NASA/TM–2020–5007394

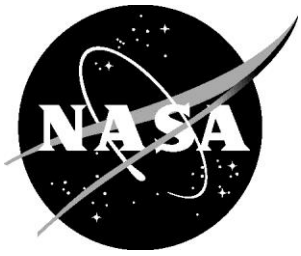

Airborne Weather Radar Observations & Analysis Results from the 2014/2015 HAIC Flight Campaigns

Steven D. Harrah
Langley Research Center, Hampton, Virginia

Patricia J. Hunt
Analytical Mechanics Associates, Inc., Hampton, Virginia

Justin K. Strickland
Analytical Mechanics Associates, Inc., Hampton, Virginia

September 2020

NASA STI Program . . . in Profile

Since its founding, NASA has been dedicated to the advancement of aeronautics and space science. The NASA scientific and technical information (STI) program plays a key part in helping NASA maintain this important role.

The NASA STI program operates under the auspices of the Agency Chief Information Officer. It collects, organizes, provides for archiving, and disseminates NASA's STI. The NASA STI program provides access to the NTRS Registered and its public interface, the NASA Technical Reports Server, thus providing one of the largest collections of aeronautical and space science STI in the world. Results are published in both non-NASA channels and by NASA in the NASA STI Report Series, which includes the following report types:

- TECHNICAL PUBLICATION. Reports of completed research or a major significant phase of research that present the results of NASA Programs and include extensive data or theoretical analysis. Includes compilations of significant scientific and technical data and information deemed to be of continuing reference value. NASA counter-part of peer-reviewed formal professional papers but has less stringent limitations on manuscript length and extent of graphic presentations.

- TECHNICAL MEMORANDUM. Scientific and technical findings that are preliminary or of specialized interest, e.g., quick release reports, working papers, and bibliographies that contain minimal annotation. Does not contain extensive analysis.

- CONTRACTOR REPORT. Scientific and technical findings by NASA-sponsored contractors and grantees.

- CONFERENCE PUBLICATION. Collected papers from scientific and technical conferences, symposia, seminars, or other meetings sponsored or co-sponsored by NASA.

- SPECIAL PUBLICATION. Scientific, technical, or historical information from NASA programs, projects, and missions, often concerned with subjects having substantial public interest.

- TECHNICAL TRANSLATION. English-language translations of foreign scientific and technical material pertinent to NASA's mission.

Specialized services also include organizing and publishing research results, distributing specialized research announcements and feeds, providing information desk and personal search support, and enabling data exchange services.

For more information about the NASA STI program, see the following:

- Access the NASA STI program home page at http://www.sti.nasa.gov

- E-mail your question to help@sti.nasa.gov

- Phone the NASA STI Information Desk at 757-864-9658

- Write to:
  NASA STI Information Desk
  Mail Stop 148
  NASA Langley Research Center
  Hampton, VA 23681-2199

NASA/TM–2020-5007394

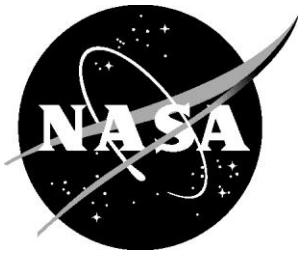

Airborne Weather Radar Observations & Analysis Results from the 2014/2015 HAIC Flight Campaigns

Steven D. Harrah
Langley Research Center, Hampton, Virginia

Patricia J. Hunt
Analytical Mechanics Associates, Inc., Hampton, Virginia

Justin K. Strickland
Analytical Mechanics Associates, Inc., Hampton, Virginia

National Aeronautics and
Space Administration

Langley Research Center
Hampton, Virginia 23681-2199

September 2020

The use of trademarks or names of manufacturers in this report is for accurate reporting and does not constitute an official endorsement, either expressed or implied, of such products or manufacturers by the National Aeronautics and Space Administration.

Available from:

NASA STI Program / Mail Stop 148
NASA Langley Research Center
Hampton, VA 23681-2199
Fax: 757-864-6500

Airborne Weather Radar Observations & Analysis Results from the 2014/2015 HAIC Flight Campaigns

Steven D. Harrah
NASA Langley Research Center, Hampton Virginia 23681

Patricia J. Hunt
Analytical Mechanics Associates, Inc., Hampton, Virginia

Justin K. Strickland
Analytical Mechanics Associates, Inc., Hampton, Virginia

ABSTRACT

This document presents a summary of the airborne weather radar observations made during joint EU/US flight campaigns to study High Altitude Ice Crystal (HAIC) atmospheric conditions. These flight campaigns were conducted near Darwin, Australia and Cayenne, French Guiana in 2014 and 2015, respectively. A variety of analyses were conducted resulting in statistical descriptions of the radar reflectivities of HAIC encountered during storm penetrations. These results are presented along with a set of visualization tools that aided flight operations and post-flight assessments. A summary of HAIC radar reflectivities observed during these flight campaigns corroborates reports by commercial pilots during HAIC encounters.

ACKNOWLEDGEMENTS

The authors would like to acknowledge these results were only possible through collaborative research and flight test support from the Federal Aviation Administration (FAA), the European Union which funded Airbus to conduct the flight campaigns, and Service des Avions Français Instrumentés pour la Recherche en Environnement (SAFIRE) who conducted the flight campaign and collected the radar data analyzed in this report. Additionally, the authors want to acknowledge the benefits from collaborative discussions with our international colleagues and their participating organizations, including (but not limited to) Environment and Climate Change Canada (ECCC), the French National Center for Scientific Research (CNRS), the French meteorological service (Météo-France), the French space agency (CNES), and the Australian Bureau of Meteorology (BoM) – all who supported and/or conducted these flight campaigns. Lastly, the authors want to thank Tom Bond (FAA), Jeanne Mason (Boeing), Alice Grandin (Airbus), Fabien Dezitter (Airbus), Walter Strapp (ECCC), and Tom Ratvasky (NASA) for the leadership and help in securing the weather radar data from these flight campaigns.

FOREWORD

This paper was originally written in 2014, after the Darwin HAIC Flight Campaign, and then updated in 2015 after the Cayenne HAIC Flight Campaign. However, its release was delayed to allow restricted use of these results by the HAIC project and the flight campaign's funding organizations. While the results contained herein are now well accepted by researchers, this report is being released now as background information and documentation of the historical development of this technology.

1 Background

For the past few years, some commercial transport flights have experienced engine events after flying in glaciated clouds. Industry researchers [Mason et al] have suggested these engine events were due to ingestion of high concentrations of small ice crystals, which produced a range of engine issues – ranging from loss of thrust to engine unstarts, and includes events that have produced significant engine damage. Pilot reports describe these encounters during cruise as flight into white-out conditions with extremely fine ice crystals impacting and flowing across the windscreen – producing a sound like sand impacting the windscreen. In some instances an electrification of the aircraft including generation of St. Elmo's fire has been observed along with a noticeable increase in cockpit humidity and the smell of ozone has been reported.

Pilots typically rely upon their weather radar to detect the presence of hydrometeors (eg, rain, sleet, hail, etc). So it was expected that increasing levels of ice particle concentrations would be visible on the weather radar display as increasing reflectivities. However, pilots consistently described these encounters as not showing any increases in radar reflectivities ahead of the aircraft. Compounding this reflectivity issue, pilots reported little to no reflectivities ahead of the aircraft both before and during engine events. This last HAIC attribute is the primary reason for: the radar observations made during the flight campaigns, the resulting radar analyses conducted thereafter, and the development of this report.

Given the threat this atmospheric condition poses to commercial aviation and the lack of detection/awareness provided by the current generation of radars, the FAA, aircraft manufacturers, and engine manufacturers recommended a series of flight campaigns to investigate this flight condition, assess if it requires a new/increased ice ingestion certification standard for modern jet engines, and develop mitigation techniques/technologies to enable continued safe flight operations in and around these environments. In response to this international call for action, aviation icing experts from the FAA, NASA, ECCC, Boeing, Airbus, and academia formed the HAIC / High Ice Water Content (HIWC) Science Team to provide structure and guidance for these investigations, provide a forum for sharing results, as well as develop plans for the recommended flight campaigns.

Initially NASA and the FAA were going to conduct a flight campaign in 2012 but were unable to get modifications to an aircraft in a satisfactory manner; however, through their participation in the HAIC/HIWC Science Team, the FAA/NASA team was able to learn of EU/Airbus plans for a HAIC flight campaign to be performed in 2014 utilizing the SAFIRE-operated Falcon 20 research aircraft. The FAA and NASA researchers travelled to Toulouse, France to investigate this opportunity and were pleased to be added to the HAIC Research Team and included in their flight campaigns.

The primary objective of the EU/Airbus flight campaigns was to characterize the HAIC atmospheric condition including measurement of Particle Size Distributions (PSD) and Ice Water Content (IWC) within the regions of HAIC and profiling of the surrounding cloud/atmosphere. In order to perform these investigations, a Dassault Falcon 20 aircraft was modified to carry a Nevzorov probe (measures IWC, Liquid Water Content (LWC), and Total Water Content (TWC)), the NASA Iso-Kinetic Probe (IKP, which measures IWC), a W-band cloud profiling radar, and several ice crystal detectors – along with their associated control and recording subsystems. NASA and Honeywell offered a new X-band weather radar but SAFIRE was unable to install a new radar due to time and certification constraints; however, a recorder was able to be added by SAFIRE to capture the existing radar's display.

As a secondary objective, radar reflectivities of HAIC conditions were measured by the pilot's weather radar and recorded for post-flight assessment and analyses by the NASA research team. The radar analyses performed included: distributions of radar reflectivity factor (RRF) inside HAIC conditions as well as the surrounding area, assessment of the pilot's need for variable gain and tilt, and an assessment of the

correlation between IWC and RRF. In addition to these analyses, various data visualization tools were developed and provided to flight team members/organizations for their own analyses and review of the flight conditions. Results of these analyses and observations made with the visualization tools are the basis for (and the balance of) this report.

2 Flight Campaigns

The record of commercial HAIC incidents were predominately over the oceans and during convective seasons so flight campaigns were planned around these conditions and near locations that had good meteorological installations and support. Darwin, Australia was selected for multiple reasons, including: the number of HAIC incidents near this region, the ability to operate relatively free of commercial traffic, the Australian Bureau of Meteorology's excellent radar network, and their interest in HAIC research. Cayenne, French Guiana was selected based upon: the preponderance of convective weather, reduced operational costs, very few traffic conflicts, and good meteorological support due to the proximity of the European Space Agency's launch site.

2.1 Hardware

The Falcon 20 research aircraft has a Honeywell Primus 660 (see Figure 1) weather radar installed to support flight operations. The radar consists of a transceiver, pedestal, and antenna located under the nose-mounted radome (see Figure 2); plus a control unit and indicator in the cockpit. Digital data from the radar display bus was captured using an ARINC 708/453 recorder. Measured RRF is encoded into 5 color bands according to the following table (expressed in dBZ):

53 ≤	magenta	
40 ≤	red	< 53
33 ≤	yellow	< 40
23 ≤	green	< 33
	black	< 23

The Primus 660 also has a variable gain control knob that allows +3 dB to –15 dB of processing gain. This knob can also be set to CAL (i.e., calibrated) which produces no additional gain (0 dB) and activates a ground clutter filter to aid SNR and weather detection.

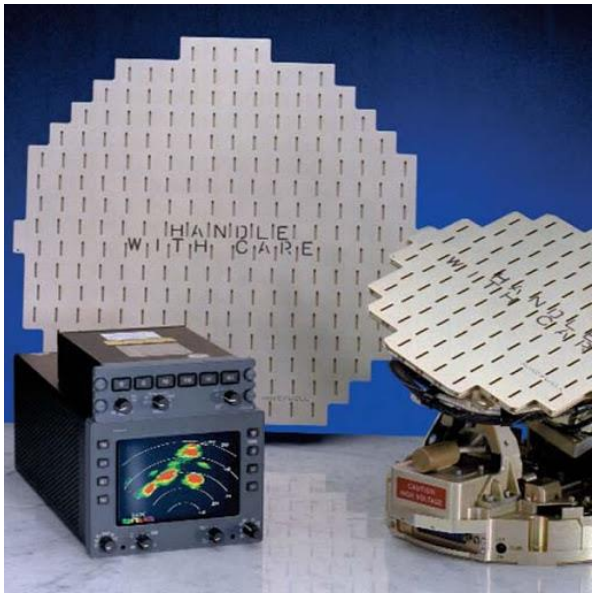

Figure 1: Primus 660 Hardware

Figure 2: Falcon aircraft with radar antenna

2.2 Deployments

Radar data was collected from two flight campaigns: the first was conducted in January and February of 2014 and based out of Darwin, Australia; the second was conducted in May of 2015 and based out of Cayenne, French Guiana. As shown in Figure 3, each flight is depicted by a French flag on the date and times they occurred. The number at the top of each flag symbol denotes the flight number. There were three types of data recorded during each flight: aircraft state, IKP (IWC data), and radar display files. A list of all the files and the start/stop times for each file type is identified in Appendix A. Recordings of each of these data sources is indicated by the bars on the flag symbol – aircraft state is blue, IKP is white, and radar is red. An "F" on the flag symbol indicates a ferry flight – typically conducted without recording research data. Each data type/file has GPS time recorded along with the measurements; during analyses the data from each source was synchronized using this recorded GPS time.

In summary, there were 23 flights (including 3 ferry flights) conducted in just 20 flight days – over a 5 week flight window, and near Darwin in 2014; similarly, there were 17 flights conducted in just 14 flight days and over a short 20 day flight window near Cayenne in 2015. The flights were generally conducted either just after dawn or just before dusk – the local diurnal cycle is shown on a UTC-based calendar in Figure 3 – with the local daytime shown as light blue and local nighttime shown as gray.

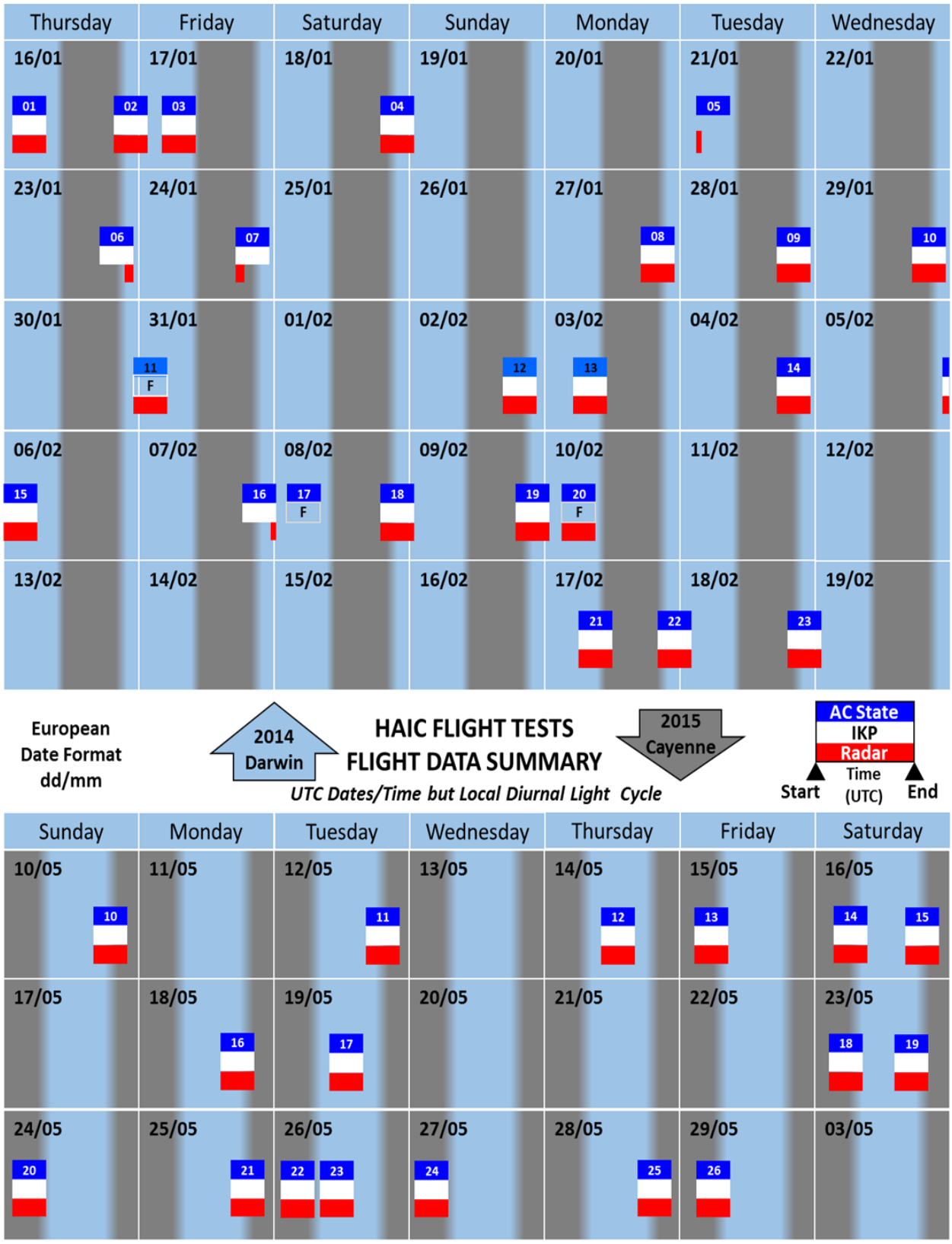

Figure 3: 2014 and 2015 HAIC Flight Campaigns

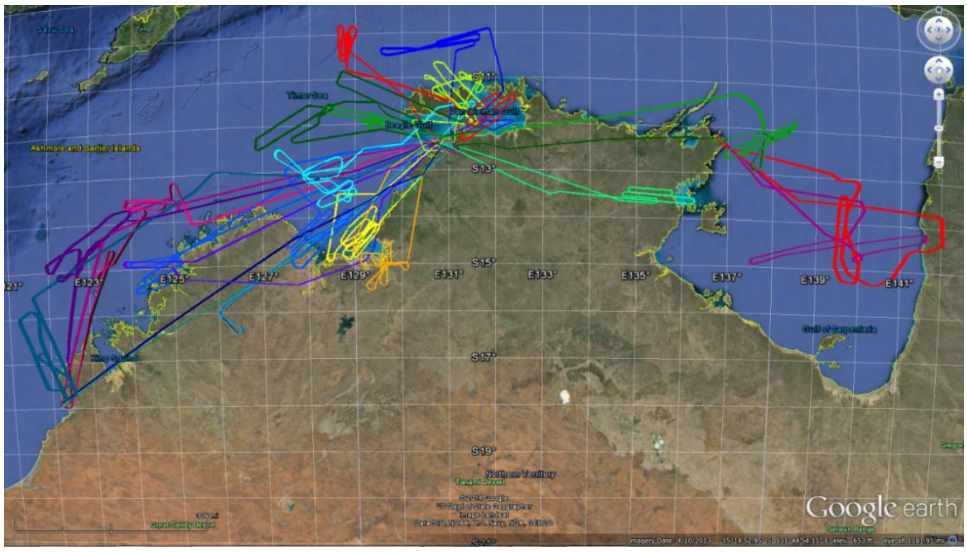

Figure 4 Summary of Flight tracks for 2014 HAIC Flight Campaign near Darwin, Australia

2.3 Flights

Figure 4 shows the flight tracks flown during the 2014 HAIC Flight Campaign. Based in Darwin, Australia, these flights were conducted primarily off-shore either down the western coast of Australia (towards Broome) or along the northern coast (towards Gove and into the Gulf of Carpentaria). These areas were favored as they had radar coverage from Australian Bureau of Meteorology radars. Figure 5 shows the flight tracks flown during the 2015 HAIC Flight Campaign. Based in Cayenne, French Guiana, these flights focused on oceanic storms but also looked at continental storms forming over the South American continent. Operations over French Guiana and Suriname were extremely limited but offered the first look at HAIC produced from continental storms. Flight tracks were dictated by existing weather conditions and the sampling strategies [Strapp et al] to assess the 99th percentile ice exposure level.

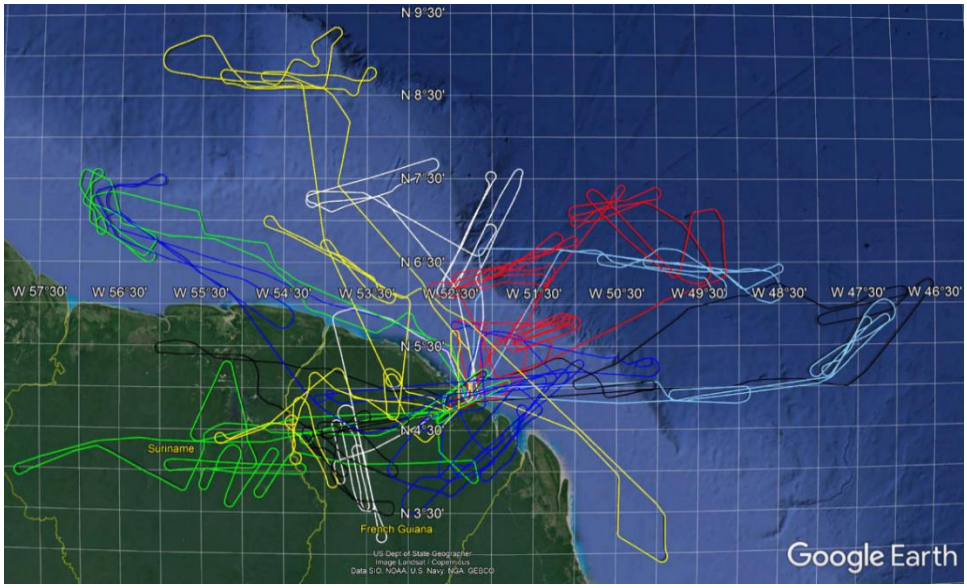

Figure 5: Summary of Flight tracks for 2015 HAIC Flight Campaign near Cayenne, French Guiana

2.4 Event Definitions

In order to easily reference specific dates and times and to specify areas of interest during a flight, a numbered list of "events" was developed for Darwin and Cayenne (see Appendix B). Ice particle concentration (i.e., IWC - measured in grams per cubic meter of air) is widely accepted as the best metric to express the severity of this aviation threat; however, at the time of writing this report, there is no accepted threshold for differentiating hazardous from non-hazardous levels of IWC. Consequently, a threshold value (i.e., IWC level) of 1 g/m^3 was selected to enable "events" to be extracted from the flight records.

The process above occasionally creates a series of smaller "events" often adjacent to each other – only separated by a momentary decrease in an IWC measurement; consequently, a process was developed to regroup these "events" into a single (i.e., continuous) "event". An analysis was performed to assess how large a time gap should be used to re-associate these fractured "events". Figure 6 shows the effect of this process on regrouping these "events". The "knee" of the curve (at 5 seconds) was chosen as the maximum allowable time gap; using this value of 5 seconds, the final listing of "events" was produced. The resulting list of 647 "events" for Darwin and 605 "events" for Cayenne are listed in Appendix B, are used in these analyses, and are referenced by these "event" numbers in the balance of this document.

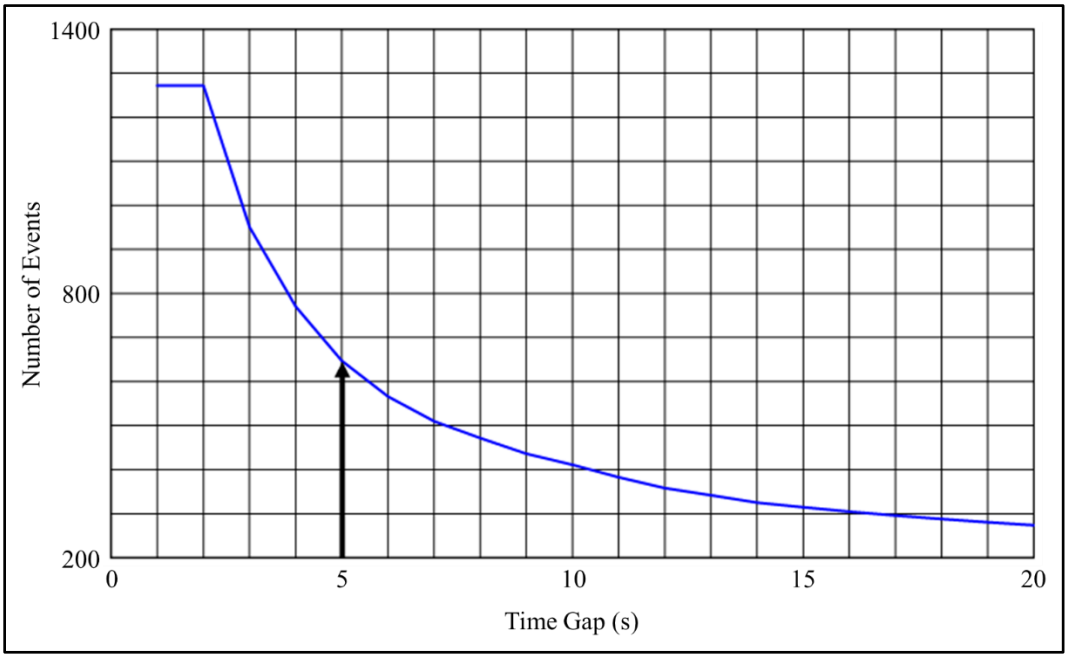

Figure 6: Assessing the Maximum Allowable Time Gap

3 Analysis Tools

Several analysis capabilities were developed and used to support the flight test campaign and analyze the resulting data. Two tools were developed to aid in visualizing the data and synchronizing/correlating multiple data types. The visualization tool provides the capability to graphically display recorded radar data. The geo-reference tool provides the capability to graphically display data from various sources in a geospatial representation.

3.1 Visualization Tool

A visualization tool was developed to read the recorded radar data files and display the ARINC 708 data in a Plan Position Indicator (PPI) format similar to a cockpit display. Radar reflectivity is shown according to the recorded color values with the Primus 660 color scale provided for reference. This application was delivered for use during flight operations to help with quick-look post-flight analysis and follow-on sortie planning. It was also useful for detailed post-flight analysis. Figure 7 below shows a snapshot of the visualization tool along with annotations (in blue) of the various radar/aircraft settings and parameters – these include:

Radar Parameters	**Display Parameters**	**Aircraft Parameters**
Azimuth angle	Date	Latitude
Tilt (Elevation) angle	Time	Longitude
Range setting	Display range	Altitude
Gain setting	Range ring spacing	Airspeed
		Heading

This visualization tool provided radar data playback capability including: continuous play, pause/restart, and/or single-frame advance. Fast-forward and re-wind options are also available to reach a desired time within the data set. Processing progress was indicated by a bar graphic at the bottom left of the display (showing percentage complete) for file-level progress and a beam indicator that moves across the top of the display to show beam location during the scan. Use of these indicators allows large-scale and fine-scale control over the data displayed for analyses. Additionally, a zoom capability was available to change the display range to focus on small areas.

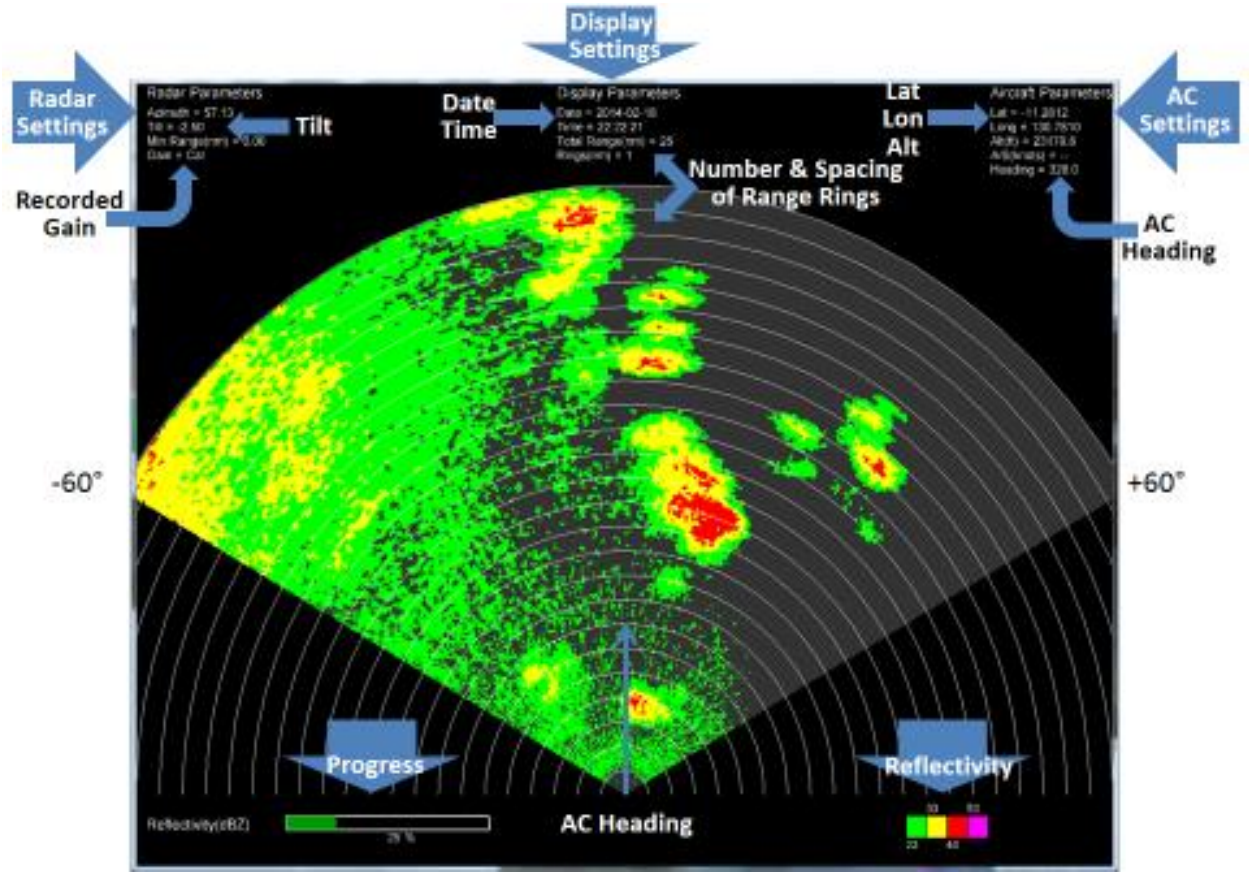

Figure 7: Weather Radar Viewer Application (708 Display)

Besides replicating an ARINC 708 display, the application provides the option to account for aircraft motion when aircraft state information is available. When enabled, the reflectivity display translates and rotates according to changes in the aircraft position and heading. Any portion of the display outside of the radar's current field of regard (i.e. beyond the azimuth scan limits) is allowed to "coast" without further updates.

An option to save screenshots is also provided. When enabled, a bitmap file is created for the entire window at the end of each sweep. The bitmap files will have the same filename as the radar data file for the same sweep with a different extension. This capability has been used to generate videos of the radar data and is the source of PPI images in this report.

Because the radar only depicts weather in front of the aircraft, it is sometimes desirable to recall what was previously shown for the current aircraft position. This is helpful for correlating in situ observations with radar measurements made prior to arriving at the current location. This visualization application provides for separate window that maintains a static snapshot of the reflectivity display, while the aircraft continues to traverse this stationary view and the primary display is updated in its window. The current aircraft position is indicated by an icon that moves relative to the stationary radar display. The current radar field of regard is drawn which indicates the current aircraft heading, radar scan limits, and radar range setting. Figure 8 below shows an example of the stationary window with a window of the current position. The window of the current position is outlined in blue with a center line showing the heading of the aircraft. The stationary window in Figure 8 had a range of 25 nm and the current window range was 10 nm.

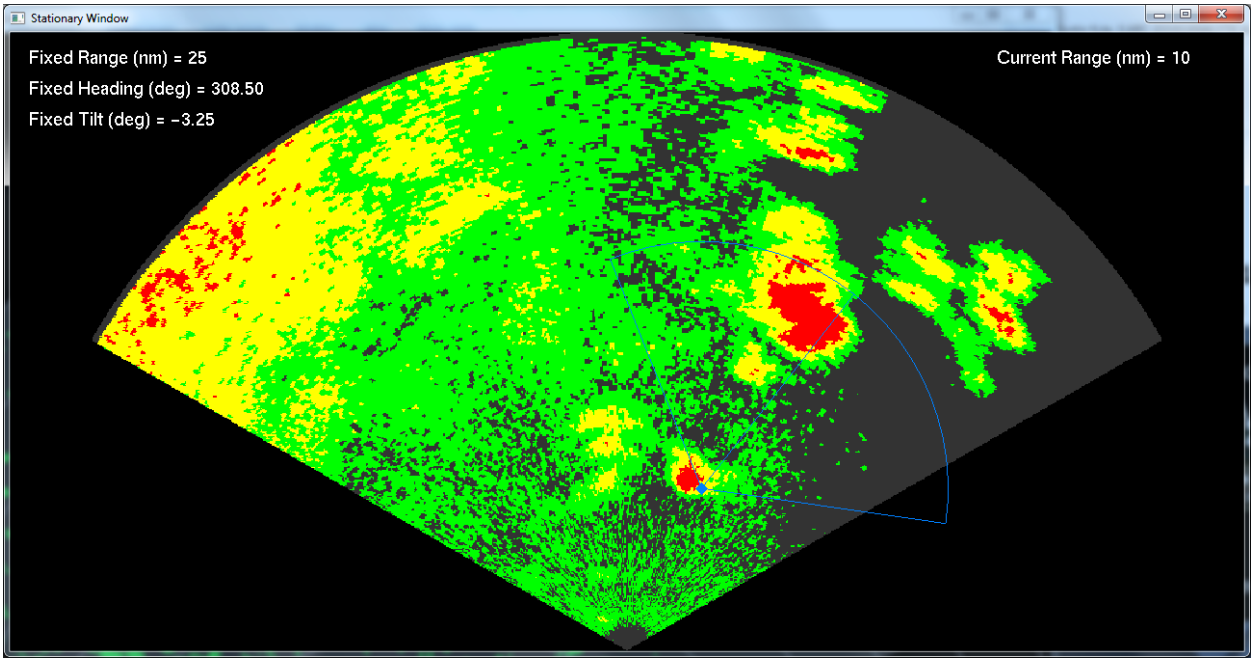

Figure 8: Weather Radar Viewer Stationary Window

3.2 Geo-Referenced Tool

Visualization of flight data in a geospatial reference frame is useful for situational awareness and correlating measurements from multiple sensors (both remote and in situ sensing systems). However, development of this new capability can be costly and very time consuming; alternatively, Google® Earth can be utilized as the graphics engine to allow limited resources to be focused on analysis rather than visualization tools. Additionally, Google® Earth is freely available and widely used, so data may be shared with many

stakeholders without the need for training or reformatting data. It provides a feature-rich Graphical User Interface (GUI) and abundant documentation/tutorials. An active user and developer communities means that it is well supported and continues to improve. Google® Earth provides the capability to import external data via the Keyhole Markup Language (KML). Therefore, custom development was simplified to merely formatting the relevant data to conform to the KML standard. By reusing capabilities provided by the visualization tool, an automatic process was created to generate KML files from recorded flight data.

The KML generated files enable the graphical display of the 4-D aircraft flight path (position and time) as well as the display of key aircraft and radar parameters in a text-based pop-up box in Google® Earth. Radar display imagery, (i.e, color-coded reflectivity) can also be conformally rendered on the display. IWC data from the NASA-developed IKP can be displayed as a color-coded 3-D track. Figure 9 below shows an example of a Google® Earth display with radar imagery overlay, IKP color-coded 3-D track, and a text-based pop-up box displaying various parameters. In addition, the figure below shows how to use the animation controls of Google® Earth to move through the flight.

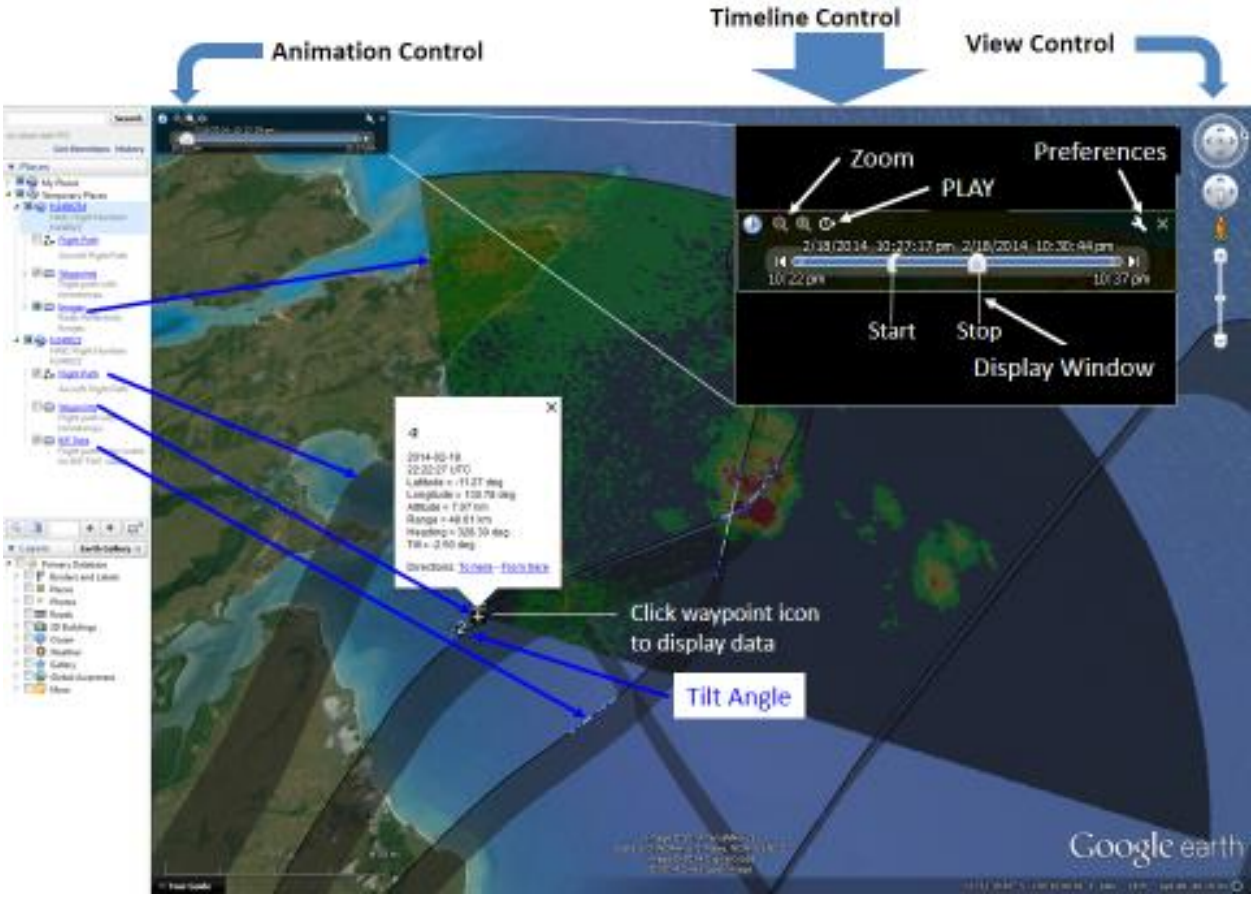

Figure 9: Visualizing aircraft, radar, and IKP data in Google® Earth

When using Google® Earth for analysis, a 3-D control feature allows for setting the observer point of view, including zoom, pan, and rotation. For data that includes a time dimension, the timeline controls may be used to animate the imagery and/or limit the time window to display only a subset of the data.

3.2.1 Representing the Iso-Kinetic Probe (IKP) data

NASA working with ECCC and Science Engineering Associates (SEA) developed an Iso-Kinetic Probe (IKP) to measure Ice Water Content (IWC) at higher concentrations than commercially available probes. The IKP instrument was used as truth data for these analyses even though the IKP and radar measure vastly different volumes of air. For these analyses and data visualizations, IKP data was quantized and color-coded into four bands:

White	$3 \leq$	IWC(g/m^3)	
Cyan	$2 \leq$	IWC(g/m^3)	< 3
Blue	$1 \leq$	IWC(g/m^3)	< 2
Black		IWC(g/m^3)	< 1

This set of colors was used on the path displayed in Google® Earth. The 3 bands of IKP data above 1 g/m^3 were used to create the statistics described in these analyses.

Simultaneously displaying radar imagery with IKP data allowed for a visualization of spatial correlation between remote and in situ measurements and helped support insights into the observed conditions.

Figure 10 is an example of the geo-referenced tool, showing a portion of a flight over the Timor Sea, north of Melville Island, on 18 February 2014 around 10:22 UTC; the image shows the aircraft overflight of two cells with high reflectivity as measured by the radar. This image depicts IKP measurements (i.e., IWC) along the entire flight path (past, present, and future) along with the current radar measurements.

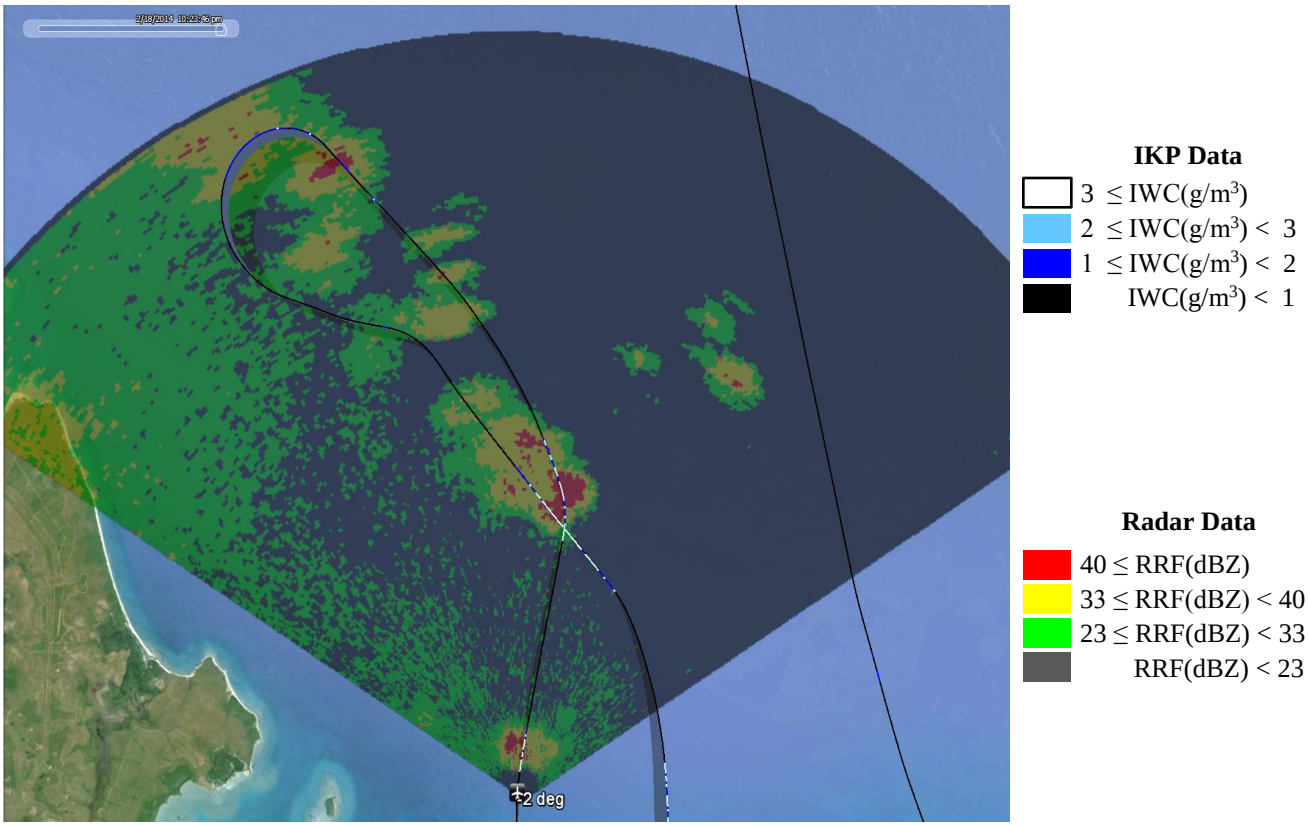

Figure 10 Spatial Correlation of IKP and Radar Reflectivity

4 Analysis

A variety of analyses were conducted, both during the flight campaign (supporting flight operations) and post-flight to assess HAIC radar properties. Specific objectives were to evaluate: use of the radar's variable gain, use of antenna tilt, flight-level IWC compared with lower-altitude RRF, and HAIC RRF statistical results. Additionally, a visual analysis was performed using the geo-referenced tool to correlate the radar reflectivities with the IKP data. This visual analysis looked for three of the four correlation outcomes in detecting HAIC conditions.

4.1 Use of Radar's Variable Gain

The Primus 660 has a variable gain controlled by a knob that allows for +3dB to -15dB gain. There is also a CAL setting that sets the gain to 0dB (i.e., no adjustment to the measured echo strength) and engages a ground-clutter filter. Pilots were requested to minimize their use of this gain as it corrupts the recorded RRF data. While both the radar display data and variable gain setting are recorded, compensation/correction for this variable gain cannot be accurately removed from the recorded data/imagery.

Note: Variable gain cannot be removed perfectly since it is applied in the radar to the measured-RRF (i.e., a floating point measurement); however, compensation is applied to recorded-RRF which is quantized into approximately 10 dBZ bands. Since some measured-RRF values are near the border between colors, application of a small amount of gain can produce a quantum (i.e., color) change in the recorded-RRF; however, this sub-quantum information is lost during quantization and cannot be recovered for use in a compensation process. During post-flight processing a value must be assumed for each recorded color, the RRF value at the middle of the color band is assumed for the purposes of analyses and compensation for variable gain adjustment. Thus the application of any variable gain less than half the width of the quantum level (e.g., 10dB / 2 = 5dB) will not produce any change in the resulting image – unlike the actual radar.

4.1.1 Minimum Gain

Figure 11 shows three PPI displays, produced from data collected on February 18, 2014 and exemplifies the difficulty compensating for variable gain. The top image was captured with the radar variable gain in CAL setting – this represents the most accurate portrayal of the atmospheric RRF measured by this radar. The lower left image shows the same scene a few seconds later, after the pilot had adjusted the variable gain to its minimum setting (i.e., maximum attenuation) of -15dB. While pilots may perform this gain adjustment to see storm structure within a single RRF band (i.e., color), this adjustment cannot easily be removed from the recorded data. The image at the lower right, shows what happens if 15dB is added back to the recorded values.

The reason for this distorted view is due to the loss of the sub-quantized values – recall only the color of the RRF was recorded so all greens are the same value, as are all yellows a single value. In order to compensate for variable gain, this analysis assumes the RRF value at the middle of the quantized band and 5 dB above the maximum yellow RRF for the red level. The gray RRF is assumed to be below measurement threshold and is unaffected by this compensation.

Since minimum gain (i.e., maximum attenuation) could not accurately be compensated, pilots were requested to minimize their use of this gain setting. For the most part, the pilots complied with this request and only used this setting briefly and sparingly; in these instances, they shifted the variable gain back to CAL after a few seconds (sweeps) to preserve data fidelity.

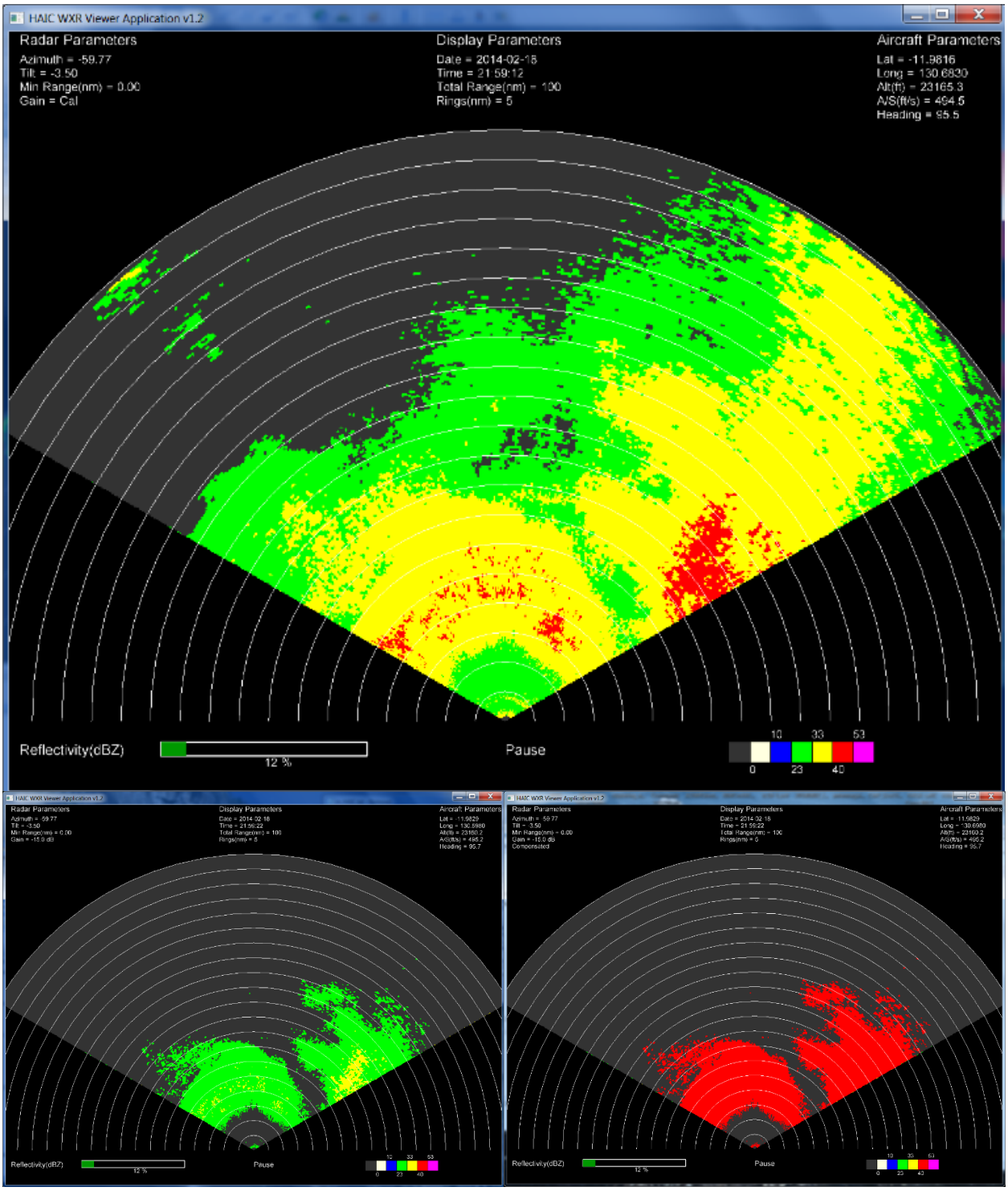

Figure 11: Comparison of Minimum Gain

4.1.2 Maximum Gain

The radar's variable gain can also be set to the other extreme – maximum gain, this is done to enhance low reflectivity regions and see below the minimum RRF level and/or see storm structure within a single RRF band. The maximum gain setting only provided 3dB of additional gain, which is less than half of any

quantized RRF band (i.e., color); therefore, compensation for this added gain will not result in any changes to recorded-RRF values (i.e., colors). Whereas the actual radar produces this amplification and results in a slightly increased RRF level on the display. An example of using maximum gain is shown in Figure 12 which was recorded on 02 February 2014. The left image was captured with the CAL variable gain setting and represents the most accurate portrayal of atmospheric RRF. The right image was recorded a few seconds later when the variable gain had been increased to maximum gain (+3dB). A comparison of the two images shows the additional gain (right image) produces slightly higher RRF levels throughout the scene. The compensated image (not shown) looks identical to the right image and thus does not restore the reflectivities to those shown in the left image. Consequently, pilots were requested to limit their use of variable gain to prevent corrupting the RRF data, analyses, and statistical results.

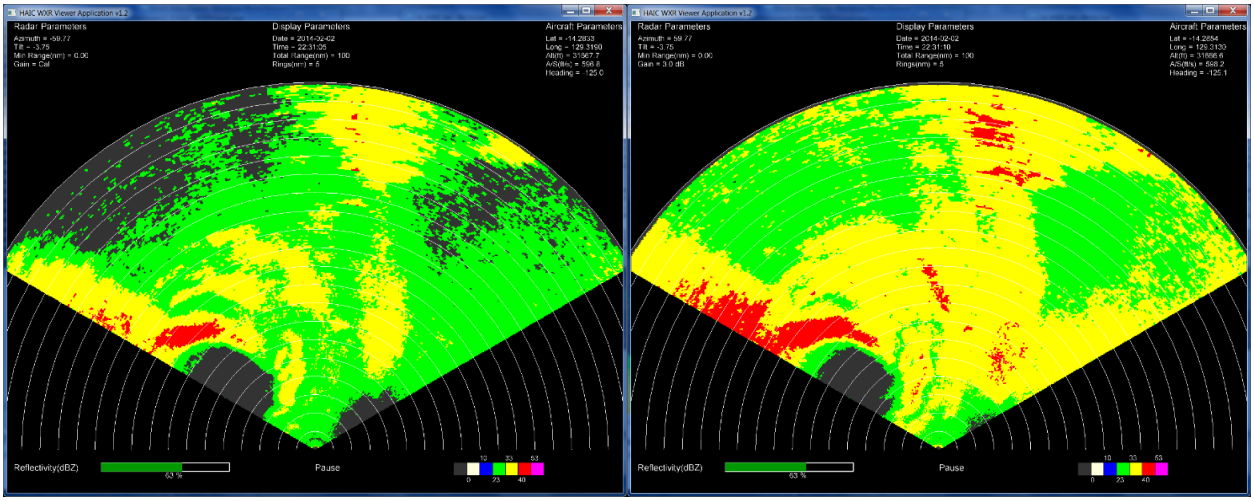

Figure 12 Comparison of CAL setting and Maximum Gain

4.2 Use of Antenna Tilt

Weather radars include an antenna and pedestal underneath the nose-mounted radome (e.g., Figure 2) and are used to scan the skies to provide situational awareness of the weather, up to hundreds of miles in front of the aircraft. Due to the limited antenna size and the operational range of airborne weather radars, echoes from the ground (i.e., clutter) often infiltrate weather returns. Pilots often use antenna tilt to discriminate ground clutter from atmospheric conditions in order to see weather descending from above or rising up from below that can affect the aircraft at its flight level.

Figure 13 shows PPI images from the 18 January 2014 flight, using the 708 visualization tool. The left image shows evidence of ground clutter contamination in the further half of range bins, from directly ahead to the right-side of the scan. Conversely, the right image shows the same scene with the antenna tilt elevated a few degrees compared to the antenna tilt used in the left image. The right image shows ground clutter is less prevalent and weather returns are more clearly evident.

The side by side images (see Figure 13) can also be shown in a conformal manner using the geo-referenced tool, described in Section 3.2 above, as shown in Figure 14. This conformal rendering shows the alignment of terrain/coastlines with RRF "features" and thereby provides confirmation that these high reflectivities come from ground clutter sources and not from weather. Aiding the interpretation of RRF imagery is the primary benefit offered by the geo-reference tool.

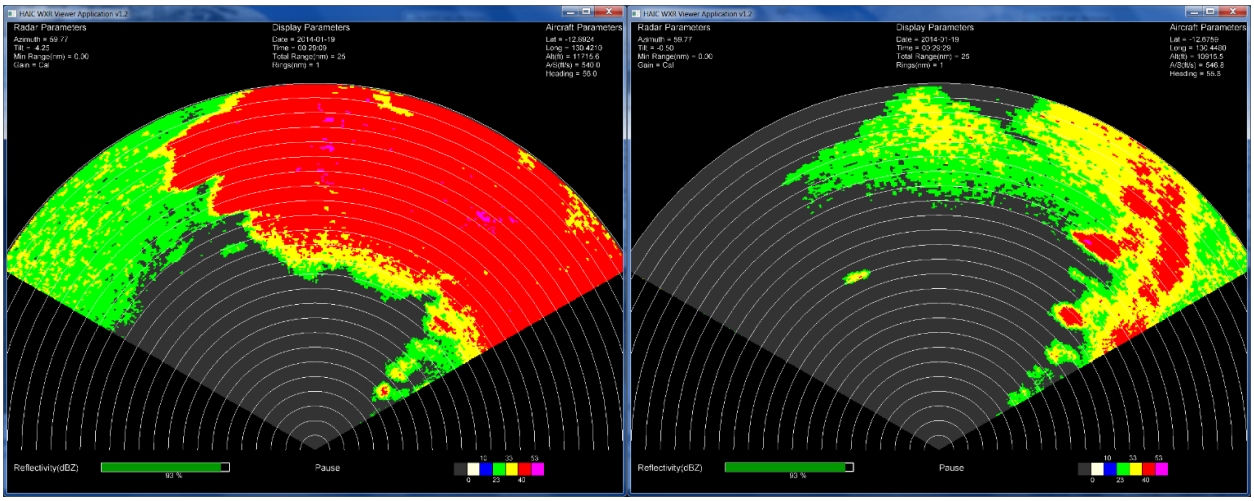

Figure 13: Ground Clutter Mitigation through Antenna Tilt Management

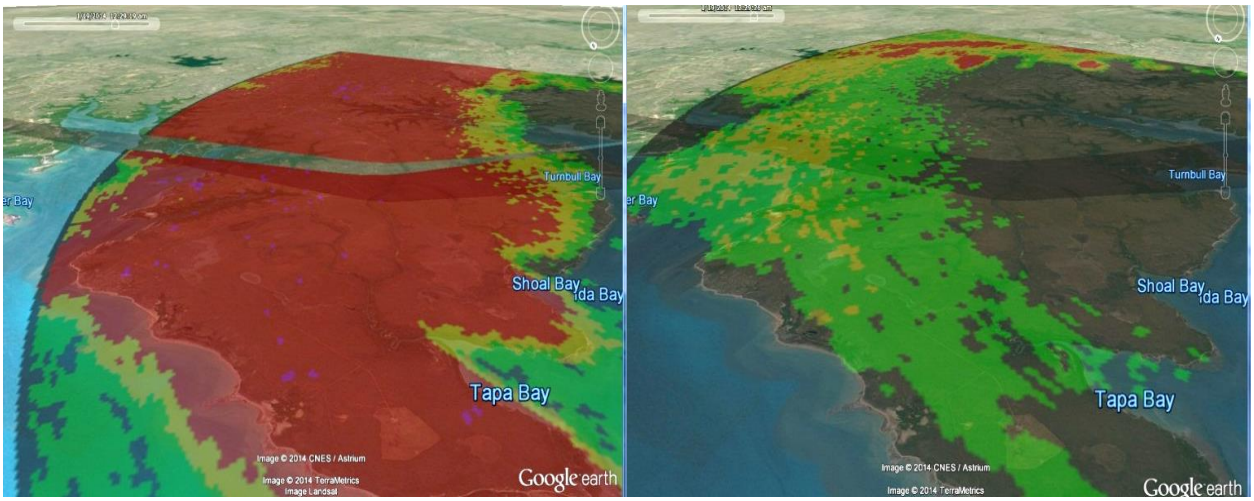

Figure 14: Confirming Ground Clutter RRF Sources Using the Geo-Reference Tool

4.3 Using Antenna Tilt to Detect HAIC Conditions

A common practice during the flight campaigns was to use the radar antenna tilt to search for possible HAIC conditions; this was achieved by tilting the antenna downward while approaching a cell to locate areas of high reflectivity below the flight level. It is believed that convection must be present in order for HAIC conditions to form, so pilots were instructed to look for high reflectivity regions below their flight altitude as an indication of potential HAIC locations. An analysis was performed using the geo-reference tool to correlate IKP measurements of IWC with locations of high radar reflectivity.

The correlation of IWC at flight level with radar reflectivity below flight level produces four possible outcomes (see Figure 15). When high radar reflectivity below flight level corresponds to high IWC at flight level, the RRF provides an indication of possible HAIC conditions (true positive) – this was the condition sought during the flight campaign. The opposite situation – when low radar reflectivity corresponds with low IWC – is not very interesting and indicates clear air conditions (true negative). Conversely, there are false indications to each of these conditions. High radar reflectivity below flight level, when IWC at flight level is low, provides an indication of HAIC conditions when none exist (false positive). Worse is when

low radar reflectivity below flight level corresponds with high IWC at flight level resulting in a missed indication of HAIC conditions (false negative).

		Radar Reflectivity Below Flight Level	
		LOW	HIGH
IKP IWC At Flight Level	LOW	True Negative (clear air)	False Positive (false indicator)
	HIGH	False Negative (miss detection)	True Positive (possible HAIC)

Figure 15: Possibility Matrix using Radar Reflectivity as an Indicator of HAIC Conditions

An analysis was performed to assess the spatial correlations between regions of high radar reflectivity below flight level and regions of HAIC at flight level. The balance of this section shows an example of False Positive, False Negative, and True Positive results observed during this analysis.

An example of a **true positive** indication was observed on 17 February 2014 around midnight UTC. During this encounter, the Falcon 20 aircraft (operating at 36,200 feet) overflew a cell with **high** radar reflectivity located about 100 nautical miles west of the Tiwi Islands over the Timor Sea. Figure 16 shows the radar measurements collected approximately 50Nm from the red reflectivities near Event 618 and with a -3° antenna tilt angle, so the regions of red RRF are about 14,000 feet below flight level.

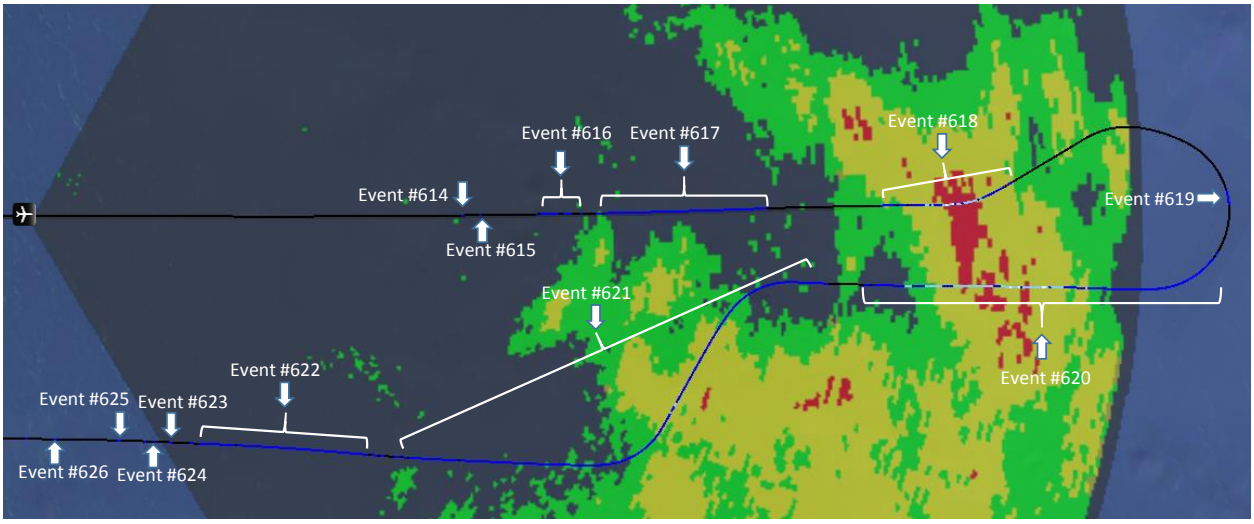

Figure 16: Radar Reflectivity and IKP Data Approaching Event #618

The antenna tilt angle was not adjusted as the aircraft approached Event 618, so the altitude of the observed radar measurements approached flight level (see Figure 17). These flight-level reflectivities were mostly low to moderate levels (i.e., green and yellow). Despite these lower flight-level reflectivities, the IKP measured significant levels of IWC with a peak at 3.4 g/m^3. This is an example of a **true positive** indication of possible higher reflectivities below HAIC conditions.

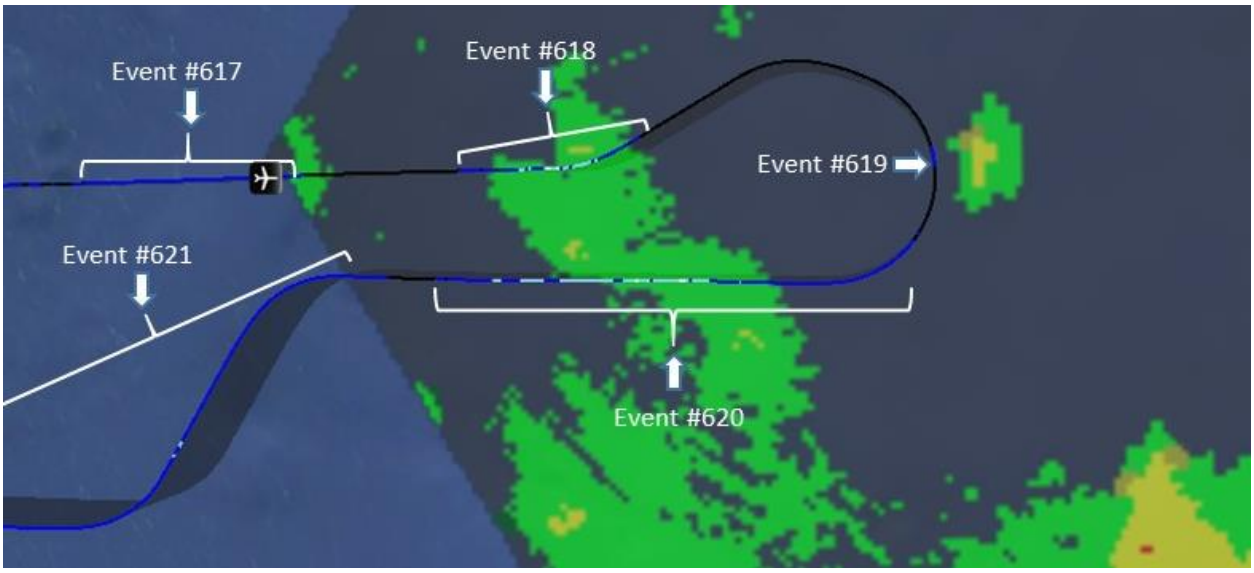

Figure 17: Radar Reflectivity and IKP Data Near Event 618

An example of a **false positive** indication was observed on 17 January 2014 around 03:33 UTC. During this encounter, the Falcon 20 aircraft (operating at 33,000 feet) overflew a cell with **high** radar reflectivity located about 200 nautical miles north of King Sound over the Indian Ocean. Figure 18 shows the radar measurements collected a little more than 20Nm from the red reflectivities near Event 012 and with a -7° antenna tilt angle, so the regions of red RRF are about 15,800 feet below flight level.

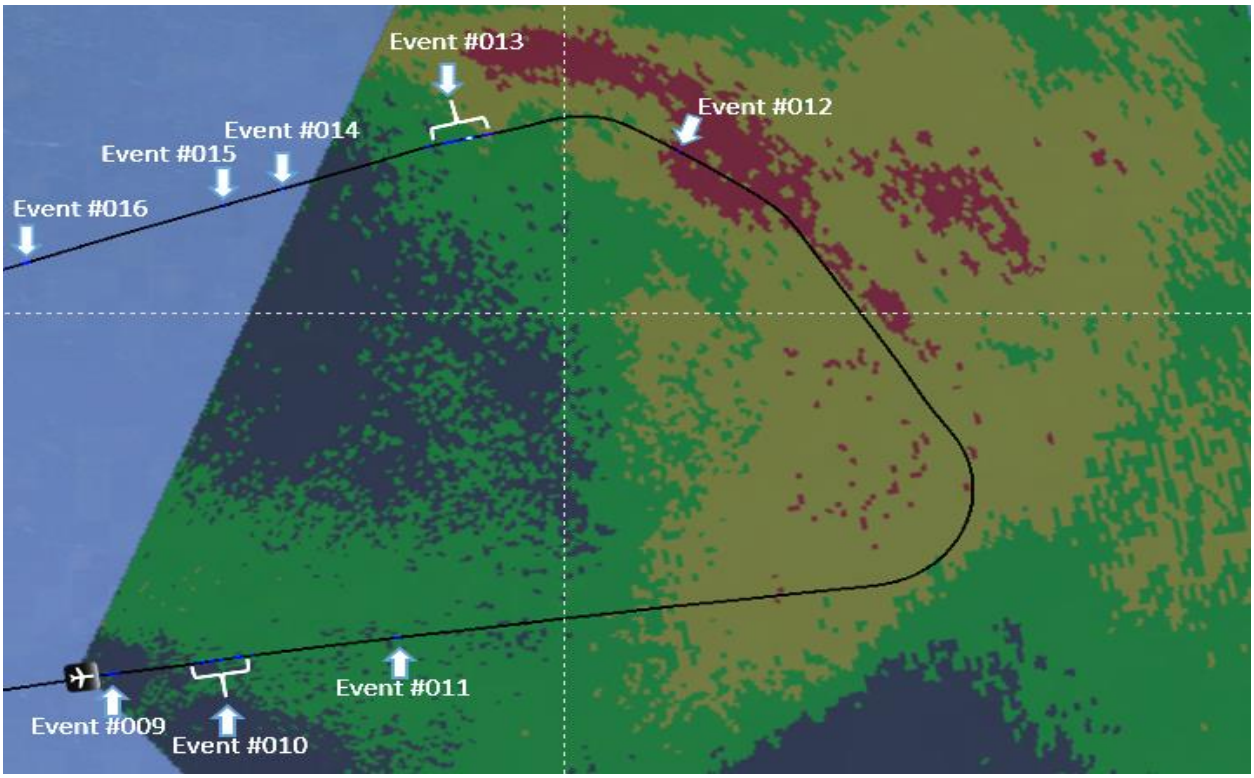

Figure 18: Radar Reflectivity and IKP Data Prior to Event 012

The antenna tilt angle was decreased (i.e., closer to 0° tilt) as the aircraft approached Event 012, so the altitude of the observed radar measurements changed to be near flight level (see Figure 19). These flight-level reflectivities were near their lowest levels (i.e., black and speckled green). Despite the high reflectivities measured below Event 012, the IKP measurements were mostly below 1 g/m^3 with a small, momentary peak of 1.6 g/m^3. This is an example of a **false positive** indication with higher reflectivities below a region without HAIC conditions.

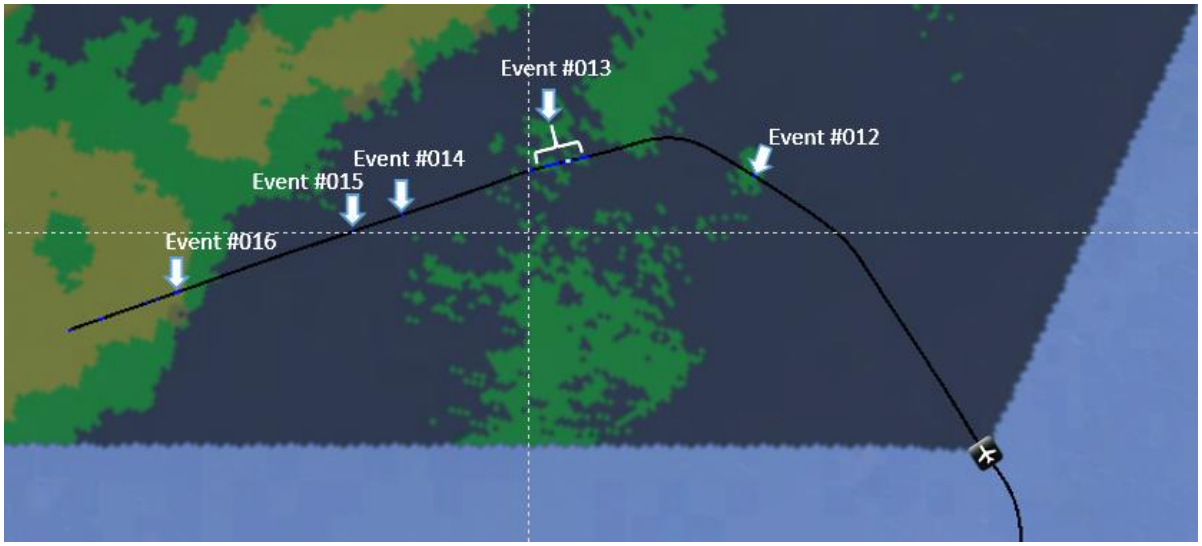

Figure 19: Radar Reflectivity and IKP Data Prior to Event 012

An example of a **false negative** indication was observed on 23 January 2014 around 10:49 UTC. During this encounter, the Falcon 20 aircraft (operating at 33,000 feet) overflew a cell with **low** radar reflectivity located over the Joseph Bonaparte Gulf. Figure 20 shows the radar measurements collected a little more than 13Nm from the beginning of Event 116 and with a -3° antenna tilt angle, so the regions of green RRF that cover Event 116 range from about 5,000 to 12,000 feet below flight level.

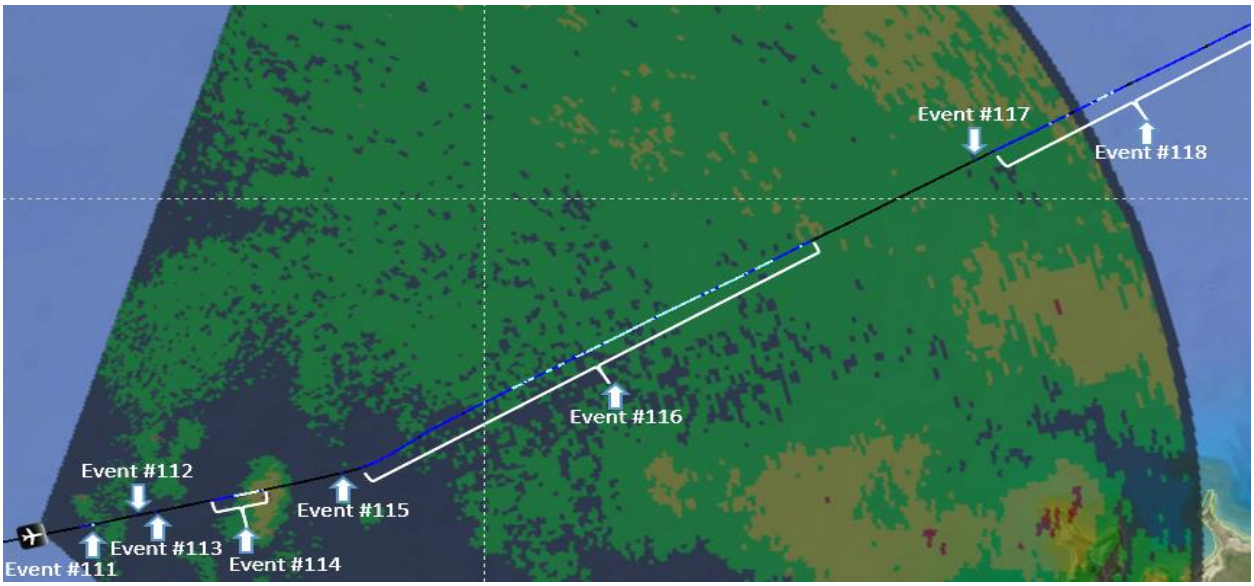

Figure 20: Radar Reflectivity and IKP Data Approaching Event 116

The antenna tilt angle was decreased (i.e., closer to 0° tilt) as the aircraft approached Event 116, so the altitude of the observed radar measurements changed to be near flight level (see Figure 21). These flight-level reflectivities were near their lowest levels (i.e., black and speckled green). Despite the low reflectivities measured prior to and during the encounter with Event 116, the IKP peak measurements were relatively high, around 2.4 to 2.7 g/m^3. This is an example of a **false negative** indication with low reflectivities below a region with HAIC conditions.

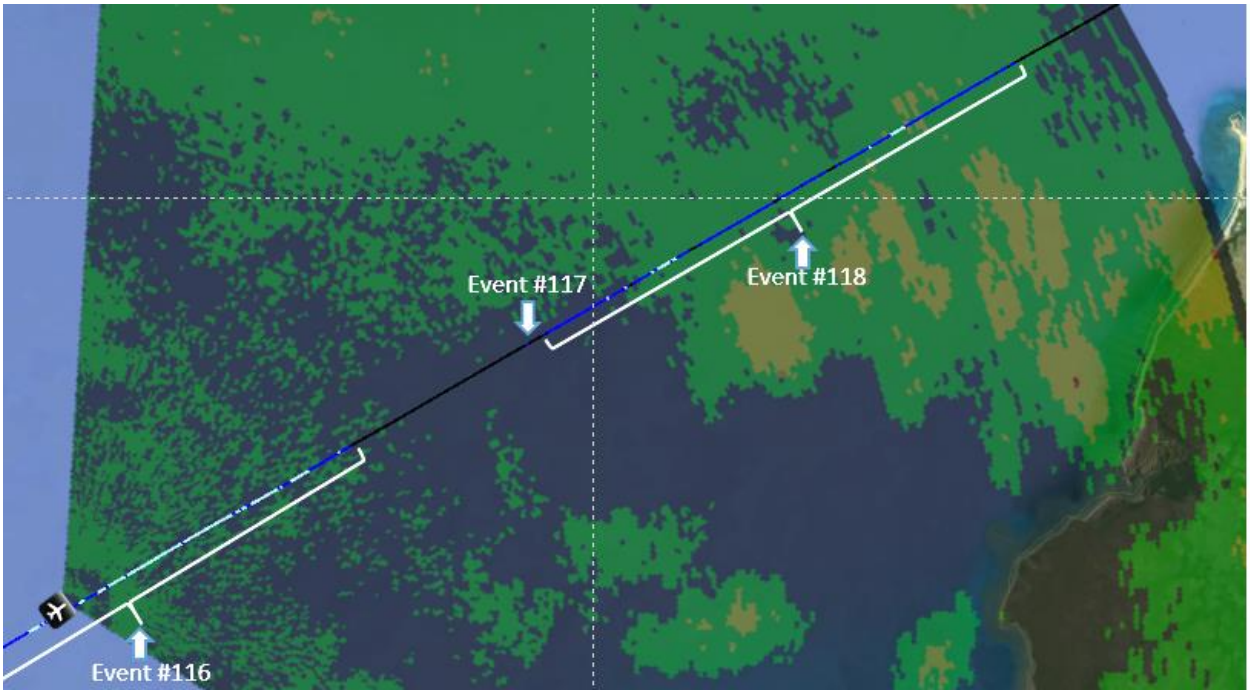

Figure 21: Radar Reflectivity and IKP Data Near Event 116

These three examples show that there is no consistent correlation between high radar reflectivity below flight level and high IWC at flight level. There are instances when high radar reflectivity are present below HAIC conditions. There are also instances when low IWC levels are present at flight level despite high radar reflectivity measurements below flight level (false positive). Conversely, there are instances when high IWC levels are present at flight level despite low radar reflectivity measurements below flight level (false negative). These inconsistencies produce significant challenges to remote detection (both direct and indirect) of HAIC conditions.

4.4 Statistical Analysis

Commercial pilots have consistently reported low radar reflectivities associated with HAIC encounters. While this seems counter-intuitive and inconsistent with accepted radar theory, it's also difficult to understand how so many pilots would report the same observations. So one of the primary radar analysis objectives was to characterize the RRF observed during these encounters.

4.4.1 Gathering the Data for Statistics

Several numerical analyses were performed to characterize radar reflectivities and develop statistical descriptions of these reflectivities for each separate IWC band: 1–2 g/m^3, 2–3 g/m^3, and >3 g/m^3. Compensating for variable gain added another challenge to these analyses. Lastly, the results reported herein were restricted to RRF values within 500 feet of flight level and the aircraft's Static Air Temperature

(SAT) was -20 °C or colder – to remove any biases that mixed phase precipitation could produce.

As previously mentioned, only the radar display bus was recorded (i.e., ARINC 708 color values). This recording attribute means each, individual RRF value could represent any of the RRF values within the band of reflectivities encoded into this single color. In order to account for this ambiguity in histogram generation, each individual RRF sample added to the entire band of RRF values for that color and was adjusted for variable gain offset. These data were used to generate histograms that estimate the Probability Density Function (PDF) of radar reflectivities for each separate IWC band.

Measured HAIC conditions were correlated with measured radar reflectivities. In order to compare and correlate IWC measurements with radar RRF measurements, an association of the data in these two recordings was needed. A technique [Strickland et al] was developed that identified which radar bins (within a scan) were coincident with future aircraft positions (i.e., where IKP measurement were located). This process relies upon an accurate, common time reference; the GPS time signal was utilized for this purpose. Using this process, radar measurements were paired with IKP measurements and could be treated as a linked pair of values throughout these analyses. Because the antenna beam width intersects the position of a single IKP value during multiple radar measurements, multiple reflectivities are associated (i.e., paired) with a single IWC value – all of these measurement pairs were used in the generation of these statistics.

RRF data, coincident with the aircraft track and within one beam width, were binned into time windows of: 10, 30, and 60 seconds in front of the aircraft. Figure 22 shows these time windows along the flight track and with a width equivalent to the antenna beam width. This time criteria had two benefits: one, to enable comparisons of different PDFs for multiple time periods in front of the aircraft (i.e., allows assessment of HAIC RRF versus range properties); and two, to eliminate associating RRF data with IWC data from crossing tracks too far into the future. An example of a future crossing track is shown in Figure 22 where a portion of the future aircraft track crosses the current aircraft track from left to right, as viewed by a pilot at the current aircraft position – thus the use of a time window prevented RRF data from the current scan from being associated with IWC measurements from too far into the future (e.g., 10min).

Note: *The longer time windows include the data from shorter time windows.*

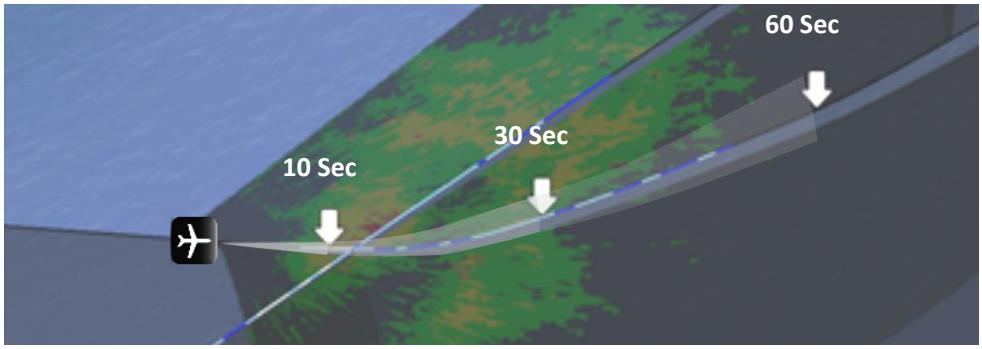

Figure 22: Employing Time Criteria for Collecting Statistical Data

4.4.2 RRF Statistical Descriptions

Figure 23 and Figure 24 show examples of statistical descriptions of the radar reflectivities observed during HAIC encounters in Darwin and Cayenne, respectively. The top left chart shows a summary of the flight track for each day, color-coded by the IWC measurements. The three other charts show RRF histograms generated for that day, segregated by IWC and for the three time windows (i.e., range regimes) as described previously. Basic statistical measures (e.g., sample size, mean RRF, and RRF standard deviation) are

provided for each histogram. These histograms have been normalized so the area under the curve equals 1 (i.e, 100%); thus these graphs represent an estimate of the RRF PDF for these conditions. Graphs of HAIC RRF PDF estimates are plotted on top of the radar reflectivity color bands used by this radar. The statistical description of HAIC radar reflectivities with the lowest concentrations of ice particles (i.e., 1-2 g/m^3) is shown in blue (lines and data); the middle band of ice particle concentrations (i.e., 2-3 g/m^3) is shown in cyan; and the highest concentrations (i.e., >3 g/m^3) is shown in white. A complete set of daily statistical results are provided in Appendix C.

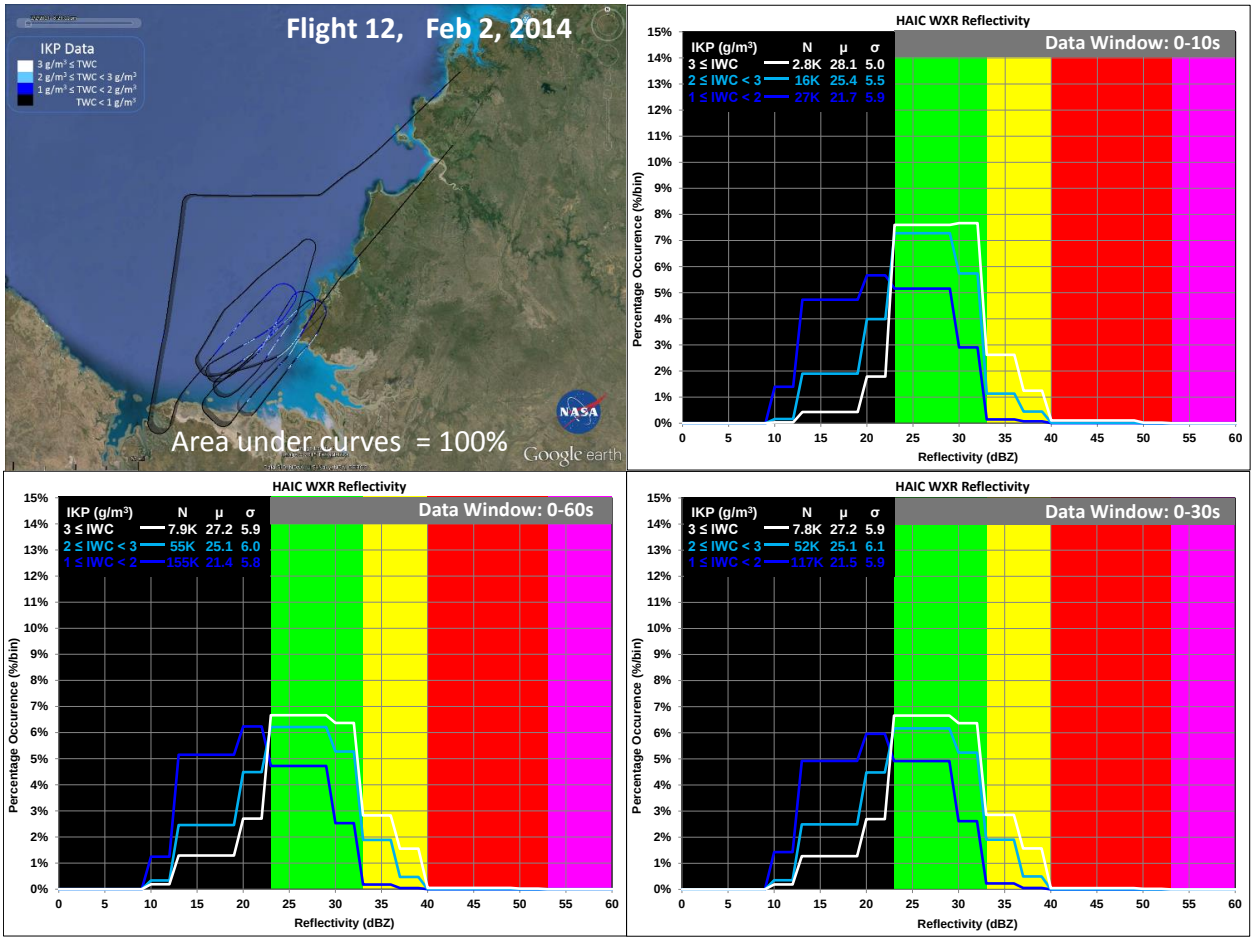

Figure 23: HAIC RRF PDF Observed on 02 February 2014 (Darwin, Australia)

The histograms in Figure 23 were created for a series of storm transits over the Timor Sea (just south and west of Darwin) on 02 February 2014. This set of race track transits provided multiple passes greater than 50Nm and short revisit times allowing observation of the evolution of the HAIC condition and in accordance with data collection strategy.

The first (and most important) observation was that the mode of these PDF are centered in the black or green bands of radar reflectivities (i.e., around 22 dBZ for the lower IWC concentrations and around 25-28 dBZ for the middle and high concentrations) – consistent with pilot reports of HAIC encounters. Also notable was the consistency of PDF across the different IWC bands; for small to moderate sample sizes, the mean RRF only varied a few decibels and even more surprising the standard deviation changed only a few decibels across the three IWC bands. Lastly, there was little variation across the three time windows, suggesting the observed HAIC condition was not a shallow/thin layer for this set of cells. The

"blocky" nature of these PDF are produced by the quantization of the RRF measurements into colors and the pilot's use of variable gain.

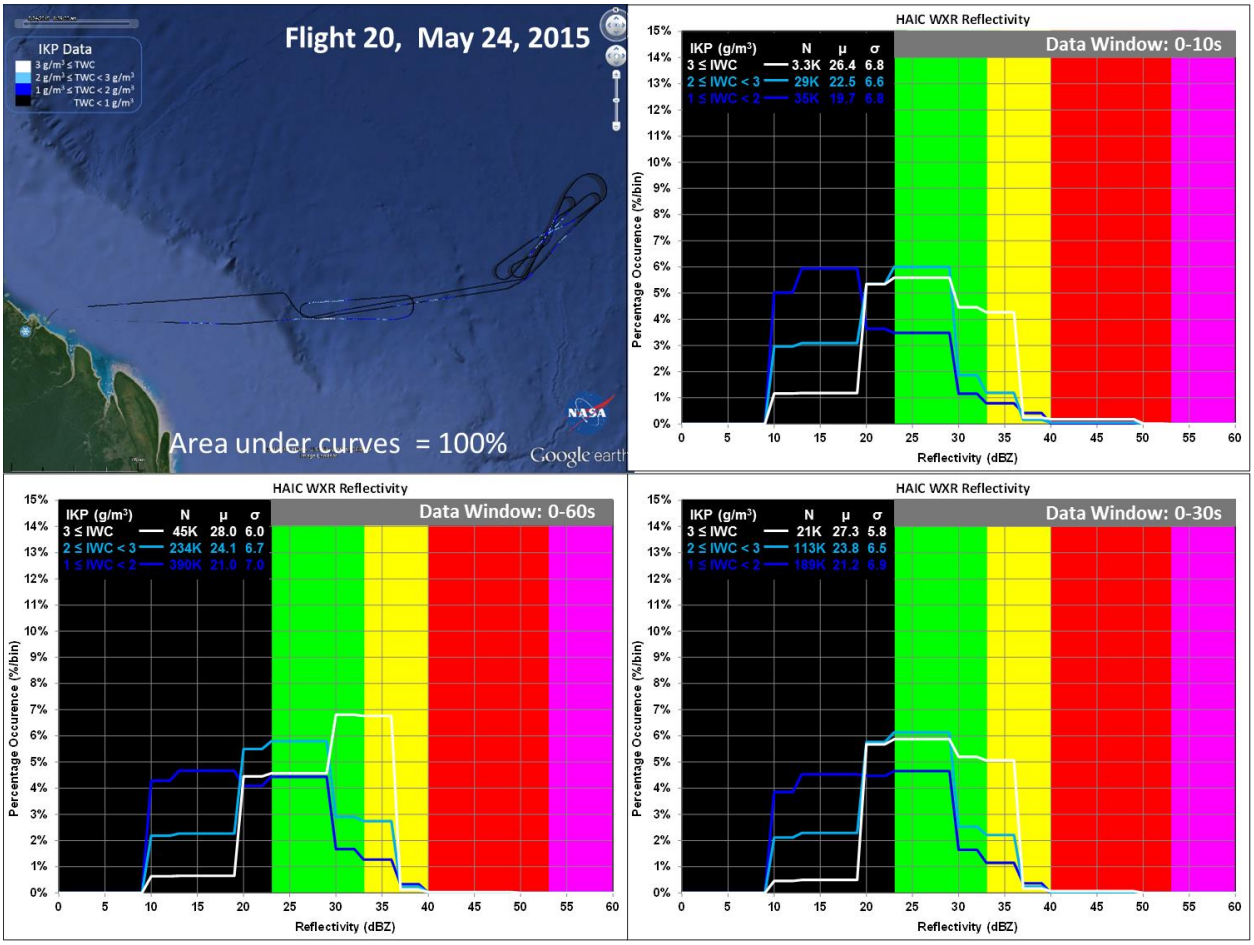

Figure 24: HAIC RRF PDF Observed on 24 May 2015 (Cayenne, French Guiana)

The histograms in Figure 24 were created for a series of storm transits over the Atlantic Ocean (just north and east of Cayenne) on 24 May 2015. This set of race track transits provided multiple passes greater than 50Nm and short revisit times allowing observation of the evolution of the HAIC condition and in accordance with data collection strategy.

These histograms show consistent reflectivity results with pilot reports and the results from Darwin a year earlier; namely, that the mean RRF for HAIC conditions is generally around 23 dBZ for low to moderate IWC and a slightly higher mean RRF around 28 dBZ for the highest IWC levels. The standard deviations for these PDF were remarkably similar to those observed in Darwin as well. The only notable difference was the slightly greater occurrence of higher RRF levels for the greater than 3 g/m^3 PDF – most noticeable in the 60s data window. This implies higher reflectivities are present at longer ranges, which suggests that there was likely higher RRF levels below flight level (where the measurement was made). As demonstrated by the results for this day and in general, Cayenne flights had more occurrences of IWC values above 3 g/m^3 than those typical for Darwin; further evidence of this and other statistical properties can be observed in the daily histograms for the Cayenne flight campaign provided in Appendix C.

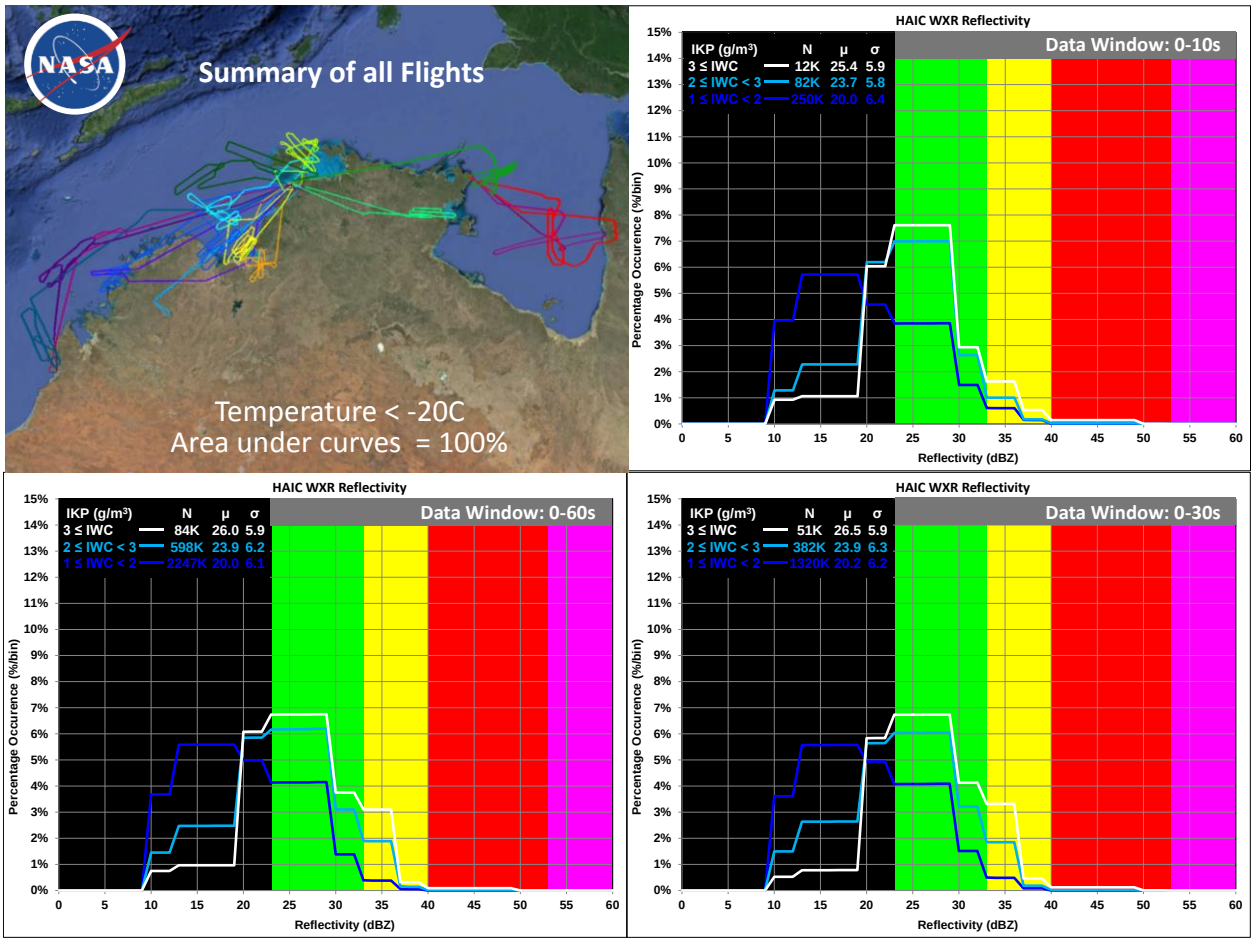

Figure 25: HAIC RRF PDF Summary for Darwin Flight Campaign

Figure 25 shows a summary set of RRF PDF for all Darwin flights. The Summary histograms are similar to the daily RRF results except that, the Summary PDF for: the lowest IWC band (blue lines) are biased toward the black reflectivities (for all distances); the middle IWC band (cyan lines) moved toward the green reflectivities; and the highest IWC band (white lines) moved toward the green reflectivities with a few yellow reflectivities. While the Darwin Summary PDF/statistics vary slightly from the daily results, it is interesting that there are almost no differences between the PDF across the different time windows (i.e., detection ranges). The means of the Summary RRF PDF increased by about 6 dBZ as IWC tripled from 1 to 3 g/m^3; however, this is expected and consistent with a 3x change in the amount of scatterers which should produce ~5 dB change in the signal.

Figure 26 shows a summary set of RRF PDF for all Cayenne flights; as can be seen from the flight tracks, the Cayenne flights consists of transits from both oceanic and continental storms. These two sources of convection appear to produce significantly different RRF PDF. Interesting, some Cayenne flights produced bi-modal RRF PDF that appears to be caused by thin HAIC layers at flight level with another RRF layer below. Additionally, Cayenne produced near 3.5 times as many measurement pairs (IWC, RRF) as observed in Darwin with a significantly larger population of higher reflectivities (i.e., yellow) than observed/flown-through in Darwin. While the Cayenne Summary PDF/statistics do vary from the daily results, it is interesting that there are almost no differences between the PDF across the different time windows (i.e., detection ranges).

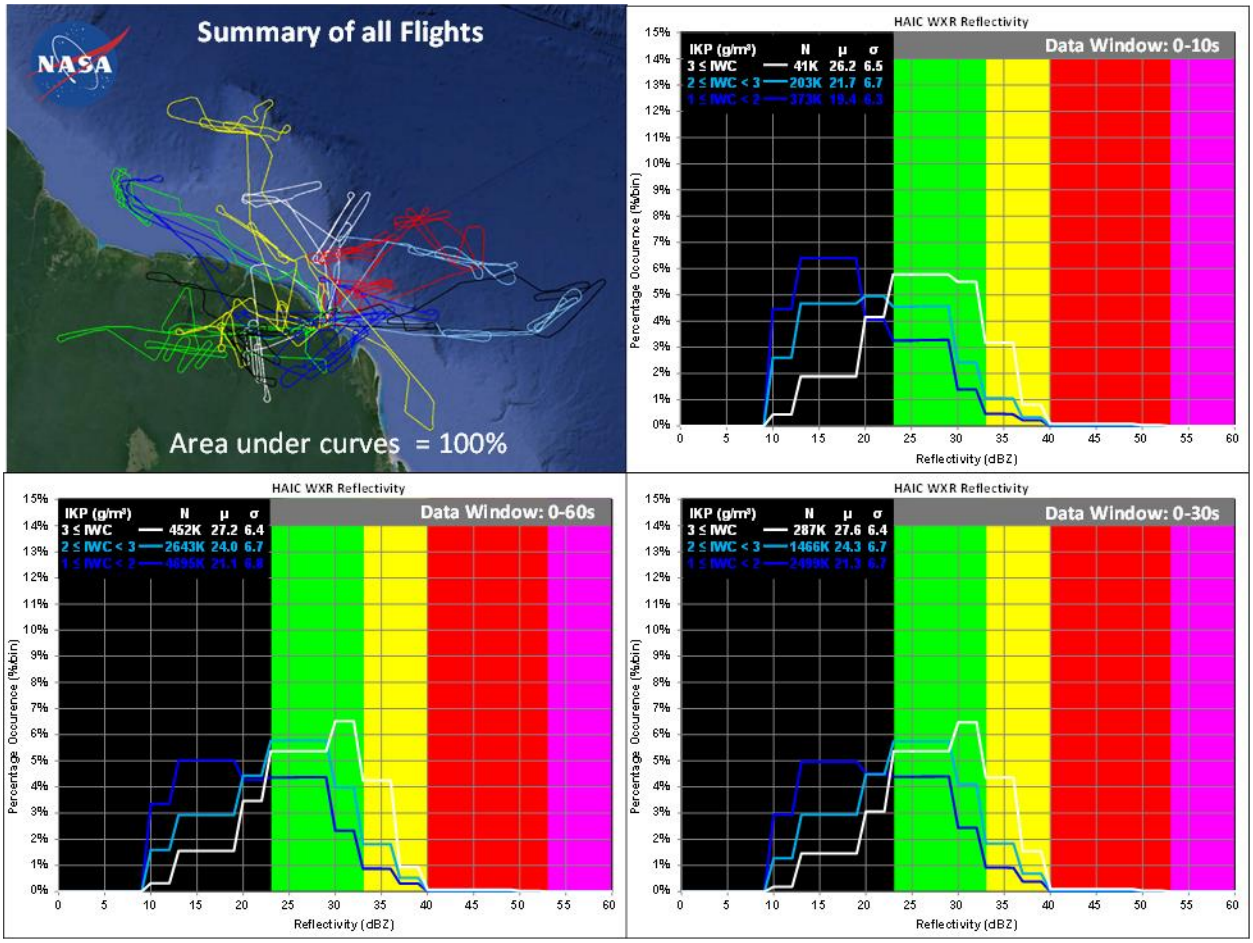

Figure 26: HAIC RRF PDF Summary for Cayenne Flight Campaign

The means of the Summary RRF PDF increased by about 6 dBZ as IWC tripled from 1 to 3 g/m^3. This is expected and consistent with a 3x change in the amount of scatterers which should produce ~5 dB change in the signal; this result suggests a correlation between RRF and IWC. It might be noted from these PDF, for a given RRF value, the probability of that RRF being produced by any of the three IWC bands is nearly equal; this contradicts the correlation result suggested above. These contradictory results are reconciled by noting that an increase in IWC (at a given location) will produce an increase in RRF, but two RRF values observed at different location does not imply the higher RRF location has a higher IWC. This is due to the fact that RRF is based upon the combination of all the scatterer sizes raised to the 6th power [Doviak et al]; whereas, IWC is the combination of all the droplet/particle sizes raised to the 3rd power. So increases in the population of small particle sizes will have a greater effect on IWC than RRF; and conversely, an increase in the population of larger particles will have a greater effect on RRF than IWC.

As was noted above, there are some differences between the two campaign summaries but the similarities are the dominant observations. Overall these reflectivity statistics show that the majority of the HAIC events occurred in the black and green reflectivities. The two campaigns show consistent reflectivity statistics for the HAIC icing conditions flown in either Australia or French Guiana. The increased number of samples of yellow reflectivity, for Cayenne, gives the apparance that the RRF PDF is different than that for Darwin; however, the statistics confirm there are no significant differences. The radar PDF/statistics do not vary greatly with distance, which implies most of the radar measurements were collected under filled beam conditions (i.e., ideal for anayses).

The fact that the standard deviation only varies by 1 dBZ across the IWC bands (for Darwin) and less than 0.5 dBZ (for Cayenne) implies the RRF PDF are insensitive to IWC (i.e., RRF variance is consistent across IWC levels). The standard deviation is also constant across the three time windows, which can only be produced by maintaining filled beam conditions (i.e., the HAIC was in thick layers and/or the radar was not at the top of the glaciated cloud). Lastly, the pilots' used variable gain occasionally in Darwin but seldom during the Cayenne fights; compensation for their use of this gain did produce a few anomalous samples of red RRF. However, this occurred so seldom that it did not adversely affect the PDF nor the statistics.

Comparing Darwin and Cayenne statistics (everything remaining constant except for the flight location) the largest difference in means is ~2 dBZ and the largest standard deviation difference is <1 dBZ. These are extemely small differences for datasets collected from numerous storms, thousands of miles and 15 months apart. This suggests the dataset and the analysis results provide consistent properties about the HAIC atmospheric condition. As a consequence of these common and self-consistent results, there is higher confidence in these results and removes many uncertainties that varied results produce.

4.4.3 Correlation of RRF & IWC

The histograms in Figure 24, especially those for the 60 second window, suggest that IWC increases as RRF increases – this is not universal. In a separate analysis, IWC was compared to RRF by presenting these associated pairs across time. In Figure 26, the blue line indicates the measured IWC and the dots indicate the measured RRF color.

It might be noted that RRF values (i.e., colors) did typically progress from black to green to yellow to red as IWC increased; but that property was only consistent for single events (i.e., localized). Looking at any specific IWC level, there are examples of every RRF value (except for black RRF at the highest IWC levels). This property is observed in all the daily correlation line plots (see Appendix C); therefore, IWC does not have a simple functional relationship with measured RRF.

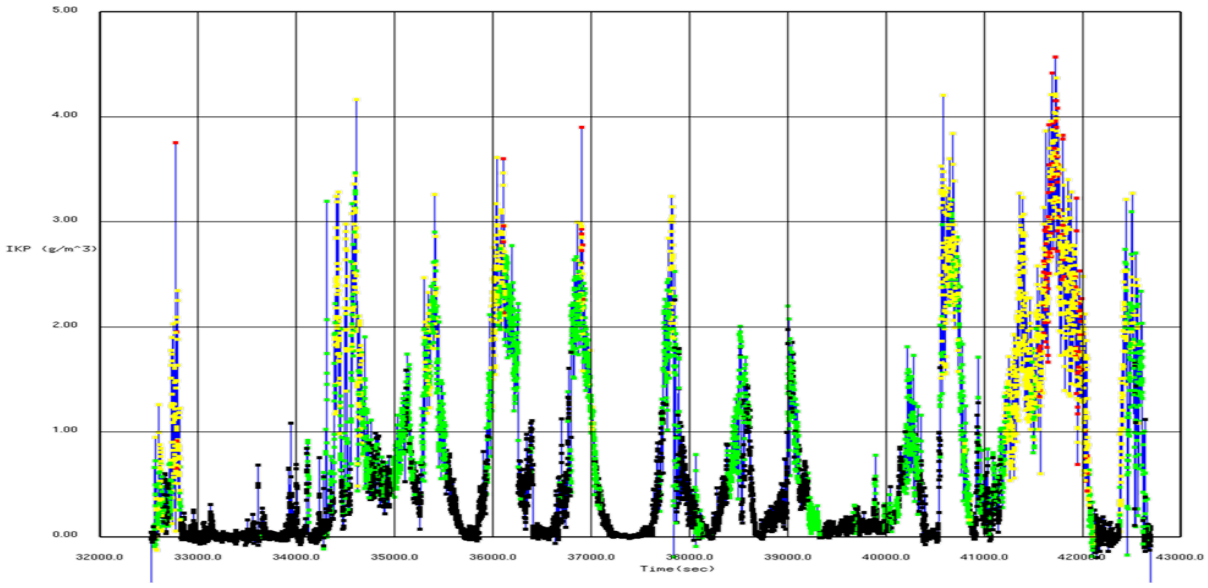

Figure 27: Time versus IKP and Reflectivity for Flight 20 on May 24, 2015

While only a few daily samples have been used to show the variety of results in this analyses section, these examples are representative of the entirety of daily results. All the Darwin and Cayenne results can be observed along with the histograms for each day in Appendix C.

5 Conclusions and Future Work

A multi-national, joint industry-government-academia, research consortium conducted a series of flight campaigns to investigate High Altitude Ice Crystal (HAIC) characteristics. These flights occurred in January and February of 2014 based out of Darwin, Australia and May of 2015 based out of Cayenne, French Guiana. These two flight campaigns produced over 145 hours of flight data through numerous HAIC events/conditions. Multiple types of data were collected including: aircraft state, particle size distributions, ice water and total water concentrations, and two types of radar data (a W-band cloud profiling radar and the pilot's X-band weather radar). Unfortunately, only the display bus could be recorded from the pilot's X-band weather radar; however, a great deal of information was confirmed and provided by this limited data source.

After analyzing the recorded data from the pilot's weather radar a number of observations/conclusions can be drawn. One of the more important observations drawn from the comparison of Darwin and Cayenne data was the similarity of the Probability Density Functions (PDF) for Radar Reflectivity Factor (RRF). Given the enormous spatial and time differences between these flight campaigns could produce significant differences in HAIC RRF PDF; however, the highly similar PDF and statistics provided confidence in the data collection and analysis processes/results. Access to these datasets can be requested through the National Center for Atmospheric Research (NCAR) at their website:

2014 HAIC Flight Campaign (Darwin, Australia) https://data.eol.ucar.edu/project/HAIC-HIWC
and
2015 HAIC Flight Campaign (Cayenne, French Guiana) https://data.eol.ucar.edu/dataset/486.031.

One of the most important conclusions was confirmation that HAIC conditions can often occur within cruise level (colder than -20 °C) regions of low RRF – consistent with the report by commercial pilots. Higher IWC bands are also produced within regions with higher reflectivities, but not at a significantly higher rate (i.e., frequency of occurrence). Thus, a specific RRF measurement has nearly the same probability of being produced by low, medium, or high IWC conditions. From which it can be concluded - RRF does not have simple functional relationship with IWC. Additionally, the analysis showed flight-level HAIC radar reflectivities are most often green or black; radar reflectivities below flight-level are often yellow or red – however, there are many examples of black and green reflectivities below flight-level too. Consequently, overflight of high reflectivity regions does not always encounter HAIC conditions.

Note: These results may have a little bias due to the fact that flight operations were conducted in accordance with commercial pilot operations (i.e., restricted from flight through RED). There was some amount of the flights that went into the yellow reflectivities but none that intentionally went into/through RED so these operations would minimize any statistical influence by high RRF regions. However, commercial pilots avoid these areas inherently so there should be no need to recommend they avoid them for HAIC purposes and the aviation hazard is therefore constrained to providing a reason to avoid areas that look benign.

Another conclusion (that was surprising) was HAIC radar reflectivity did not vary greatly with distance; this implies most radar measurements were made with a nearly filled beam. This condition produces more consistent measurements and analysis results. It also suggests HAIC conditions may often occur in thick layers, reducing the number of conditions needed in detection algorithms.

Lastly, use of the radar display bus (i.e., colors instead of actual RRF values) worked pretty well (much better than expected). The pilots' minimized their use of variable gain, which improved the consistency of these results. However, as each RRF color represented about 10dBZ of variability, this loss of precision produces uncertainties in all RRF results and conclusions that would not exist if RRF values had been recorded. Future flight campaigns are being planned that will provide recording of the fundamental radar

measurement of In-phase and Quadrature (I/Q) voltages, which should improve these results and allow additional analyses to be performed. These fundamental radar measurements will be correlated with other scientific data including drop size distributions collected by probes, satellite imagery, and other remote sensing instruments. Once the flight data is acquired, an analysis can be performed to define and assess HAIC detection possibilities with current weather radars or define the changes to this technology that would be required to perform HAIC detection.

References

Mason, J., Strapp, J.W., Chow, P., "The Ice Particle Threat to Engines in Flight," AIAA 2006-0206, https://doi.org/10.2514/6.2006-206.

Strapp, J. W., Isaac, G., Korolev, A, Ratvasky, T., et al., "The High Ice Water Content (HIWC) Study of Deep Convective Clouds: Science and Technical Plan," DOT/FAA/TC-14/31, 2016, http://www.tc.faa.gov/its/worldpac/techrpt/tc14-31.pdf.

Strickland, J. K., Hunt, P. J., Harrah, S. D., and Switzer, G. F., "A Method for Correlating Forward-Looking Remote Sensor Measurements with In-Situ Measurements on Flying Platforms," NASA/TM-2020-5002898, 2020, https://ntrs.nasa.gov/api/citations/20205002898/downloads/NASA-TM-2020-5002898%20corrected.pdf.

Doviak, Richard J. and Zrnic, Dusan S., Doppler Radar and Weather Observations. Academic Press, Inc., 1984.

Appendix A: Table of data files from HAIC Flight Campaign data for 2014 in Darwin, Australia. The times in red are an indication of missing data (due to either a late start or an early shutdown); the flights/times in gray were ferry flights.

Flight Number	Date	Radar Data (UTC)		AC State Data (UTC)		IKP (UTC)	
		Start	Stop	Start	Stop	Start	Stop
fs140001	1/16/2014	2:10	5:09	1:22	5:24	1:22	5:11
fs140002	1/16/2014	21:25	0:10	21:03	0:30	21:03	0:24
fs140003	1/17/2014	2:30	4:50	2:07	5:15	1:59	5:10
fs140004	1/18/2014	21:51	0:40	21:18	0:50	21:34	0:46
fs140005	1/21/2014	4:34	5:39	4:12	7:25		
fs140006	1/23/2014	22:09	23:19	19:34	23:25	19:36	23:20
fs140007	1/24/2014	20:08	21:24	19:38	22:40	20:10	22:36
fs140008	1/27/2014	20:43	23:14	20:03	23:16	20:16	23:14
fs140009	1/28/2014	21:08	23:38	20:46	23:49	20:55	23:44
fs140010	1/29/2014	20:06	23:07	19:34	23:22	19:27	23:22
fs140011	1/30/2014	1:13	2:16	0:45	2:26	0:52	2:23
fs140012	2/2/2014	20:35	23:39	19:49	23:50	20:24	23:46
fs140013	2/3/2014	4:05	6:28	2:37	6:36	3:40	6:33
fs140014	2/4/2014	20:34	23:45	19:51	23:56	20:26	23:50
fs140015	2/5/2014	23:27	2:29	22:56	2:35	22:58	2:32
fs140016	2/7/2014	23:23	0:12	19:42	0:20	19:44	0:19
fs140017	2/8/2014			1:36	3:57	1:36	3:53
fs140018	2/8/2014	20:48	23:56	20:16	0:12	20:13	0:03
fs140019	2/9/2014	20:48	0:14	20:11	0:19	20:06	0:16
fs140020	2/10/2014	2:07	3:56	1:33	4:04	1:33	3:59
fs140021	2/17/2014	6:27	8:27	6:07	8:36	5:58	8:33
fs140022	2/17/2014	21:43	0:48	20:56	1:07	20:56	1:05
fs140023	2/18/2014	21:37	0:38	20:51	0:52	20:51	0:47

Table of data files from HAIC Flight Campaign data for 2015 in Cayenne, French Guiana.

Flight Number	Date	Radar Data(UTC)		AC State Data (UTC)		IKP (UTC)	
		Start	Stop	Start	Stop	Start	Stop
fs150009	5/9/2015	16:09	18:36	15:35	18:43		
fs150010	5/10/2015	18:55	21:17	18:33	21:27	19:39	21:05
fs150011	5/12/2015	19:54	22:15	19:37	22:34	20:28	22:06
fs150012	5/14/2015	13:57	17:07	13:40	17:21	14:49	16:57
fs150013	5/15/2015	8:35	12:06	8:09	12:14	8:56	11:36
fs150014	5/16/2015	8:08	11:50	8:01	12:01	8:37	11:33
fs150015	5/16/2015	15:51	18:29	15:35	18:37	16:20	18:16
fs150016	5/18/2015	19:27	22:29	19:27	22:47	19:47	22:20
fs150017	5/19/2015	14:19	17:27	13:49	17:33	14:51	17:08
fs150018	5/23/2015	9:14	12:36	8:49	12:53	9:29	12:18
fs150019	5/23/2015	15:23	18:59	15:00	19:12	15:35	18:40
fs150020	5/24/2015	8:51	12:08	8:36	12:11	9:02	11:51
fs150021	5/25/2015	19:07	22:30	18:54	22:45	19:24	22:15
fs150022	5/26/2015	8:33	11:59	8:08	12:02	8:42	11:42
fs150023	5/26/2015	13:10	15:51	12:54	16:00	13:23	15:32
fs150024	5/27/2015	8:27	11:58	8:06	12:12	8:36	11:37
fs150025	5/28/2015	19:25	22:50	19:00	22:58	19:39	22:31
fs150026	5/29/2015	8:47	12:06	8:25	12:10	9:01	11:49

Appendix B: Table of IWC events for 2014 HAIC Flight Campaign in Darwin, Australia. There were 647 events encountered over 19 flight days. The table is organized by date and by time.

Event	Time (sec)		Event	Time (sec)		Event	Time (sec)		Event	Time (sec)	
#	Start	End	#	Start	End	#	Start	End	#	Start	End
20140116			20140123 (cont)			20140123 (cont)			20140124 (cont)		
1	81197	81199	48	75858	75869	98	79046	79057	147	76983	76992
2	81230	81249	49	75875	75878	99	79064	79066	148	77000	77000
3	82446	82709	50	75889	75890	100	79076	79395	149	77006	77006
4	84189	84190	51	75929	75929	101	80304	80327	150	77022	77026
5	84198	84199	52	75943	75943	102	80333	80338	151	77032	77047
6	84212	84212	53	76037	76037	103	80353	80497	152	77053	77066
7	84218	84220	54	76105	76105	104	80506	80527	153	77076	77084
8	84256	84256	55	76144	76155	105	80537	80537	154	77102	77102
20140117			56	76162	76361	106	80558	80659	155	77108	77108
9	12390	12396	57	76372	76414	107	80678	80702	156	77146	77147
10	12422	12440	58	76427	76427	108	80895	80895	157	77194	77194
11	12486	12487	59	76443	76450	109	81048	81063	158	77456	77456
12	12861	12861	60	76456	76456	110	81098	81784	159	77485	77485
13	12928	12950	61	76462	76468	111	81827	81837	160	77510	77510
14	13001	13001	62	76534	76541	112	81853	81853	161	77522	77522
15	13021	13021	63	76552	76564	113	81862	81862	162	77530	77530
16	13089	13091	64	76572	76572	114	81888	81911	163	77541	77542
17	13098	13102	65	76587	76592	115	81945	81945	164	77575	77579
18	13119	13120	66	76606	76714	116	81954	82182	165	77596	77600
19	13132	13132	67	76720	76743	117	82268	82268	166	77606	77624
20	16450	16461	68	76756	76757	118	82276	82505	167	77637	77637
20140118			69	76796	76802	20140124			168	77649	77651
21	80153	80154	70	76815	76825	119	75553	75553	169	77657	77659
22	80163	80163	71	76848	76855	120	75592	75592	170	77671	77677
23	80170	80170	72	76936	76951	121	75603	75603	171	77685	77694
24	80560	80565	73	76962	76977	122	75610	75616	172	77700	77717
25	80577	80601	74	77088	77088	123	75629	75636	173	77724	77724
26	80607	80607	75	77096	77617	124	75644	75745	174	77736	77736
27	80616	80626	76	77624	77625	125	75752	75752	175	77745	77804
28	80833	80833	77	77634	77634	126	75761	75764	176	77810	77811
29	80840	80841	78	77888	77893	127	75770	75781	177	77817	77888
30	83291	83291	79	77928	77928	128	75788	75865	178	77896	77896
31	83300	83412	80	77939	77957	129	75872	75872	179	77909	77909
32	83560	83580	81	77965	77978	130	75883	75888	180	77918	77918
33	83589	83636	82	77987	78002	131	75908	75908	181	77932	77935
34	84724	84724	83	78008	78528	132	75940	75940	182	77941	77947
35	84819	84846	84	78536	78540	133	75950	75950	183	77955	77955
36	84862	84872	85	78547	78555	134	75960	75969	184	77973	77973
37	84886	84900	86	78561	78561	135	75975	75996	185	77982	77982
38	85007	85009	87	78572	78575	136	76008	76049	186	78279	78279
39	85015	85019	88	78583	78583	137	76066	76079	187	79244	79244
40	85026	85031	89	78667	78678	138	76088	76094	188	79263	79263
20140123			90	78684	78685	139	76101	76111	189	79270	79298
41	74054	74062	91	78695	78707	140	76129	76140	190	79305	79305
42	75749	75749	92	78714	78714	141	76152	76162	191	79320	79320
43	75762	75768	93	78850	78899	142	76169	76177	20140127		
44	75774	75784	94	78910	78916	143	76602	76602	192	76339	76401
45	75792	75817	95	78952	78952	144	76627	76627	193	76432	76432
46	75824	75836	96	78988	78994	145	76675	76685	194	76830	76830
47	75846	75851	97	79024	79034	146	76949	76974	195	77276	77276

Event	Time (sec)		Event	Time (sec)		Event	Time (sec)		Event	Time (sec)	
#	Start	End	#	Start	End	#	Start	End	#	Start	End
20140127 (cont)			20140128 (cont)			20140202 (cont)			20140203 (cont)		
196	77282	77290	246	79138	79173	295	76551	76562	345	18143	18146
197	77567	77569	247	79179	79266	296	76571	76585	346	18155	18167
198	77588	77590	248	80311	80372	297	76795	76796	347	18207	18274
199	77596	77725	249	80755	80756	298	77225	77225	348	18568	18568
200	77755	77968	250	80805	80805	299	77231	77231	349	18718	18718
201	77979	77979	251	80828	80847	300	77273	77273	350	18770	18933
202	78023	78040	252	80867	80924	301	77286	77462	351	18940	18940
203	78268	78358	253	80942	80951	302	77478	77479	352	18988	18996
204	78378	78380	254	80959	80959	303	77505	77958	353	19578	19781
205	78390	78405	255	80971	80973	304	77967	77968	354	19791	19791
206	78412	78607	256	81609	81621	305	77974	77975	355	20072	20081
207	78614	78617	257	81627	81628	306	77981	77987	356	20089	20125
208	79020	79043	258	81635	81635	307	77996	78014	357	20140	20182
209	79460	79591	259	81645	81645	308	78077	78079	358	20192	20436
210	79602	79606	20140129			309	78289	78294	359	20448	20451
211	79613	79688	260	76448	76448	310	78340	78522	360	20865	20865
212	79694	79944	261	76468	76468	311	78541	78545	361	20888	21176
213	80094	80108	262	76816	76816	312	78551	78595	362	21182	21191
214	80170	80175	263	76985	76993	313	78601	78601	20140204		
215	80187	80192	264	77067	77067	314	78608	78891	363	77904	77941
216	80198	80201	265	77126	77127	315	78915	78942	364	77952	77958
217	80395	80429	266	77166	77586	316	78997	79008	365	78028	78029
218	80438	80439	267	77597	77604	317	79019	79028	366	78036	78045
219	80446	80446	268	77721	77733	318	79085	79107	367	78059	78062
220	80461	80461	269	77744	77750	319	79139	79142	368	78083	78100
221	80470	80479	270	77756	77776	320	79618	79799	369	78128	78129
222	80485	80489	271	77782	77843	321	79809	79813	370	78136	78218
223	80499	80540	272	77849	78281	322	79828	79828	371	78226	78226
224	80812	80837	273	78551	78940	323	79852	79854	372	78391	78410
225	81609	81610	274	78992	79021	324	79860	79860	373	79552	79569
226	81621	81621	275	79028	79065	325	79869	79944	374	79579	79582
227	81635	81670	276	79644	79659	326	79966	79970	375	79590	79596
228	81900	81900	277	79665	79672	327	79978	79980	376	79618	79632
229	81942	81962	278	79678	79692	328	79994	79995	377	79878	79879
230	81971	81972	279	79705	79705	329	80005	80124	378	79890	79994
231	82100	82100	280	79737	79737	330	80138	80171	379	80004	80004
232	82106	82267	281	79753	80158	331	81221	81328	380	80067	80080
233	82303	82315	282	80175	80181	332	81334	81336	381	80087	80087
234	82325	82325	283	80688	80693	333	81353	81357	382	80095	80095
235	82712	82735	284	80699	80715	334	81713	81901	383	80107	80108
236	82747	82748	285	80722	80772	335	81917	81917	384	80120	80120
237	82780	82850	286	80778	81103	336	83198	83198	385	80154	80161
238	82877	82882	287	81242	81252	337	83208	83345	386	80201	80205
239	83216	83417	288	81500	81500	20140203			387	80212	80276
240	83426	83426	289	81631	81636	338	17482	17484	388	80288	80360
20140128			290	81645	81884	339	17509	17523	389	80622	80632
241	78891	78891	291	81904	82066	340	17529	17555	390	80651	80666
242	78899	78899	292	82257	82394	341	17576	17597	391	80684	80684
243	78907	78910	293	82421	82665	342	17618	17633	392	80785	80786
244	78940	78940	20140202			343	17640	17640	393	81365	81365
245	78962	78962	294	76540	76540	344	17697	17697	394	81692	81693

Event	Time (sec)		Event	Time (sec)		Event	Time (sec)		Event	Time (sec)	
#	Start	End	#	Start	End	#	Start	End	#	Start	End
20140204 (cont)			20140205 (cont)			20140207 (cont)			20140208 (cont)		
395	81717	81718	445	90891	90910	495	84096	84100	545	82266	82271
396	81737	81741	446	90947	90961	496	84111	84181	546	82297	82298
397	81749	81749	447	90968	91174	497	84188	84218	547	82313	82313
398	81762	81768	448	91384	91385	498	84272	84341	548	82393	82439
399	81780	81802	449	91397	91493	499	84351	84359	549	82488	82493
400	82477	82496	450	92143	92368	500	84366	84383	550	82507	82549
401	82502	82503	451	92582	92621	501	84389	84392	551	82563	82563
402	82517	82529	452	92628	92630	502	84724	84725	20140209		
403	83125	83154	453	92645	92683	503	84732	84735	552	81207	81207
404	83163	83163	454	92702	92737	504	84761	84790	553	81248	81312
405	83169	83338	455	92747	92747	505	84801	84801	554	81318	81322
406	83885	83890	456	92895	92904	506	84814	85200	555	81344	81448
407	83907	83969	457	92910	92966	507	85211	85213	556	81456	81462
408	83992	83993	458	92988	92993	508	85290	85291	557	81493	81499
409	84005	84012	459	93041	93044	509	85297	85297	558	81547	81565
410	84020	84020	460	93101	93104	510	85332	85332	559	81602	81603
411	84026	84053	461	93425	93443	511	85493	85591	560	81609	81619
20140205			20140207			512	85597	85597	561	81625	81628
412	87621	87762	462	79389	79395	20140208			562	81943	81943
413	87845	87855	463	79406	79445	513	12570	12574	563	81991	81999
414	87865	87865	464	80102	80105	514	12586	12586	564	82027	82027
415	87970	87973	465	80123	80129	515	78988	78995	565	82035	82057
416	87999	88077	466	80135	80135	516	79011	79020	566	82092	82121
417	88093	88097	467	80267	80305	517	79027	79148	567	82141	82166
418	88111	88131	468	80313	80349	518	79155	79258	568	82173	82204
419	88210	88548	469	80356	80356	519	79266	79272	569	82254	82256
420	88554	88569	470	80489	81070	520	79400	79400	570	82739	82747
421	88576	88576	471	81077	81081	521	79870	80036	571	83326	83327
422	88594	88595	472	81089	81089	522	80047	80051	572	83367	83591
423	88606	88606	473	81102	81102	523	80058	80063	573	83597	83598
424	88612	88632	474	81152	81152	524	80071	80088	574	83606	83608
425	88641	88667	475	81169	81169	525	80095	80097	575	85542	85543
426	88676	88677	476	81187	81581	526	80111	80122	576	85556	85556
427	88685	88709	477	81641	81641	527	80144	80149	577	85562	85563
428	88723	88723	478	81667	81669	528	80158	80159	578	85573	85578
429	89308	89308	479	81691	82032	529	80266	80278	579	85602	85604
430	89318	89320	480	82048	82176	530	80287	80288	580	85615	85644
431	89326	89327	481	82183	82197	531	80378	80404	20140210		
432	89377	89407	482	82204	82215	532	80410	80444	581	9739	9740
433	89467	89467	483	82337	82365	533	80874	80874	20140217		
434	89507	89518	484	82371	82901	534	80954	80990	582	80265	80284
435	89524	89533	485	82927	82932	535	81031	81191	583	80292	80299
436	89545	89554	486	82946	82956	536	81197	81219	584	80306	80581
437	89560	89563	487	82962	82968	537	81234	81247	585	80595	80607
438	89569	89586	488	83114	83119	538	81255	81255	586	80615	80618
439	89592	89871	489	83125	83695	539	81287	81310	587	81673	81673
440	90222	90238	490	83702	83710	540	81333	81333	588	81781	81781
441	90255	90258	491	83716	83722	541	81818	81818	589	81820	81820
442	90393	90467	492	83914	83962	542	81826	81851	590	81856	81856
443	90473	90473	493	83970	84056	543	81857	81860	591	81868	81886
444	90488	90493	494	84062	84089	544	82238	82244	592	81895	81908

Event #	Time (sec)		Event #	Time (sec)		Event #	Time (sec)		Event #	Time (sec)	
	Start	End		Start	End		Start	End		Start	End
20140217 (cont)			20140218								
593	81919	81919	638	82132	82164						
594	82078	82078	639	82176	82181						
595	82124	82124	640	82777	82784						
596	82134	82134	641	82845	82848						
597	82155	82166	642	82855	82855						
598	82179	82181	643	83173	83177						
599	82187	82201	644	83588	83591						
600	82207	82243	645	83602	83632						
601	82257	82258	646	83644	83644						
602	82305	82503	647	85131	85131						
603	82722	82722									
604	82731	82760									
605	82767	82774									
606	82783	82786									
607	82795	82948									
608	82958	82958									
609	82982	82982									
610	82989	82989									
611	83017	83119									
612	83235	83272									
613	83303	83303									
614	86126	86126									
615	86135	86135									
616	86161	86182									
617	86189	86266									
618	86319	86378									
619	86492	86498									
620	86522	86689									
621	86706	86955									
622	86961	87054									
623	87063	87064									
624	87072	87076									
625	87088	87089									
626	87119	87120									
627	87133	87133									
628	87159	87159									
629	87199	87199									
630	87246	87246									
631	87438	87439									
632	87547	87547									
633	87588	88025									
634	88120	88124									
635	88321	88328									
636	88334	88371									
637	88398	88437									

Table of IWC events for 2015 HAIC Flight Campaign in Cayenne, French Guiana. There were 605 events encountered over 14 flight days. The table is organized by date and by time.

Event #	Time (sec)		Event #	Time (sec)		Event #	Time (sec)		Event #	Time (sec)	
	Start	End		Start	End		Start	End		Start	End
20150510			20150512 (cont)			20150516 (cont)			20150516 (cont)		
1	71739	71741	50	78943	78943	97	35831	35831	147	60746	60759
2	71761	71761	51	78961	78967	98	35837	35840	148	60775	60788
3	71771	71806	52	78975	78982	99	35909	35912	149	60796	60800
4	71826	71826	53	79059	79059	100	35940	35940	150	60808	60808
5	72307	72311	54	79066	79121	101	35946	35946	151	60927	61028
6	72327	72327	55	79135	79154	102	36280	36280	152	61235	61240
7	72335	72335	56	79160	79160	103	36286	36286	153	61250	61294
8	72423	72437	20150514			104	36321	36325	154	61303	61303
9	72905	72906	57	57478	57482	105	36401	36401	155	61342	61368
10	72913	72913	58	57488	57493	106	36409	36411	156	62345	62399
11	72933	72933	59	57516	57516	107	36607	36607	157	62405	62405
12	72975	72975	60	60463	60475	108	36613	36616	158	62417	62432
13	73699	73746	20150515			109	38194	38202	159	62438	62465
14	73759	73779	61	35645	35645	110	38211	38260	160	62885	62885
15	73788	73788	62	35703	35936	111	38267	38301	161	62944	62944
16	73821	73822	63	35945	36109	112	38349	38349	162	63301	63481
17	73828	73841	64	36125	36132	113	39265	39301	20150518		
18	74374	74388	65	36146	36151	114	39608	39623	163	72904	72906
19	74408	74408	66	36161	36162	115	39635	39813	164	73095	73095
20	74414	74414	67	36228	36393	116	39833	39837	165	74257	74326
21	74423	74423	68	36800	36800	117	39894	39901	166	74346	74348
22	74440	74441	69	36809	36822	118	39913	39915	167	74382	74382
23	74453	74463	70	36828	36835	119	39922	39924	168	74388	74395
24	74551	74557	71	36857	36941	120	39949	39956	169	74457	74457
25	74575	74583	72	36951	37059	121	39968	39990	170	74463	74471
26	74870	74893	73	37066	37066	122	40009	40020	171	74735	74735
27	74901	74908	74	37075	37115	123	40027	40129	172	74780	74780
28	74916	74916	75	37495	37511	124	40137	40142	173	74814	74879
29	74961	74965	76	37545	37545	125	40149	40198	174	76434	76444
30	74971	75022	77	37554	37560	126	40220	40226	175	76610	76614
31	75372	75428	78	37571	37571	127	40373	40373	176	76622	76622
20150512			79	37606	37606	128	40383	40391	177	76634	76634
32	74133	74133	80	37630	37643	129	40863	40863	178	76698	76698
33	74143	74143	81	37650	37650	130	40870	40881	179	77562	77578
34	74211	74215	82	38478	38478	131	40926	40938	20150519		
35	74224	74227	83	38484	38484	132	40986	40991	180	53632	53632
36	74234	74236	84	38490	38524	133	40997	40998	181	54374	54377
37	74488	74537	85	38564	38742	134	41022	41287	182	56461	56476
38	74566	74571	86	38748	38772	135	41293	41342	183	56483	56483
39	74577	74578	87	38801	38806	136	59649	59745	184	56489	56489
40	74595	74620	88	38815	38829	137	59805	59805	185	56789	56789
41	75490	75490	89	39752	39752	138	59816	59825	186	57076	57151
42	75511	75511	90	39765	39771	139	60184	60199	187	57157	57157
43	75522	75539	91	39777	39777	140	60209	60210	188	57326	57330
44	75572	75573	92	39783	39897	141	60219	60234	189	57610	57688
45	75585	75585	20150516			142	60243	60252	190	58492	58495
46	77310	77310	93	35580	35590	143	60269	60269	191	58503	58504
47	78007	78007	94	35596	35596	144	60281	60298	192	58614	58644
48	78887	78887	95	35607	35618	145	60312	60331	193	58654	58654
49	78911	78936	96	35646	35646	146	60358	60358	194	58953	58953

Event #	Time (sec)		Event #	Time (sec)		Event #	Time (sec)		Event #	Time (sec)	
	Start	End		Start	End		Start	End		Start	End
20150519 (cont)			20150523 (cont)			20150524 (cont)			20150525 (cont)		
195	59013	59019	245	42906	42922	295	35454	35488	345	71550	71550
196	61081	61081	246	43354	43372	296	35494	35497	346	71557	71582
197	61089	61089	247	43383	43386	297	35503	35505	347	71590	71590
198	61095	61095	248	43546	43548	298	35513	35513	348	71599	71600
199	61146	61146	249	43573	43574	299	35936	35936	349	71796	71796
200	61163	61163	250	43584	43586	300	35950	36260	350	71833	71833
201	61591	61603	251	43593	43598	301	36381	36388	351	71847	71847
20150523			252	43609	43609	302	36395	36396	352	71854	71876
202	34744	34860	253	43620	43692	303	36700	36700	353	71887	71903
203	34891	34891	254	43730	43742	304	36765	36778	354	71915	71915
204	35890	35916	255	43755	43766	305	36796	37023	355	72061	72061
205	36997	37005	256	43783	43791	306	37712	37861	356	72071	72090
206	37016	37020	257	43808	43936	307	37880	37897	357	72304	72304
207	37047	37255	258	43976	44027	308	37907	37912	358	72315	72414
208	37264	37264	259	44080	44136	309	38443	38458	359	72422	72427
209	37270	37280	260	62639	62639	310	38473	38482	360	72466	72471
210	37286	37291	261	62654	62687	311	38498	38528	361	72968	72968
211	37299	37299	262	62696	62752	312	38547	38554	362	73610	73614
212	37421	37421	263	62758	62773	313	38562	38611	363	73623	73623
213	38122	38300	264	63057	63057	314	38997	39064	364	74042	74046
214	38312	38316	265	63095	63143	315	39072	39073	365	74148	74148
215	38439	38444	266	63155	63166	316	39079	39099	366	74164	74176
216	38484	38490	267	63172	63173	317	40195	40195	367	74182	74185
217	38502	38518	268	63179	63180	318	40202	40207	368	74194	74226
218	38524	38570	269	63192	63195	319	40213	40213	369	74785	74944
219	38580	38580	270	63222	63226	320	40219	40243	370	74951	74952
220	39261	39266	271	65549	65549	321	40249	40295	371	74959	74959
221	39272	39303	272	65594	65612	322	40324	40324	372	74965	74968
222	39314	39459	273	66345	66401	323	40361	40361	373	74977	74977
223	39492	39492	274	66412	66434	324	40549	40781	374	74984	74984
224	39502	39508	275	66498	66498	325	40789	40789	375	74990	75043
225	39540	39541	276	66729	66730	326	40808	40811	376	75243	75260
226	39547	39548	277	66736	66792	327	40926	40928	377	75269	75324
227	39565	39733	20150524			328	40935	40943	378	75331	75379
228	39740	39740	278	33944	33944	20150525			379	75387	75421
229	40089	40089	279	34302	34311	329	70359	70359	380	75427	75429
230	40095	40294	280	34383	34449	330	70431	70438	381	75435	75435
231	40364	40393	281	34496	34518	331	70904	70917	382	75623	75623
232	40403	40403	282	34552	34678	332	70955	70966	383	75639	75639
233	40409	40409	283	34684	34702	333	70973	70977	384	75692	75696
234	40417	40417	284	34716	34724	334	70984	71007	385	75704	75713
235	40428	40497	285	34763	34763	335	71119	71151	386	75719	75754
236	40503	40524	286	35020	35020	336	71172	71179	387	75802	75802
237	40532	40532	287	35034	35039	337	71376	71376	388	75821	75821
238	40541	40541	288	35070	35091	338	71404	71407	389	75827	75855
239	40784	40964	289	35099	35099	339	71429	71431	390	76183	76188
240	40972	40976	290	35106	35153	340	71446	71446	391	76278	76283
241	41396	41397	291	35162	35162	341	71460	71463	392	76340	76419
242	41423	41464	292	35277	35279	342	71483	71492	393	76425	76425
243	42819	42881	293	35286	35288	343	71510	71513	394	76431	76439
244	42890	42898	294	35298	35446	344	71519	71531	395	76445	76445

Event #	Time (sec)		Event #	Time (sec)		Event #	Time (sec)		Event #	Time (sec)	
	Start	End		Start	End		Start	End		Start	End
20150525 (cont)			20150526 (cont)			20150527 (cont)			20140208 (cont)		
396	76451	76451	446	35772	35788	496	33836	33837	546	75673	75734
397	76913	76916	447	35796	35796	497	34062	34064	547	75755	75759
398	76930	77054	448	35810	35810	498	34070	34071	548	75770	75794
399	77066	77073	449	35819	35823	499	34077	34086	549	75922	75934
400	77091	77091	450	35846	35846	500	34095	34166	550	75942	75982
401	77099	77099	451	35997	35997	501	34197	34217	551	75989	76026
402	77107	77113	452	36050	36266	502	34331	34331	552	76041	76137
403	77350	77460	453	36276	36276	503	34898	34908	553	76145	76149
404	77649	77660	454	36293	36293	504	34918	34935	554	76158	76159
405	77709	77916	455	36517	36517	505	35198	35198	555	76192	76192
406	77924	77924	456	36590	36663	506	35422	35550	556	77765	77765
407	77944	77944	457	37962	37966	507	35557	35680	557	77773	77773
408	77950	77950	458	38121	38121	508	36154	36245	558	77797	77811
409	77961	77961	459	38127	38139	509	36252	36252	559	78048	78048
410	78298	78312	460	38338	38340	510	36260	36316	560	78088	78088
411	78318	78321	461	38346	38352	511	36327	36335	561	78110	78113
412	78331	78406	462	38358	38366	512	36814	36814	562	78866	78925
413	78667	78787	463	38374	38374	513	36824	36998	563	78931	78935
414	78943	78943	464	38493	38498	514	37010	37010	564	79470	79470
415	79055	79064	465	38515	38523	515	37016	37063	565	79490	79493
416	79072	79100	466	38532	38533	516	37083	37091	566	79610	79610
417	79109	79109	467	39211	39211	517	37103	37131	567	79774	79774
418	79118	79122	468	39232	39241	518	37137	37149	568	79868	79868
419	79312	79313	469	40024	40024	519	37157	37171	569	79874	79912
420	79328	79340	470	40371	40371	520	37190	37215	570	80397	80397
421	79346	79350	471	40430	40430	521	37226	37248	571	80427	80427
422	79357	79477	472	40890	40890	522	37338	37338	572	80438	80443
423	79485	79497	473	40899	41139	523	37346	37351	573	80459	80460
424	79688	79688	474	41145	41160	524	37808	37851	574	80468	80468
425	79699	79836	475	41709	41709	525	37858	37862	575	80484	80484
426	79844	79849	476	41723	41727	526	37868	37899	20150529		
20150526			477	41738	41743	527	37917	37935	576	35589	35589
427	34661	34813	478	53145	53151	528	38027	38246	577	35648	35649
428	34824	34824	479	53162	53187	20150528			578	35660	35660
429	34853	34855	480	53278	53288	529	73619	73619	579	35667	35667
430	34878	34878	481	53474	53475	530	73627	73627	580	35678	35692
431	34887	34887	482	53490	53499	531	73634	73634	581	35700	35734
432	34895	34899	483	53514	53514	532	73642	73643	582	35742	35755
433	34908	34908	484	54767	54771	533	73650	73681	583	35761	35840
434	34915	34932	485	54779	54779	534	73688	73688	584	35846	35851
435	34954	34954	486	54788	54790	535	73694	73762	585	35865	36045
436	34965	34987	487	54797	54811	536	73783	73783	586	36052	36062
437	35021	35023	488	54825	54850	537	73982	74168	587	36070	36487
438	35029	35034	20150527			538	74174	74188	588	36566	36573
439	35040	35046	489	33163	33183	539	74194	74197	589	36597	36628
440	35070	35075	490	33224	33275	540	74208	74208	590	36785	36788
441	35082	35089	491	33403	33404	541	74549	74551	591	36835	36835
442	35164	35164	492	33416	33416	542	74557	74779	592	37331	37331
443	35182	35182	493	33446	33669	543	74788	74793	593	37350	37521
444	35569	35570	494	33678	33682	544	74807	74807	594	37728	37730
445	35576	35585	495	33828	33828	545	75204	75204	595	37780	37799

Event	Time (sec)		Event	Time (sec)		Event	Time (sec)		Event	Time (sec)	
#	Start	End	#	Start	End	#	Start	End	#	Start	End
20150529 (cont)											
596	37860	37860									
597	38942	38942									
598	38982	38982									
599	39054	39054									
600	40500	40510									
601	40791	40874									
602	40882	40892									
603	40908	40921									
604	41011	41180									
605	41190	41203									

Appendix C: The follow series of histograms and line plots are from flights near Darwin, Australia in 2014. The first chart (below) is a summary for all flights; subsequent pages are the results for each daily flight. Unless indicated otherwise, line plots have a maximum value of 5g/m^3 for the IWC axis.

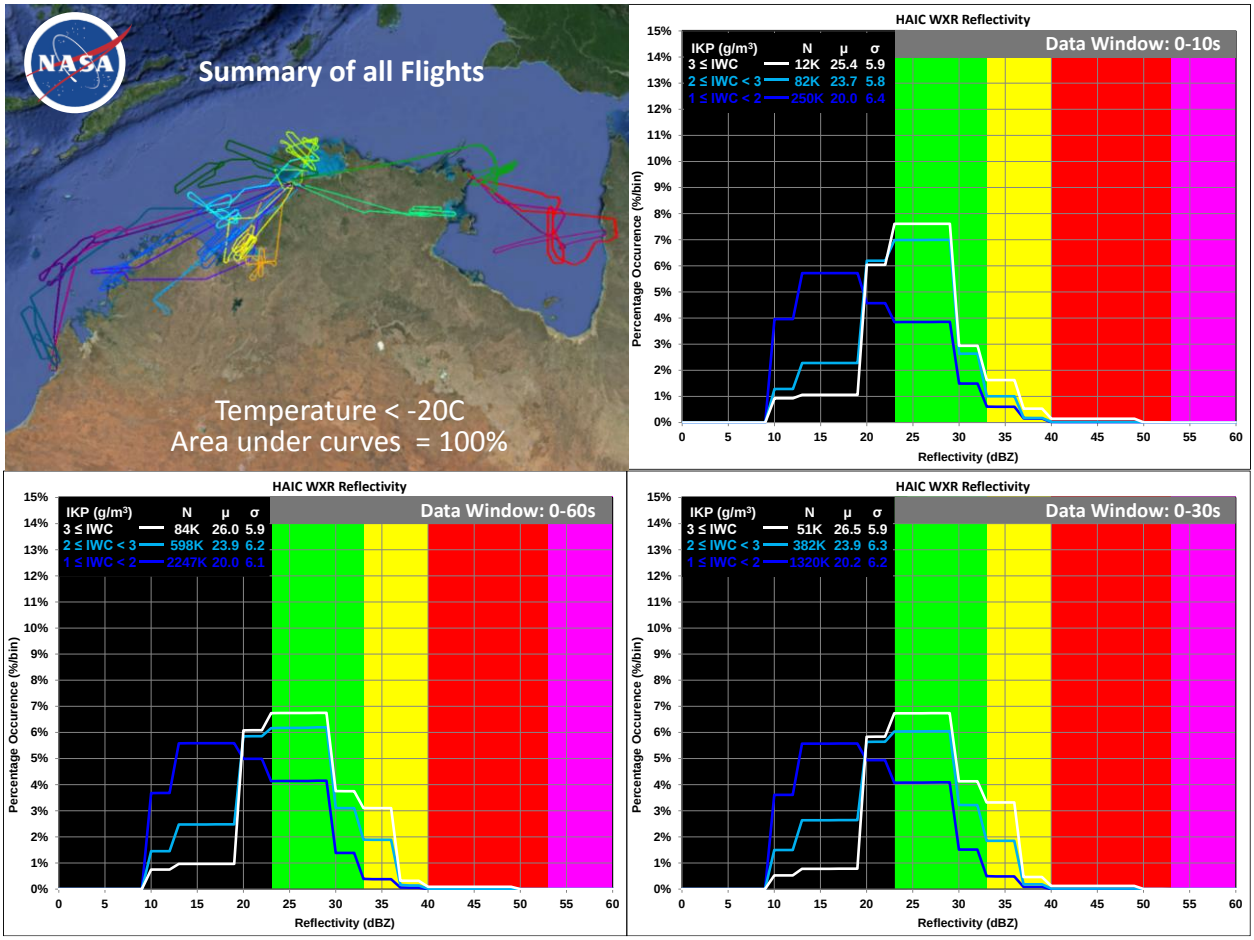

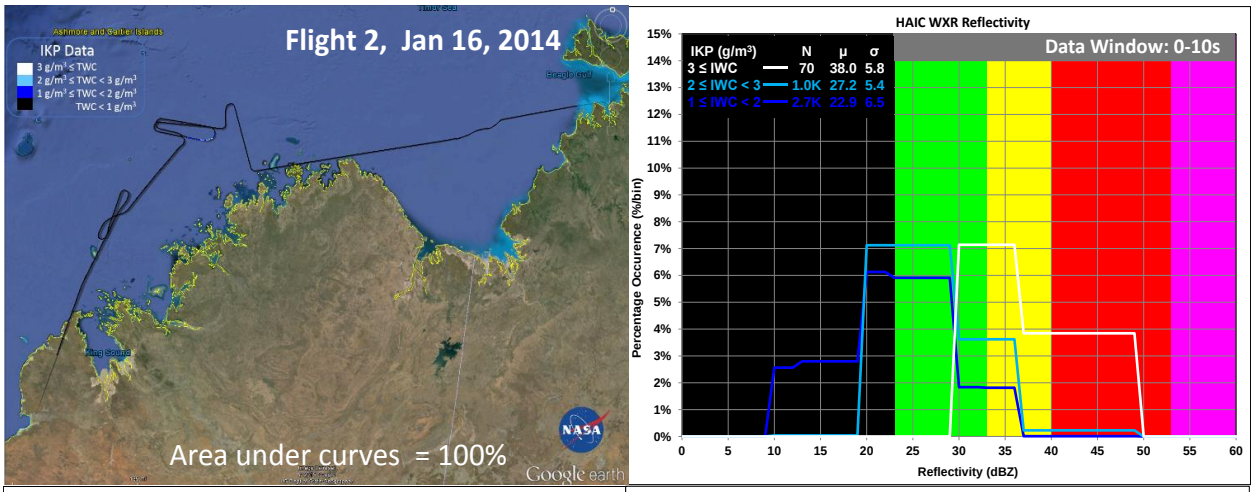
Flight 2, Jan 16, 2014
IKP Data
3 g/m³ ≤ TWC
2 g/m³ ≤ TWC < 3 g/m³
1 g/m³ ≤ TWC < 2 g/m³
TWC < 1 g/m³
Area under curves = 100%
Google earth
HAIC WXR Reflectivity
IKP (g/m³) N μ σ
3 ≤ IWC 70 38.0 5.8
2 ≤ IWC < 3 1.0K 27.2 5.4
1 ≤ IWC < 2 2.7K 22.9 6.5
Data Window: 0-10s
Percentage Occurence (%/bin)
Reflectivity (dBZ)

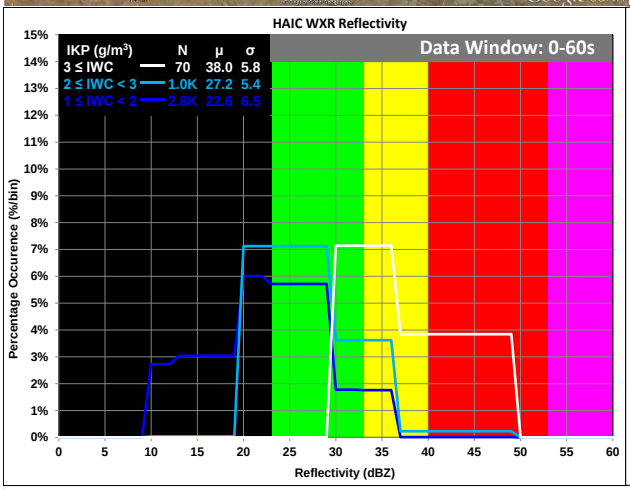
HAIC WXR Reflectivity
IKP (g/m³) N μ σ
3 ≤ IWC 70 38.0 5.8
2 ≤ IWC < 3 1.0K 27.2 5.4
1 ≤ IWC < 2 2.8K 22.6 6.5
Data Window: 0-60s
Percentage Occurence (%/bin)
Reflectivity (dBZ)

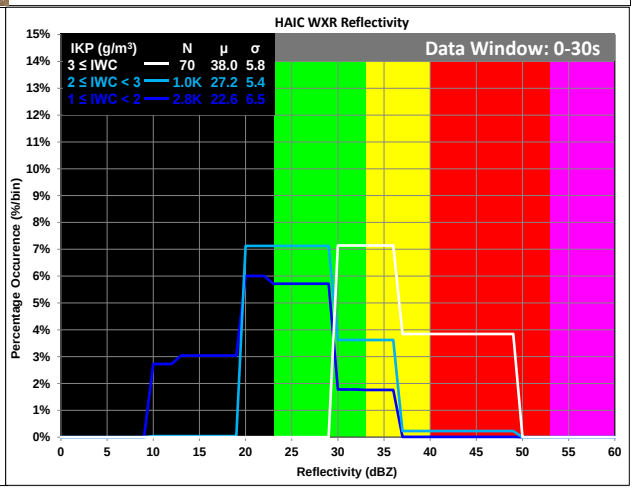
HAIC WXR Reflectivity
IKP (g/m³) N μ σ
3 ≤ IWC 70 38.0 5.8
2 ≤ IWC < 3 1.0K 27.2 5.4
1 ≤ IWC < 2 2.8K 22.6 6.5
Data Window: 0-30s
Percentage Occurence (%/bin)
Reflectivity (dBZ)

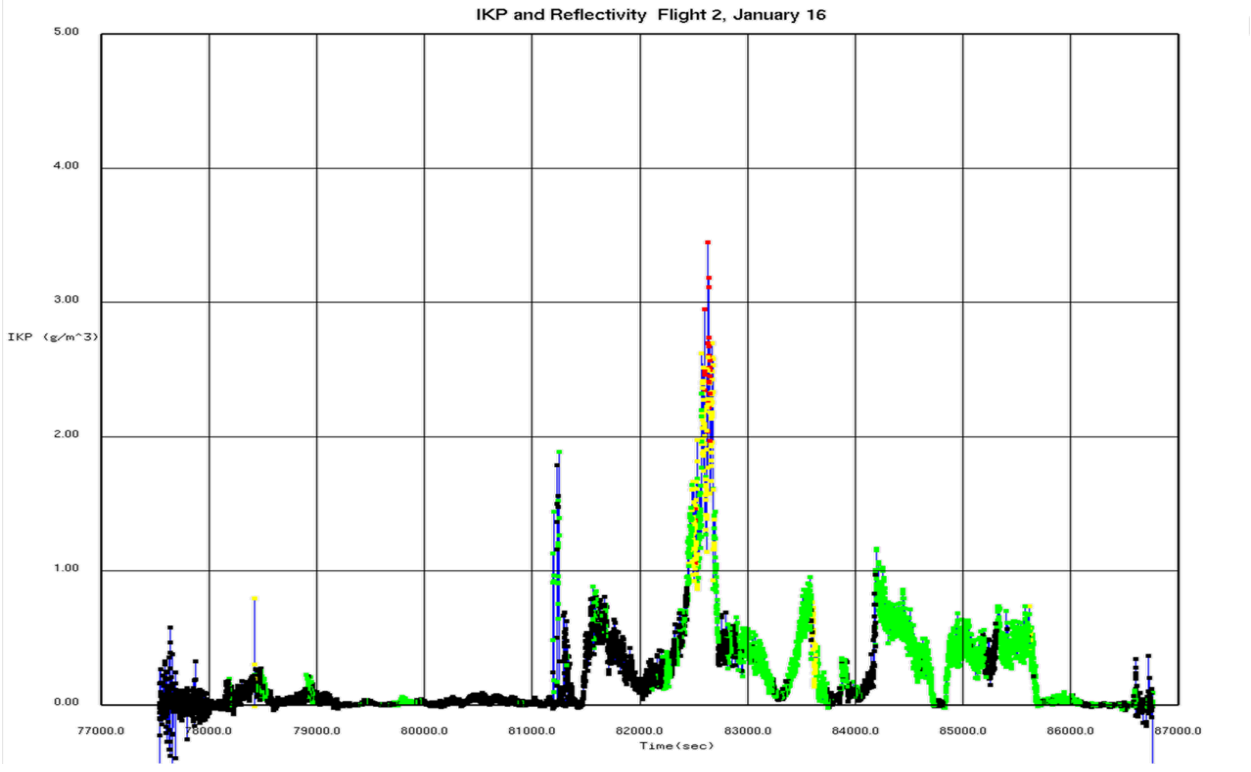
IKP and Reflectivity Flight 2, January 16
IKP (g/m^3)
Time(sec)

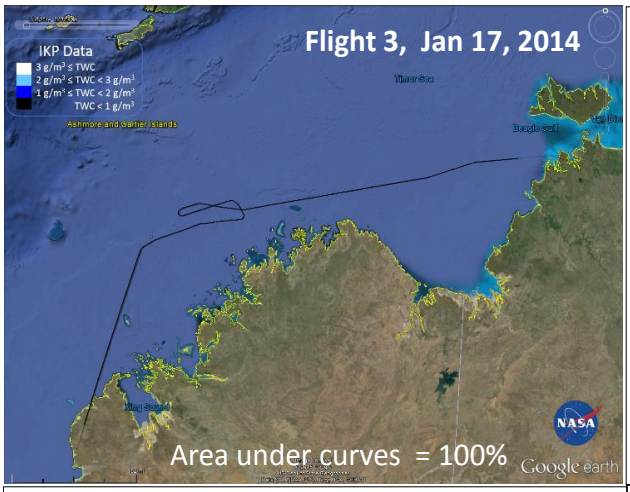
Flight 3, Jan 17, 2014
IKP Data
3 g/m³ ≤ TWC
2 g/m³ ≤ TWC < 3 g/m³
1 g/m³ ≤ TWC < 2 g/m³
TWC < 1 g/m³
Area under curves = 100%
NASA
Google earth

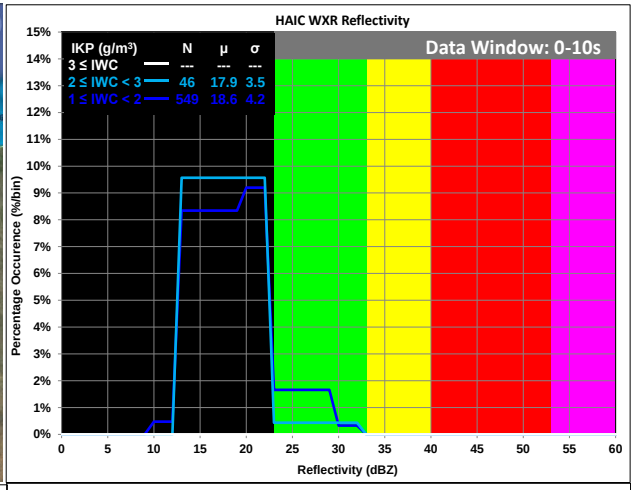
HAIC WXR Reflectivity
Data Window: 0-10s
IKP (g/m³) N μ σ
3 ≤ IWC --- --- ---
2 ≤ IWC < 3 46 17.9 3.5
1 ≤ IWC < 2 549 18.6 4.2
Percentage Occurence (%/bin)
Reflectivity (dBZ)

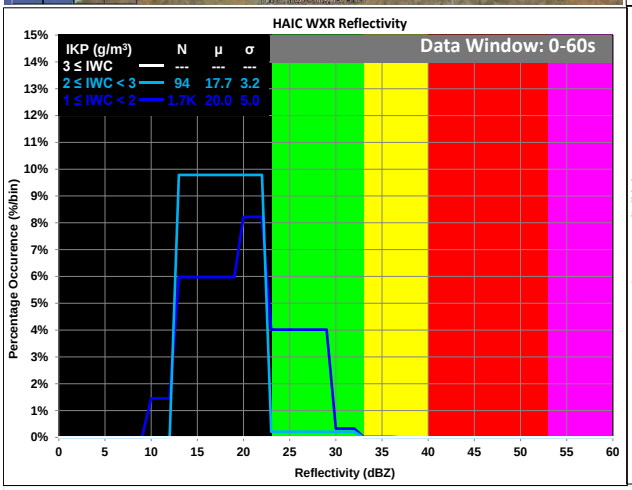
HAIC WXR Reflectivity
Data Window: 0-60s
IKP (g/m³) N μ σ
3 ≤ IWC --- --- ---
2 ≤ IWC < 3 94 17.7 3.2
1 ≤ IWC < 2 1.7K 20.0 5.0
Percentage Occurence (%/bin)
Reflectivity (dBZ)

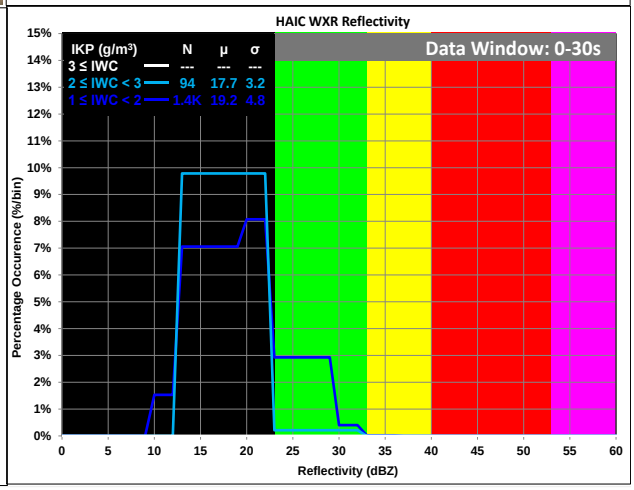
HAIC WXR Reflectivity
Data Window: 0-30s
IKP (g/m³) N μ σ
3 ≤ IWC --- --- ---
2 ≤ IWC < 3 94 17.7 3.2
1 ≤ IWC < 2 1.4K 19.2 4.8
Percentage Occurence (%/bin)
Reflectivity (dBZ)

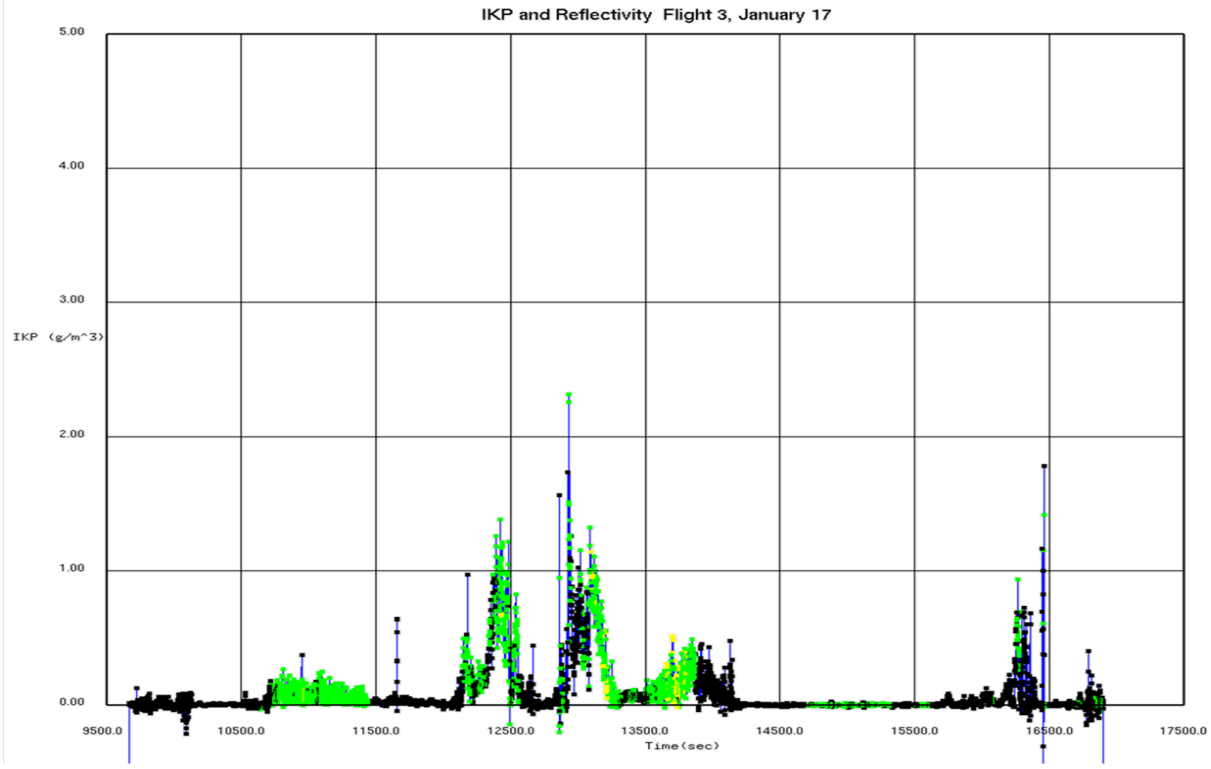
IKP and Reflectivity Flight 3, January 17
IKP (g/m^3)
Time(sec)

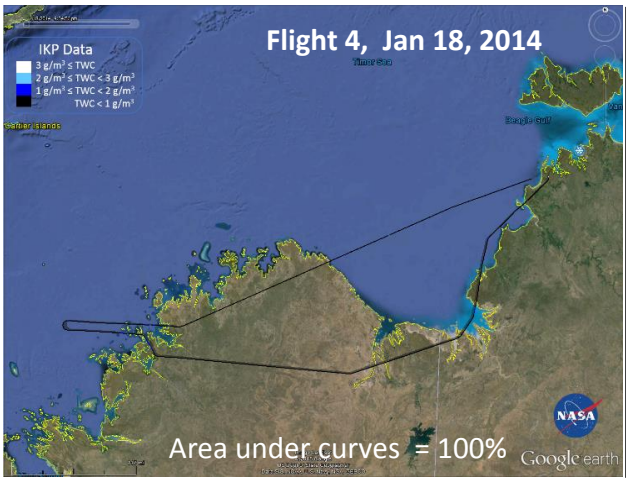
Flight 4, Jan 18, 2014
IKP Data
3 g/m³ ≤ TWC
2 g/m³ ≤ TWC < 3 g/m³
1 g/m³ ≤ TWC < 2 g/m³
TWC < 1 g/m³
Area under curves = 100%
Google earth

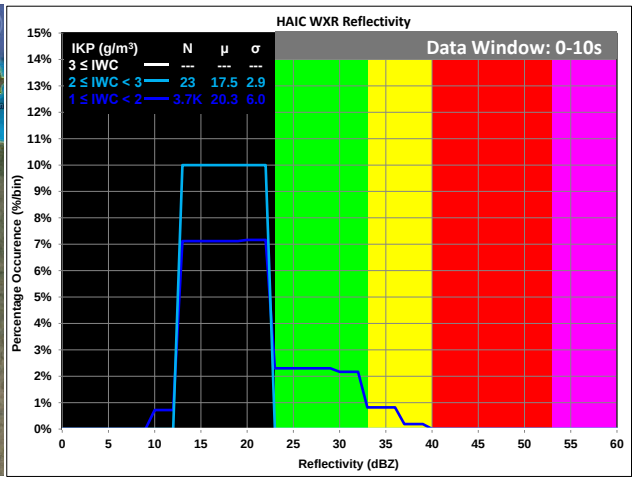
HAIC WXR Reflectivity
Data Window: 0-10s
IKP (g/m³) N μ σ
3 ≤ IWC --- --- ---
2 ≤ IWC < 3 23 17.5 2.9
1 ≤ IWC < 2 3.7K 20.3 6.0
Percentage Occurence (%/bin)
Reflectivity (dBZ)

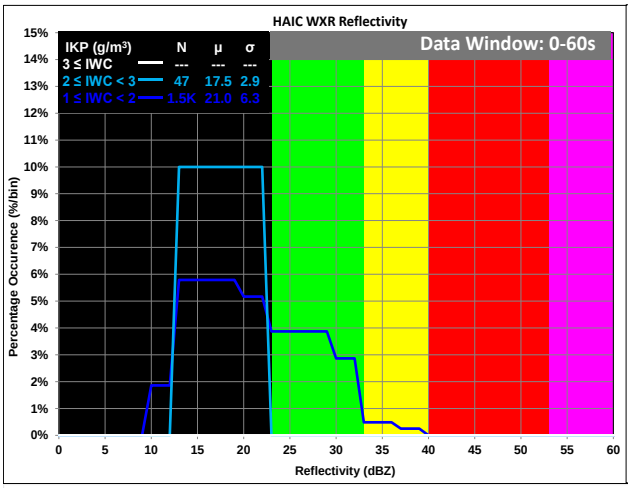
HAIC WXR Reflectivity
Data Window: 0-60s
IKP (g/m³) N μ σ
3 ≤ IWC --- --- ---
2 ≤ IWC < 3 47 17.5 2.9
1 ≤ IWC < 2 1.5K 21.0 6.3
Percentage Occurence (%/bin)
Reflectivity (dBZ)

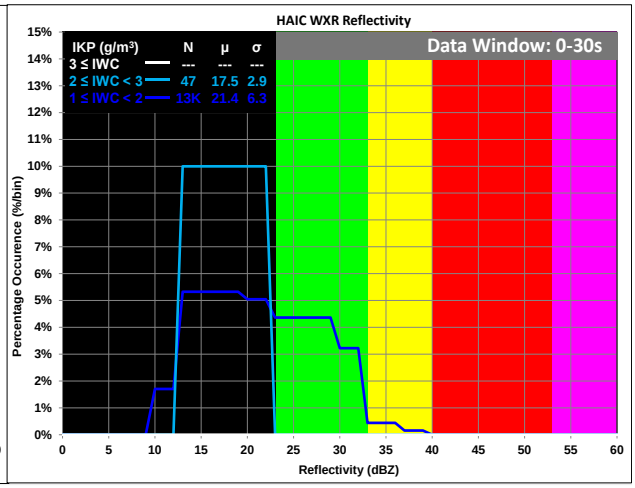
HAIC WXR Reflectivity
Data Window: 0-30s
IKP (g/m³) N μ σ
3 ≤ IWC --- --- ---
2 ≤ IWC < 3 47 17.5 2.9
1 ≤ IWC < 2 13K 21.4 6.3
Percentage Occurence (%/bin)
Reflectivity (dBZ)

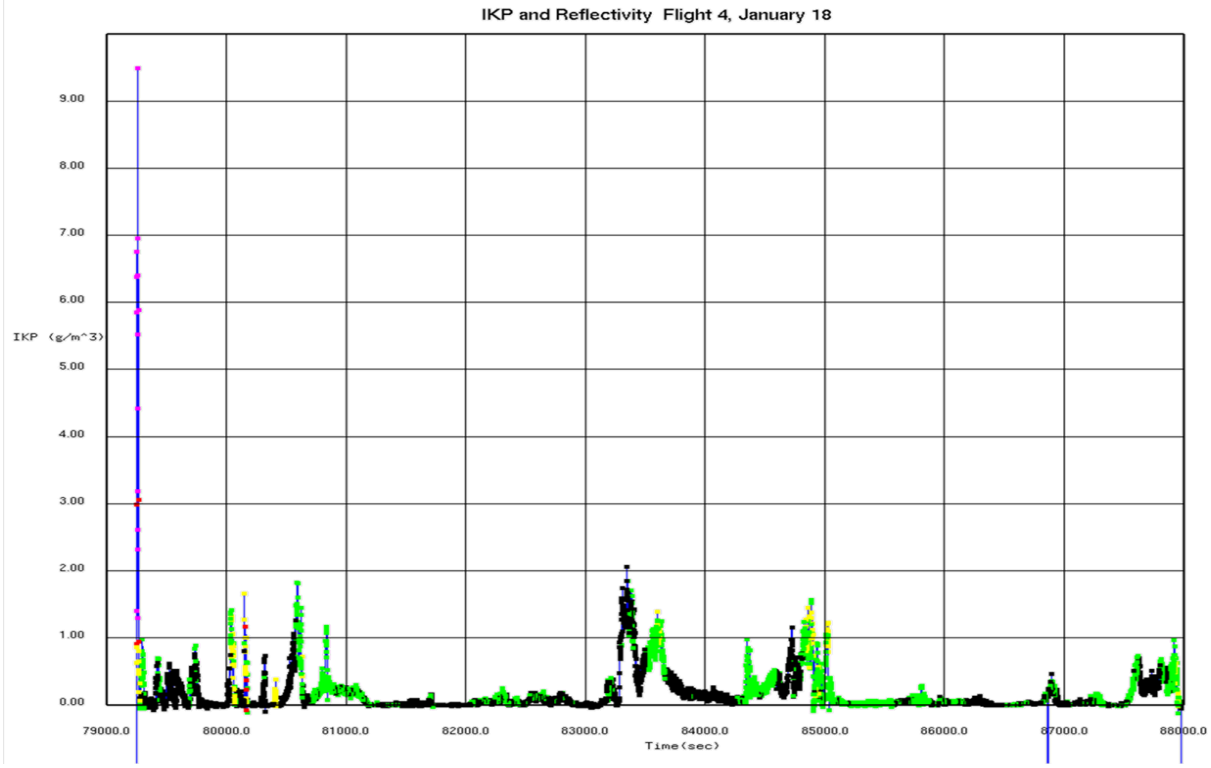
IKP and Reflectivity Flight 4, January 18
IKP (g/m^3)
Time(sec)

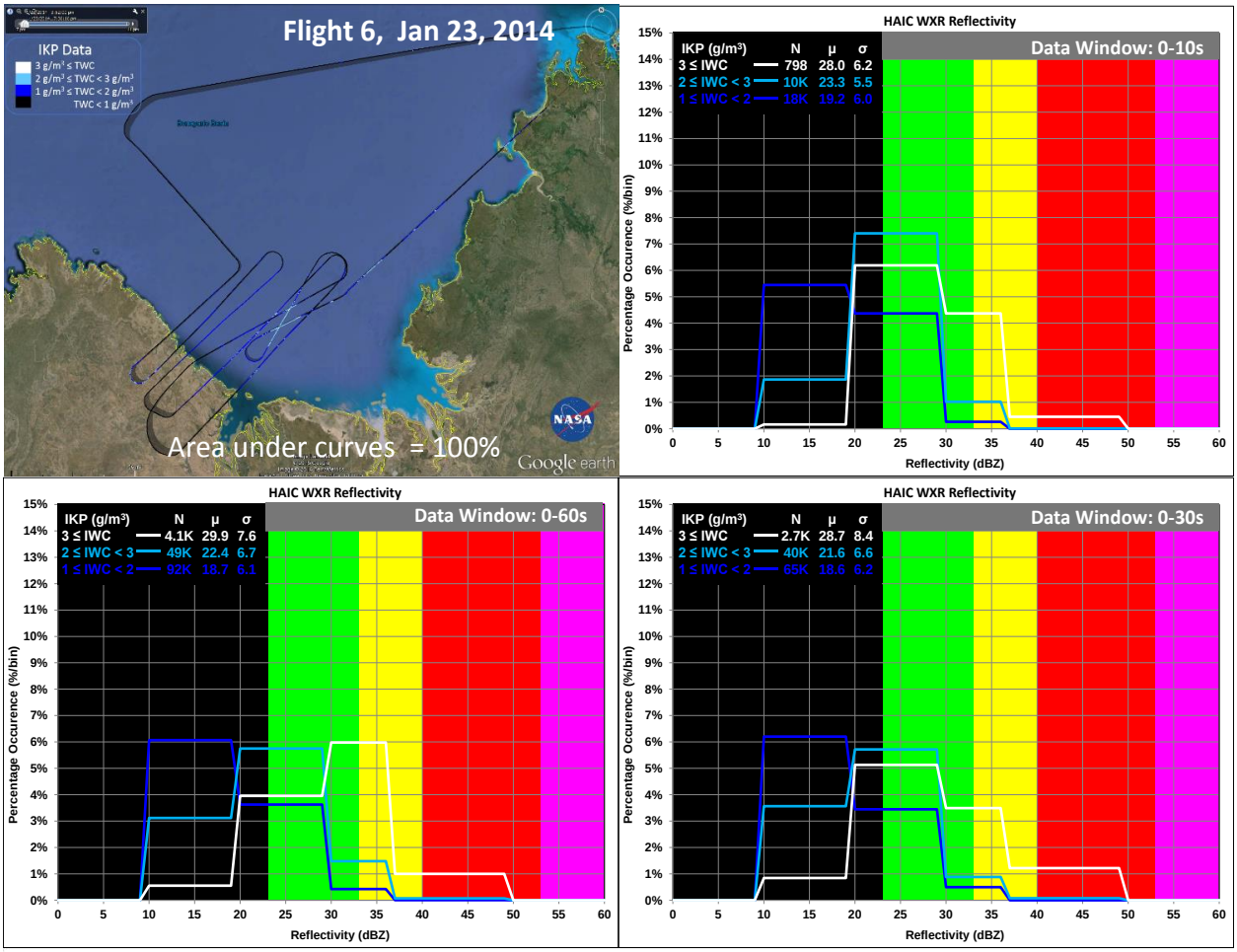
Flight 6, Jan 23, 2014
IKP Data
3 g/m³ ≤ TWC
2 g/m³ ≤ TWC < 3 g/m³
1 g/m³ ≤ TWC < 2 g/m³
TWC < 1 g/m³
Area under curves = 100%
Google earth
HAIC WXR Reflectivity
Data Window: 0-10s
IKP (g/m³) N μ σ
3 ≤ IWC 798 28.0 6.2
2 ≤ IWC < 3 10K 23.3 5.5
1 ≤ IWC < 2 18K 19.2 6.0
Percentage Occurence (%/bin)
Reflectivity (dBZ)
HAIC WXR Reflectivity
Data Window: 0-60s
IKP (g/m³) N μ σ
3 ≤ IWC 4.1K 29.9 7.6
2 ≤ IWC < 3 49K 22.4 6.7
1 ≤ IWC < 2 92K 18.7 6.1
Percentage Occurence (%/bin)
Reflectivity (dBZ)
HAIC WXR Reflectivity
Data Window: 0-30s
IKP (g/m³) N μ σ
3 ≤ IWC 2.7K 28.7 8.4
2 ≤ IWC < 3 40K 21.6 6.6
1 ≤ IWC < 2 65K 18.6 6.2
Percentage Occurence (%/bin)
Reflectivity (dBZ)

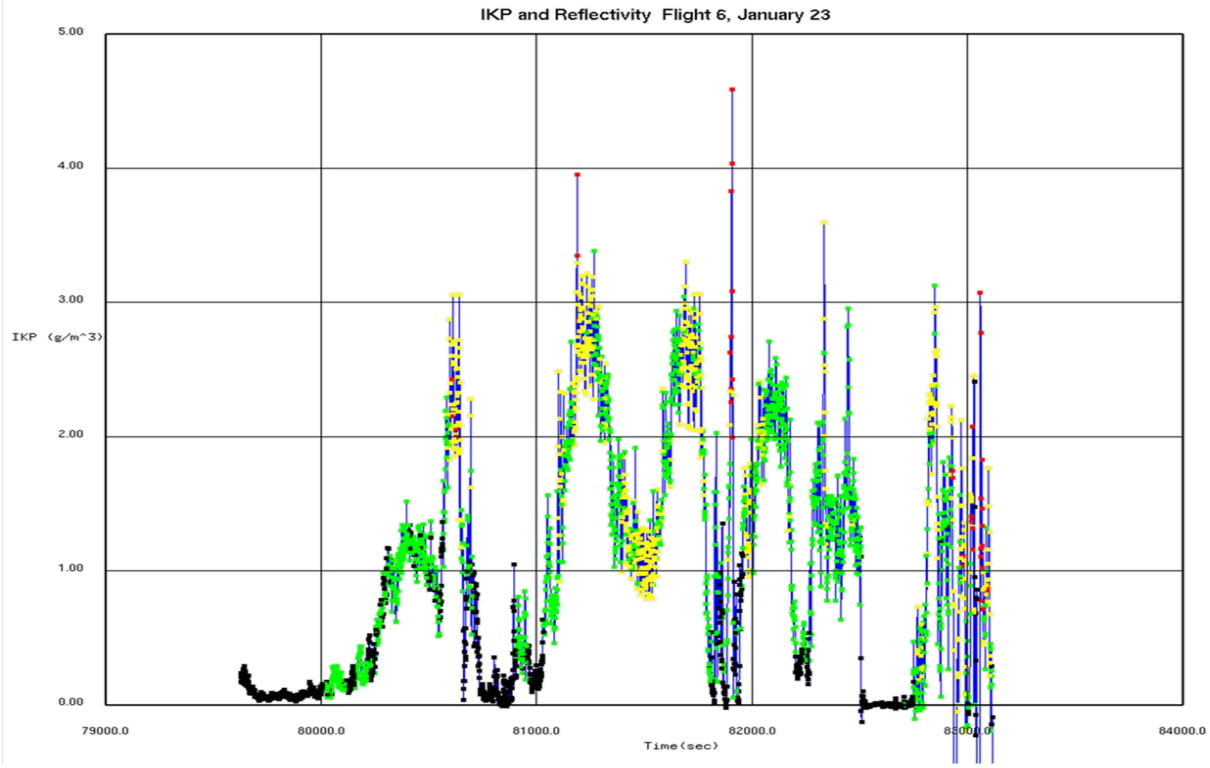
IKP and Reflectivity Flight 6, January 23
IKP (g/m^3)
Time(sec)

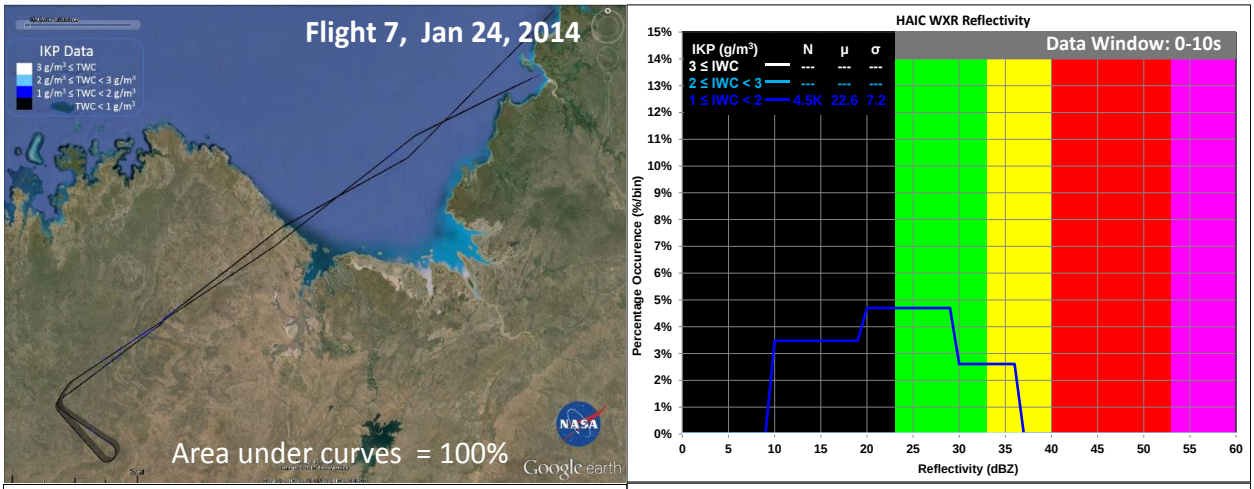
Flight 7, Jan 24, 2014
IKP Data
3 g/m³ ≤ TWC
2 g/m³ ≤ TWC < 3 g/m³
1 g/m³ ≤ TWC < 2 g/m³
TWC < 1 g/m³
Area under curves = 100%
Google earth

HAIC WXR Reflectivity
Data Window: 0-10s
IKP (g/m³) N μ σ
3 ≤ IWC --- --- ---
2 ≤ IWC < 3 --- --- ---
1 ≤ IWC < 2 4.5K 22.6 7.2
Percentage Occurence (%/bin)
Reflectivity (dBZ)

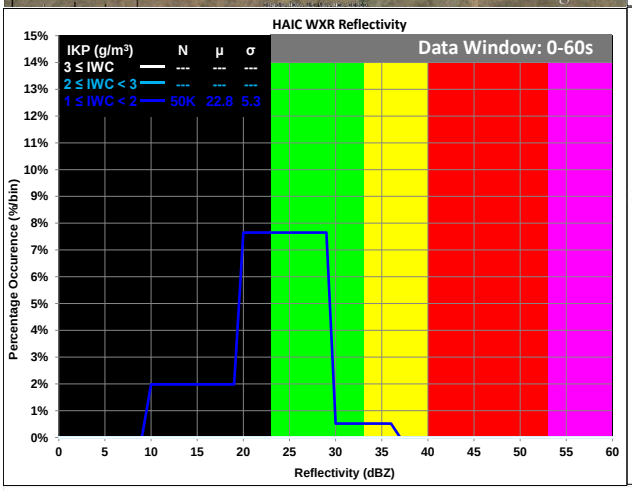
HAIC WXR Reflectivity
Data Window: 0-60s
IKP (g/m³) N μ σ
3 ≤ IWC --- --- ---
2 ≤ IWC < 3 --- --- ---
1 ≤ IWC < 2 50K 22.8 5.3
Percentage Occurence (%/bin)
Reflectivity (dBZ)

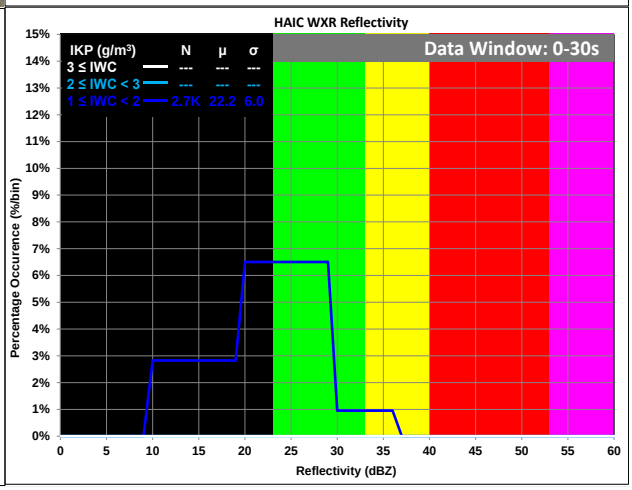
HAIC WXR Reflectivity
Data Window: 0-30s
IKP (g/m³) N μ σ
3 ≤ IWC --- --- ---
2 ≤ IWC < 3 --- --- ---
1 ≤ IWC < 2 2.7K 22.2 6.0
Percentage Occurence (%/bin)
Reflectivity (dBZ)

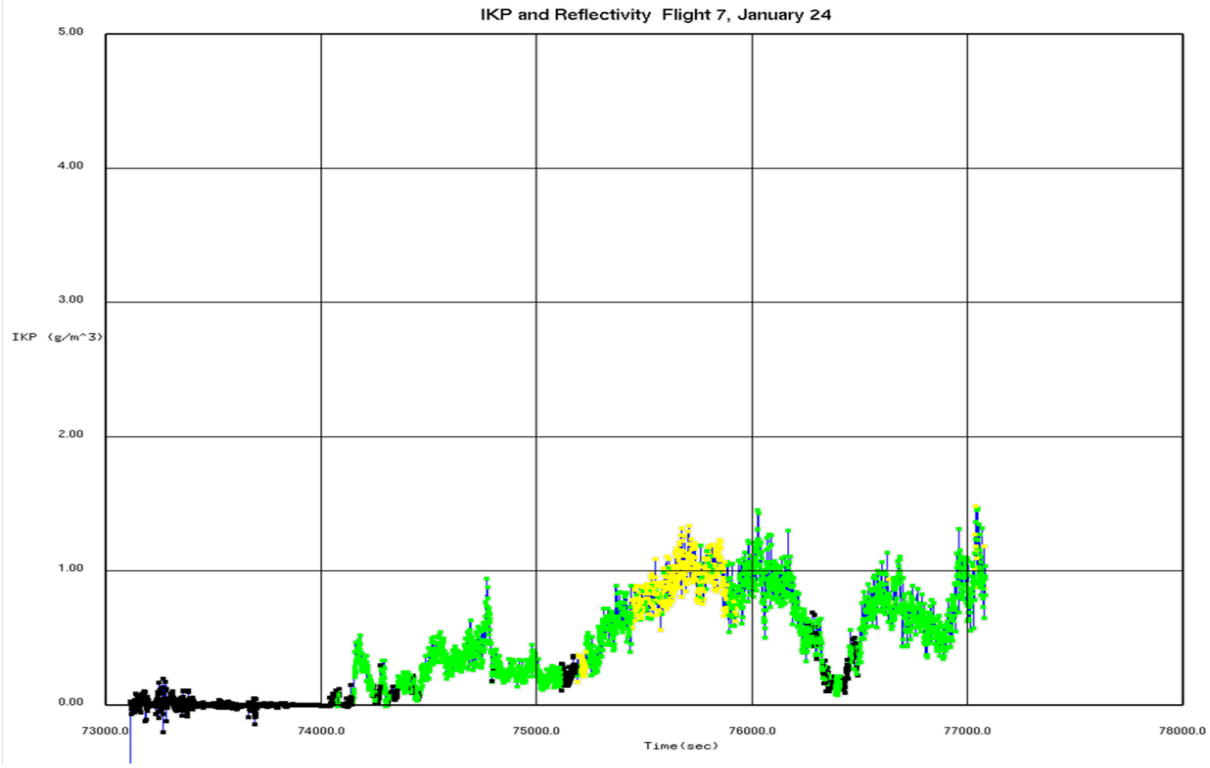
IKP and Reflectivity Flight 7, January 24
IKP (g/m^3)
Time(sec)

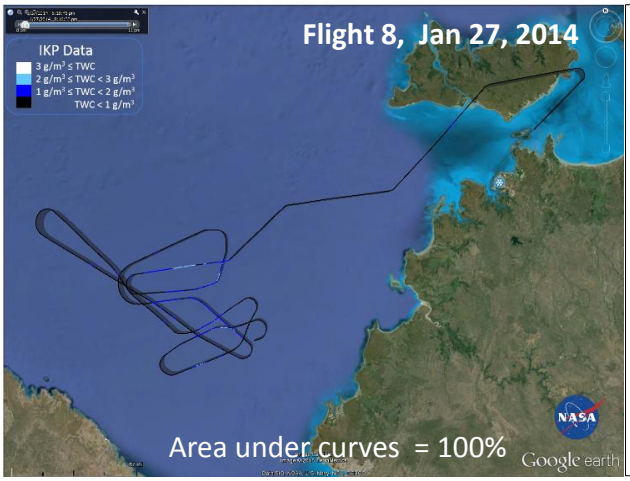
Flight 8, Jan 27, 2014
IKP Data
3 g/m³ ≤ TWC
2 g/m³ ≤ TWC < 3 g/m³
1 g/m³ ≤ TWC < 2 g/m³
TWC < 1 g/m³
Area under curves = 100%
Google earth

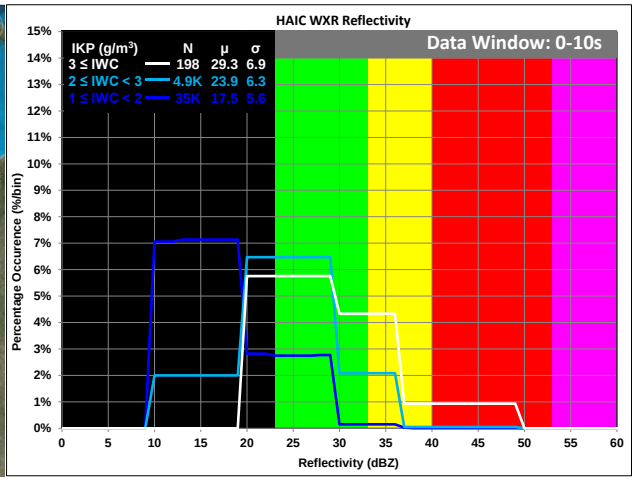
HAIC WXR Reflectivity
Data Window: 0-10s
IKP (g/m³) N μ σ
3 ≤ IWC 198 29.3 6.9
2 ≤ IWC < 3 4.9K 23.9 6.3
1 ≤ IWC < 2 35K 17.5 5.6
Percentage Occurence (%/bin)
Reflectivity (dBZ)

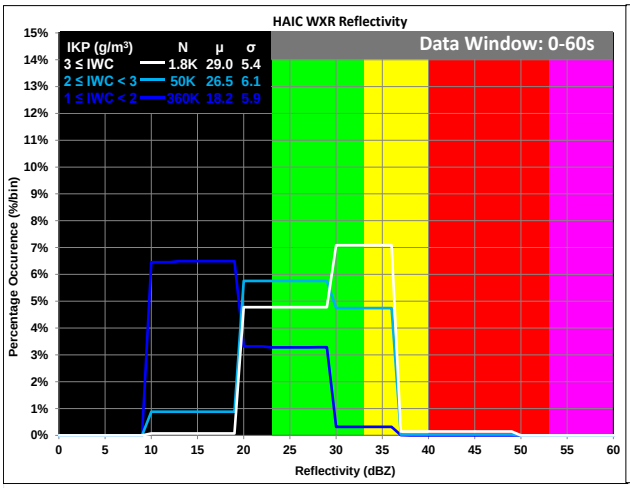
HAIC WXR Reflectivity
Data Window: 0-60s
IKP (g/m³) N μ σ
3 ≤ IWC 1.8K 29.0 5.4
2 ≤ IWC < 3 50K 26.5 6.1
1 ≤ IWC < 2 360K 18.2 5.9
Percentage Occurence (%/bin)
Reflectivity (dBZ)

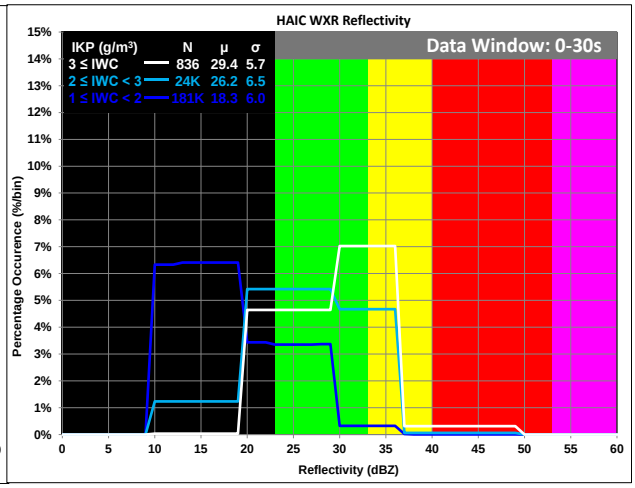
HAIC WXR Reflectivity
Data Window: 0-30s
IKP (g/m³) N μ σ
3 ≤ IWC 836 29.4 5.7
2 ≤ IWC < 3 24K 26.2 6.5
1 ≤ IWC < 2 181K 18.3 6.0
Percentage Occurence (%/bin)
Reflectivity (dBZ)

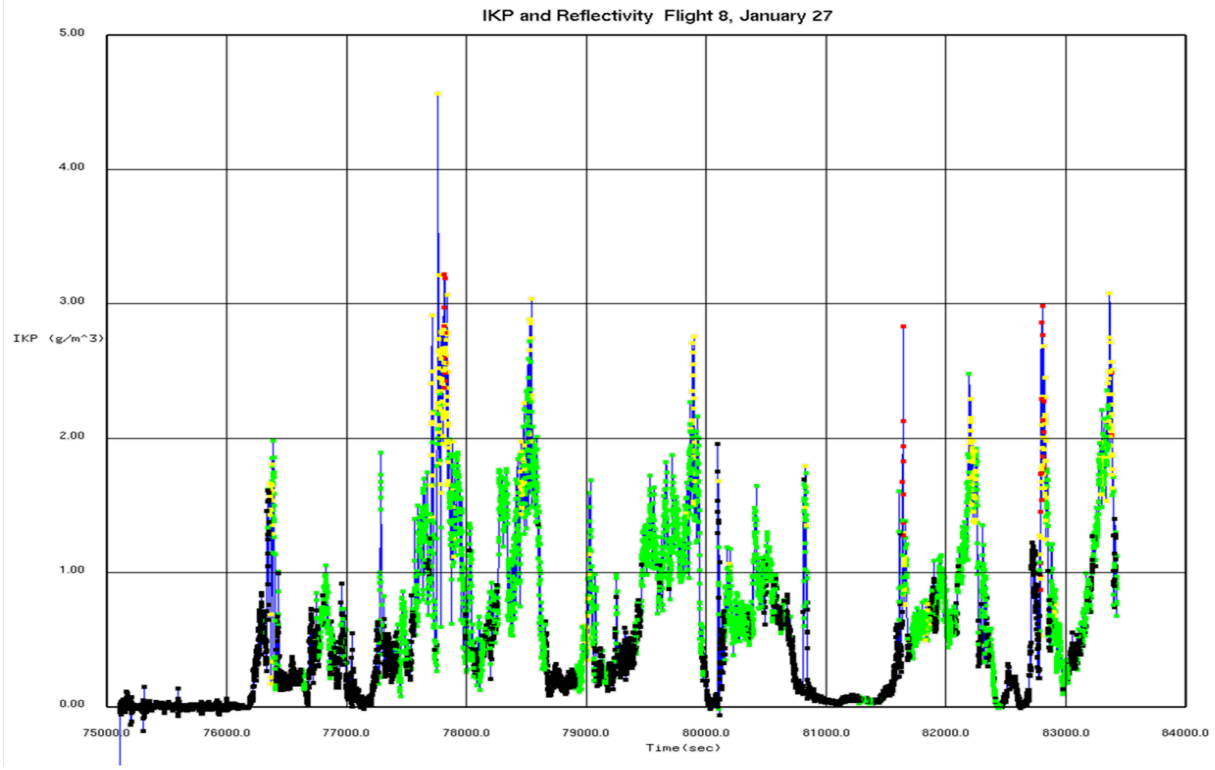
IKP and Reflectivity Flight 8, January 27
IKP (g/m^3)
Time(sec)

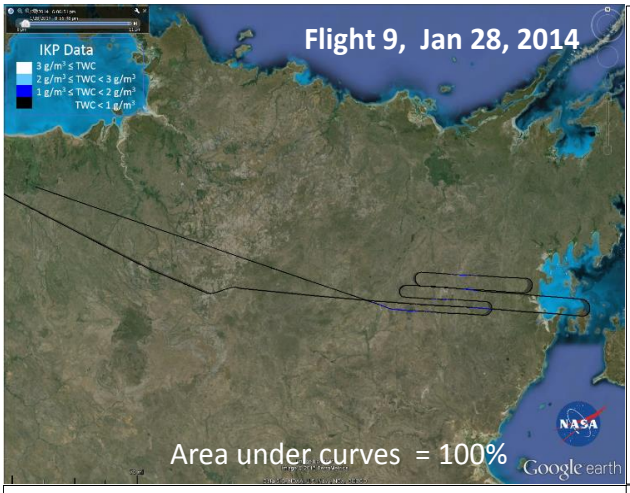
Flight 9, Jan 28, 2014
IKP Data
3 g/m³ ≤ TWC
2 g/m³ ≤ TWC < 3 g/m³
1 g/m³ ≤ TWC < 2 g/m³
TWC < 1 g/m³
Area under curves = 100%
Google earth

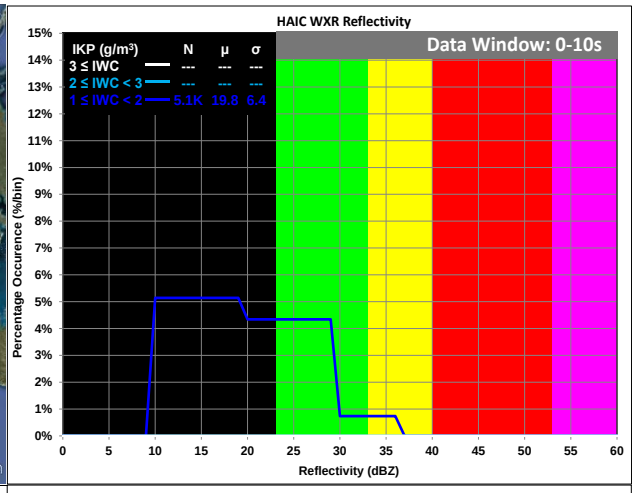
HAIC WXR Reflectivity
Data Window: 0-10s
IKP (g/m³) N μ σ
3 ≤ IWC --- --- ---
2 ≤ IWC < 3 --- --- ---
1 ≤ IWC < 2 5.1K 19.8 6.4
Percentage Occurence (%/bin)
Reflectivity (dBZ)

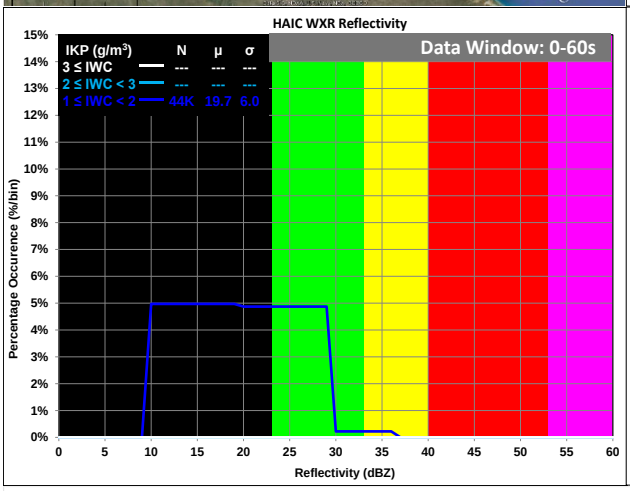
HAIC WXR Reflectivity
Data Window: 0-60s
IKP (g/m³) N μ σ
3 ≤ IWC --- --- ---
2 ≤ IWC < 3 --- --- ---
1 ≤ IWC < 2 44K 19.7 6.0
Percentage Occurence (%/bin)
Reflectivity (dBZ)

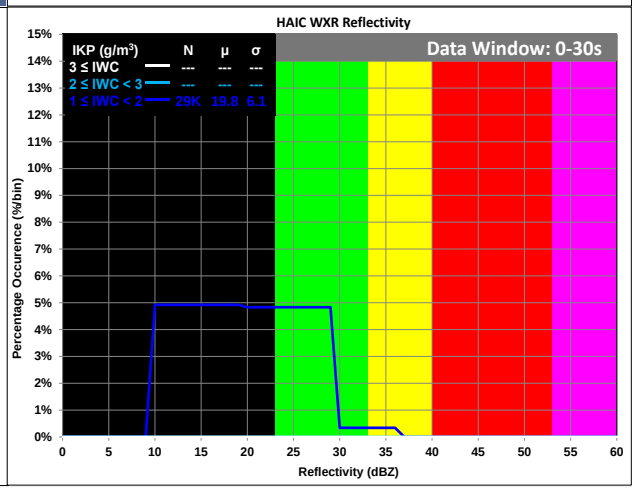
HAIC WXR Reflectivity
Data Window: 0-30s
IKP (g/m³) N μ σ
3 ≤ IWC --- --- ---
2 ≤ IWC < 3 --- --- ---
1 ≤ IWC < 2 29K 19.8 6.1
Percentage Occurence (%/bin)
Reflectivity (dBZ)

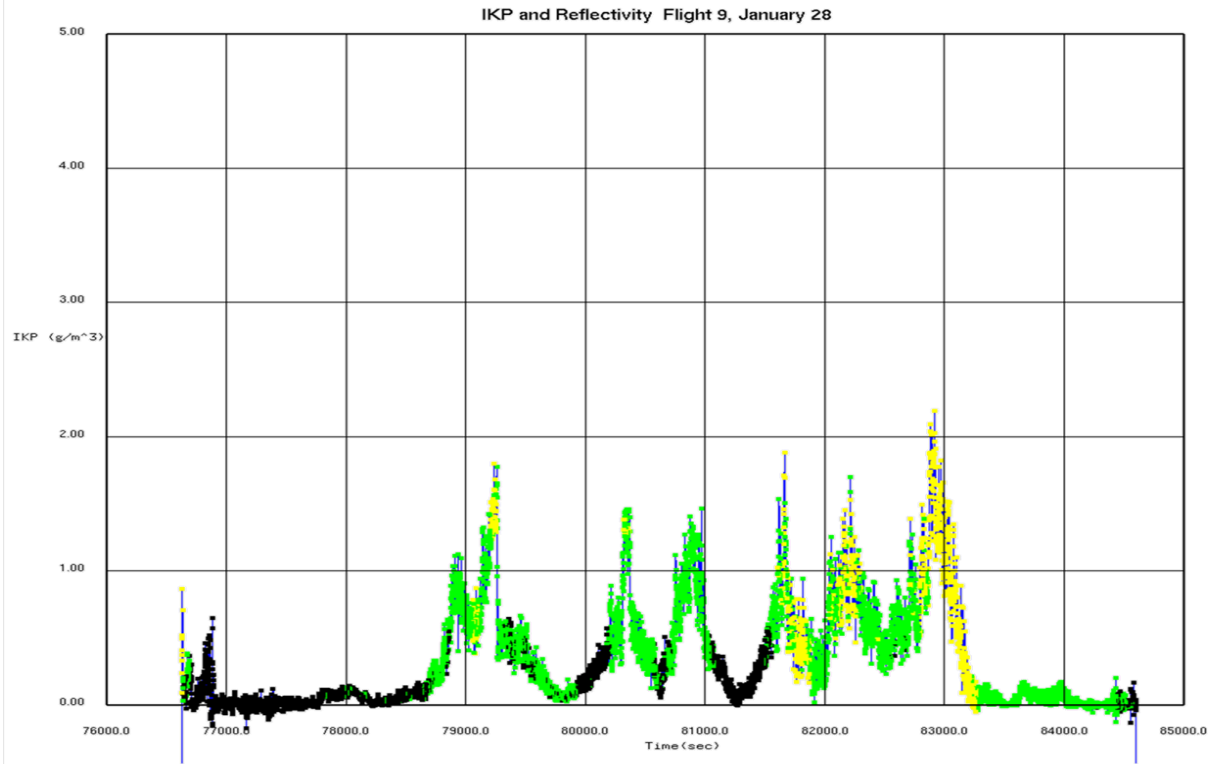
IKP and Reflectivity Flight 9, January 28
IKP (g/m^3)
Time(sec)

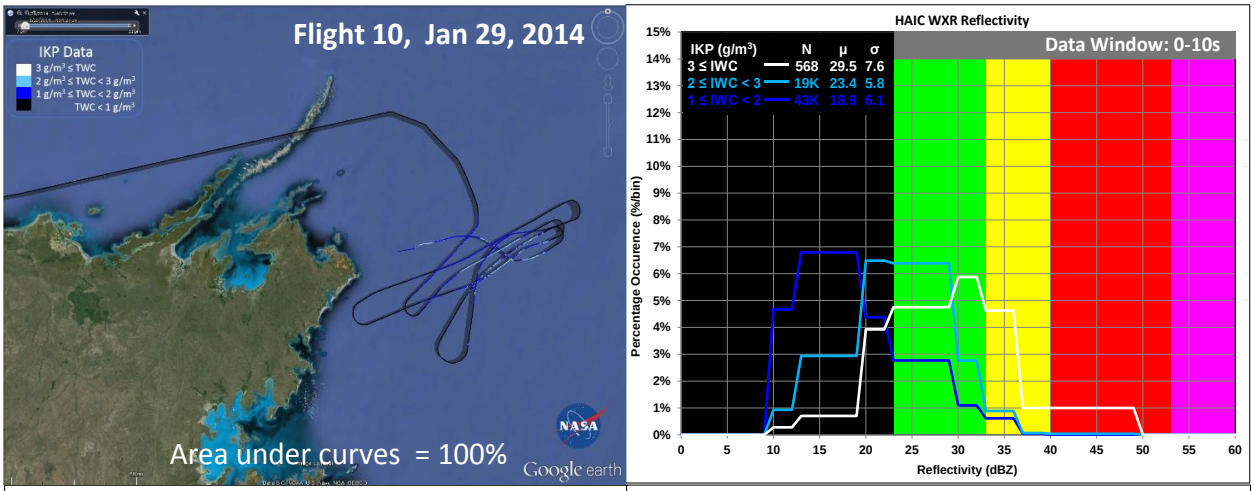
Flight 10, Jan 29, 2014
IKP Data
3 g/m³ ≤ TWC
2 g/m³ ≤ TWC < 3 g/m³
1 g/m³ ≤ TWC < 2 g/m³
TWC < 1 g/m³
Area under curves = 100%
Google earth
NASA

HAIC WXR Reflectivity
Data Window: 0-10s
IKP (g/m³) N μ σ
3 ≤ IWC 568 29.5 7.6
2 ≤ IWC < 3 19K 23.4 5.8
1 ≤ IWC < 2 43K 18.9 6.1
Percentage Occurence (%/bin)
Reflectivity (dBZ)

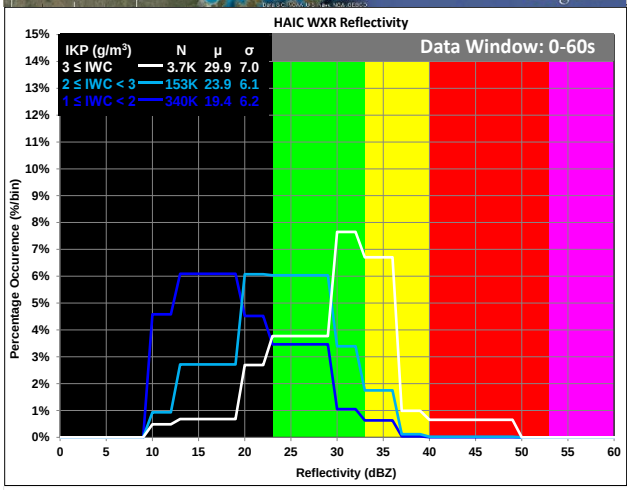
HAIC WXR Reflectivity
Data Window: 0-60s
IKP (g/m³) N μ σ
3 ≤ IWC 3.7K 29.9 7.0
2 ≤ IWC < 3 153K 23.9 6.1
1 ≤ IWC < 2 340K 19.4 6.2
Percentage Occurence (%/bin)
Reflectivity (dBZ)

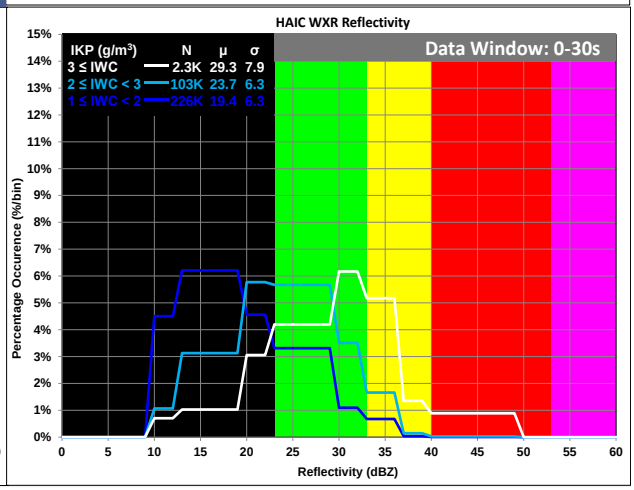
HAIC WXR Reflectivity
Data Window: 0-30s
IKP (g/m³) N μ σ
3 ≤ IWC 2.3K 29.3 7.9
2 ≤ IWC < 3 103K 23.7 6.3
1 ≤ IWC < 2 226K 19.4 6.3
Percentage Occurence (%/bin)
Reflectivity (dBZ)

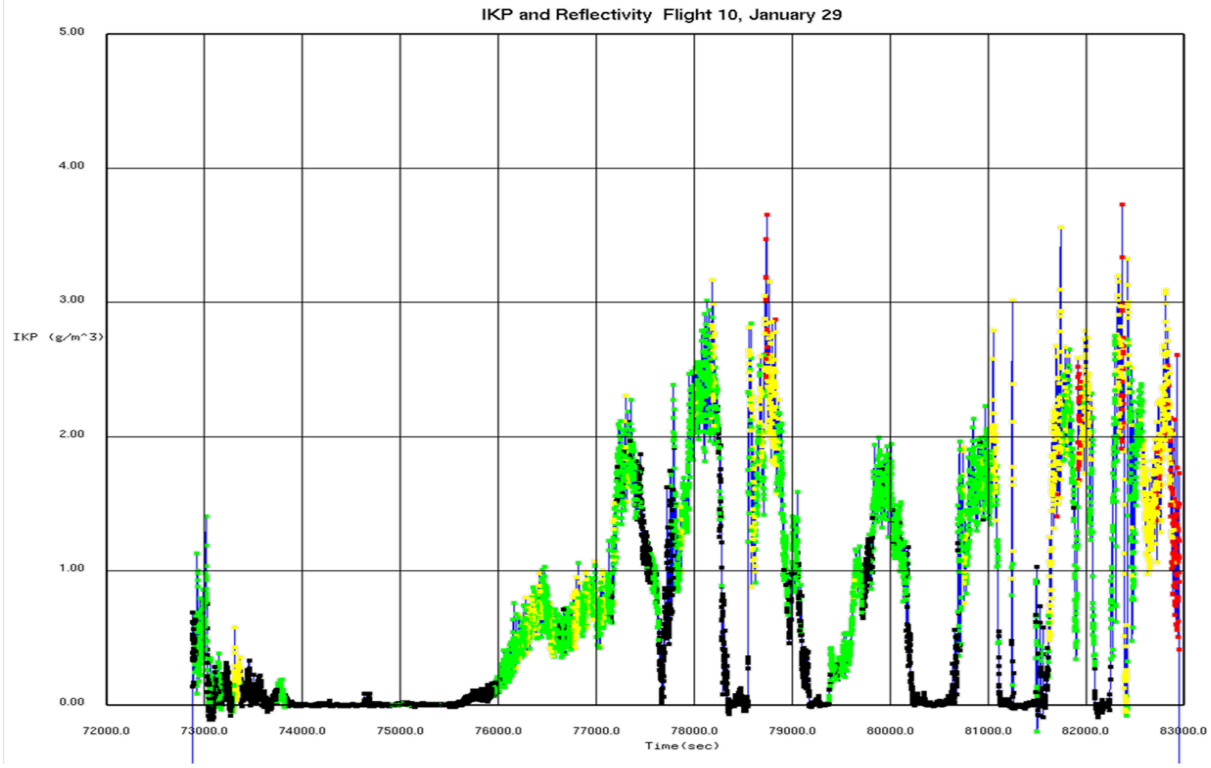
IKP and Reflectivity Flight 10, January 29
IKP (g/m^3)
Time(sec)

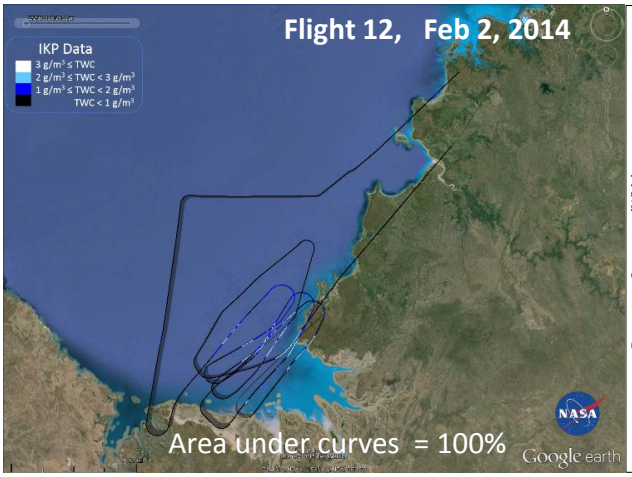
Flight 12, Feb 2, 2014
IKP Data
3 g/m³ ≤ TWC
2 g/m³ ≤ TWC < 3 g/m³
1 g/m³ ≤ TWC < 2 g/m³
TWC < 1 g/m³
Area under curves = 100%
Google earth

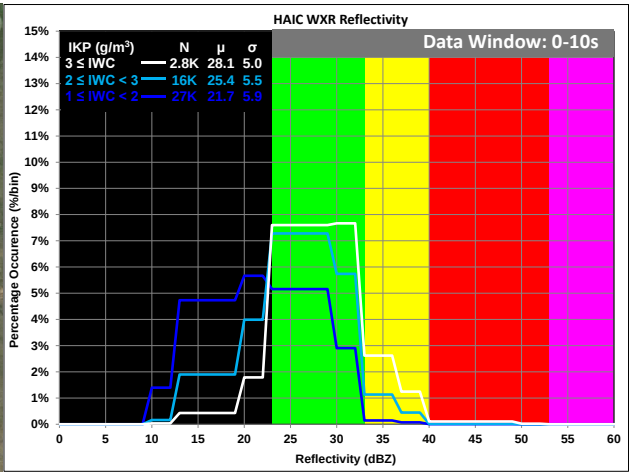
HAIC WXR Reflectivity
Data Window: 0-10s
IKP (g/m³) N μ σ
3 ≤ IWC 2.8K 28.1 5.0
2 ≤ IWC < 3 16K 25.4 5.5
1 ≤ IWC < 2 27K 21.7 5.9
Percentage Occurence (%/bin)
Reflectivity (dBZ)

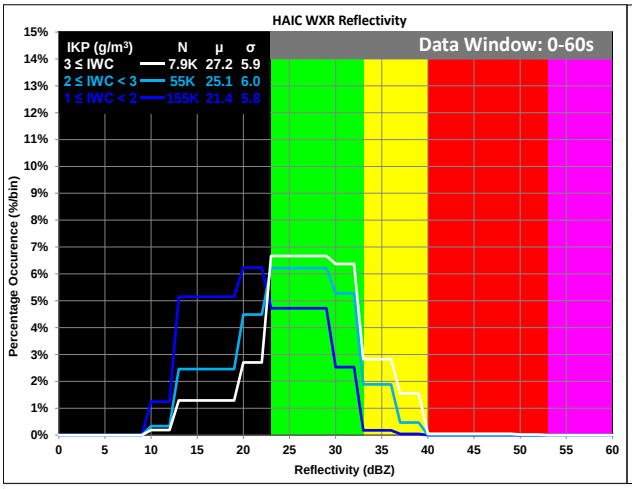
HAIC WXR Reflectivity
Data Window: 0-60s
IKP (g/m³) N μ σ
3 ≤ IWC 7.9K 27.2 5.9
2 ≤ IWC < 3 55K 25.1 6.0
1 ≤ IWC < 2 155K 21.4 5.8
Percentage Occurence (%/bin)
Reflectivity (dBZ)

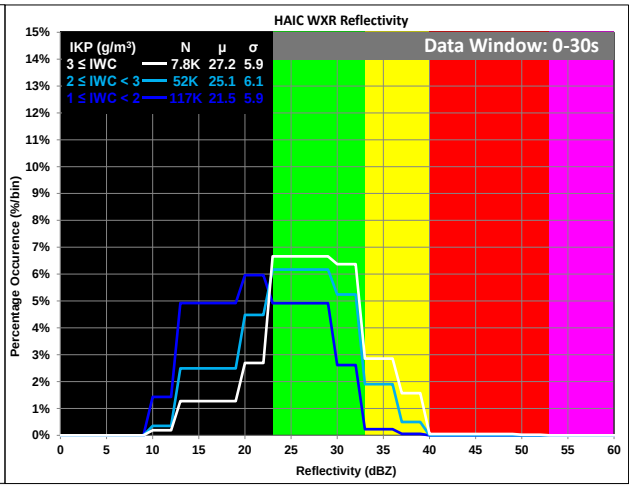
HAIC WXR Reflectivity
Data Window: 0-30s
IKP (g/m³) N μ σ
3 ≤ IWC 7.8K 27.2 5.9
2 ≤ IWC < 3 52K 25.1 6.1
1 ≤ IWC < 2 117K 21.5 5.9
Percentage Occurence (%/bin)
Reflectivity (dBZ)

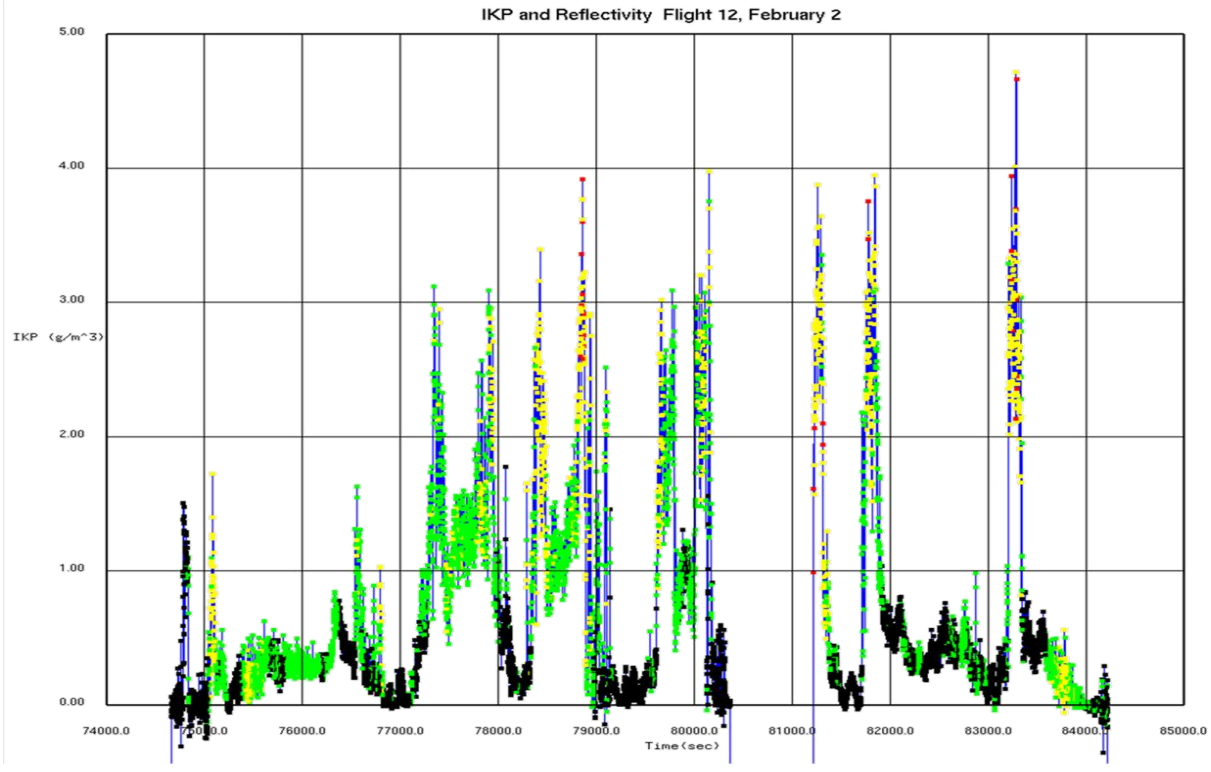
IKP and Reflectivity Flight 12, February 2
IKP (g/m^3)
Time(sec)

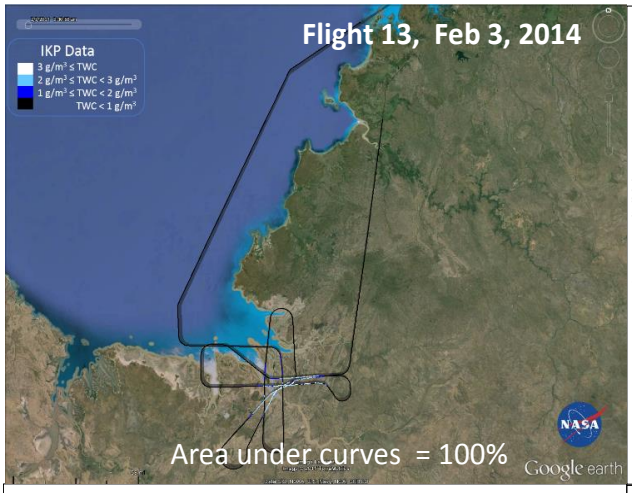
Flight 13, Feb 3, 2014
IKP Data
3 g/m³ ≤ TWC
2 g/m³ ≤ TWC < 3 g/m³
1 g/m³ ≤ TWC < 2 g/m³
TWC < 1 g/m³
Area under curves = 100%
Google earth

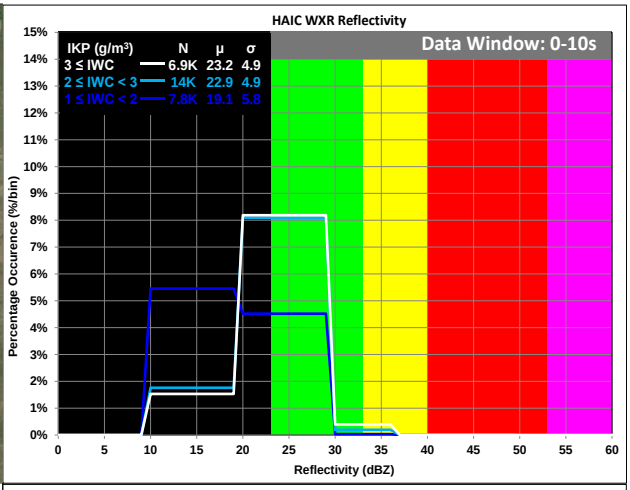
HAIC WXR Reflectivity
Data Window: 0-10s
IKP (g/m³) N μ σ
3 ≤ IWC 6.9K 23.2 4.9
2 ≤ IWC < 3 14K 22.9 4.9
1 ≤ IWC < 2 7.8K 19.1 5.8
Percentage Occurence (%/bin)
Reflectivity (dBZ)

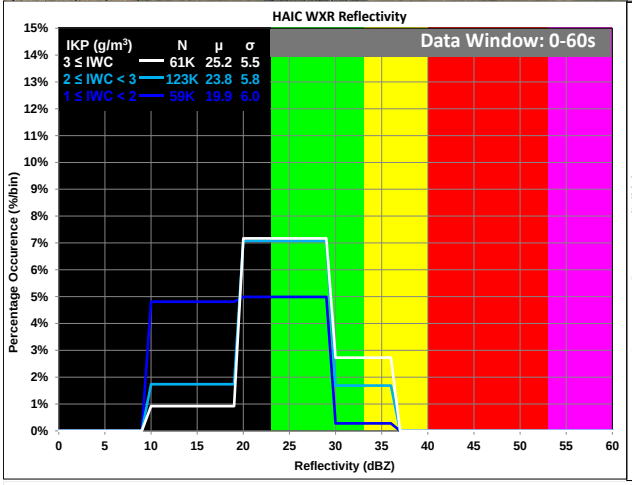
HAIC WXR Reflectivity
Data Window: 0-60s
IKP (g/m³) N μ σ
3 ≤ IWC 61K 25.2 5.5
2 ≤ IWC < 3 123K 23.8 5.8
1 ≤ IWC < 2 59K 19.9 6.0
Percentage Occurence (%/bin)
Reflectivity (dBZ)

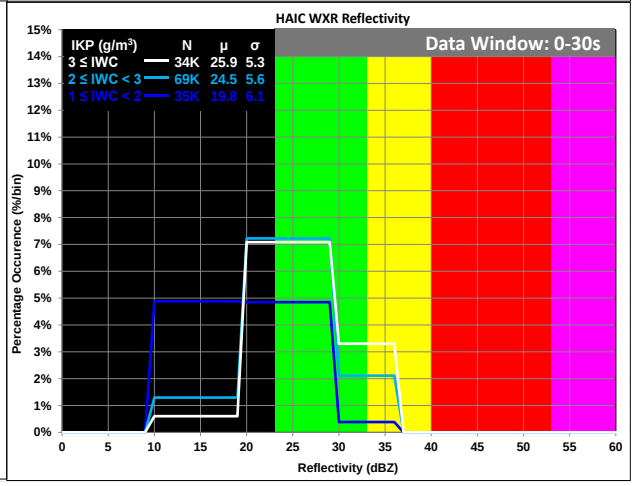
HAIC WXR Reflectivity
Data Window: 0-30s
IKP (g/m³) N μ σ
3 ≤ IWC 34K 25.9 5.3
2 ≤ IWC < 3 69K 24.5 5.6
1 ≤ IWC < 2 35K 19.8 6.1
Percentage Occurence (%/bin)
Reflectivity (dBZ)

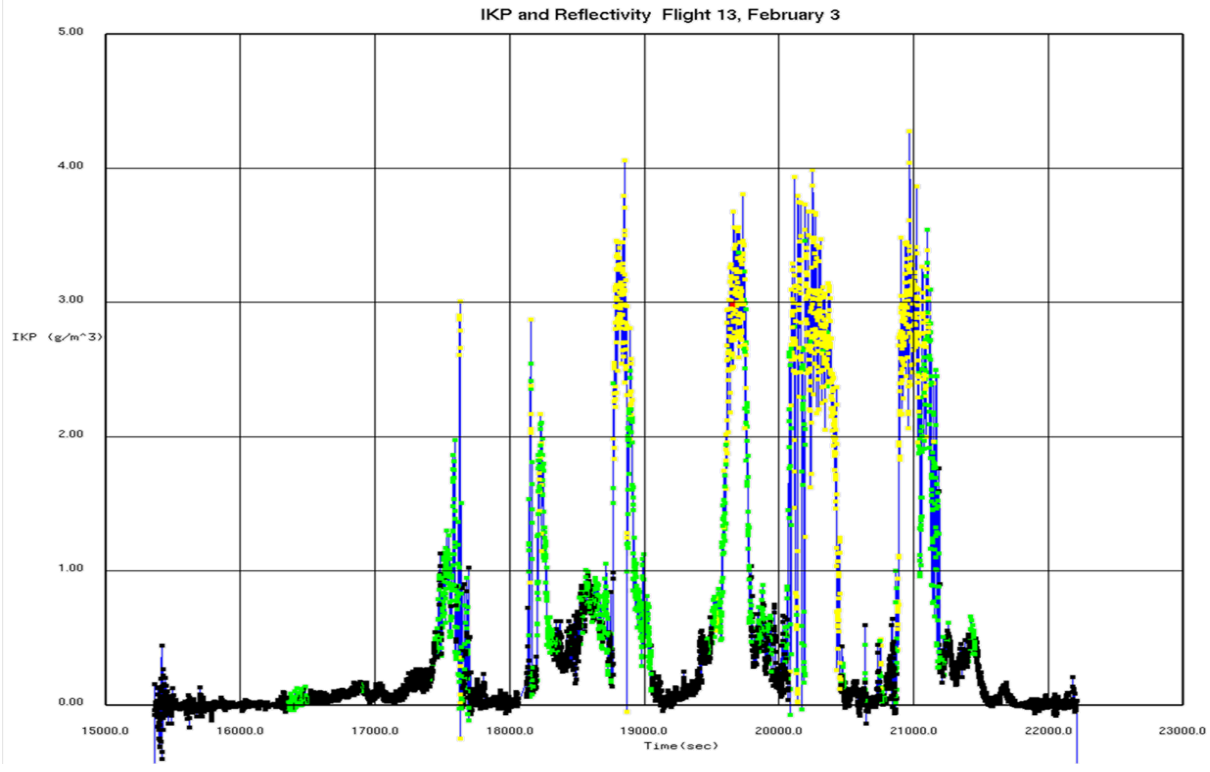
IKP and Reflectivity Flight 13, February 3
IKP (g/m^3)
Time(sec)

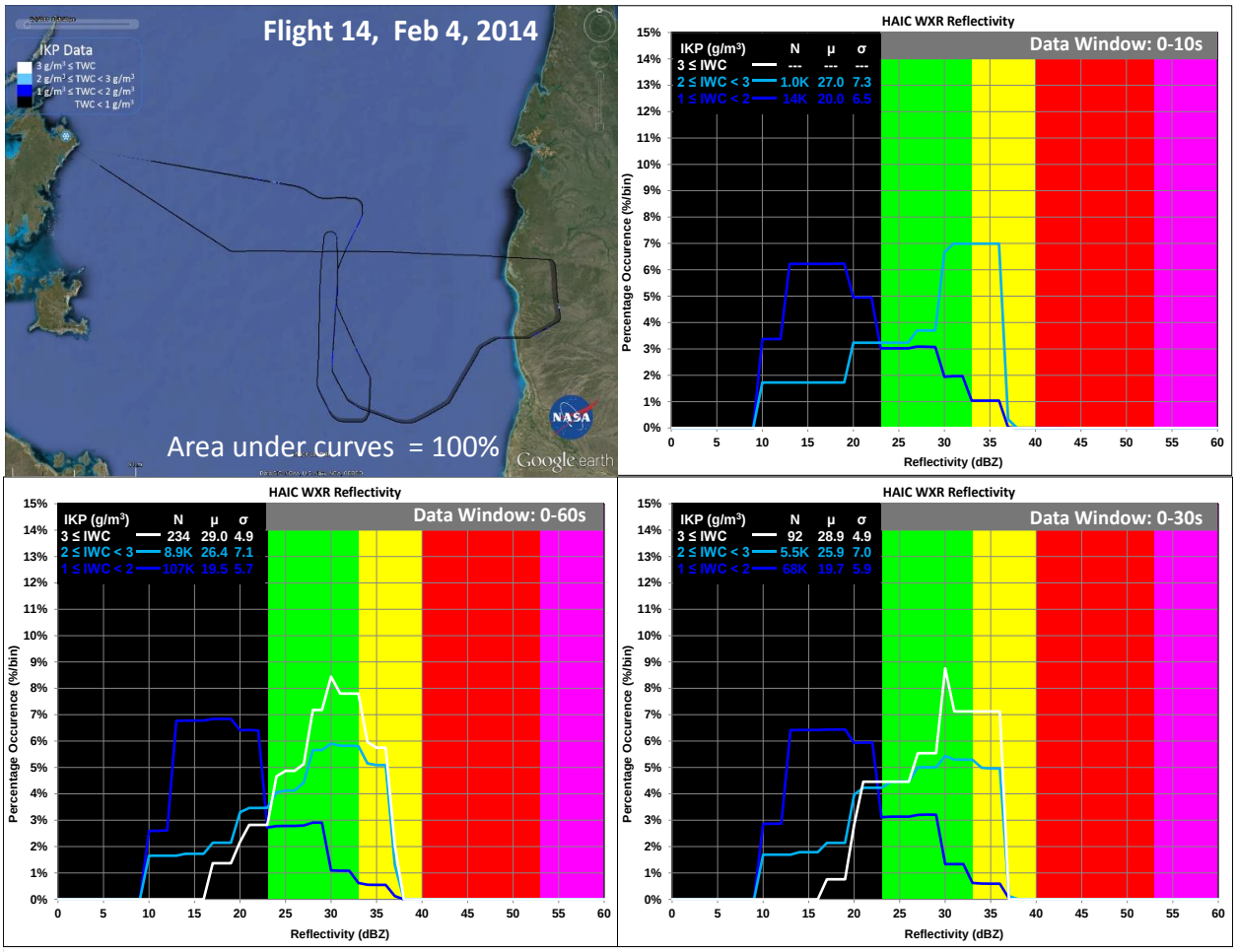
Flight 14, Feb 4, 2014
IKP Data
3 g/m³ ≤ TWC
2 g/m³ ≤ TWC < 3 g/m³
1 g/m³ ≤ TWC < 2 g/m³
TWC < 1 g/m³
Area under curves = 100%
Google earth
HAIC WXR Reflectivity
Data Window: 0-10s
IKP (g/m³) N μ σ
3 ≤ IWC --- --- ---
2 ≤ IWC < 3 1.0K 27.0 7.3
1 ≤ IWC < 2 14K 20.0 6.5
Percentage Occurence (%/bin)
Reflectivity (dBZ)
HAIC WXR Reflectivity
Data Window: 0-60s
IKP (g/m³) N μ σ
3 ≤ IWC 234 29.0 4.9
2 ≤ IWC < 3 8.9K 26.4 7.1
1 ≤ IWC < 2 107K 19.5 5.7
Percentage Occurence (%/bin)
Reflectivity (dBZ)
HAIC WXR Reflectivity
Data Window: 0-30s
IKP (g/m³) N μ σ
3 ≤ IWC 92 28.9 4.9
2 ≤ IWC < 3 5.5K 25.9 7.0
1 ≤ IWC < 2 68K 19.7 5.9
Percentage Occurence (%/bin)
Reflectivity (dBZ)

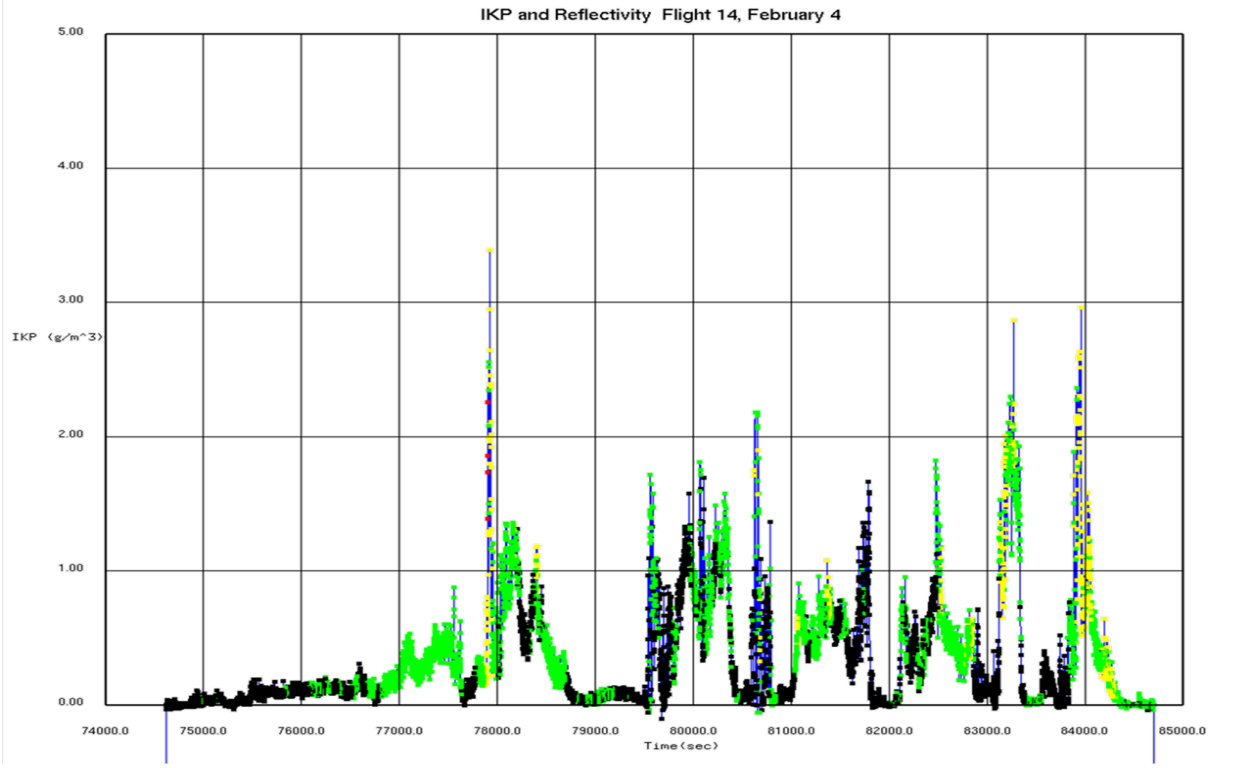
IKP and Reflectivity Flight 14, February 4
IKP (g/m^3)
Time(sec)

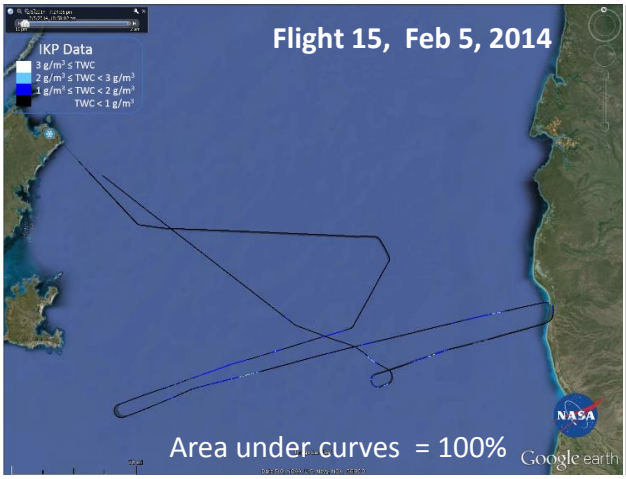
Flight 15, Feb 5, 2014
IKP Data
3 g/m³ ≤ TWC
2 g/m³ ≤ TWC < 3 g/m³
1 g/m³ ≤ TWC < 2 g/m³
TWC < 1 g/m³
Area under curves = 100%
Google earth

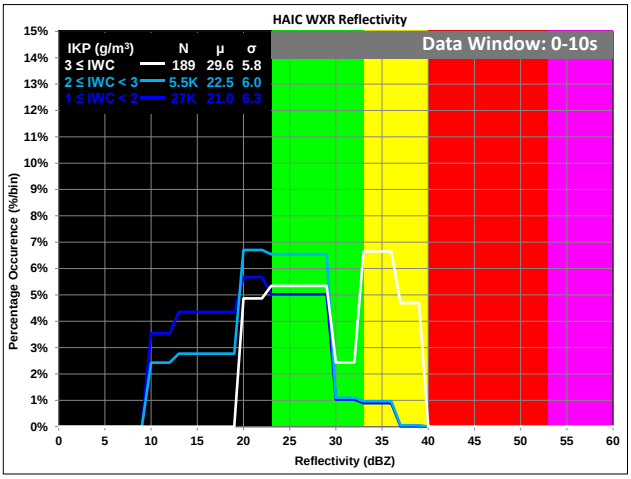
HAIC WXR Reflectivity
Data Window: 0-10s
IKP (g/m³) N μ σ
3 ≤ IWC 189 29.6 5.8
2 ≤ IWC < 3 5.5K 22.5 6.0
1 ≤ IWC < 2 27K 21.0 6.3
Percentage Occurence (%/bin)
Reflectivity (dBZ)

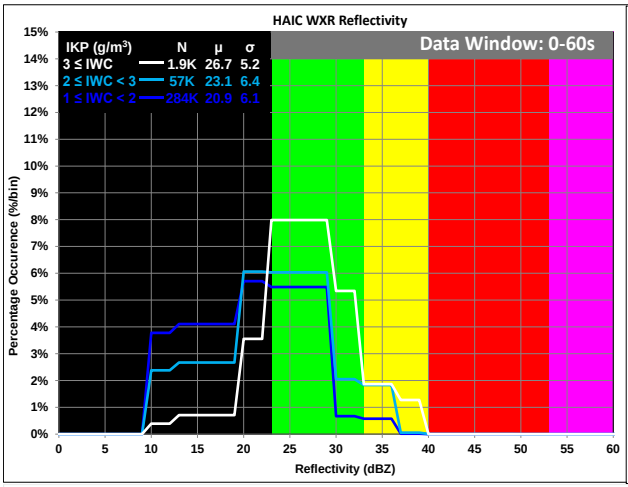
HAIC WXR Reflectivity
Data Window: 0-60s
IKP (g/m³) N μ σ
3 ≤ IWC 1.9K 26.7 5.2
2 ≤ IWC < 3 57K 23.1 6.4
1 ≤ IWC < 2 284K 20.9 6.1
Percentage Occurence (%/bin)
Reflectivity (dBZ)

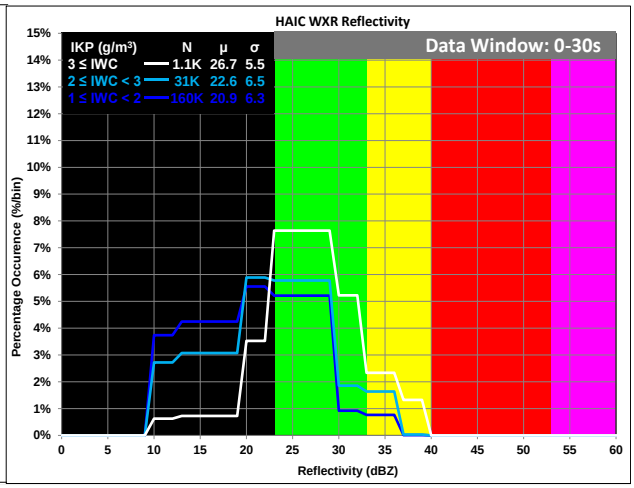
HAIC WXR Reflectivity
Data Window: 0-30s
IKP (g/m³) N μ σ
3 ≤ IWC 1.1K 26.7 5.5
2 ≤ IWC < 3 31K 22.6 6.5
1 ≤ IWC < 2 160K 20.9 6.3
Percentage Occurence (%/bin)
Reflectivity (dBZ)

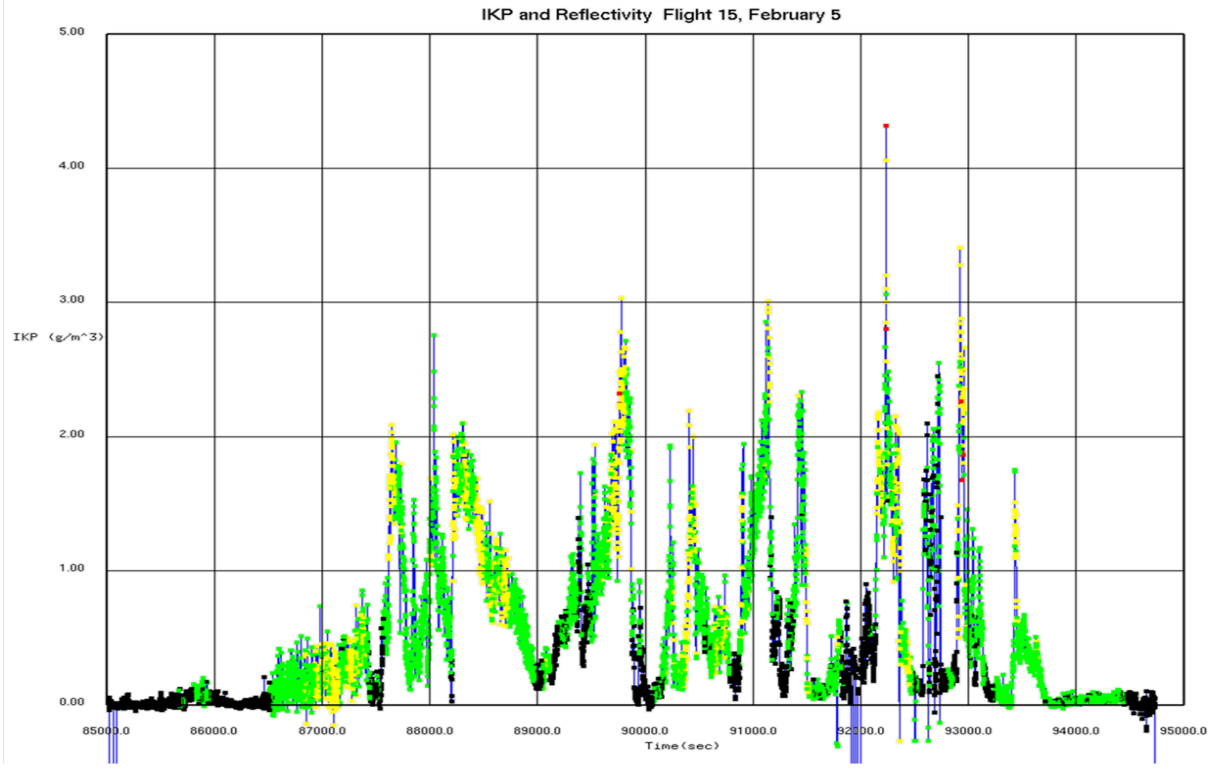
IKP and Reflectivity Flight 15, February 5
IKP (g/m^3)
Time(sec)

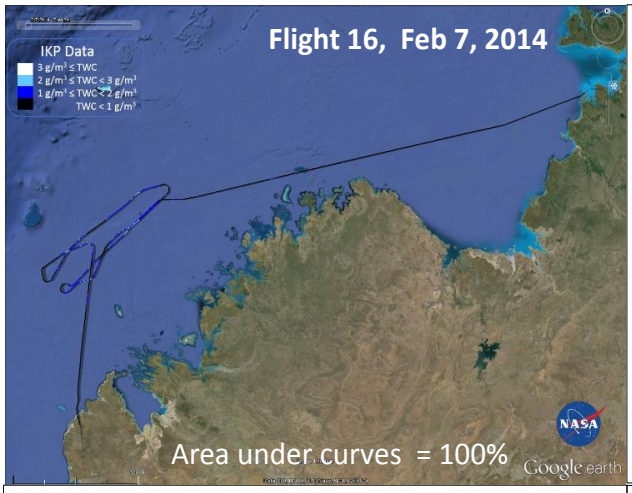
Flight 16, Feb 7, 2014
IKP Data
3 g/m³ ≤ TWC
2 g/m³ ≤ TWC < 3 g/m³
1 g/m³ ≤ TWC < 2 g/m³
TWC < 1 g/m³
Area under curves = 100%
Google earth

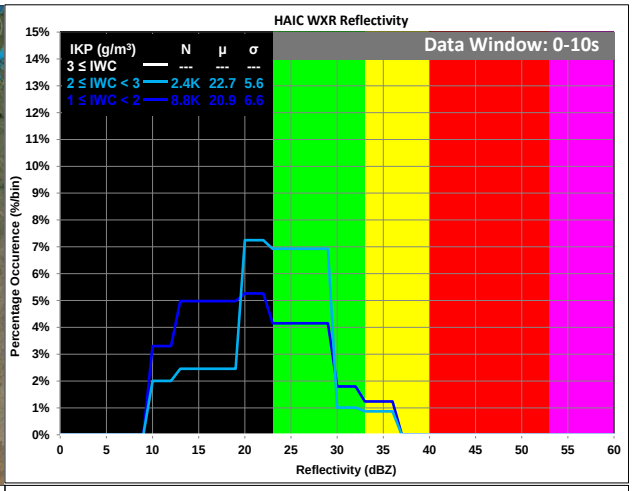
HAIC WXR Reflectivity
Data Window: 0-10s
IKP (g/m³) N μ σ
3 ≤ IWC --- --- ---
2 ≤ IWC < 3 2.4K 22.7 5.6
1 ≤ IWC < 2 8.8K 20.9 6.6
Percentage Occurence (%/bin)
Reflectivity (dBZ)

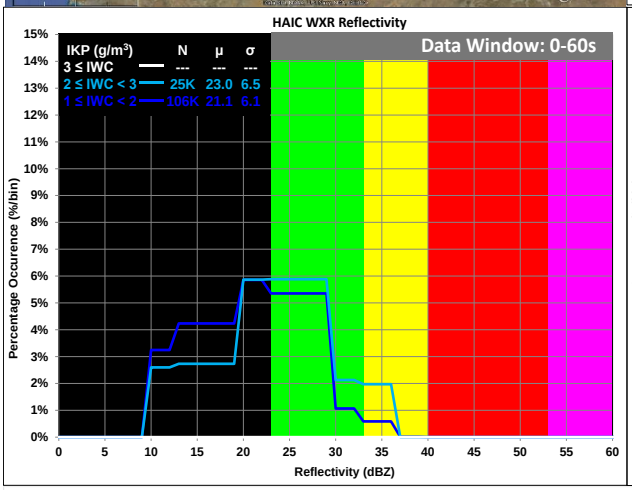
HAIC WXR Reflectivity
Data Window: 0-60s
IKP (g/m³) N μ σ
3 ≤ IWC --- --- ---
2 ≤ IWC < 3 25K 23.0 6.5
1 ≤ IWC < 2 106K 21.1 6.1
Percentage Occurence (%/bin)
Reflectivity (dBZ)

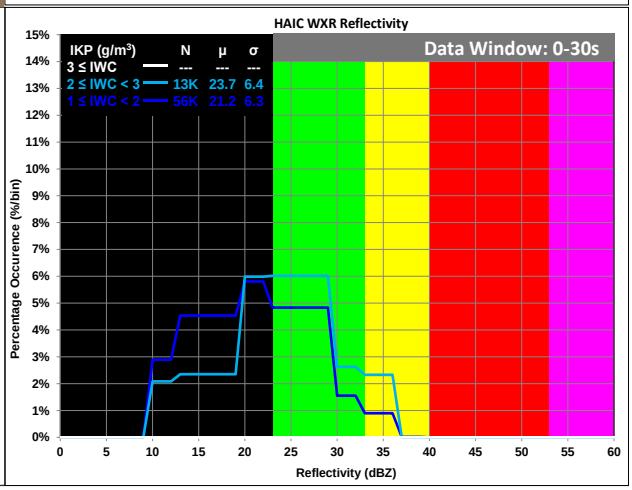
HAIC WXR Reflectivity
Data Window: 0-30s
IKP (g/m³) N μ σ
3 ≤ IWC --- --- ---
2 ≤ IWC < 3 13K 23.7 6.4
1 ≤ IWC < 2 56K 21.2 6.3
Percentage Occurence (%/bin)
Reflectivity (dBZ)

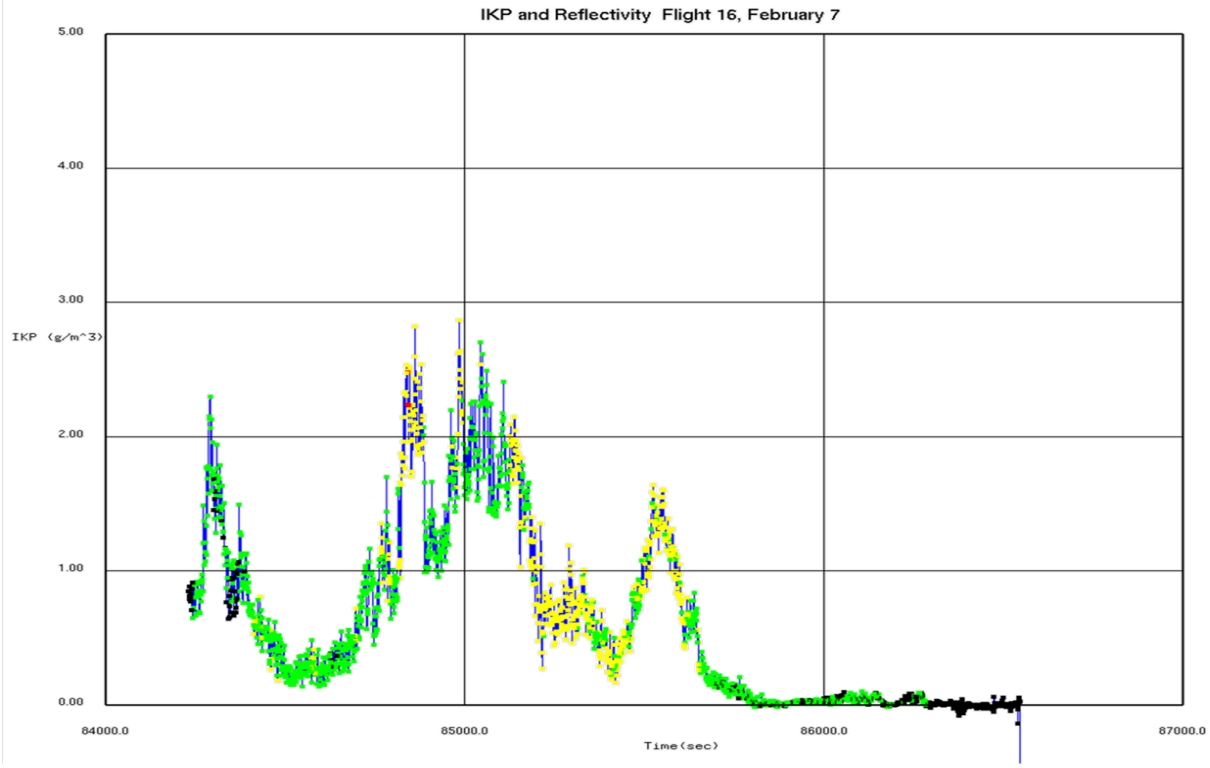
IKP and Reflectivity Flight 16, February 7
IKP (g/m^3)
Time(sec)

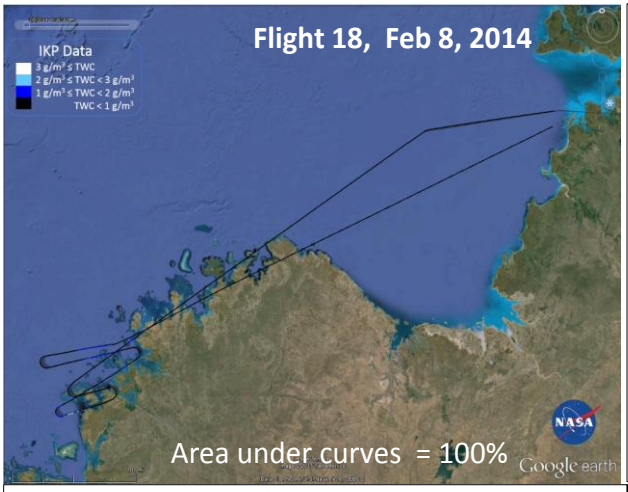
Flight 18, Feb 8, 2014
IKP Data
3 g/m³ ≤ TWC
2 g/m³ ≤ TWC < 3 g/m³
1 g/m³ ≤ TWC < 2 g/m³
TWC < 1 g/m³
Area under curves = 100%
Google earth

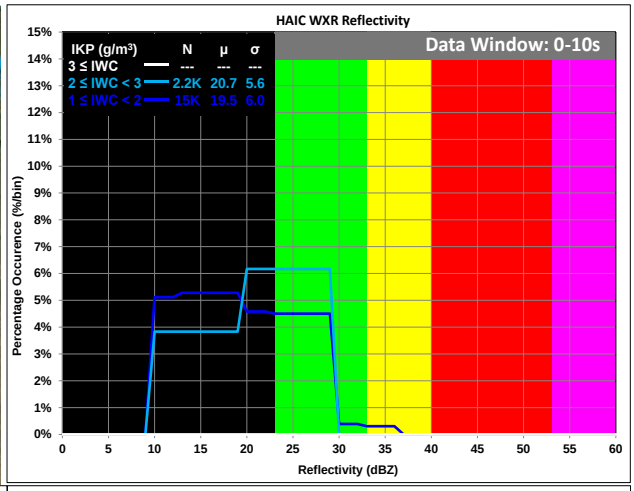
HAIC WXR Reflectivity
Data Window: 0-10s
IKP (g/m³) N μ σ
3 ≤ IWC --- --- ---
2 ≤ IWC < 3 2.2K 20.7 5.6
1 ≤ IWC < 2 15K 19.5 6.0
Percentage Occurence (%/bin)
Reflectivity (dBZ)

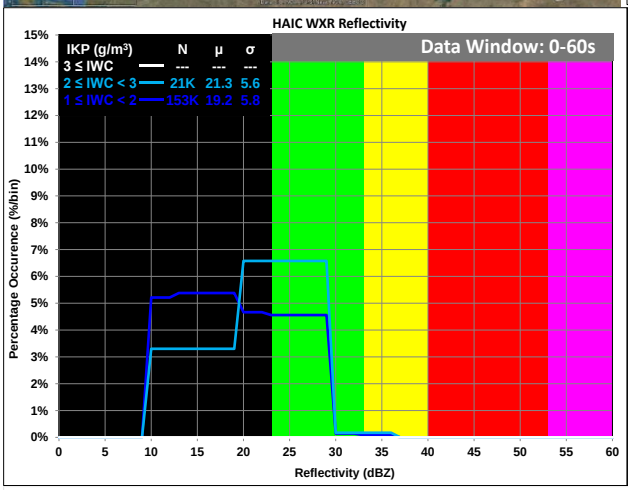
HAIC WXR Reflectivity
Data Window: 0-60s
IKP (g/m³) N μ σ
3 ≤ IWC --- --- ---
2 ≤ IWC < 3 21K 21.3 5.6
1 ≤ IWC < 2 153K 19.2 5.8
Percentage Occurence (%/bin)
Reflectivity (dBZ)

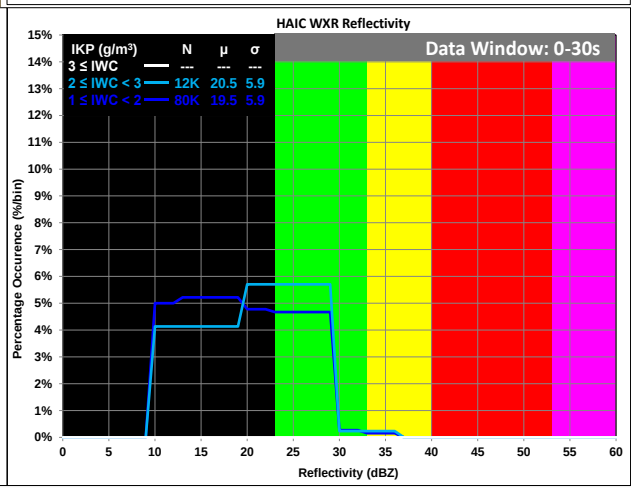
HAIC WXR Reflectivity
Data Window: 0-30s
IKP (g/m³) N μ σ
3 ≤ IWC --- --- ---
2 ≤ IWC < 3 12K 20.5 5.9
1 ≤ IWC < 2 80K 19.5 5.9
Percentage Occurence (%/bin)
Reflectivity (dBZ)

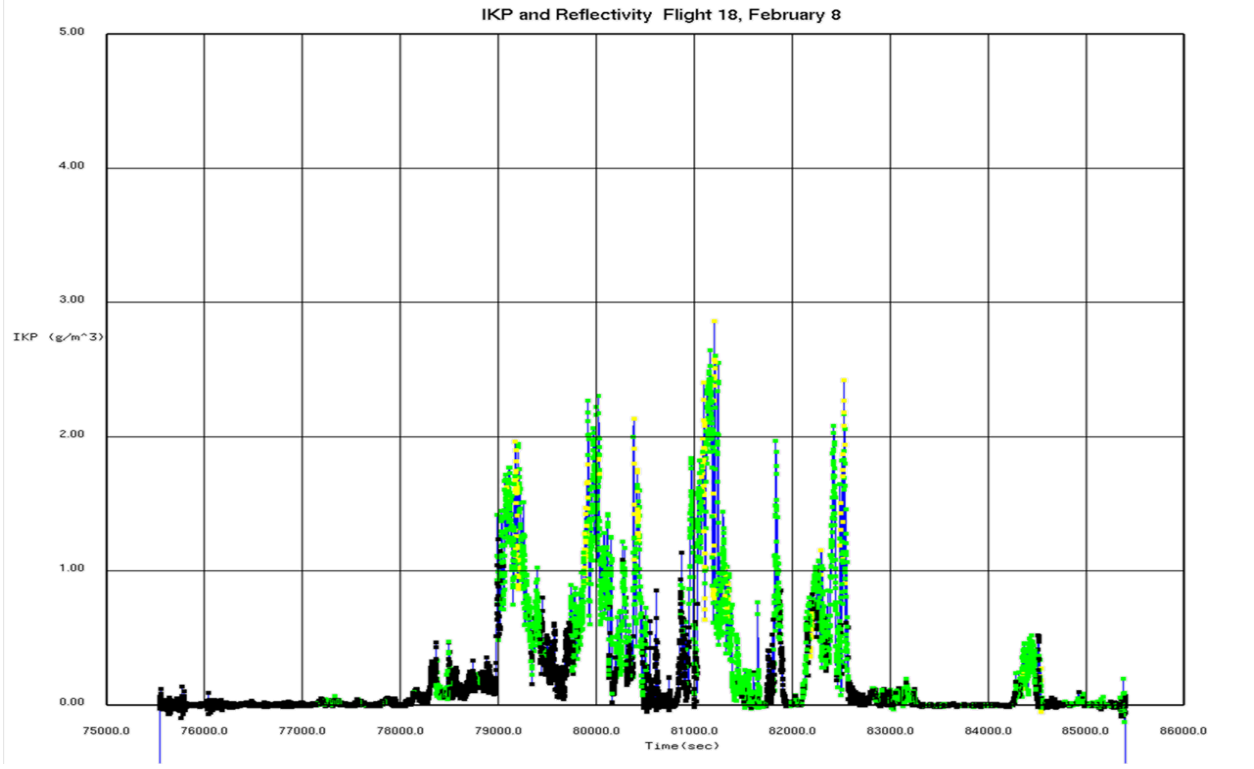
IKP and Reflectivity Flight 18, February 8
IKP (g/m^3)
Time(sec)

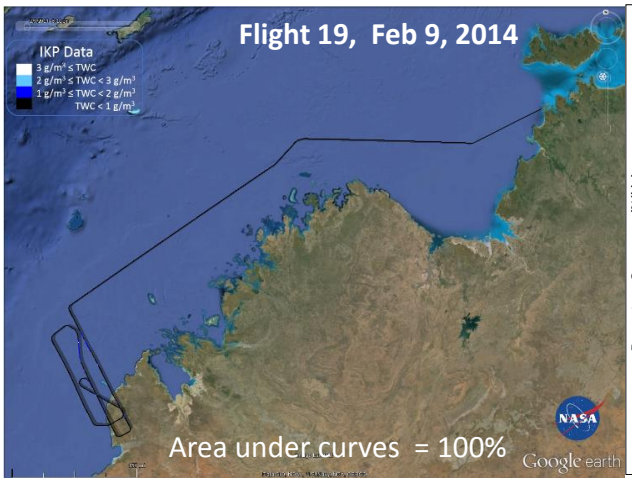
Flight 19, Feb 9, 2014
IKP Data
3 g/m³ ≤ TWC
2 g/m³ ≤ TWC < 3 g/m³
1 g/m³ ≤ TWC < 2 g/m³
TWC < 1 g/m³
Area under curves = 100%
NASA
Google earth

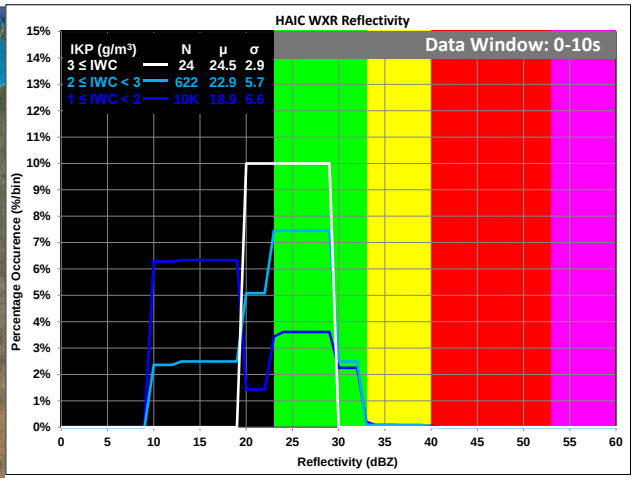
HAIC WXR Reflectivity
Data Window: 0-10s
IKP (g/m³) N μ σ
3 ≤ IWC 24 24.5 2.9
2 ≤ IWC < 3 622 22.9 5.7
1 ≤ IWC < 2 10K 18.9 6.6
Percentage Occurence (%/bin)
Reflectivity (dBZ)

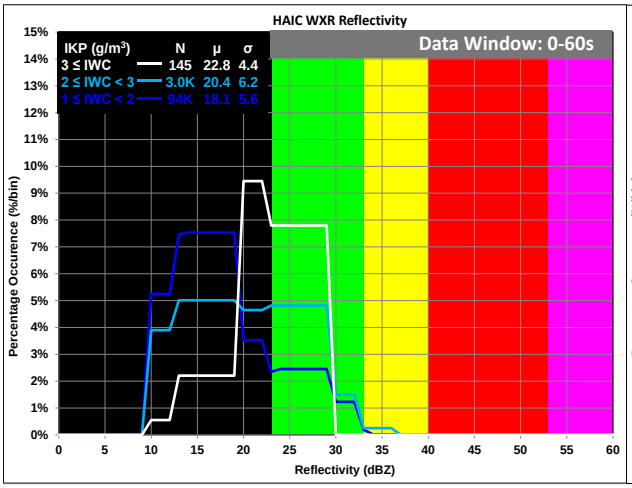
HAIC WXR Reflectivity
Data Window: 0-60s
IKP (g/m³) N μ σ
3 ≤ IWC 145 22.8 4.4
2 ≤ IWC < 3 3.0K 20.4 6.2
1 ≤ IWC < 2 94K 18.1 5.6
Percentage Occurence (%/bin)
Reflectivity (dBZ)

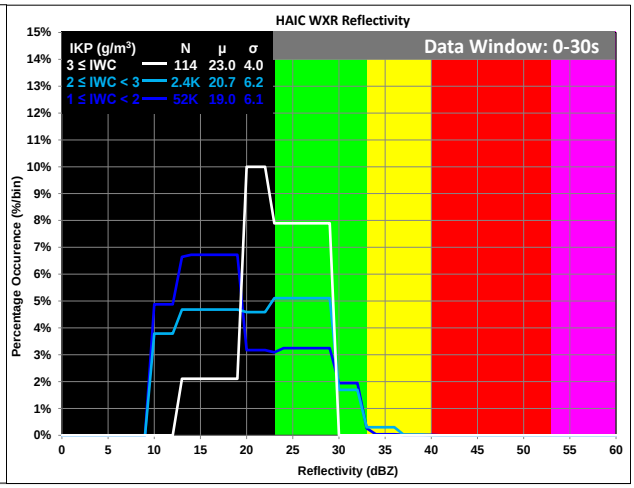
HAIC WXR Reflectivity
Data Window: 0-30s
IKP (g/m³) N μ σ
3 ≤ IWC 114 23.0 4.0
2 ≤ IWC < 3 2.4K 20.7 6.2
1 ≤ IWC < 2 52K 19.0 6.1
Percentage Occurence (%/bin)
Reflectivity (dBZ)

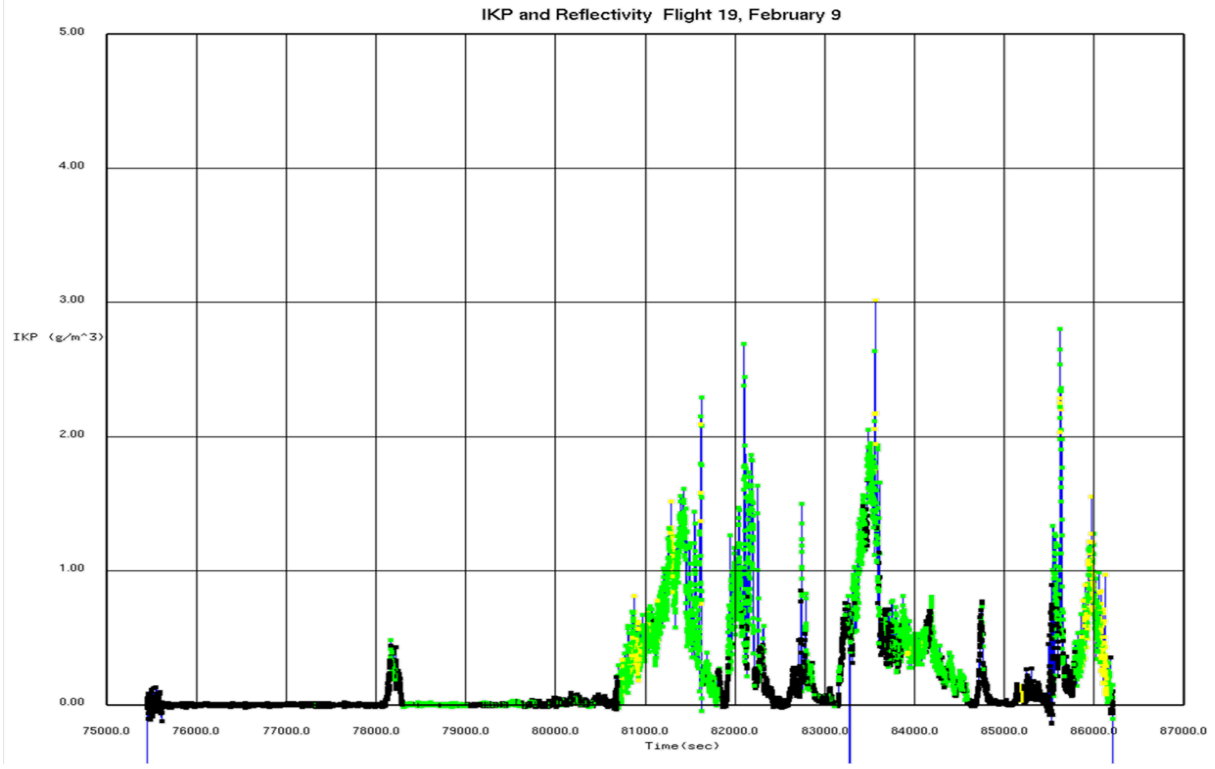
IKP and Reflectivity Flight 19, February 9
IKP (g/m^3)
Time(sec)

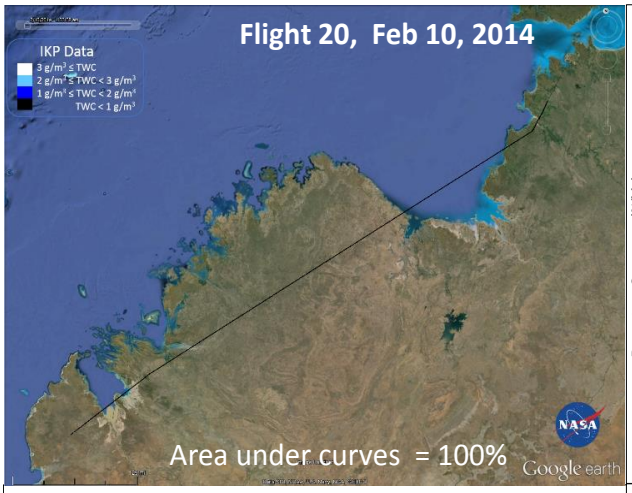
Flight 20, Feb 10, 2014
IKP Data
3 g/m³ ≤ TWC
2 g/m³ ≤ TWC < 3 g/m³
1 g/m³ ≤ TWC < 2 g/m³
TWC < 1 g/m³
Area under curves = 100%
NASA
Google earth

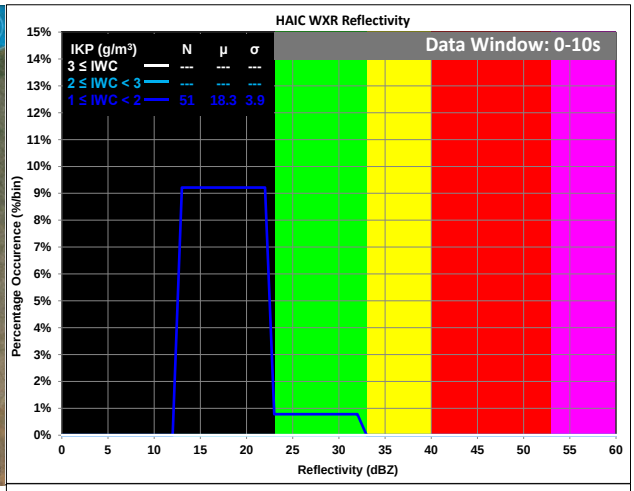
HAIC WXR Reflectivity
Data Window: 0-10s
IKP (g/m³) N μ σ
3 ≤ IWC --- --- ---
2 ≤ IWC < 3 --- --- ---
1 ≤ IWC < 2 51 18.3 3.9
Percentage Occurence (%/bin)
Reflectivity (dBZ)

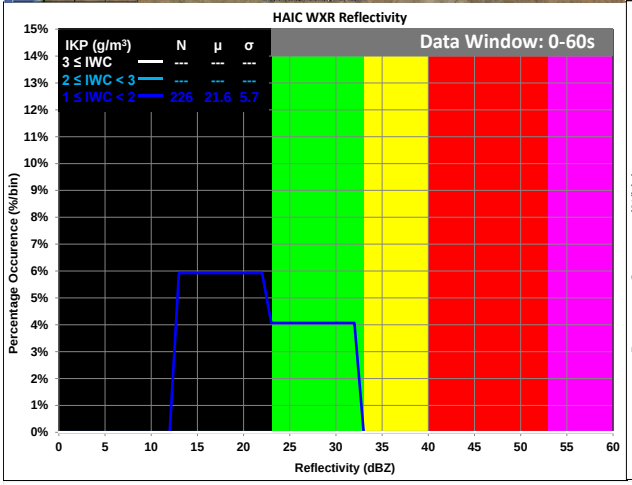
HAIC WXR Reflectivity
Data Window: 0-60s
IKP (g/m³) N μ σ
3 ≤ IWC --- --- ---
2 ≤ IWC < 3 --- --- ---
1 ≤ IWC < 2 226 21.6 5.7
Percentage Occurence (%/bin)
Reflectivity (dBZ)

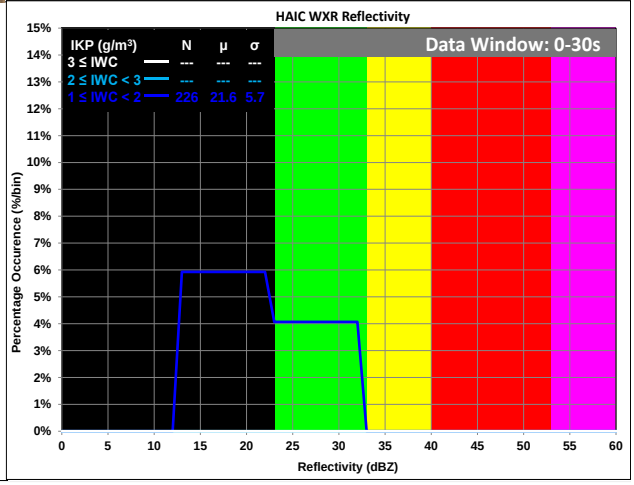
HAIC WXR Reflectivity
Data Window: 0-30s
IKP (g/m³) N μ σ
3 ≤ IWC --- --- ---
2 ≤ IWC < 3 --- --- ---
1 ≤ IWC < 2 226 21.6 5.7
Percentage Occurence (%/bin)
Reflectivity (dBZ)

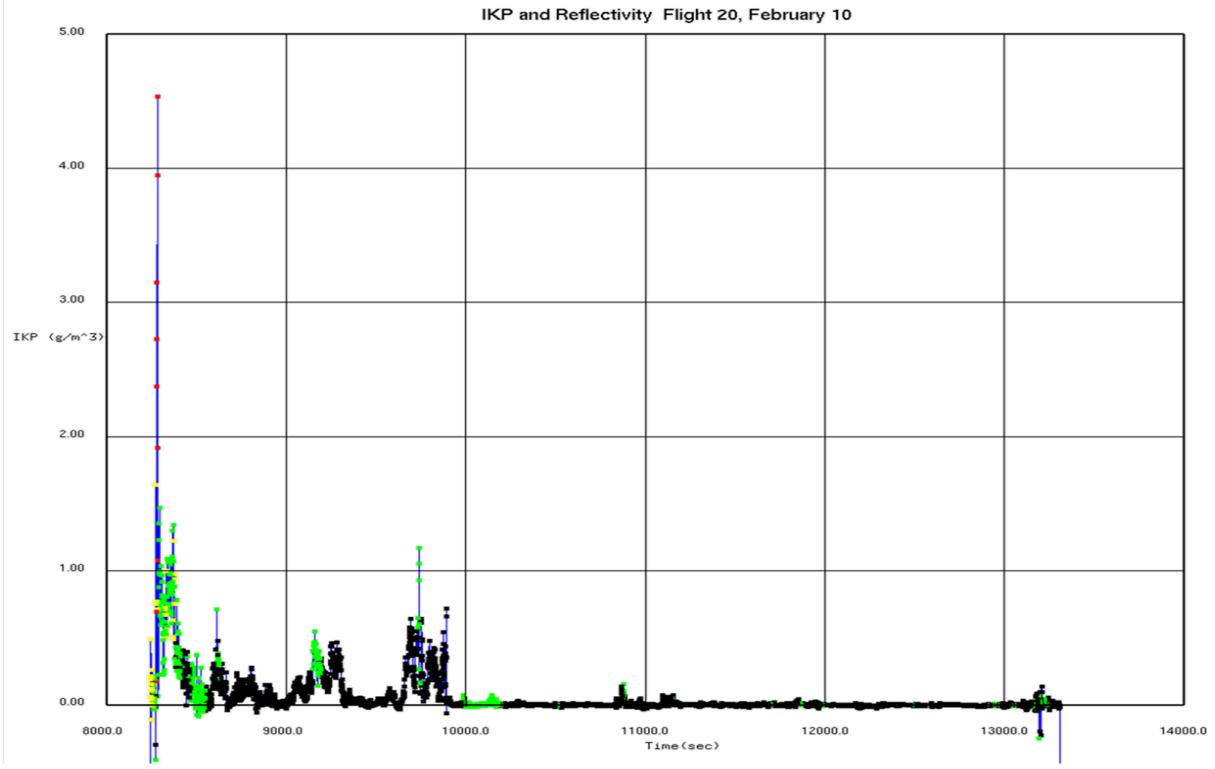
IKP and Reflectivity Flight 20, February 10
IKP (g/m^3)
Time(sec)

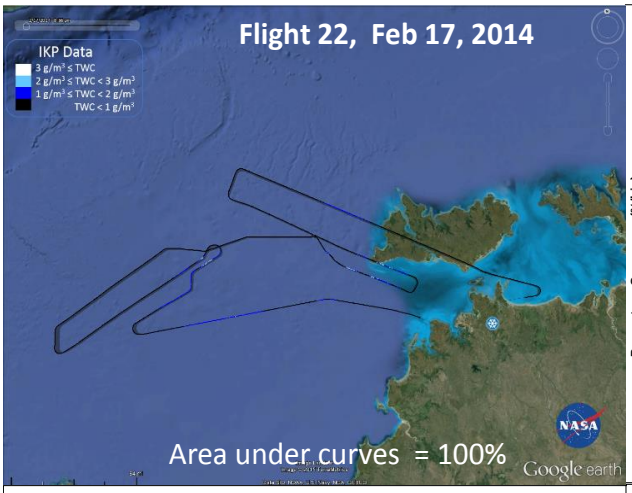
Flight 22, Feb 17, 2014
IKP Data
3 g/m³ ≤ TWC
2 g/m³ ≤ TWC < 3 g/m³
1 g/m³ ≤ TWC < 2 g/m³
TWC < 1 g/m³
Area under curves = 100%
NASA
Google earth

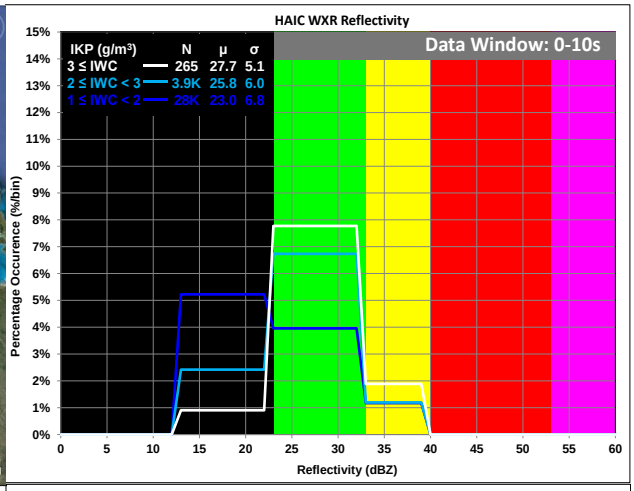
HAIC WXR Reflectivity
Data Window: 0-10s
IKP (g/m³) N μ σ
3 ≤ IWC 265 27.7 5.1
2 ≤ IWC < 3 3.9K 25.8 6.0
1 ≤ IWC < 2 28K 23.0 6.8
Percentage Occurence (%/bin)
Reflectivity (dBZ)

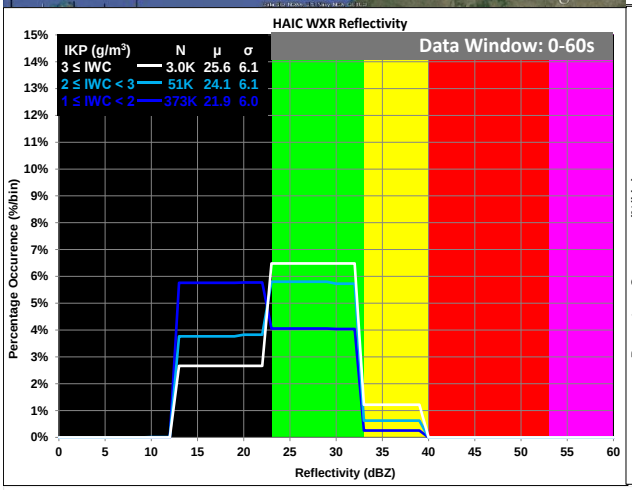
HAIC WXR Reflectivity
Data Window: 0-60s
IKP (g/m³) N μ σ
3 ≤ IWC 3.0K 25.6 6.1
2 ≤ IWC < 3 51K 24.1 6.1
1 ≤ IWC < 2 373K 21.9 6.0
Percentage Occurence (%/bin)
Reflectivity (dBZ)

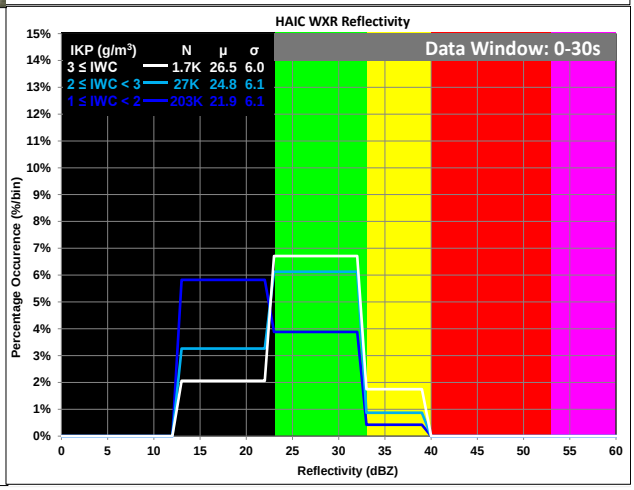
HAIC WXR Reflectivity
Data Window: 0-30s
IKP (g/m³) N μ σ
3 ≤ IWC 1.7K 26.5 6.0
2 ≤ IWC < 3 27K 24.8 6.1
1 ≤ IWC < 2 203K 21.9 6.1
Percentage Occurence (%/bin)
Reflectivity (dBZ)

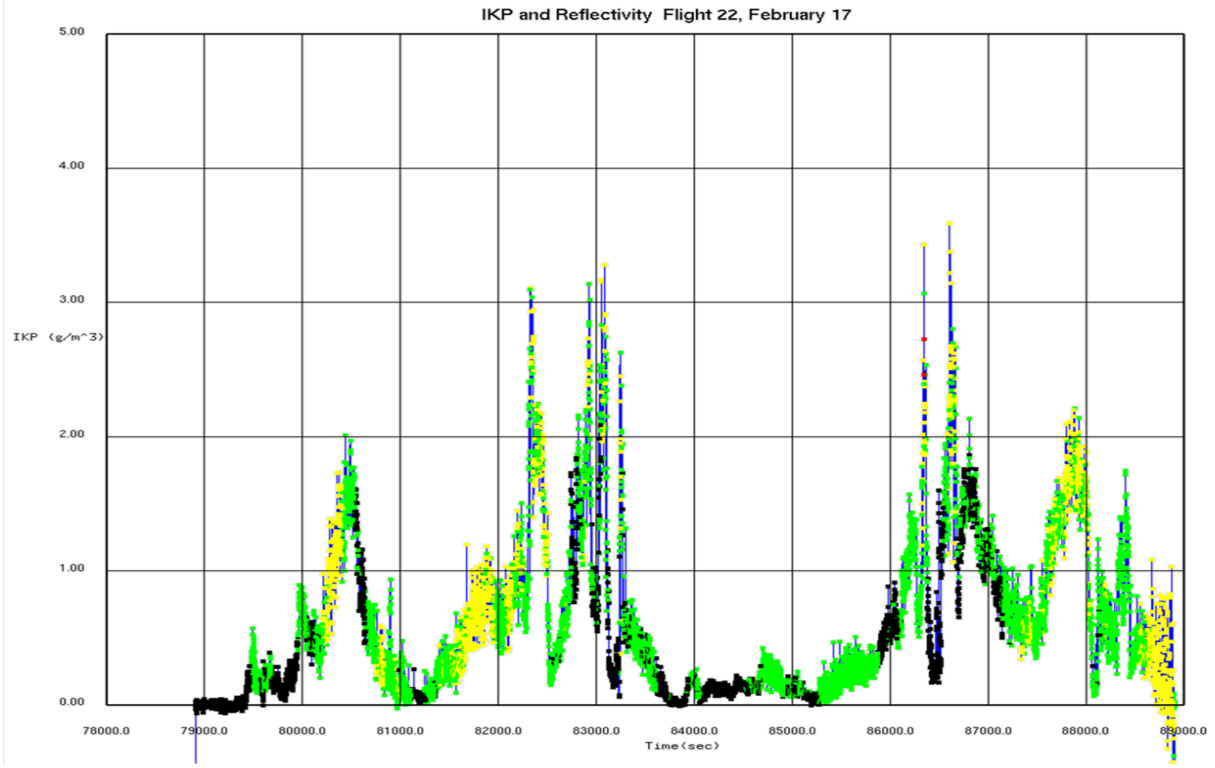
IKP and Reflectivity Flight 22, February 17
IKP (g/m^3)
Time(sec)

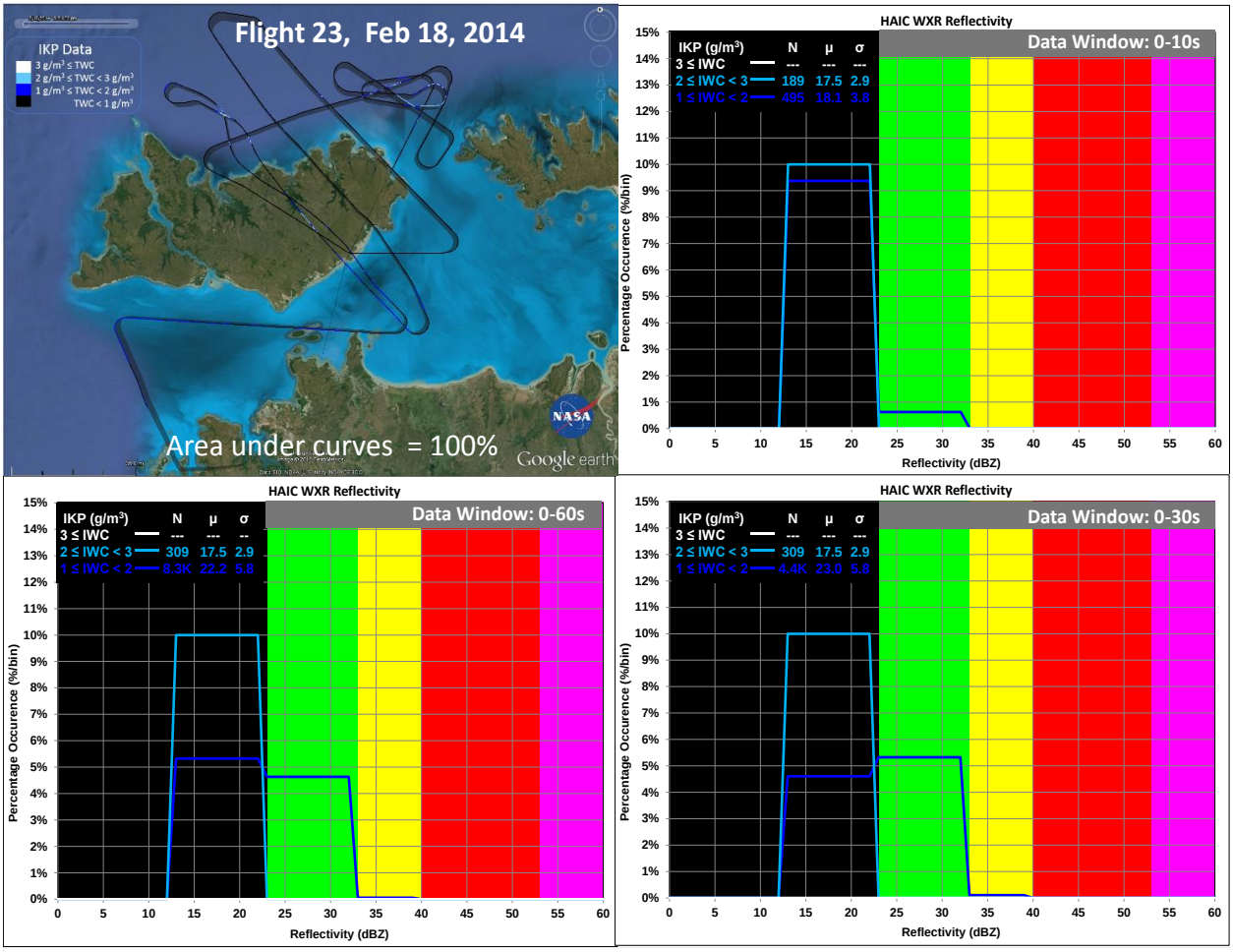
Flight 23, Feb 18, 2014
IKP Data
3 g/m³ ≤ TWC
2 g/m³ ≤ TWC < 3 g/m³
1 g/m³ ≤ TWC < 2 g/m³
TWC < 1 g/m³
Area under curves = 100%
Google earth
HAIC WXR Reflectivity
Data Window: 0-10s
IKP (g/m³) N μ σ
3 ≤ IWC --- --- ---
2 ≤ IWC < 3 189 17.5 2.9
1 ≤ IWC < 2 495 18.1 3.8
Percentage Occurence (%/bin)
Reflectivity (dBZ)
HAIC WXR Reflectivity
Data Window: 0-60s
IKP (g/m³) N μ σ
3 ≤ IWC --- --- --
2 ≤ IWC < 3 309 17.5 2.9
1 ≤ IWC < 2 8.3K 22.2 5.8
Percentage Occurence (%/bin)
Reflectivity (dBZ)
HAIC WXR Reflectivity
Data Window: 0-30s
IKP (g/m³) N μ σ
3 ≤ IWC --- --- ---
2 ≤ IWC < 3 309 17.5 2.9
1 ≤ IWC < 2 4.4K 23.0 5.8
Percentage Occurence (%/bin)
Reflectivity (dBZ)

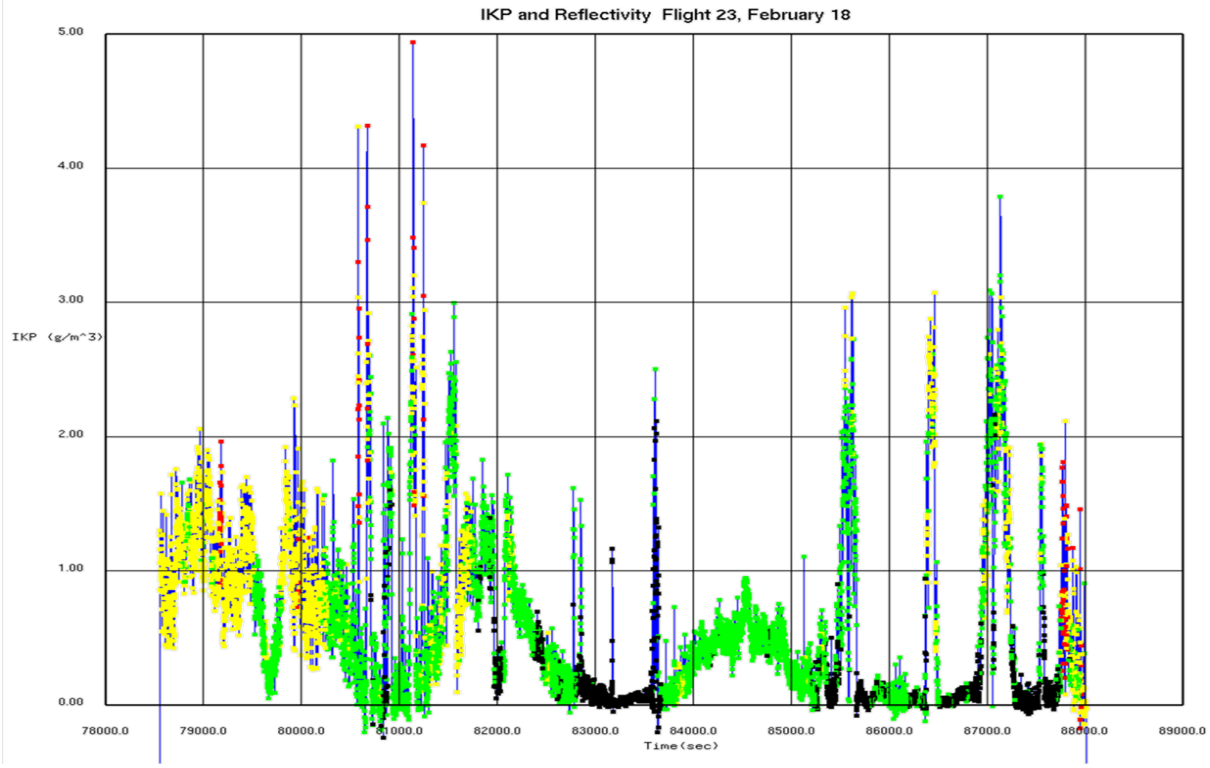
IKP and Reflectivity Flight 23, February 18
IKP (g/m^3)
Time(sec)

The follow series of histograms and line plots are from flights near Cayenne, French Guiana in 2015. The first chart (below) is a summary for all flights; subsequent pages are the results for each daily flight. Unless indicated otherwise, line plots have a maximum value of 5g/m^3 for the IWC axis.

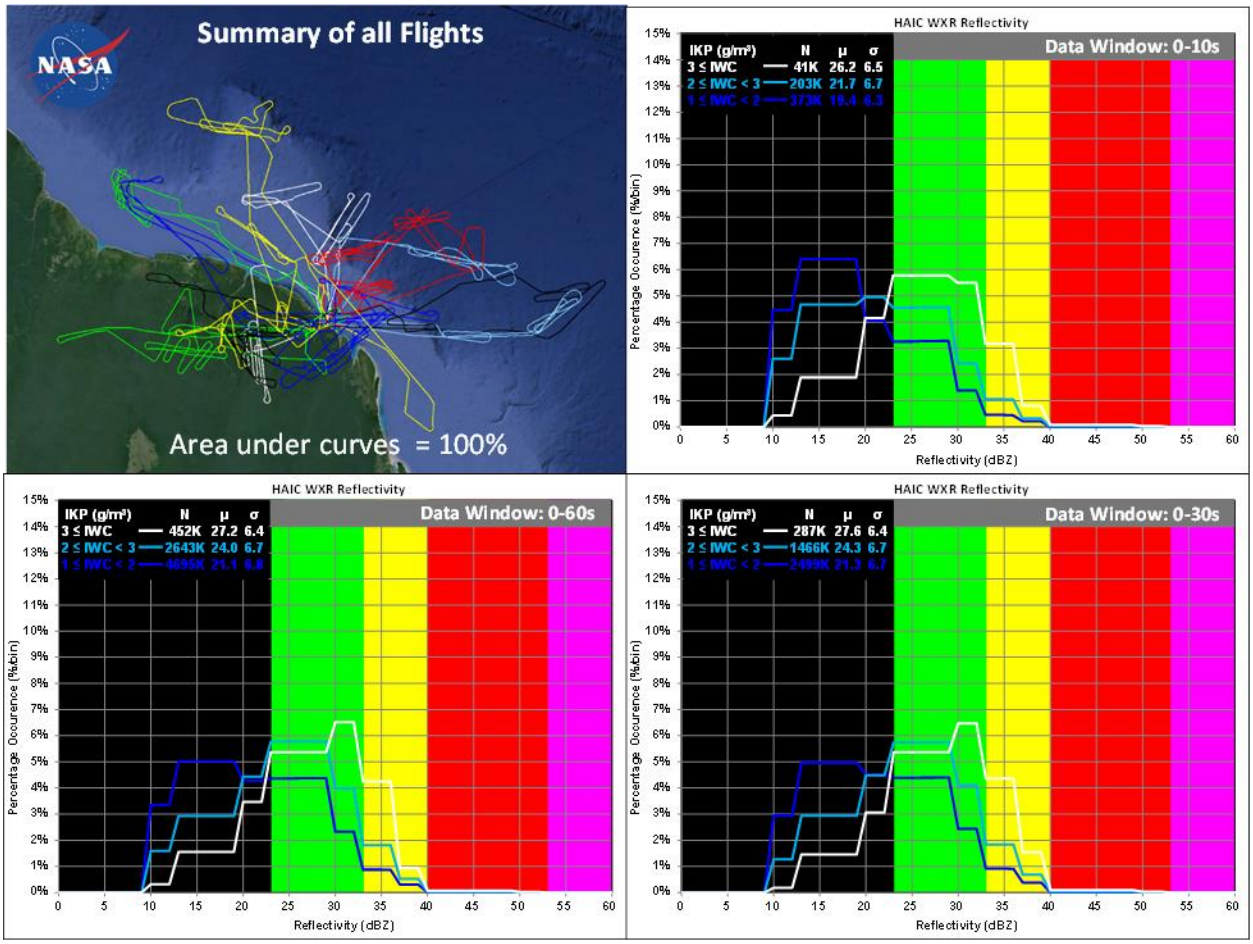

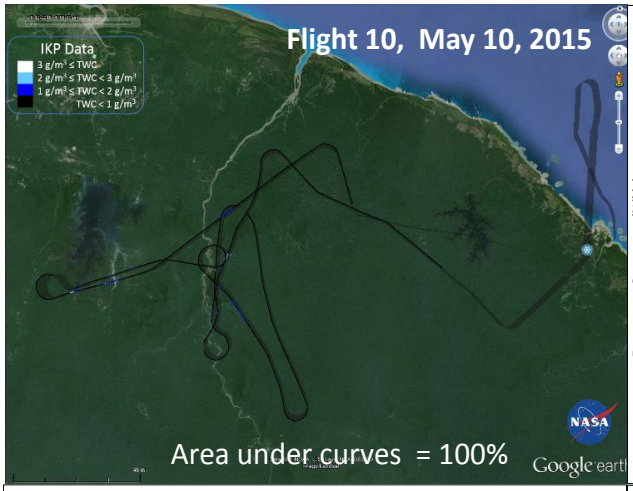
Flight 10, May 10, 2015
IKP Data
3 g/m³ ≤ TWC
2 g/m³ ≤ TWC < 3 g/m³
1 g/m³ ≤ TWC < 2 g/m³
TWC < 1 g/m³
Area under curves = 100%
NASA
Google earth

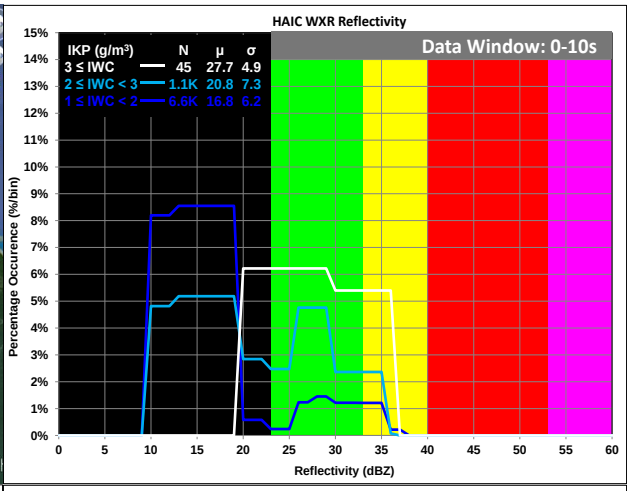
HAIC WXR Reflectivity
Data Window: 0-10s
IKP (g/m³) N μ σ
3 ≤ IWC 45 27.7 4.9
2 ≤ IWC < 3 1.1K 20.8 7.3
1 ≤ IWC < 2 6.6K 16.8 6.2
Percentage Occurence (%/bin)
Reflectivity (dBZ)

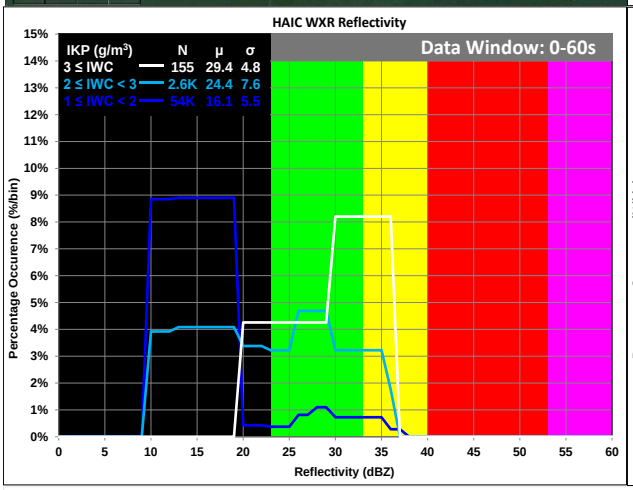
HAIC WXR Reflectivity
Data Window: 0-60s
IKP (g/m³) N μ σ
3 ≤ IWC 155 29.4 4.8
2 ≤ IWC < 3 2.6K 24.4 7.6
1 ≤ IWC < 2 54K 16.1 5.5
Percentage Occurence (%/bin)
Reflectivity (dBZ)

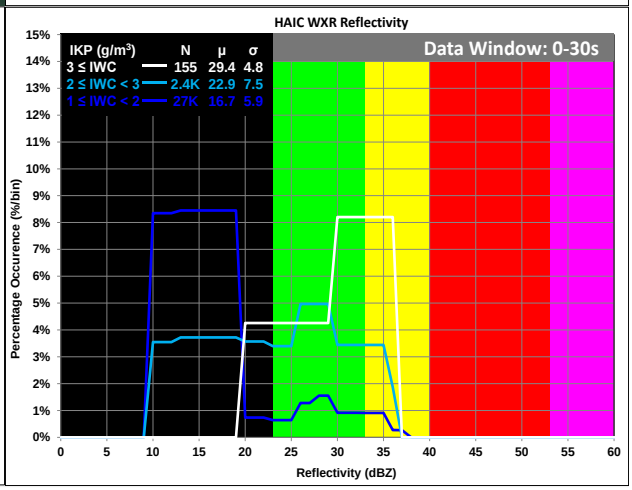
HAIC WXR Reflectivity
Data Window: 0-30s
IKP (g/m³) N μ σ
3 ≤ IWC 155 29.4 4.8
2 ≤ IWC < 3 2.4K 22.9 7.5
1 ≤ IWC < 2 27K 16.7 5.9
Percentage Occurence (%/bin)
Reflectivity (dBZ)

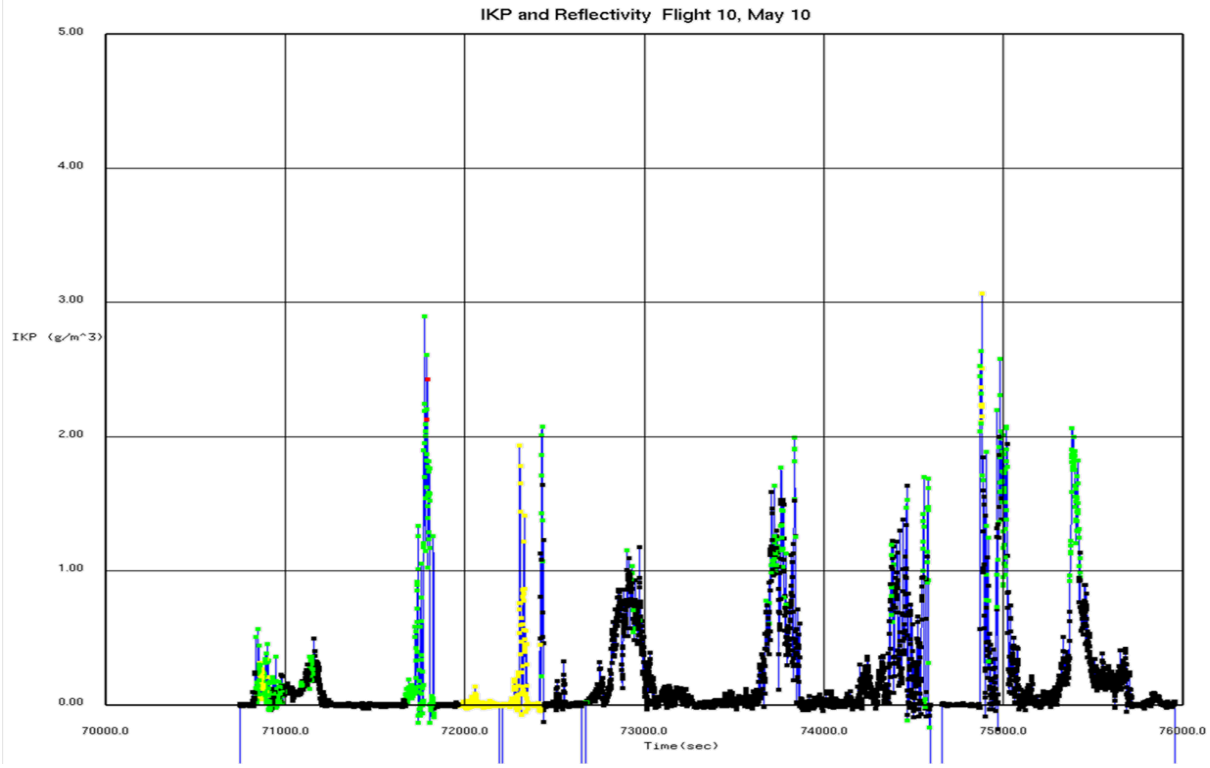
IKP and Reflectivity Flight 10, May 10
IKP (g/m^3)
Time(sec)

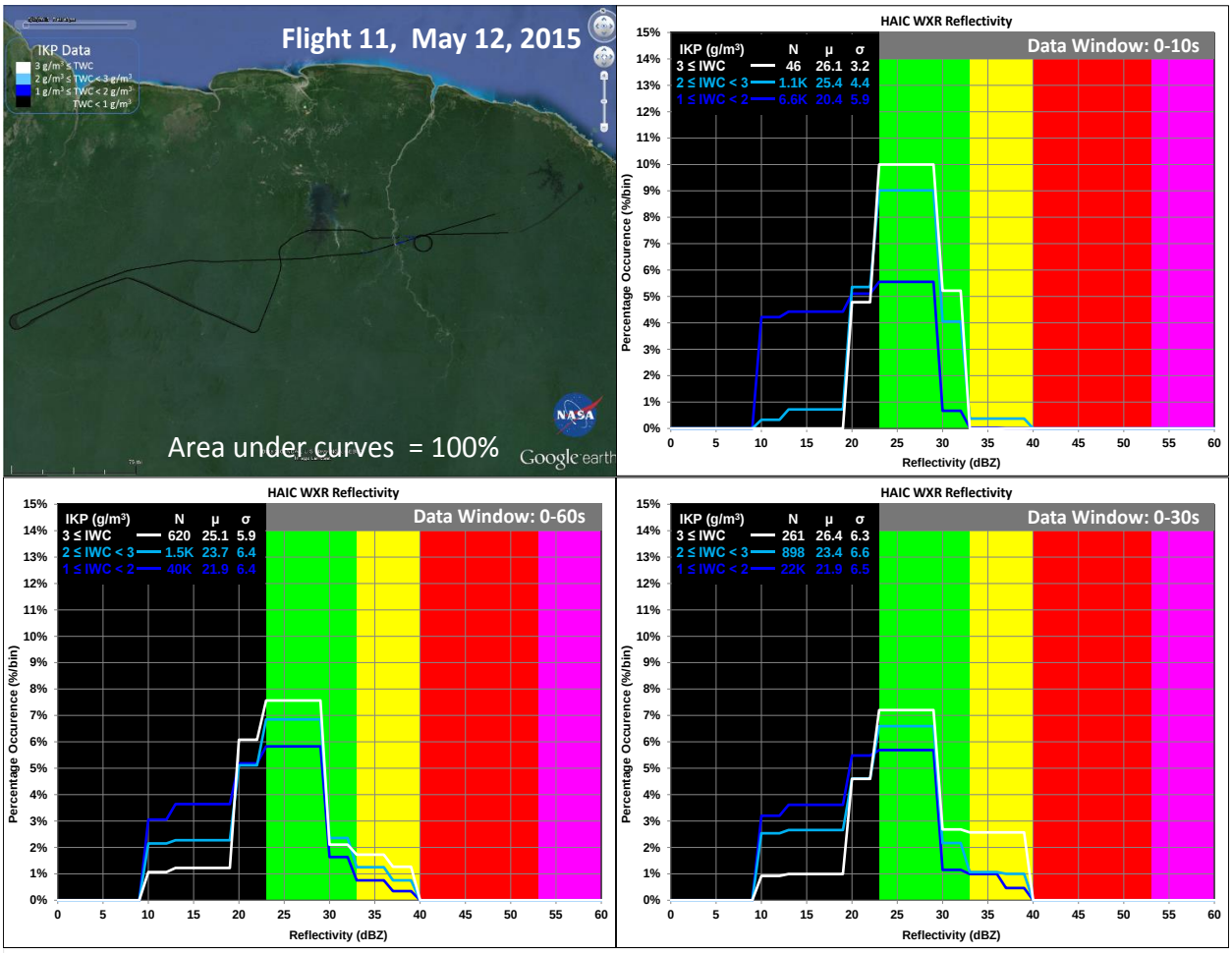
Flight 11, May 12, 2015
IKP Data
3 g/m³ ≤ TWC
2 g/m³ ≤ TWC < 3 g/m³
1 g/m³ ≤ TWC < 2 g/m³
TWC < 1 g/m³
Area under curves = 100%
Google earth
HAIC WXR Reflectivity
Data Window: 0-10s
IKP (g/m³) N μ σ
3 ≤ IWC 46 26.1 3.2
2 ≤ IWC < 3 1.1K 25.4 4.4
1 ≤ IWC < 2 6.6K 20.4 5.9
Percentage Occurence (%/bin)
Reflectivity (dBZ)
HAIC WXR Reflectivity
Data Window: 0-60s
IKP (g/m³) N μ σ
3 ≤ IWC 620 25.1 5.9
2 ≤ IWC < 3 1.5K 23.7 6.4
1 ≤ IWC < 2 40K 21.9 6.4
Percentage Occurence (%/bin)
Reflectivity (dBZ)
HAIC WXR Reflectivity
Data Window: 0-30s
IKP (g/m³) N μ σ
3 ≤ IWC 261 26.4 6.3
2 ≤ IWC < 3 898 23.4 6.6
1 ≤ IWC < 2 22K 21.9 6.5
Percentage Occurence (%/bin)
Reflectivity (dBZ)

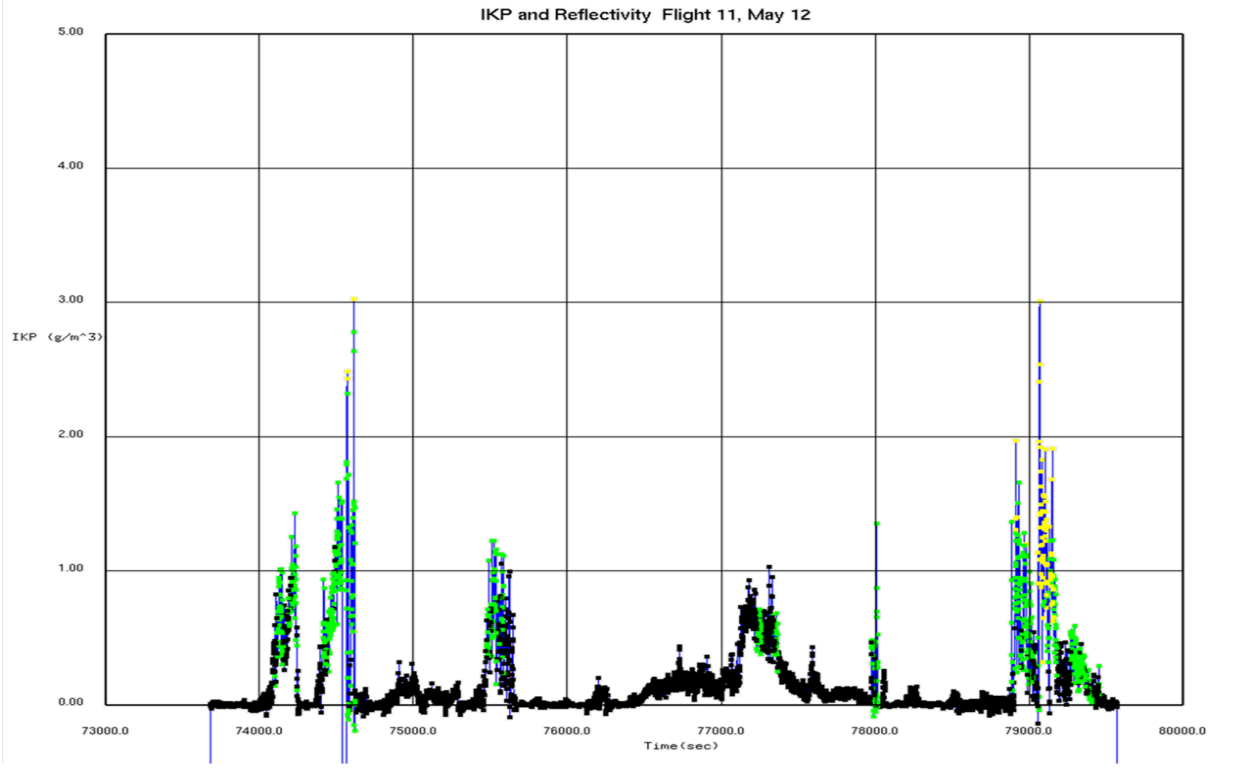
IKP and Reflectivity Flight 11, May 12
IKP (g/m^3)
Time(sec)

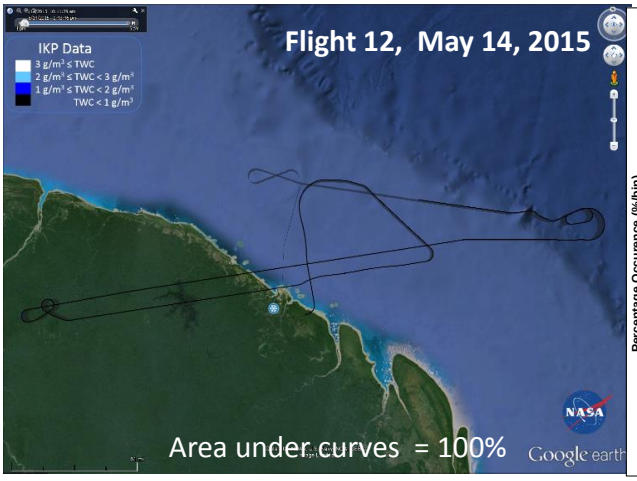
Flight 12, May 14, 2015
IKP Data
3 g/m³ ≤ TWC
2 g/m³ ≤ TWC < 3 g/m³
1 g/m³ ≤ TWC < 2 g/m³
TWC < 1 g/m³
Area under curves = 100%
NASA
Google earth

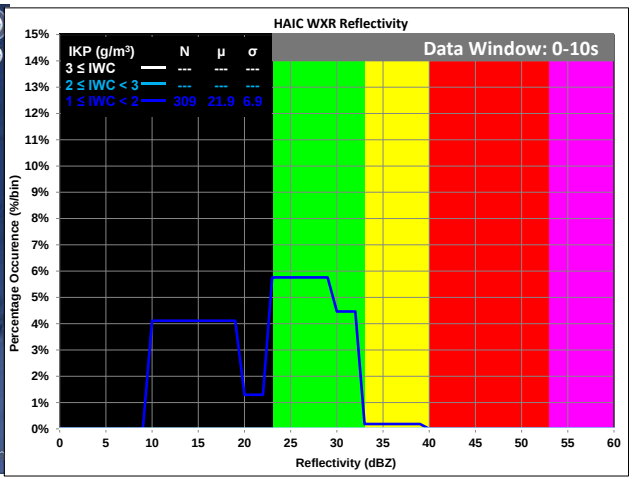
HAIC WXR Reflectivity
Data Window: 0-10s
IKP (g/m³) N μ σ
3 ≤ IWC --- --- ---
2 ≤ IWC < 3 --- --- ---
1 ≤ IWC < 2 309 21.9 6.9
Percentage Occurence (%/bin)
Reflectivity (dBZ)

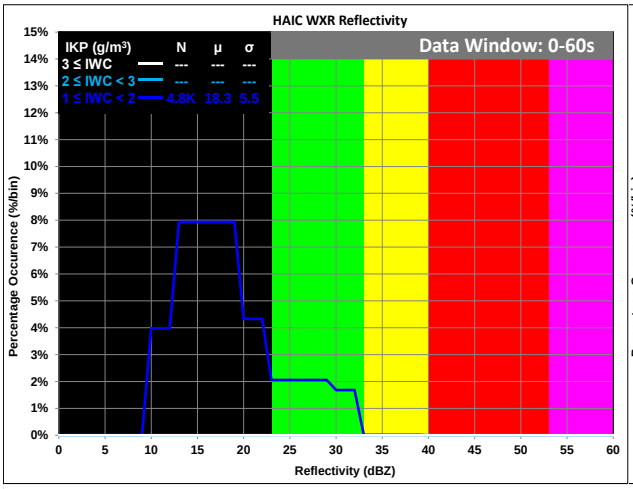
HAIC WXR Reflectivity
Data Window: 0-60s
IKP (g/m³) N μ σ
3 ≤ IWC --- --- ---
2 ≤ IWC < 3 --- --- ---
1 ≤ IWC < 2 4.8K 18.3 5.5
Percentage Occurence (%/bin)
Reflectivity (dBZ)

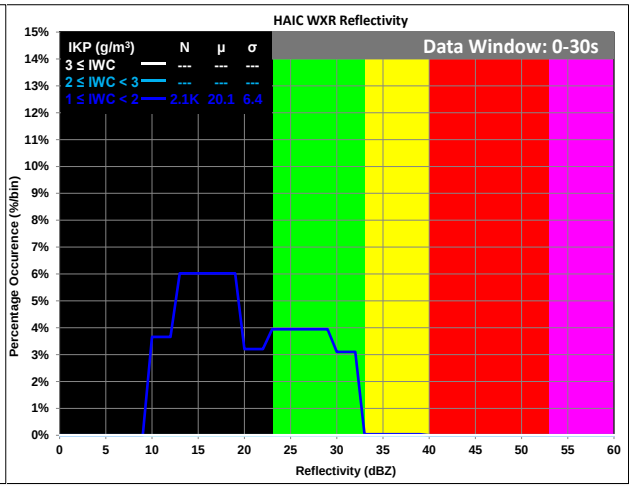
HAIC WXR Reflectivity
Data Window: 0-30s
IKP (g/m³) N μ σ
3 ≤ IWC --- --- ---
2 ≤ IWC < 3 --- --- ---
1 ≤ IWC < 2 2.1K 20.1 6.4
Percentage Occurence (%/bin)
Reflectivity (dBZ)

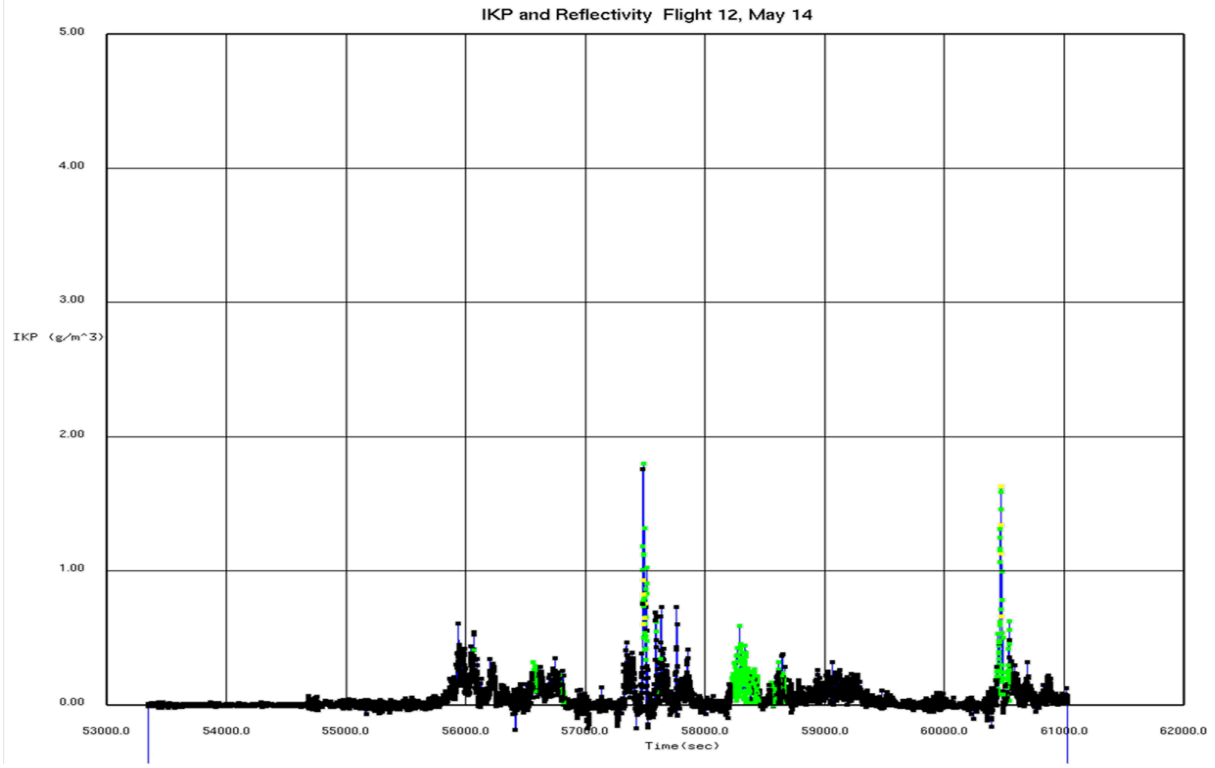
IKP and Reflectivity Flight 12, May 14
IKP (g/m^3)
Time(sec)

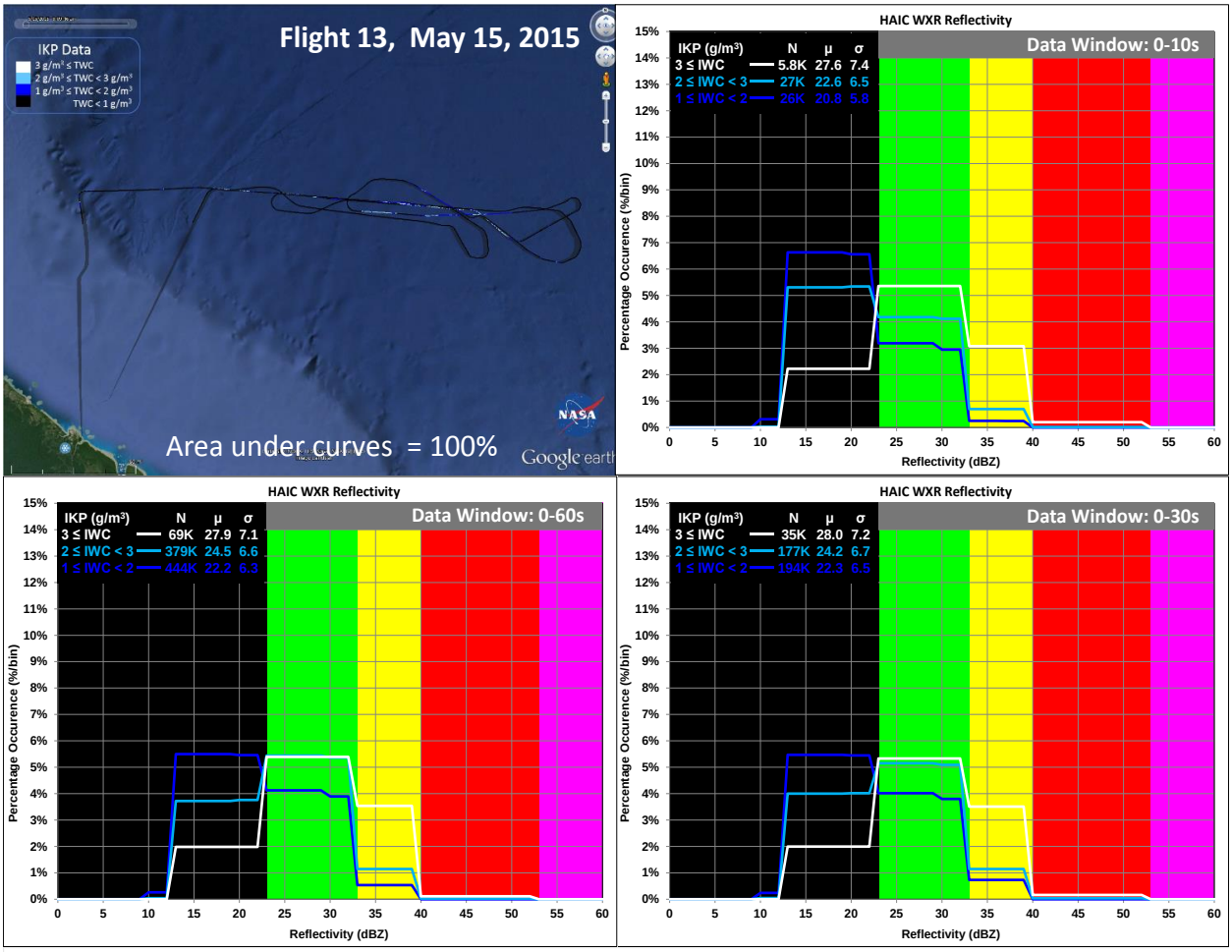
Flight 13, May 15, 2015
IKP Data
3 g/m³ ≤ TWC
2 g/m³ ≤ TWC < 3 g/m³
1 g/m³ ≤ TWC < 2 g/m³
TWC < 1 g/m³
Area under curves = 100%
Google earth
HAIC WXR Reflectivity
Data Window: 0-10s
IKP (g/m³) N μ σ
3 ≤ IWC 5.8K 27.6 7.4
2 ≤ IWC < 3 27K 22.6 6.5
1 ≤ IWC < 2 26K 20.8 5.8
Percentage Occurence (%/bin)
Reflectivity (dBZ)
HAIC WXR Reflectivity
Data Window: 0-60s
IKP (g/m³) N μ σ
3 ≤ IWC 69K 27.9 7.1
2 ≤ IWC < 3 379K 24.5 6.6
1 ≤ IWC < 2 444K 22.2 6.3
Percentage Occurence (%/bin)
Reflectivity (dBZ)
HAIC WXR Reflectivity
Data Window: 0-30s
IKP (g/m³) N μ σ
3 ≤ IWC 35K 28.0 7.2
2 ≤ IWC < 3 177K 24.2 6.7
1 ≤ IWC < 2 194K 22.3 6.5
Percentage Occurence (%/bin)
Reflectivity (dBZ)

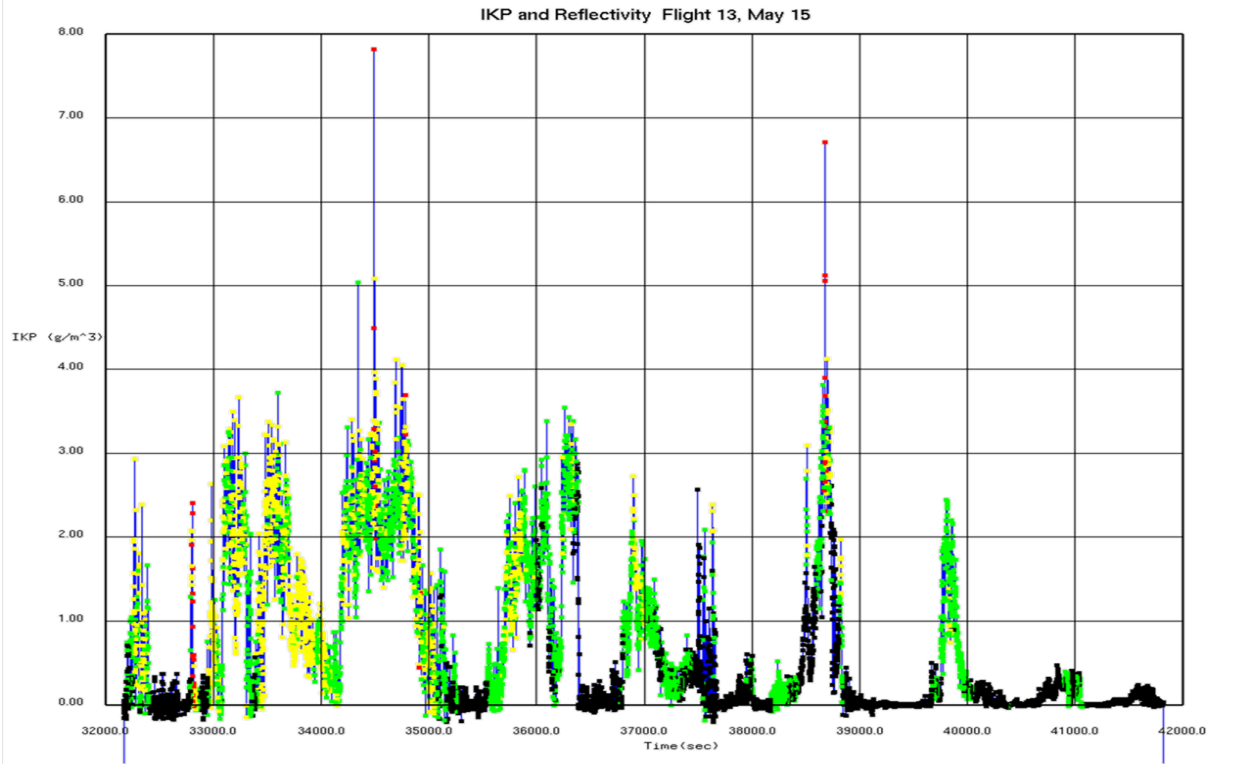
IKP and Reflectivity Flight 13, May 15
IKP (g/m^3)
Time(sec)

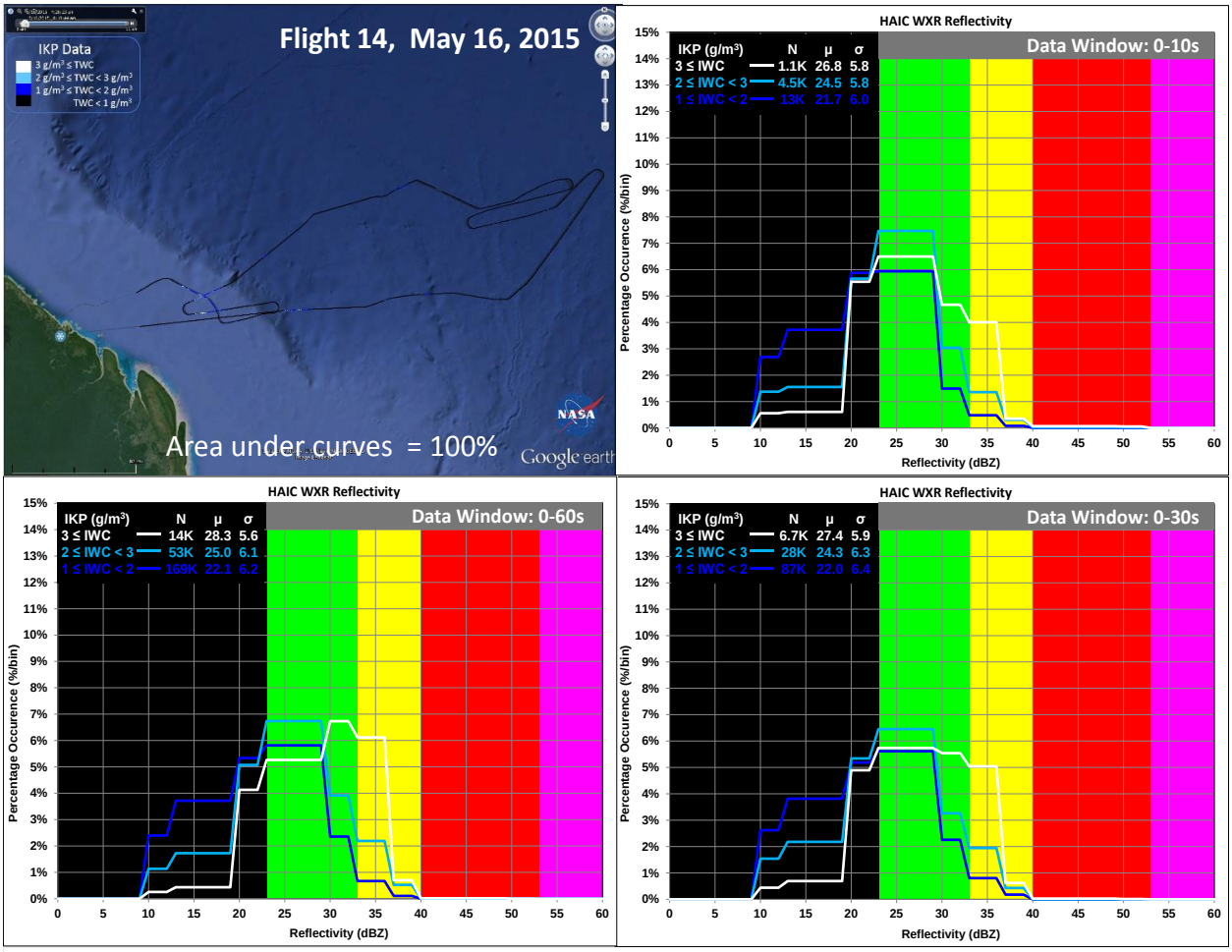
Flight 14, May 16, 2015
IKP Data
3 g/m³ ≤ TWC
2 g/m³ ≤ TWC < 3 g/m³
1 g/m³ ≤ TWC < 2 g/m³
TWC < 1 g/m³
Area under curves = 100%
Google earth
HAIC WXR Reflectivity
Data Window: 0-10s
IKP (g/m³) N μ σ
3 ≤ IWC 1.1K 26.8 5.8
2 ≤ IWC < 3 4.5K 24.5 5.8
1 ≤ IWC < 2 13K 21.7 6.0
Percentage Occurence (%/bin)
Reflectivity (dBZ)
HAIC WXR Reflectivity
Data Window: 0-60s
IKP (g/m³) N μ σ
3 ≤ IWC 14K 28.3 5.6
2 ≤ IWC < 3 53K 25.0 6.1
1 ≤ IWC < 2 169K 22.1 6.2
Percentage Occurence (%/bin)
Reflectivity (dBZ)
HAIC WXR Reflectivity
Data Window: 0-30s
IKP (g/m³) N μ σ
3 ≤ IWC 6.7K 27.4 5.9
2 ≤ IWC < 3 28K 24.3 6.3
1 ≤ IWC < 2 87K 22.0 6.4
Percentage Occurence (%/bin)
Reflectivity (dBZ)

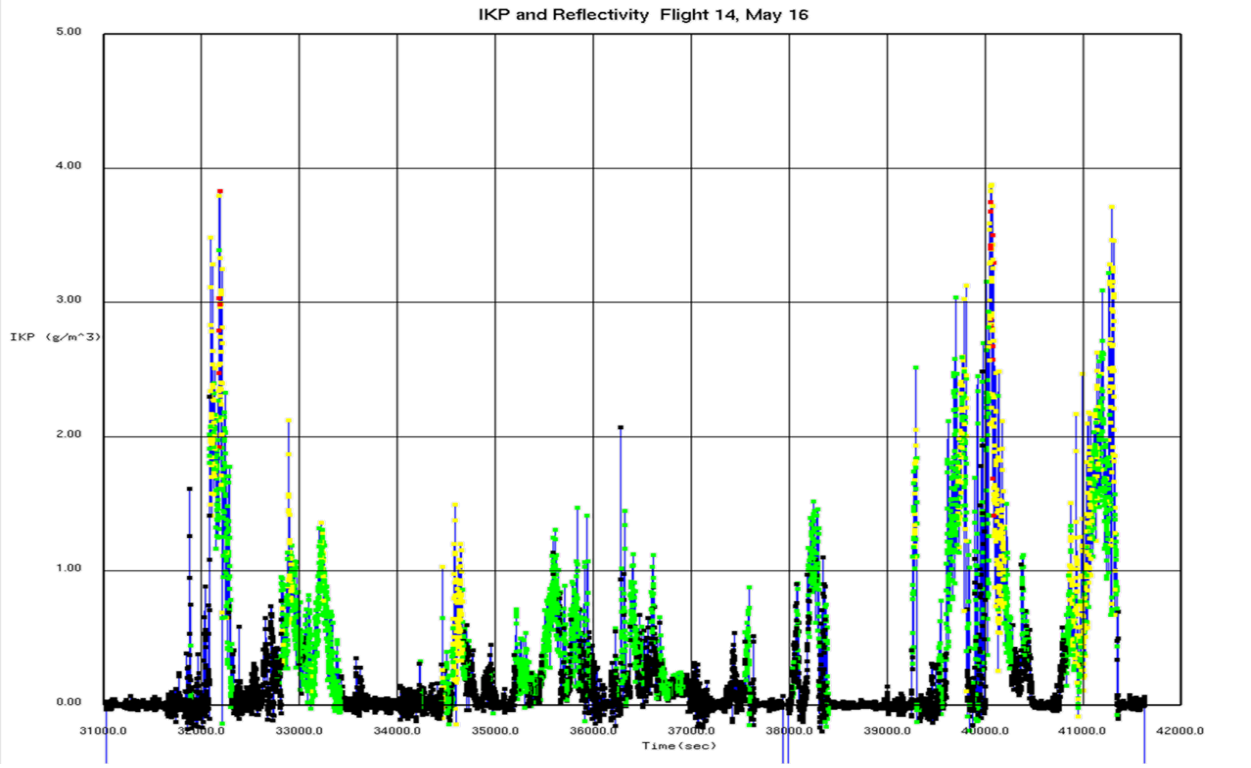
IKP and Reflectivity Flight 14, May 16
IKP (g/m^3)
Time(sec)

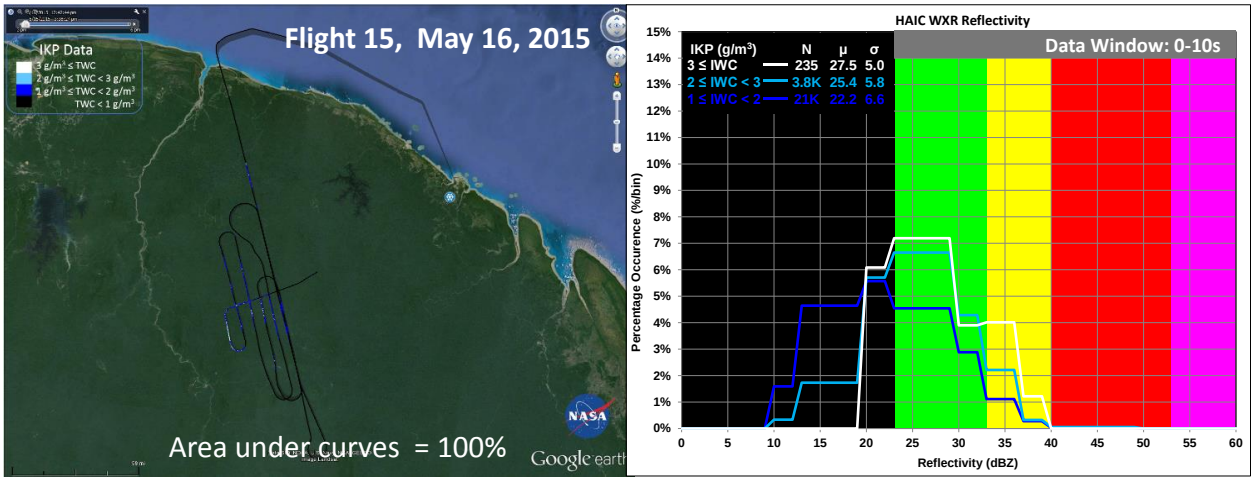
Flight 15, May 16, 2015
IKP Data
3 g/m³ ≤ TWC
2 g/m³ ≤ TWC < 3 g/m³
1 g/m³ ≤ TWC < 2 g/m³
TWC < 1 g/m³
Area under curves = 100%
Google earth
HAIC WXR Reflectivity
Data Window: 0-10s
IKP (g/m³) N μ σ
3 ≤ IWC 235 27.5 5.0
2 ≤ IWC < 3 3.8K 25.4 5.8
1 ≤ IWC < 2 21K 22.2 6.6
Percentage Occurence (%/bin)
Reflectivity (dBZ)

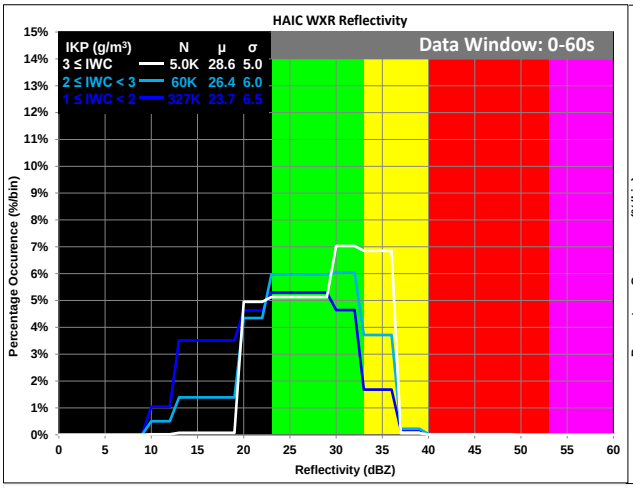
HAIC WXR Reflectivity
Data Window: 0-60s
IKP (g/m³) N μ σ
3 ≤ IWC 5.0K 28.6 5.0
2 ≤ IWC < 3 60K 26.4 6.0
1 ≤ IWC < 2 327K 23.7 6.5
Percentage Occurence (%/bin)
Reflectivity (dBZ)

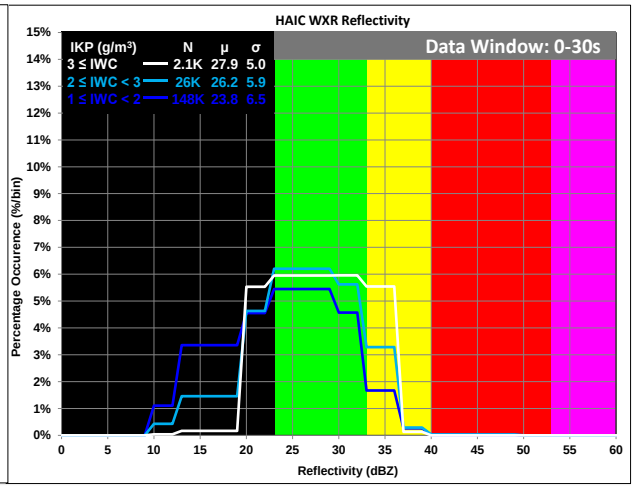
HAIC WXR Reflectivity
Data Window: 0-30s
IKP (g/m³) N μ σ
3 ≤ IWC 2.1K 27.9 5.0
2 ≤ IWC < 3 26K 26.2 5.9
1 ≤ IWC < 2 148K 23.8 6.5
Percentage Occurence (%/bin)
Reflectivity (dBZ)

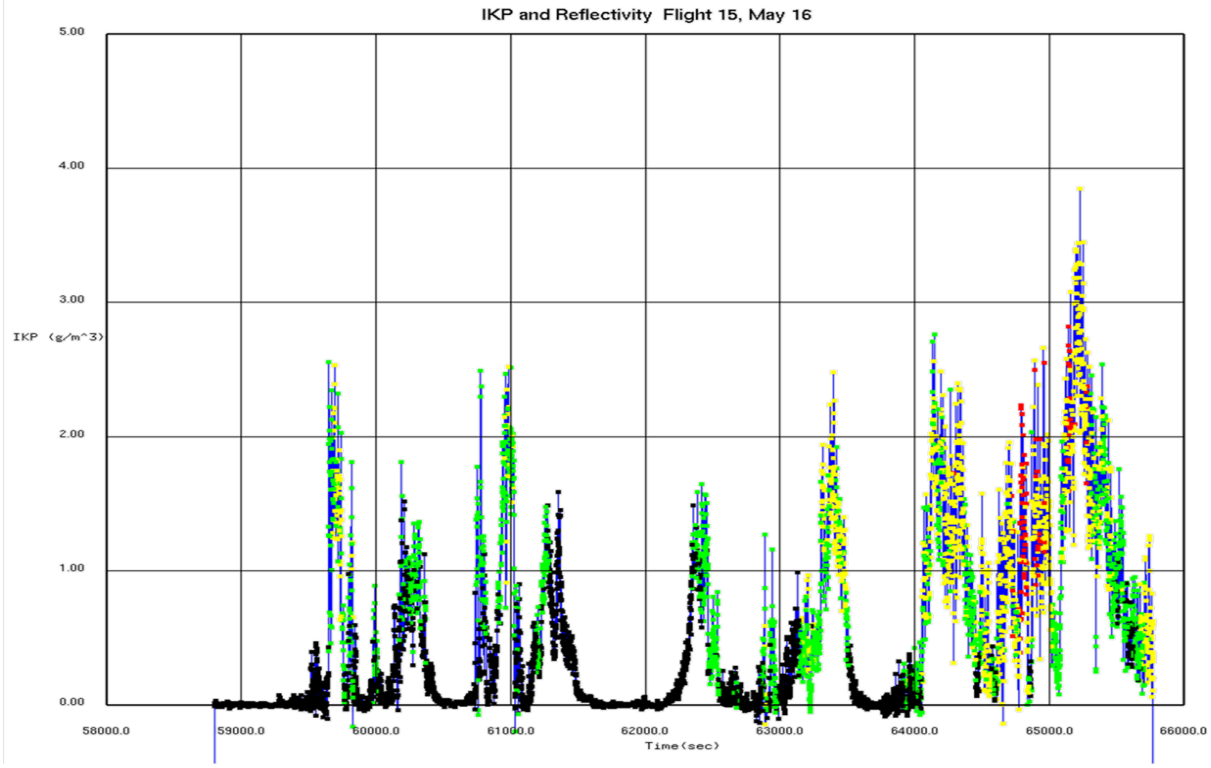
IKP and Reflectivity Flight 15, May 16
IKP (g/m^3)
Time(sec)

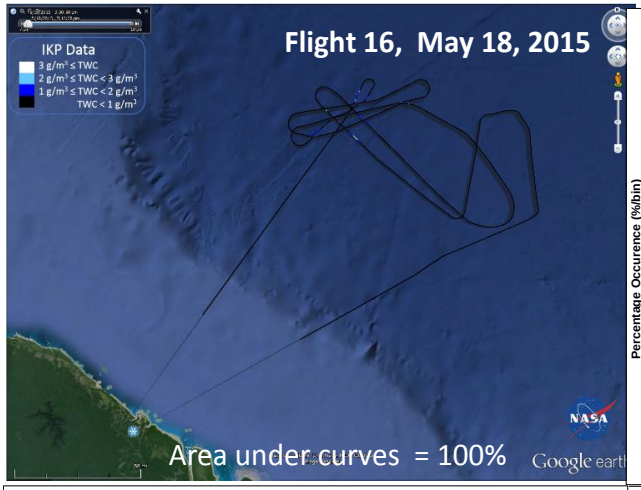
Flight 16, May 18, 2015
IKP Data
3 g/m³ ≤ TWC
2 g/m³ ≤ TWC < 3 g/m³
1 g/m³ ≤ TWC < 2 g/m³
TWC < 1 g/m³
Area under curves = 100%
Google earth

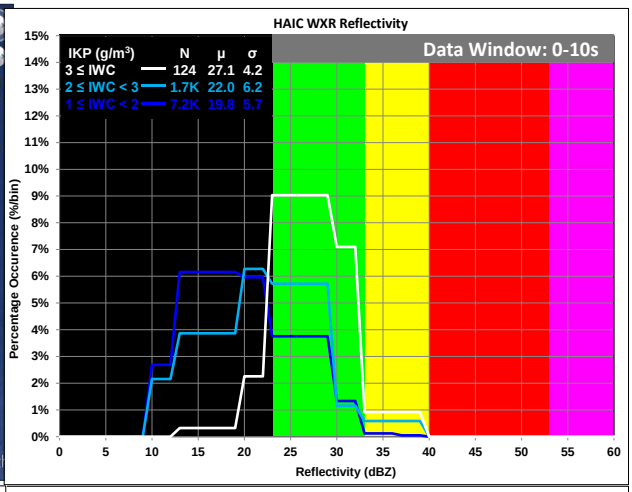
HAIC WXR Reflectivity
Data Window: 0-10s
IKP (g/m³) N μ σ
3 ≤ IWC 124 27.1 4.2
2 ≤ IWC < 3 1.7K 22.0 6.2
1 ≤ IWC < 2 7.2K 19.8 5.7
Percentage Occurence (%/bin)
Reflectivity (dBZ)

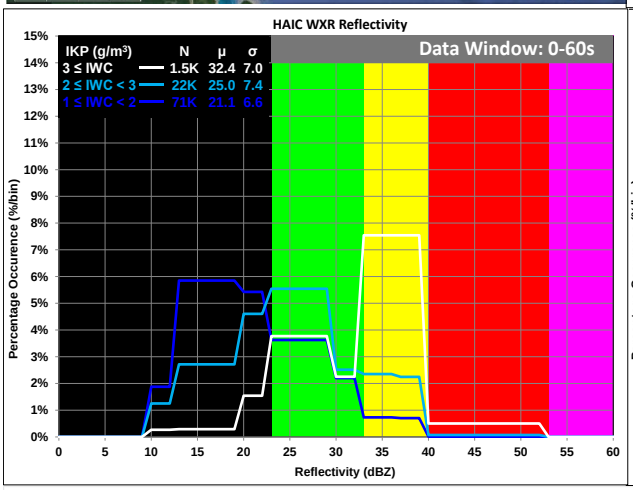
HAIC WXR Reflectivity
Data Window: 0-60s
IKP (g/m³) N μ σ
3 ≤ IWC 1.5K 32.4 7.0
2 ≤ IWC < 3 22K 25.0 7.4
1 ≤ IWC < 2 71K 21.1 6.6
Percentage Occurence (%/bin)
Reflectivity (dBZ)

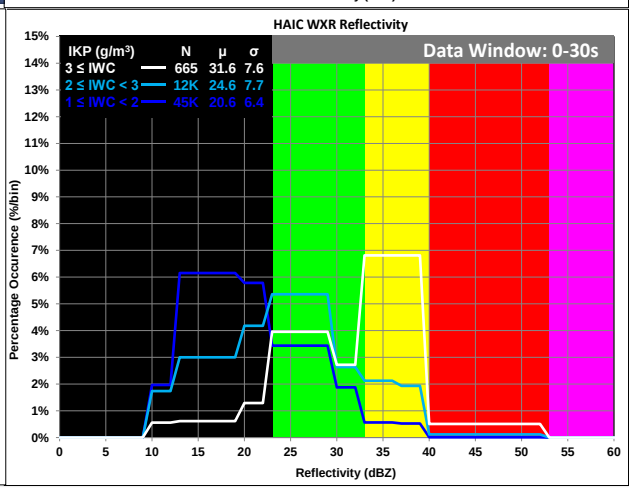
HAIC WXR Reflectivity
Data Window: 0-30s
IKP (g/m³) N μ σ
3 ≤ IWC 665 31.6 7.6
2 ≤ IWC < 3 12K 24.6 7.7
1 ≤ IWC < 2 45K 20.6 6.4
Percentage Occurence (%/bin)
Reflectivity (dBZ)

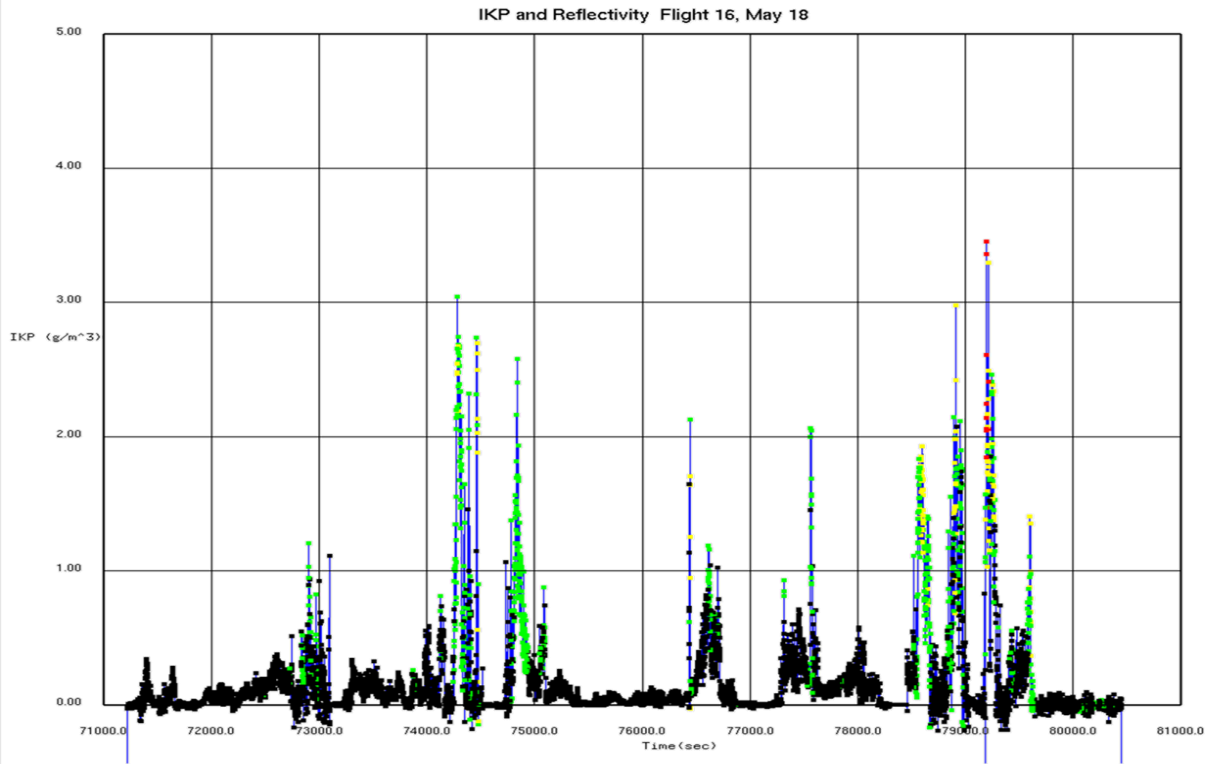
IKP and Reflectivity Flight 16, May 18
IKP (g/m^3)
Time(sec)

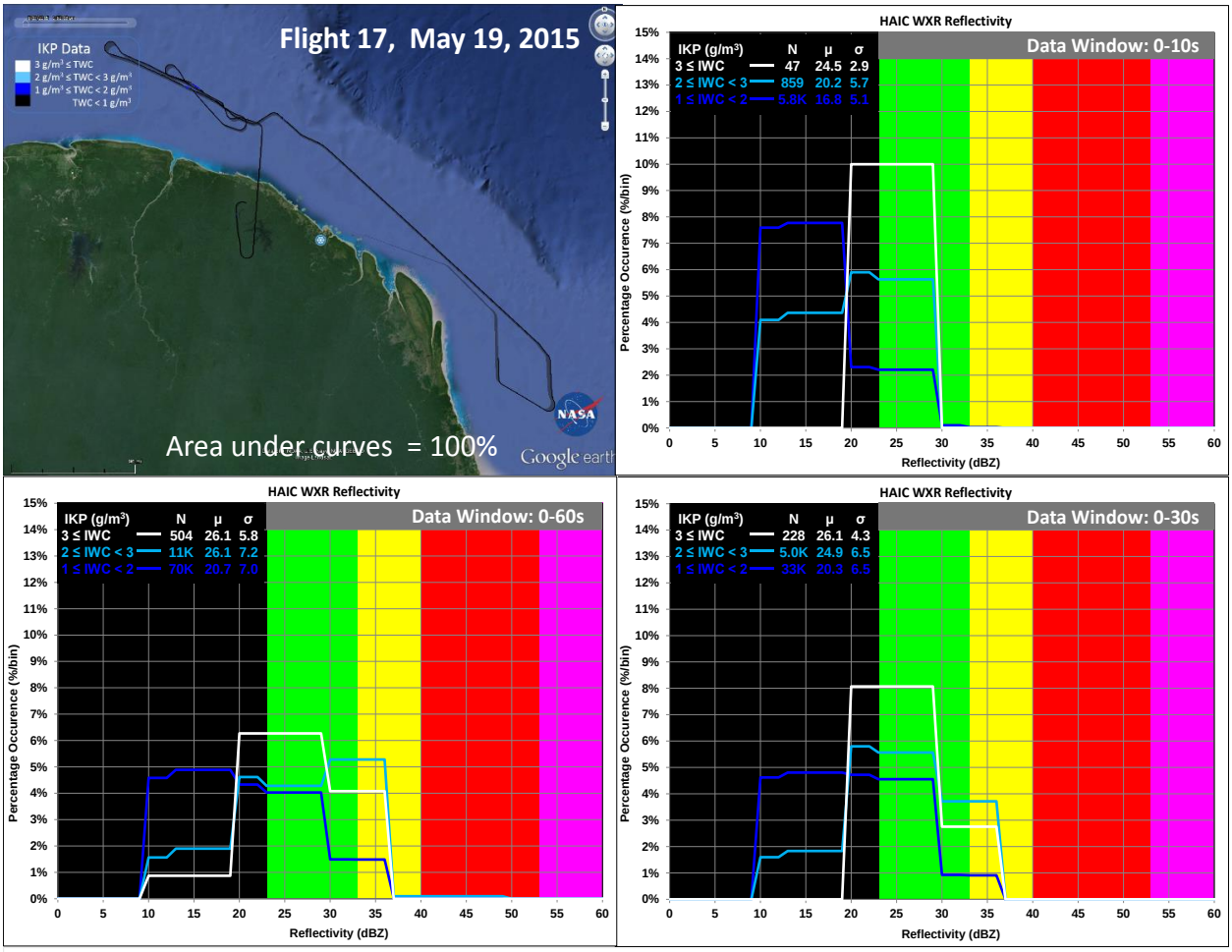
Flight 17, May 19, 2015
IKP Data
3 g/m³ ≤ TWC
2 g/m³ ≤ TWC < 3 g/m³
1 g/m³ ≤ TWC < 2 g/m³
TWC < 1 g/m³
Area under curves = 100%
Google earth
HAIC WXR Reflectivity
Data Window: 0-10s
IKP (g/m³) N μ σ
3 ≤ IWC 47 24.5 2.9
2 ≤ IWC < 3 859 20.2 5.7
1 ≤ IWC < 2 5.8K 16.8 5.1
Percentage Occurence (%/bin)
Reflectivity (dBZ)
HAIC WXR Reflectivity
Data Window: 0-60s
IKP (g/m³) N μ σ
3 ≤ IWC 504 26.1 5.8
2 ≤ IWC < 3 11K 26.1 7.2
1 ≤ IWC < 2 70K 20.7 7.0
Percentage Occurence (%/bin)
Reflectivity (dBZ)
HAIC WXR Reflectivity
Data Window: 0-30s
IKP (g/m³) N μ σ
3 ≤ IWC 228 26.1 4.3
2 ≤ IWC < 3 5.0K 24.9 6.5
1 ≤ IWC < 2 33K 20.3 6.5
Percentage Occurence (%/bin)
Reflectivity (dBZ)

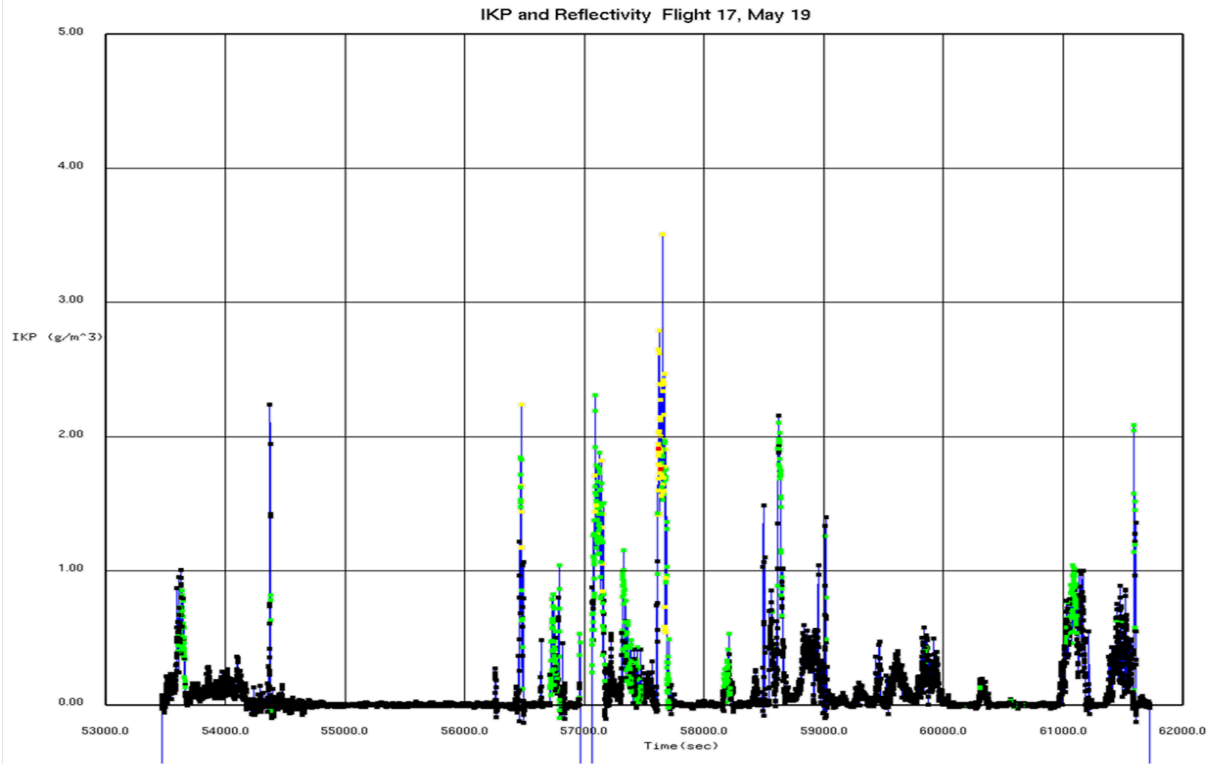
IKP and Reflectivity Flight 17, May 19
IKP (g/m^3)
Time(sec)

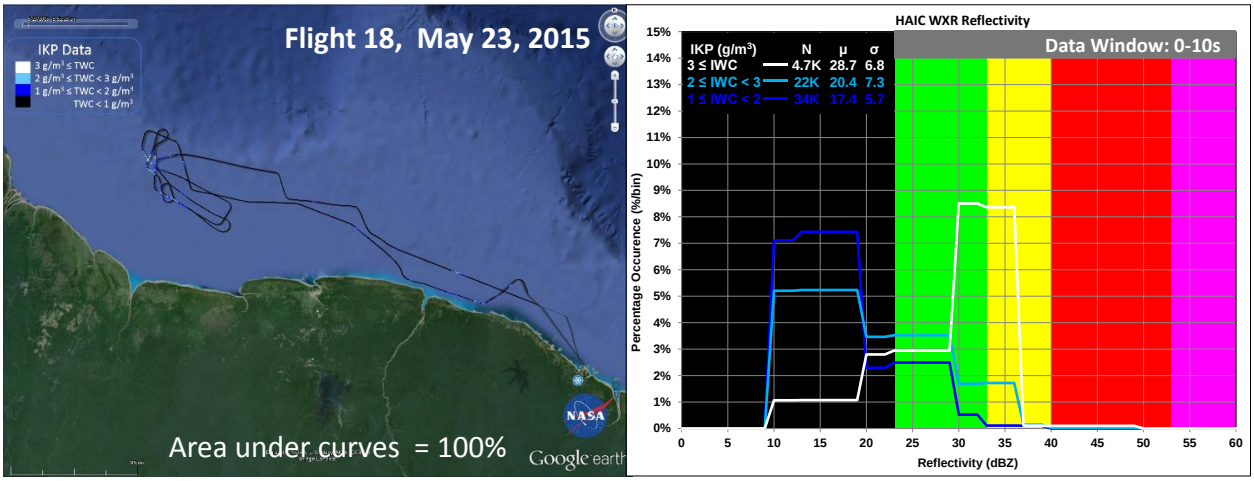
Flight 18, May 23, 2015
IKP Data
3 g/m³ ≤ TWC
2 g/m³ ≤ TWC < 3 g/m³
1 g/m³ ≤ TWC < 2 g/m³
TWC < 1 g/m³
Area under curves = 100%
Google earth
HAIC WXR Reflectivity
Data Window: 0-10s
IKP (g/m³) N μ σ
3 ≤ IWC 4.7K 28.7 6.8
2 ≤ IWC < 3 22K 20.4 7.3
1 ≤ IWC < 2 34K 17.4 5.7
Percentage Occurence (%/bin)
Reflectivity (dBZ)

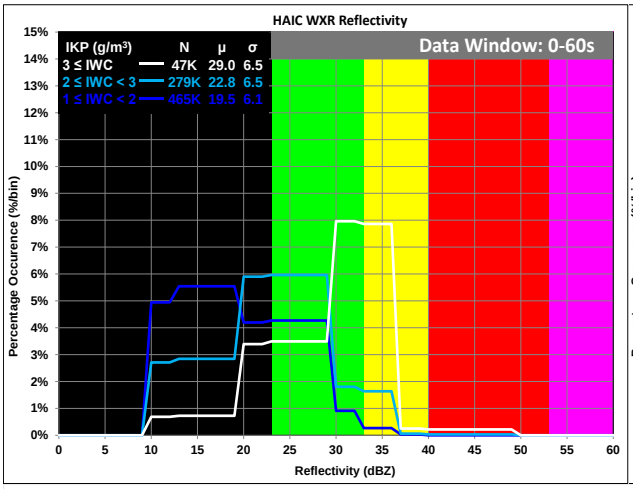
HAIC WXR Reflectivity
Data Window: 0-60s
IKP (g/m³) N μ σ
3 ≤ IWC 47K 29.0 6.5
2 ≤ IWC < 3 279K 22.8 6.5
1 ≤ IWC < 2 465K 19.5 6.1
Percentage Occurence (%/bin)
Reflectivity (dBZ)

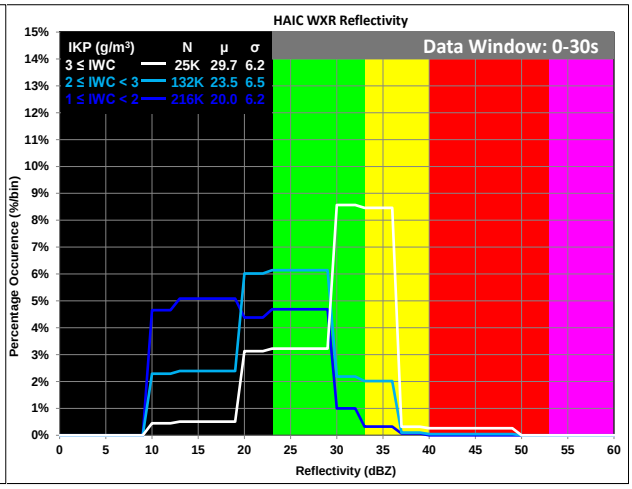
HAIC WXR Reflectivity
Data Window: 0-30s
IKP (g/m³) N μ σ
3 ≤ IWC 25K 29.7 6.2
2 ≤ IWC < 3 132K 23.5 6.5
1 ≤ IWC < 2 216K 20.0 6.2
Percentage Occurence (%/bin)
Reflectivity (dBZ)

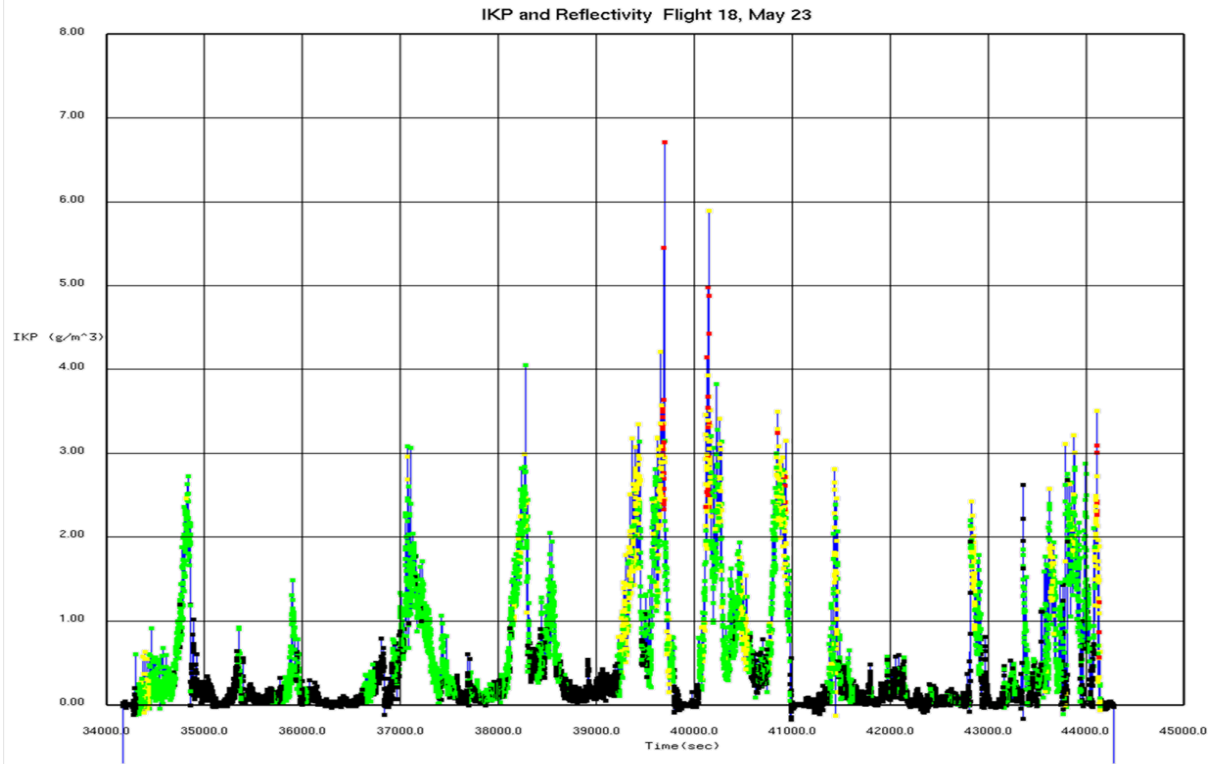
IKP and Reflectivity Flight 18, May 23
IKP (g/m^3)
Time(sec)

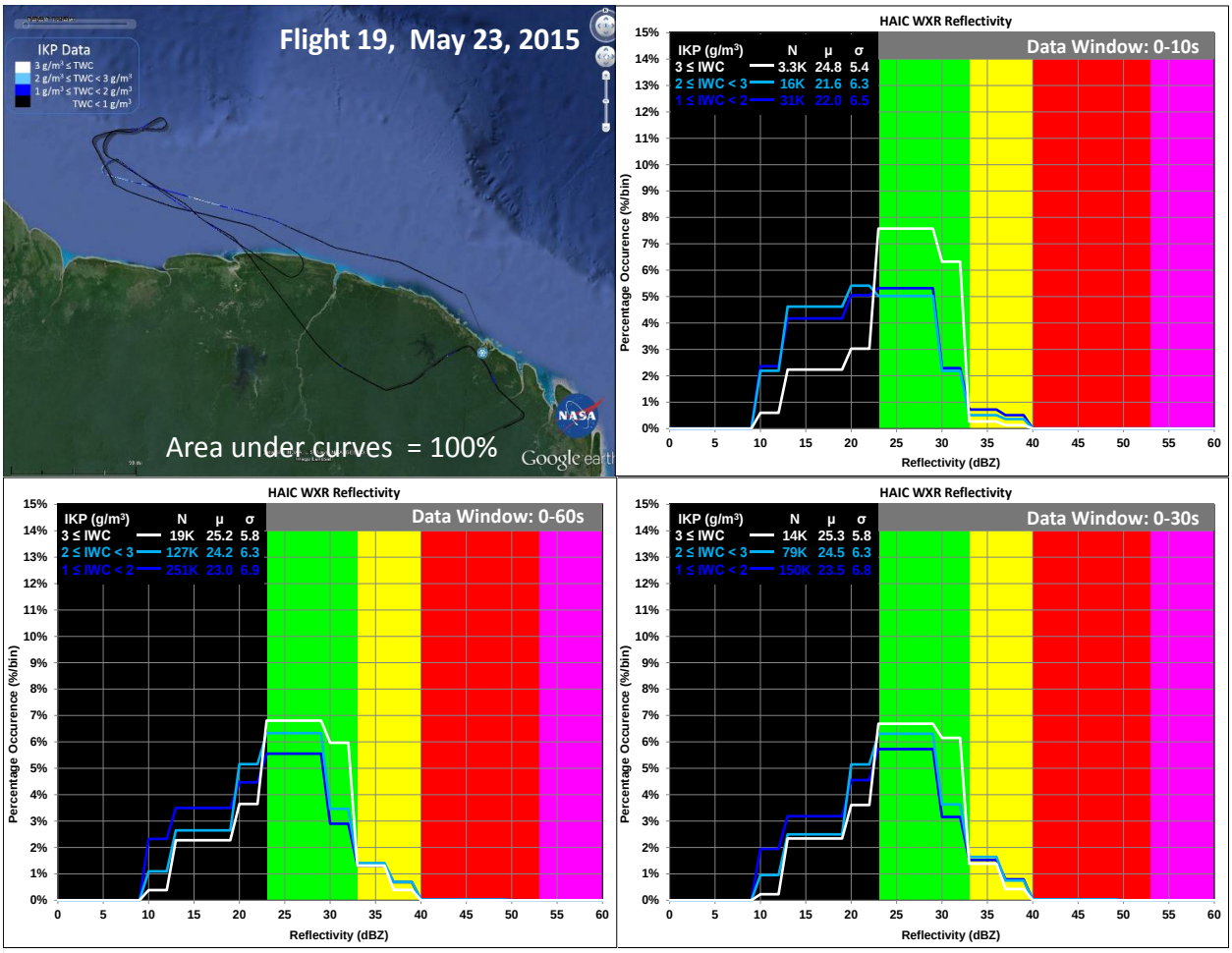
Flight 19, May 23, 2015
IKP Data
3 g/m³ ≤ TWC
2 g/m³ ≤ TWC < 3 g/m³
1 g/m³ ≤ TWC < 2 g/m³
TWC < 1 g/m³
Area under curves = 100%
Google earth
HAIC WXR Reflectivity
Data Window: 0-10s
IKP (g/m³) N μ σ
3 ≤ IWC 3.3K 24.8 5.4
2 ≤ IWC < 3 16K 21.6 6.3
1 ≤ IWC < 2 31K 22.0 6.5
Percentage Occurence (%/bin)
Reflectivity (dBZ)
HAIC WXR Reflectivity
Data Window: 0-60s
IKP (g/m³) N μ σ
3 ≤ IWC 19K 25.2 5.8
2 ≤ IWC < 3 127K 24.2 6.3
1 ≤ IWC < 2 251K 23.0 6.9
Percentage Occurence (%/bin)
Reflectivity (dBZ)
HAIC WXR Reflectivity
Data Window: 0-30s
IKP (g/m³) N μ σ
3 ≤ IWC 14K 25.3 5.8
2 ≤ IWC < 3 79K 24.5 6.3
1 ≤ IWC < 2 150K 23.5 6.8
Percentage Occurence (%/bin)
Reflectivity (dBZ)

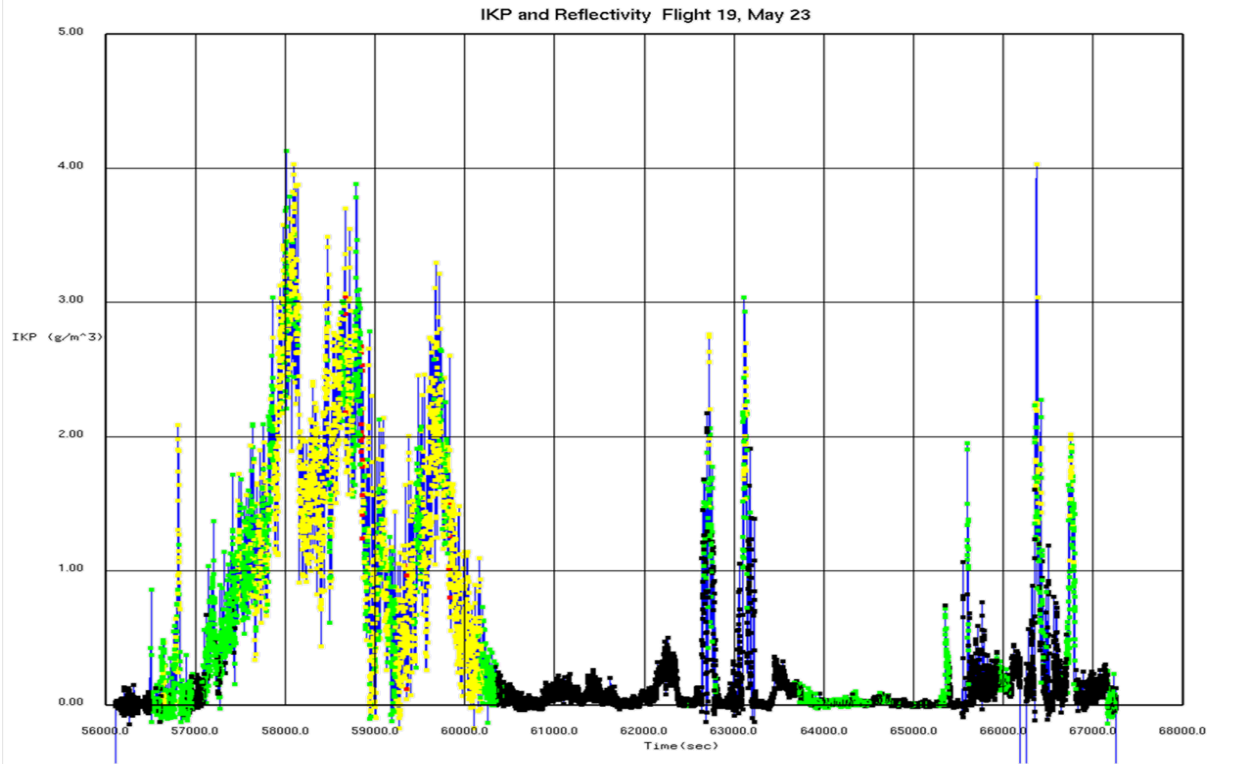
IKP and Reflectivity Flight 19, May 23
IKP (g/m^3)
Time(sec)

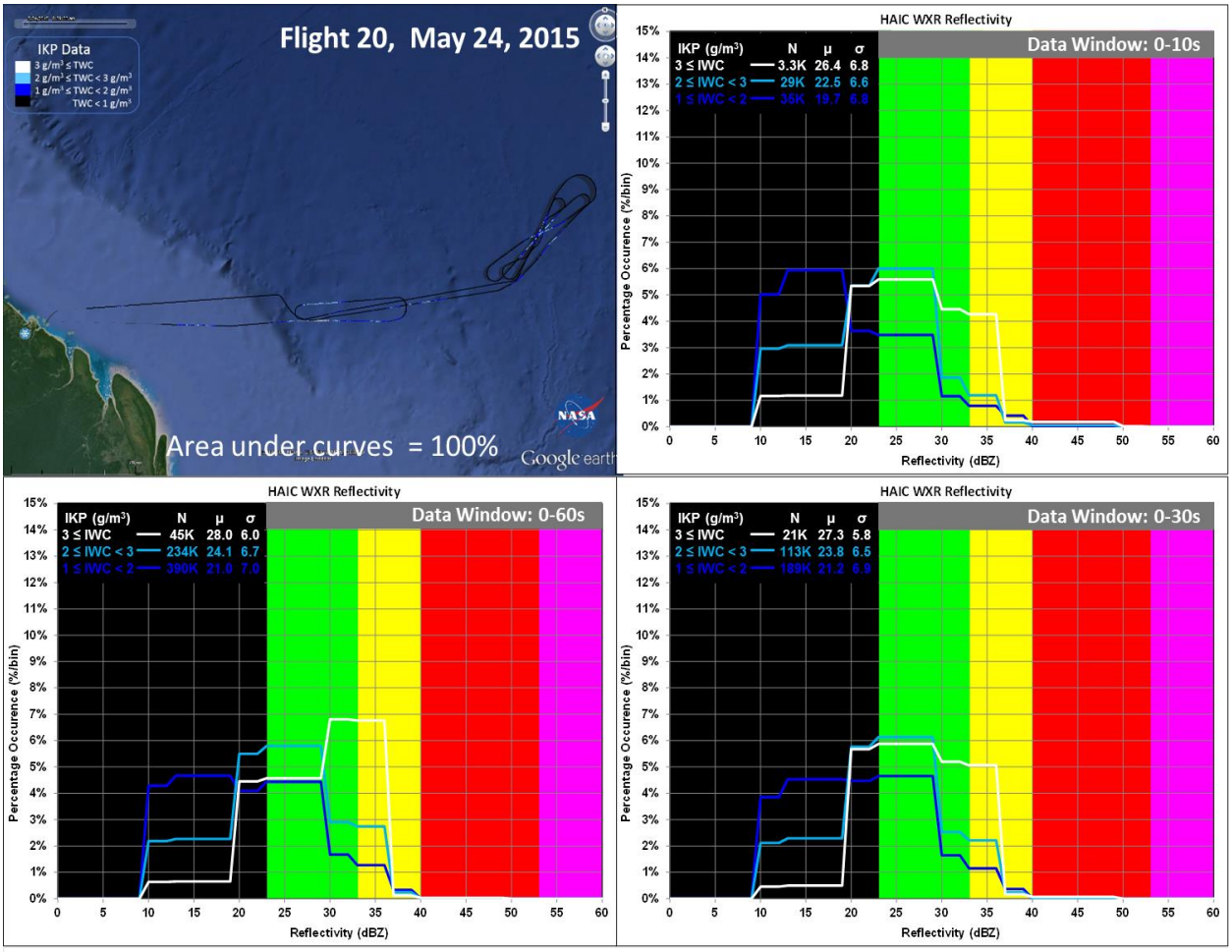
Flight 20, May 24, 2015
IKP Data
3 g/m³ ≤ TWC
2 g/m³ ≤ TWC < 3 g/m³
1 g/m³ ≤ TWC < 2 g/m³
TWC < 1 g/m³
Area under curves = 100%
Google earth
HAIC WXR Reflectivity
Data Window: 0-10s
IKP (g/m³) N μ σ
3 ≤ IWC 3.3K 26.4 6.8
2 ≤ IWC < 3 29K 22.5 6.6
1 ≤ IWC < 2 35K 19.7 6.8
Percentage Occurence (%/bin)
Reflectivity (dBZ)
HAIC WXR Reflectivity
Data Window: 0-60s
IKP (g/m³) N μ σ
3 ≤ IWC 45K 28.0 6.0
2 ≤ IWC < 3 234K 24.1 6.7
1 ≤ IWC < 2 390K 21.0 7.0
Percentage Occurence (%/bin)
Reflectivity (dBZ)
HAIC WXR Reflectivity
Data Window: 0-30s
IKP (g/m³) N μ σ
3 ≤ IWC 21K 27.3 5.8
2 ≤ IWC < 3 113K 23.8 6.5
1 ≤ IWC < 2 189K 21.2 6.9
Percentage Occurence (%/bin)
Reflectivity (dBZ)

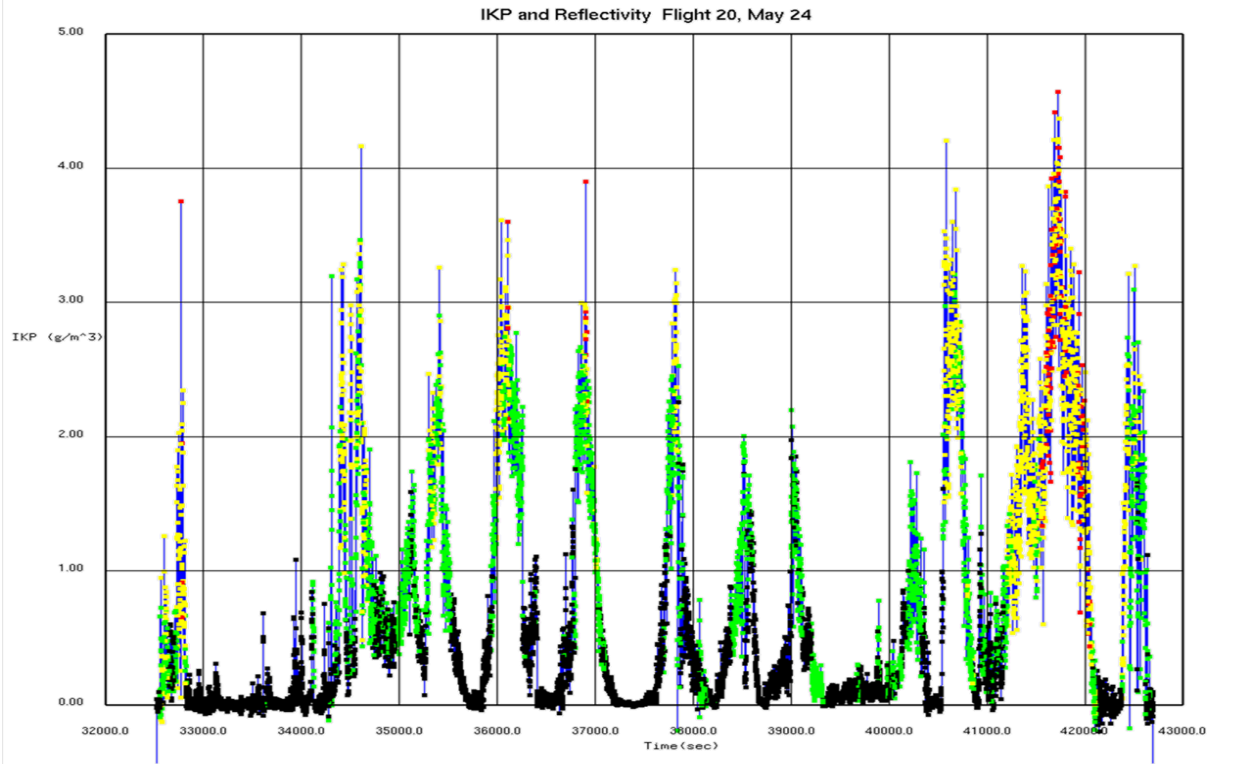
IKP and Reflectivity Flight 20, May 24
IKP (g/m^3)
Time(sec)

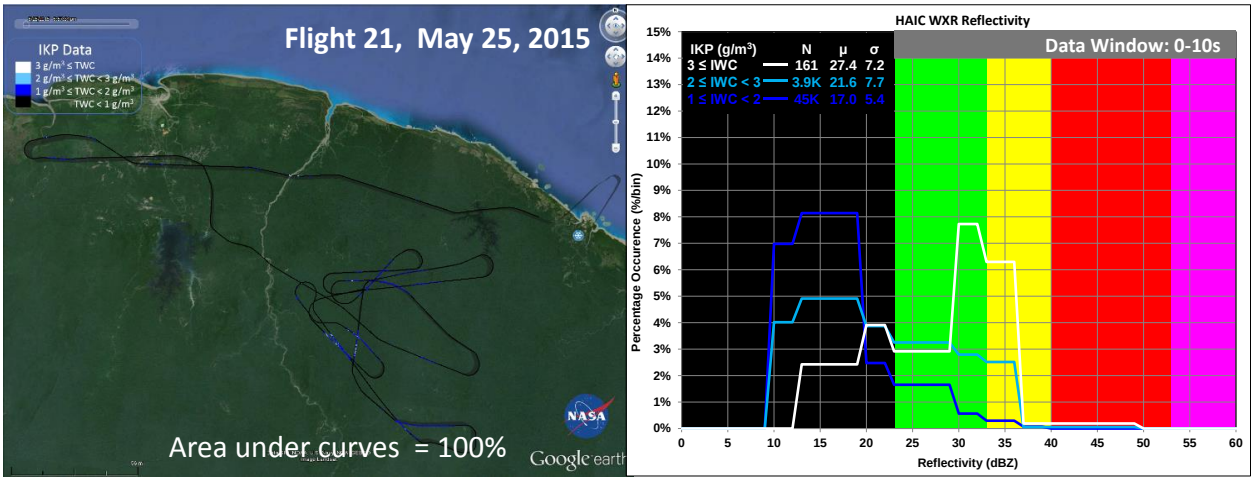
Flight 21, May 25, 2015
IKP Data
3 g/m³ ≤ TWC
2 g/m³ ≤ TWC < 3 g/m³
1 g/m³ ≤ TWC < 2 g/m³
TWC < 1 g/m³
Area under curves = 100%
Google earth
HAIC WXR Reflectivity
Data Window: 0-10s
IKP (g/m³) N μ σ
3 ≤ IWC 161 27.4 7.2
2 ≤ IWC < 3 3.9K 21.6 7.7
1 ≤ IWC < 2 45K 17.0 5.4
Percentage Occurence (%/bin)
Reflectivity (dBZ)

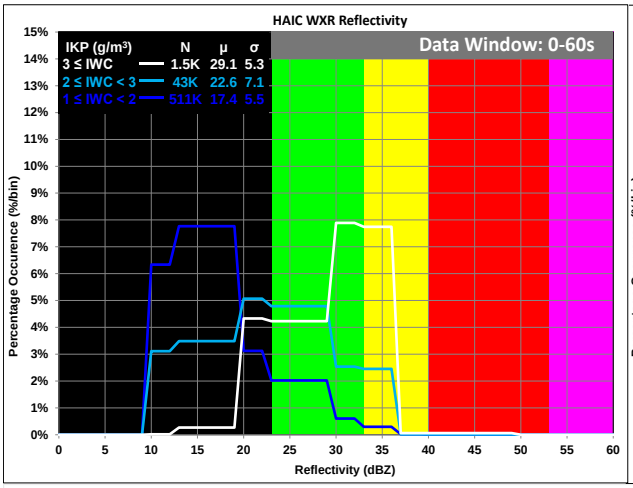
HAIC WXR Reflectivity
Data Window: 0-60s
IKP (g/m³) N μ σ
3 ≤ IWC 1.5K 29.1 5.3
2 ≤ IWC < 3 43K 22.6 7.1
1 ≤ IWC < 2 511K 17.4 5.5
Percentage Occurence (%/bin)
Reflectivity (dBZ)

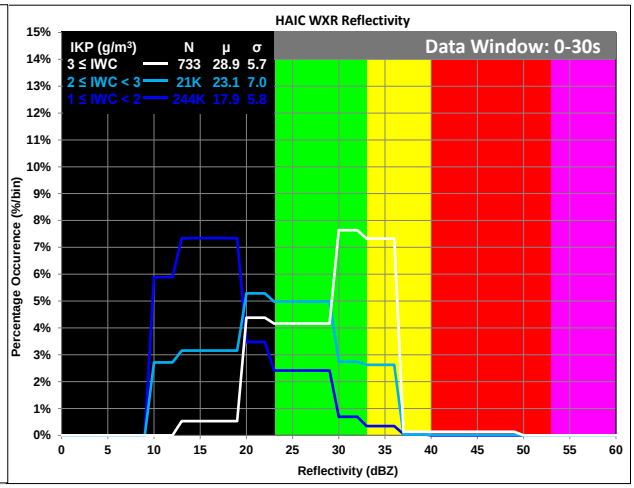
HAIC WXR Reflectivity
Data Window: 0-30s
IKP (g/m³) N μ σ
3 ≤ IWC 733 28.9 5.7
2 ≤ IWC < 3 21K 23.1 7.0
1 ≤ IWC < 2 244K 17.9 5.8
Percentage Occurence (%/bin)
Reflectivity (dBZ)

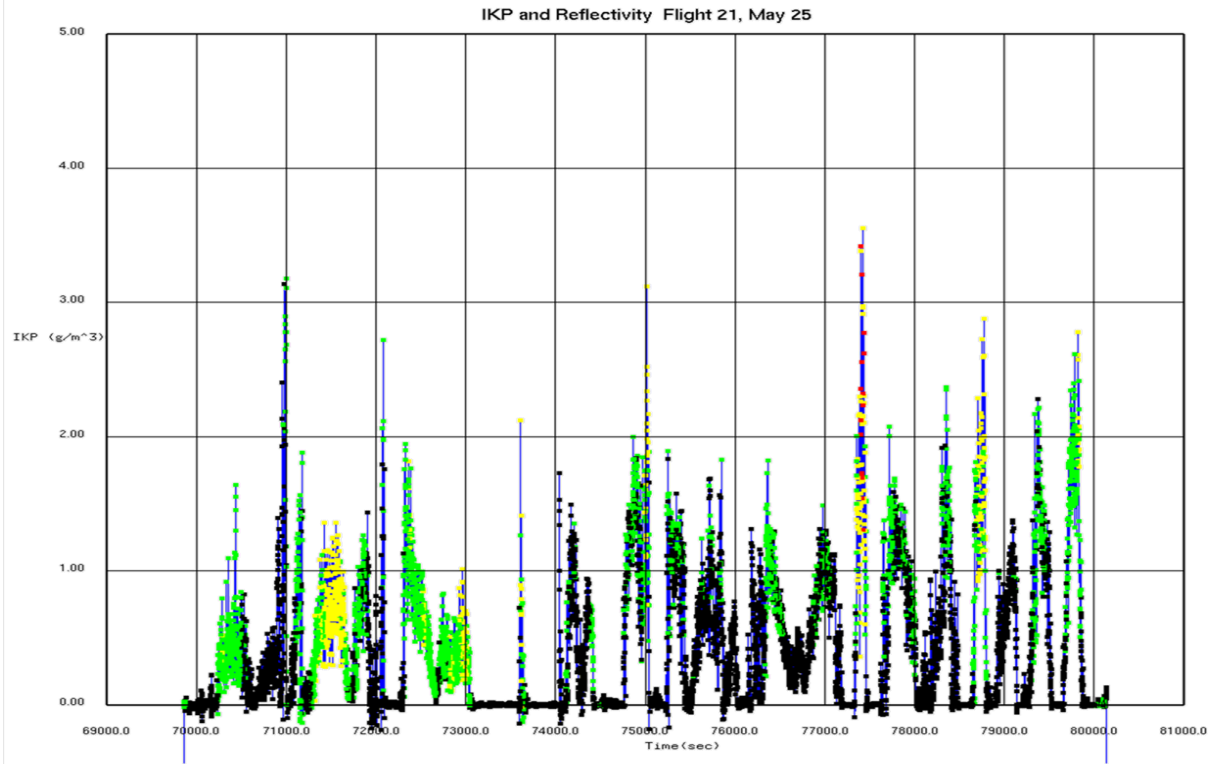
IKP and Reflectivity Flight 21, May 25
IKP (g/m^3)
Time(sec)

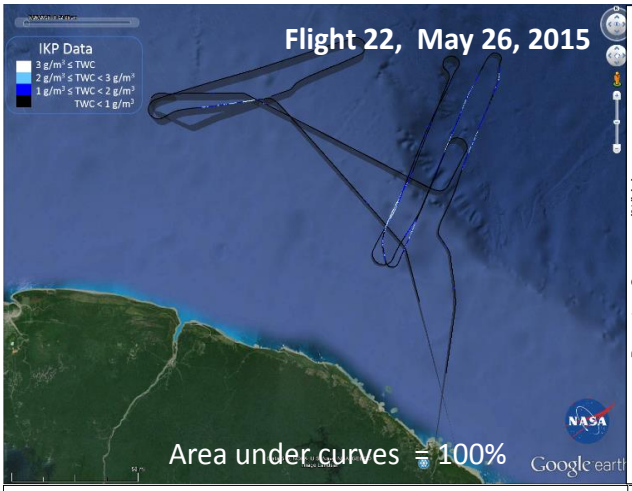
IKP Data
3 g/m³ ≤ TWC
2 g/m³ ≤ TWC < 3 g/m³
1 g/m³ ≤ TWC < 2 g/m³
TWC < 1 g/m³
Flight 22, May 26, 2015
Area under curves = 100%
NASA
Google earth

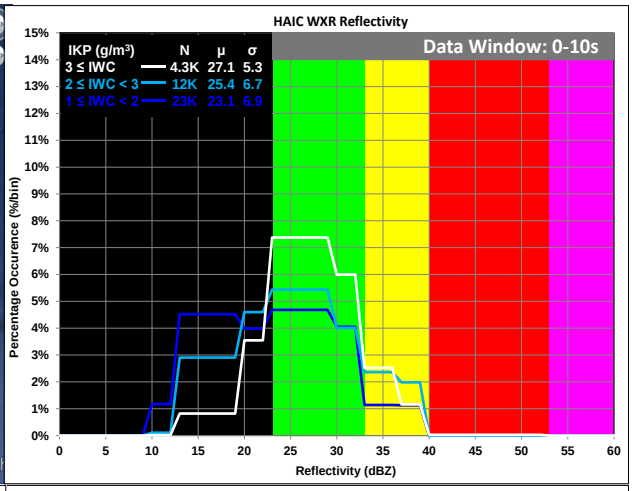
HAIC WXR Reflectivity
Data Window: 0-10s
IKP (g/m³) N μ σ
3 ≤ IWC 4.3K 27.1 5.3
2 ≤ IWC < 3 12K 25.4 6.7
1 ≤ IWC < 2 23K 23.1 6.9
Percentage Occurence (%/bin)
Reflectivity (dBZ)

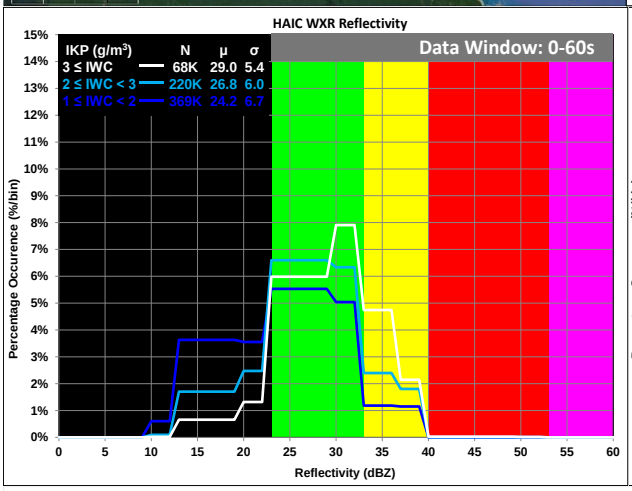
HAIC WXR Reflectivity
Data Window: 0-60s
IKP (g/m³) N μ σ
3 ≤ IWC 68K 29.0 5.4
2 ≤ IWC < 3 220K 26.8 6.0
1 ≤ IWC < 2 369K 24.2 6.7
Percentage Occurence (%/bin)
Reflectivity (dBZ)

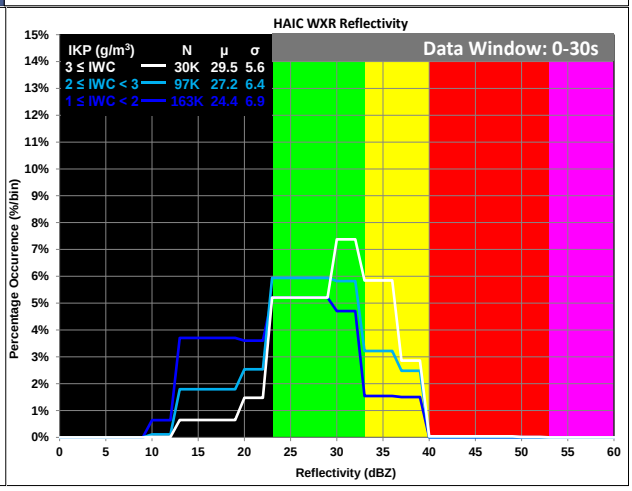
HAIC WXR Reflectivity
Data Window: 0-30s
IKP (g/m³) N μ σ
3 ≤ IWC 30K 29.5 5.6
2 ≤ IWC < 3 97K 27.2 6.4
1 ≤ IWC < 2 163K 24.4 6.9
Percentage Occurence (%/bin)
Reflectivity (dBZ)

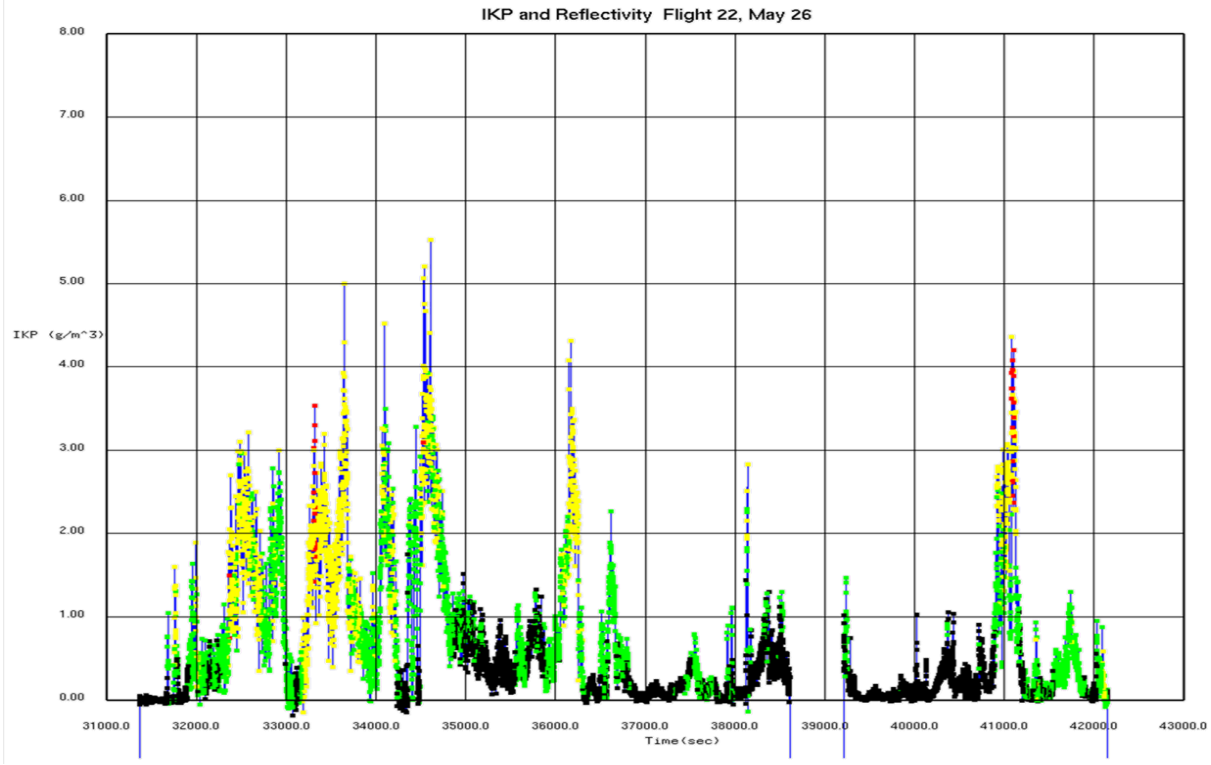
IKP and Reflectivity Flight 22, May 26
IKP (g/m^3)
Time(sec)

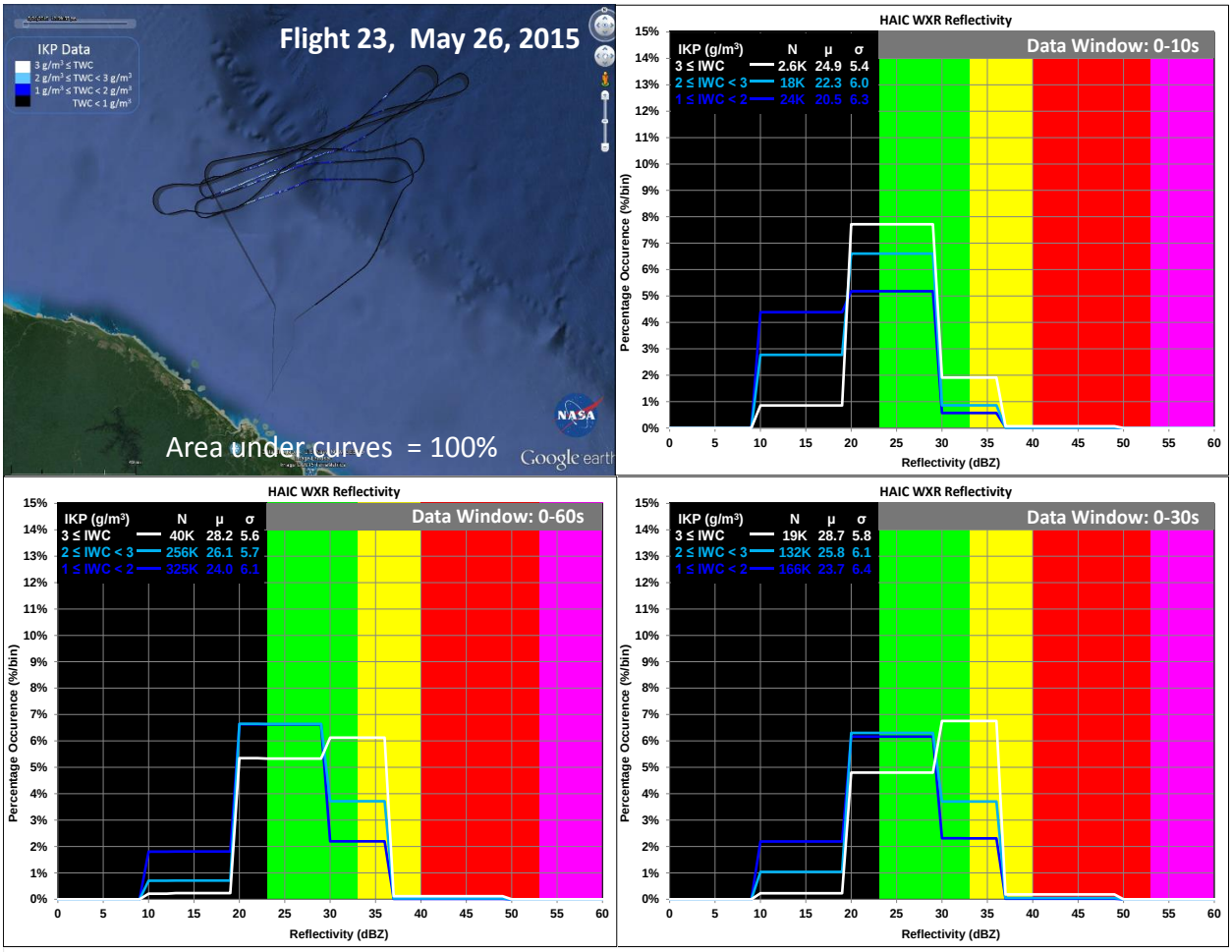
Flight 23, May 26, 2015
IKP Data
3 g/m³ ≤ TWC
2 g/m³ ≤ TWC < 3 g/m³
1 g/m³ ≤ TWC < 2 g/m³
TWC < 1 g/m³
Area under curves = 100%
Google earth
HAIC WXR Reflectivity
Data Window: 0-10s
IKP (g/m³) N μ σ
3 ≤ IWC 2.6K 24.9 5.4
2 ≤ IWC < 3 18K 22.3 6.0
1 ≤ IWC < 2 24K 20.5 6.3
Percentage Occurence (%/bin)
Reflectivity (dBZ)
HAIC WXR Reflectivity
Data Window: 0-60s
IKP (g/m³) N μ σ
3 ≤ IWC 40K 28.2 5.6
2 ≤ IWC < 3 256K 26.1 5.7
1 ≤ IWC < 2 325K 24.0 6.1
Percentage Occurence (%/bin)
Reflectivity (dBZ)
HAIC WXR Reflectivity
Data Window: 0-30s
IKP (g/m³) N μ σ
3 ≤ IWC 19K 28.7 5.8
2 ≤ IWC < 3 132K 25.8 6.1
1 ≤ IWC < 2 166K 23.7 6.4
Percentage Occurence (%/bin)
Reflectivity (dBZ)

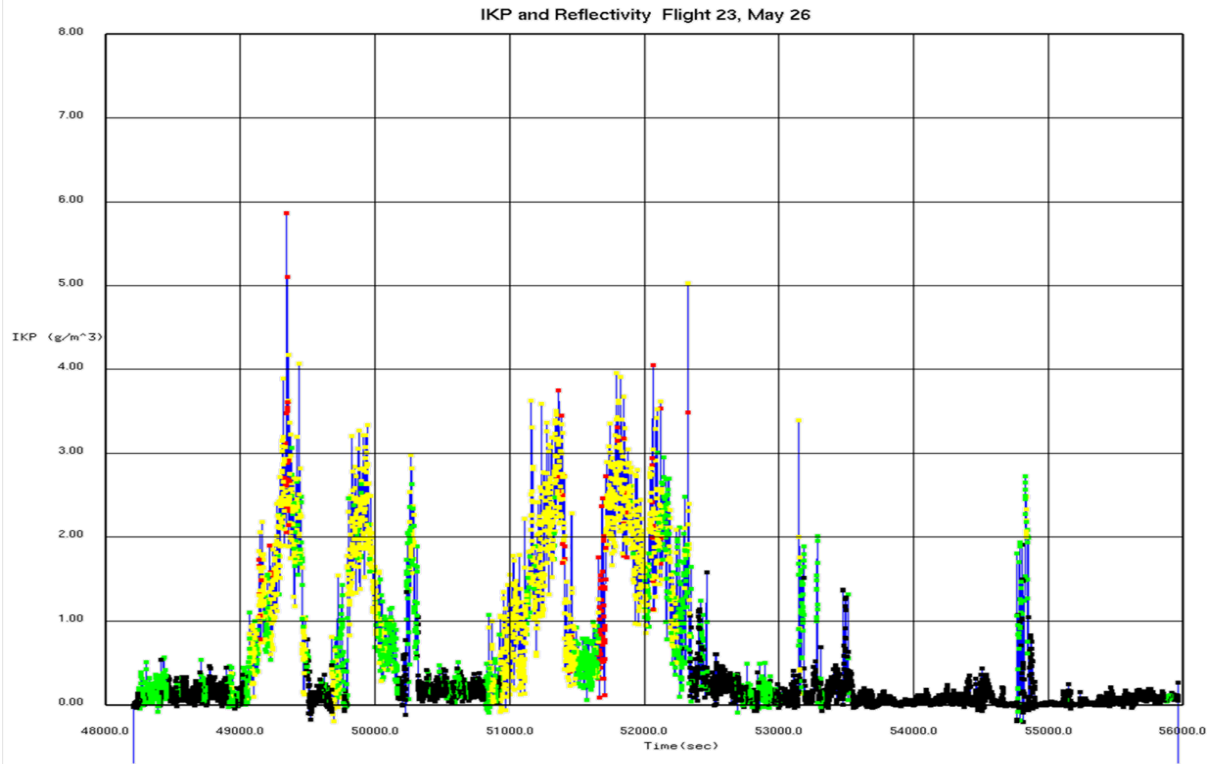
IKP and Reflectivity Flight 23, May 26
IKP (g/m^3)
Time(sec)

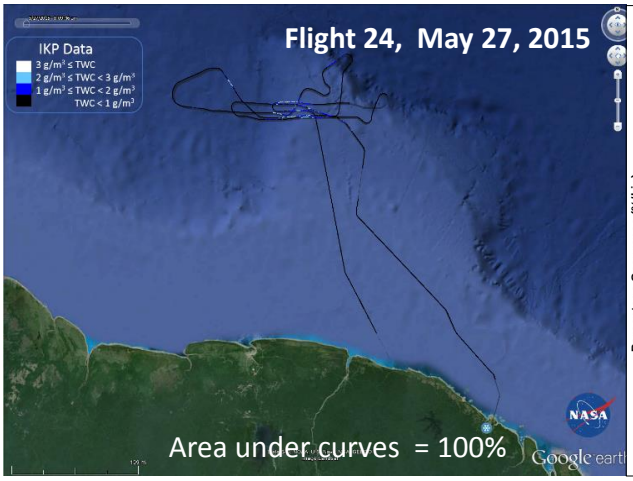
Flight 24, May 27, 2015
IKP Data
3 g/m³ ≤ TWC
2 g/m³ ≤ TWC < 3 g/m³
1 g/m³ ≤ TWC < 2 g/m³
TWC < 1 g/m³
Area under curves = 100%
NASA
Google earth

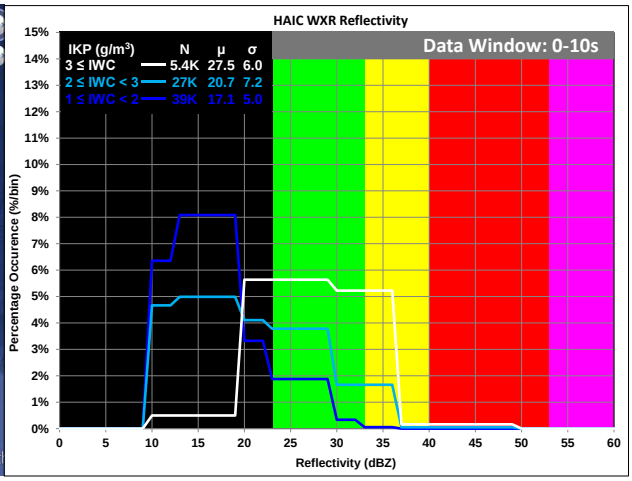
HAIC WXR Reflectivity
Data Window: 0-10s
IKP (g/m³) N μ σ
3 ≤ IWC 5.4K 27.5 6.0
2 ≤ IWC < 3 27K 20.7 7.2
1 ≤ IWC < 2 39K 17.1 5.0
Percentage Occurence (%/bin)
Reflectivity (dBZ)

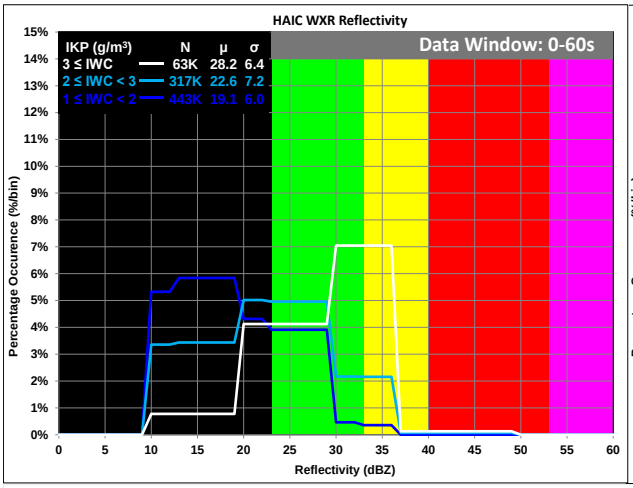
HAIC WXR Reflectivity
Data Window: 0-60s
IKP (g/m³) N μ σ
3 ≤ IWC 63K 28.2 6.4
2 ≤ IWC < 3 317K 22.6 7.2
1 ≤ IWC < 2 443K 19.1 6.0
Percentage Occurence (%/bin)
Reflectivity (dBZ)

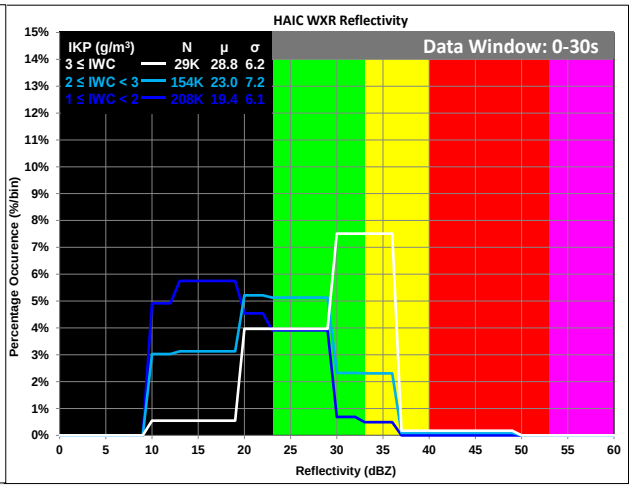
HAIC WXR Reflectivity
Data Window: 0-30s
IKP (g/m³) N μ σ
3 ≤ IWC 29K 28.8 6.2
2 ≤ IWC < 3 154K 23.0 7.2
1 ≤ IWC < 2 208K 19.4 6.1
Percentage Occurence (%/bin)
Reflectivity (dBZ)

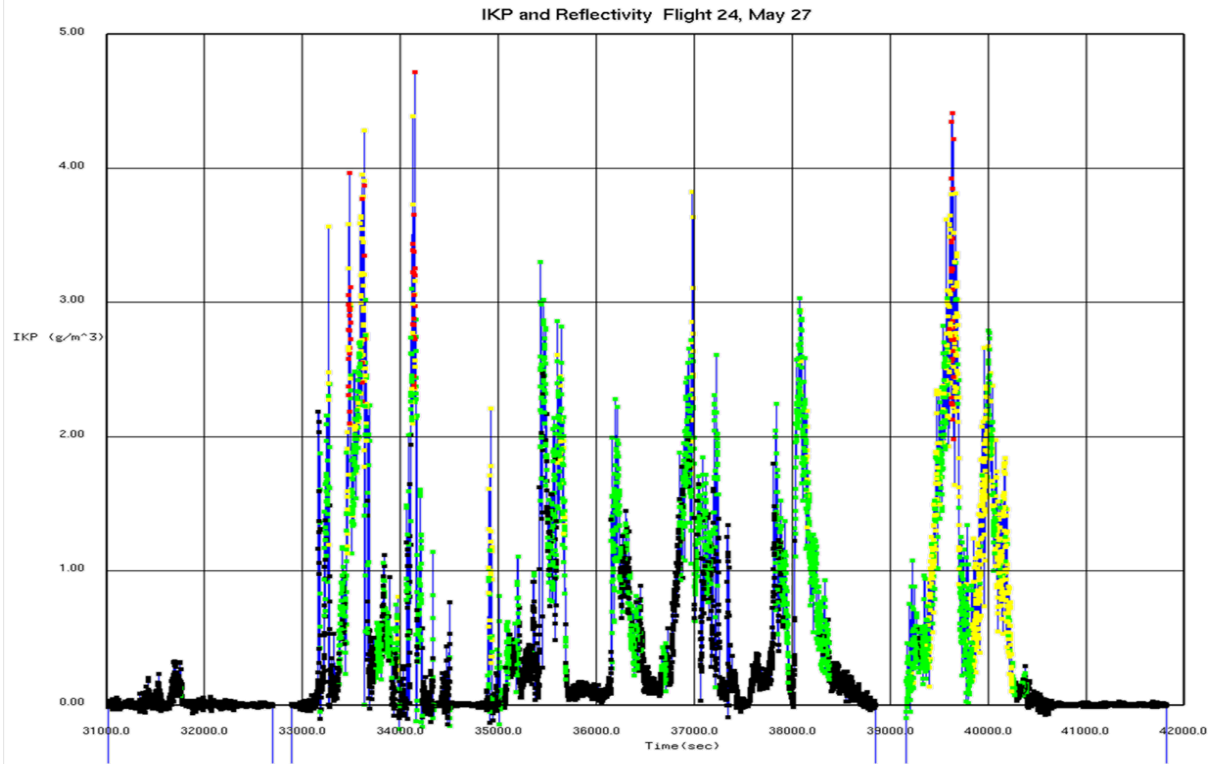
IKP and Reflectivity Flight 24, May 27
IKP (g/m^3)
Time(sec)

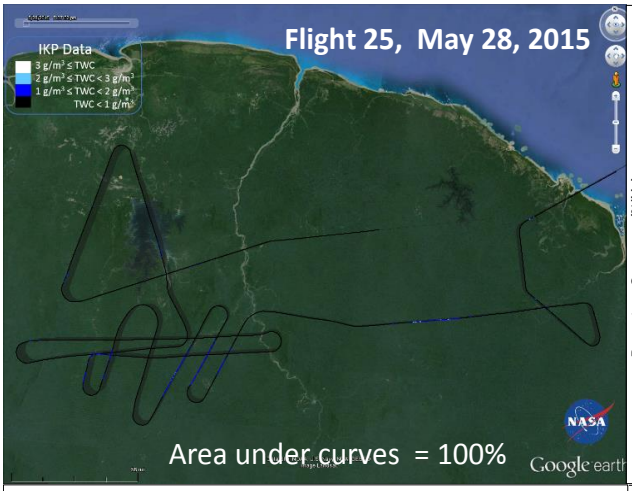
Flight 25, May 28, 2015
IKP Data
3 g/m³ ≤ TWC
2 g/m³ ≤ TWC < 3 g/m³
1 g/m³ ≤ TWC < 2 g/m³
TWC < 1 g/m³
Area under curves = 100%
Google earth

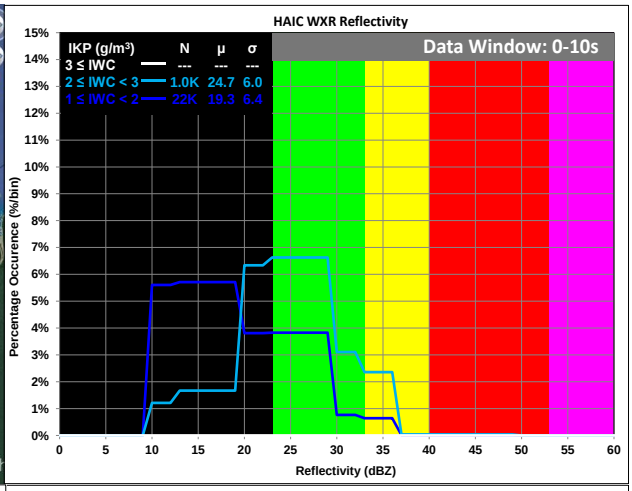
HAIC WXR Reflectivity
Data Window: 0-10s
IKP (g/m³) N μ σ
3 ≤ IWC --- --- ---
2 ≤ IWC < 3 1.0K 24.7 6.0
1 ≤ IWC < 2 22K 19.3 6.4
Percentage Occurence (%/bin)
Reflectivity (dBZ)

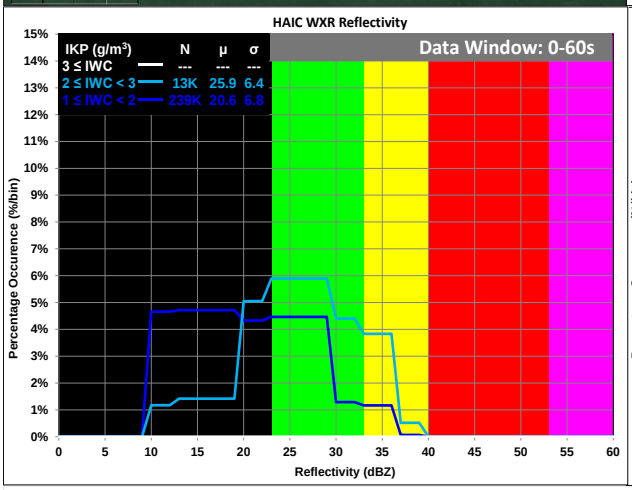
HAIC WXR Reflectivity
Data Window: 0-60s
IKP (g/m³) N μ σ
3 ≤ IWC --- --- ---
2 ≤ IWC < 3 13K 25.9 6.4
1 ≤ IWC < 2 239K 20.6 6.8
Percentage Occurence (%/bin)
Reflectivity (dBZ)

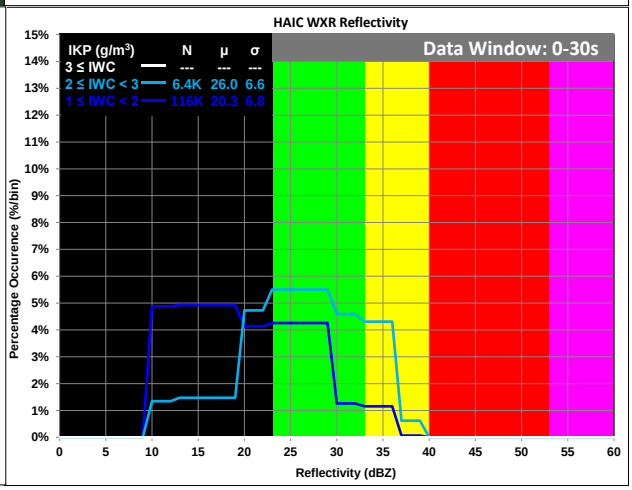
HAIC WXR Reflectivity
Data Window: 0-30s
IKP (g/m³) N μ σ
3 ≤ IWC --- --- ---
2 ≤ IWC < 3 6.4K 26.0 6.6
1 ≤ IWC < 2 116K 20.3 6.8
Percentage Occurence (%/bin)
Reflectivity (dBZ)

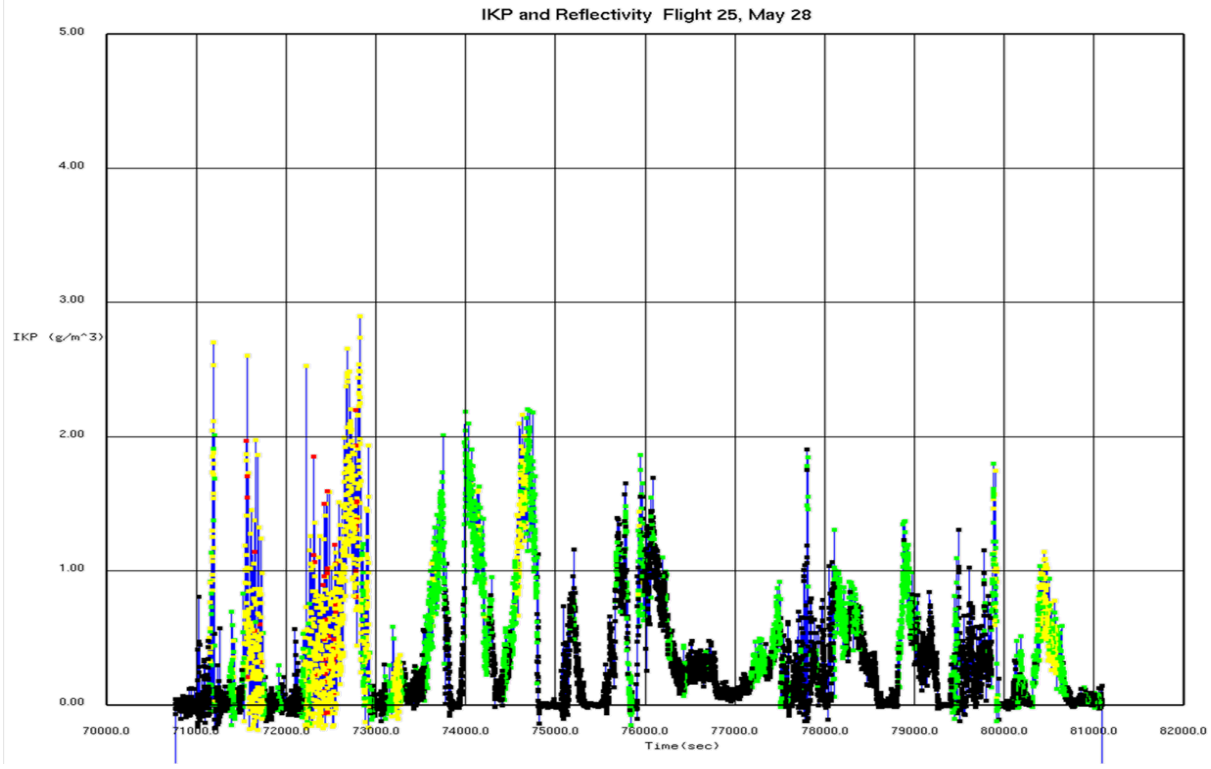
IKP and Reflectivity Flight 25, May 28
IKP (g/m^3)
Time(sec)

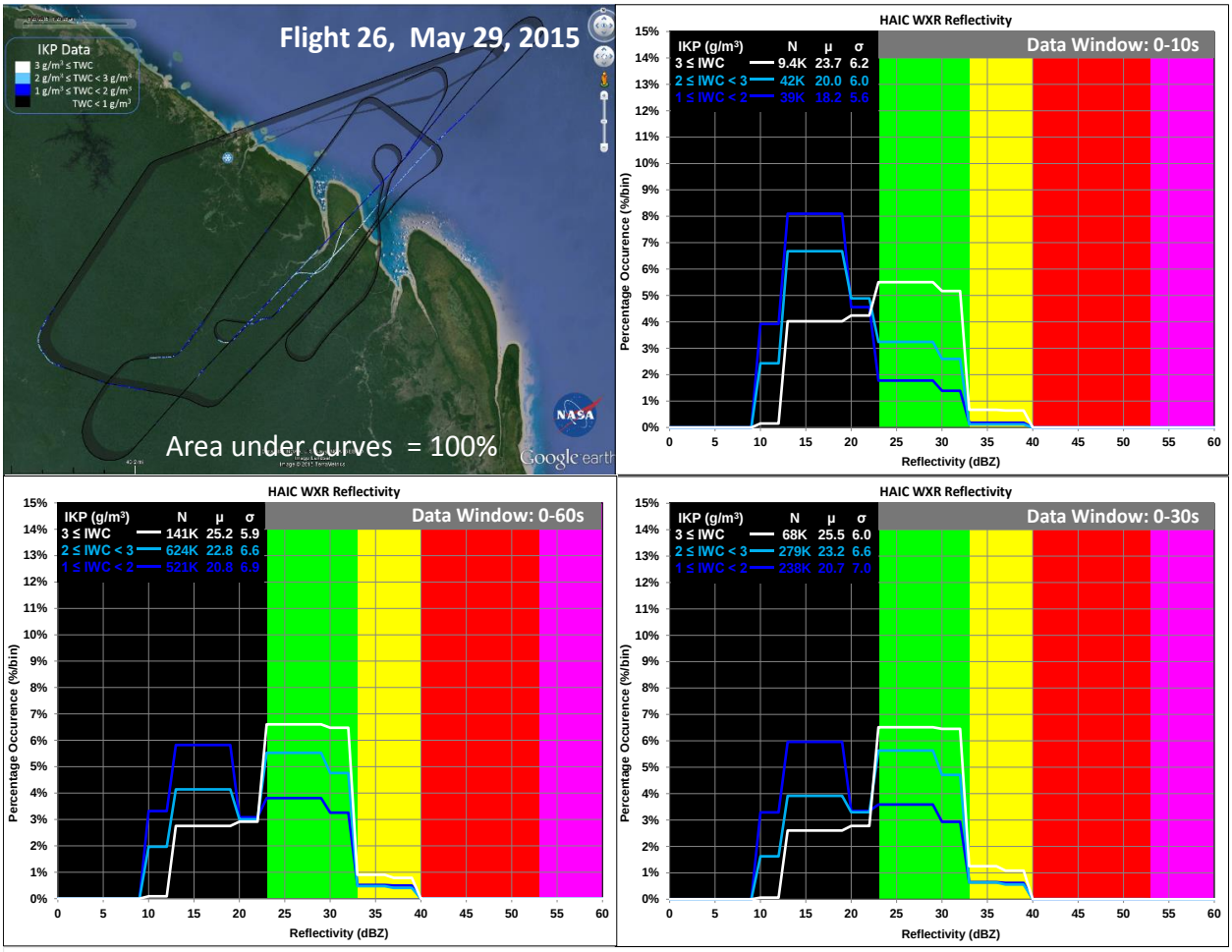
Flight 26, May 29, 2015
IKP Data
3 g/m³ ≤ TWC
2 g/m³ ≤ TWC < 3 g/m³
1 g/m³ ≤ TWC < 2 g/m³
TWC < 1 g/m³
Area under curves = 100%
Google earth
HAIC WXR Reflectivity
Data Window: 0-10s
IKP (g/m³) N μ σ
3 ≤ IWC 9.4K 23.7 6.2
2 ≤ IWC < 3 42K 20.0 6.0
1 ≤ IWC < 2 39K 18.2 5.6
Percentage Occurence (%/bin)
Reflectivity (dBZ)
HAIC WXR Reflectivity
Data Window: 0-60s
IKP (g/m³) N μ σ
3 ≤ IWC 141K 25.2 5.9
2 ≤ IWC < 3 624K 22.8 6.6
1 ≤ IWC < 2 521K 20.8 6.9
Percentage Occurence (%/bin)
Reflectivity (dBZ)
HAIC WXR Reflectivity
Data Window: 0-30s
IKP (g/m³) N μ σ
3 ≤ IWC 68K 25.5 6.0
2 ≤ IWC < 3 279K 23.2 6.6
1 ≤ IWC < 2 238K 20.7 7.0
Percentage Occurence (%/bin)
Reflectivity (dBZ)

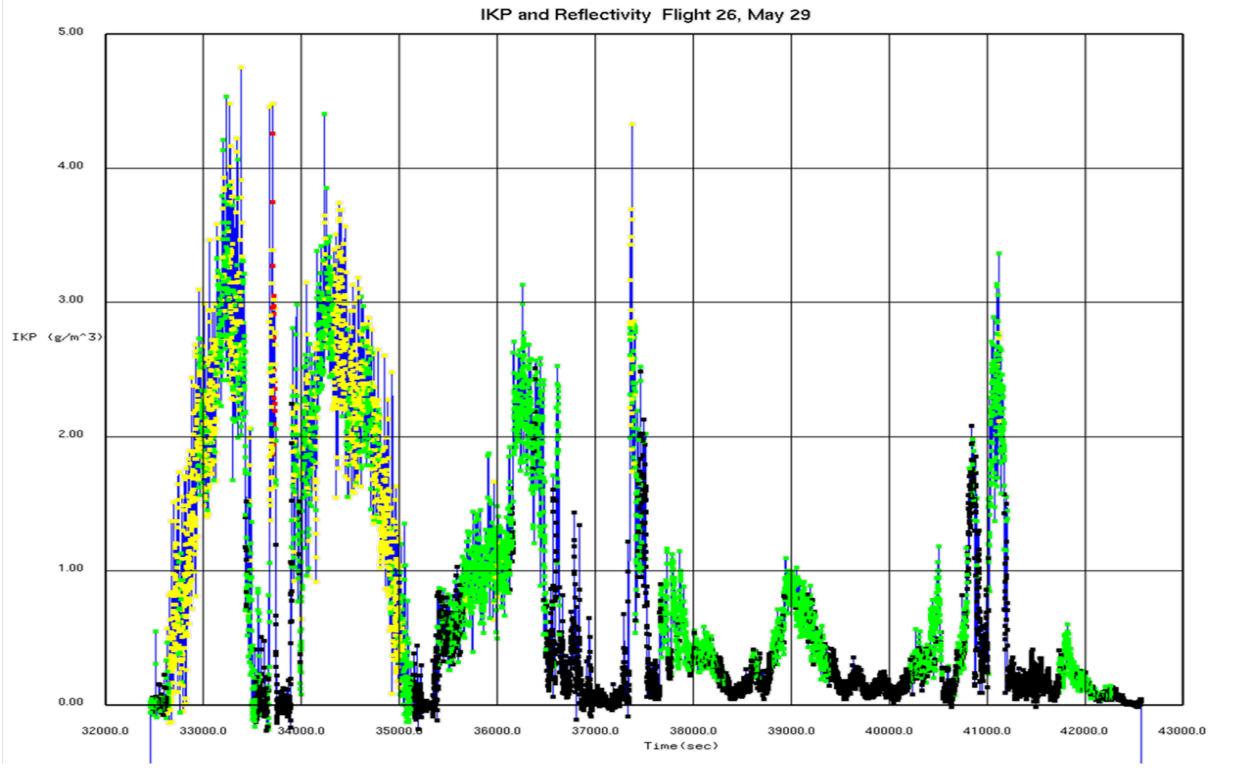
IKP and Reflectivity Flight 26, May 29
IKP (g/m^3)
Time(sec)

REPORT DOCUMENTATION PAGE

Form Approved
OMB No. 0704-0188

The public reporting burden for this collection of information is estimated to average 1 hour per response, including the time for reviewing instructions, searching existing data sources, gathering and maintaining the data needed, and completing and reviewing the collection of information. Send comments regarding this burden estimate or any other aspect of this collection of information, including suggestions for reducing the burden, to Department of Defense, Washington Headquarters Services, Directorate for Information Operations and Reports (0704-0188), 1215 Jefferson Davis Highway, Suite 1204, Arlington, VA 22202-4302. Respondents should be aware that notwithstanding any other provision of law, no person shall be subject to any penalty for failing to comply with a collection of information if it does not display a currently valid OMB control number.
PLEASE DO NOT RETURN YOUR FORM TO THE ABOVE ADDRESS.

1. REPORT DATE *(DD-MM-YYYY)*	2. REPORT TYPE	3. DATES COVERED *(From - To)*
09/23/2020	Technical Memorandum	

4. TITLE AND SUBTITLE
Airborne Weather Radar Observations & Analysis Results from the 2014/2015 HAIC Flight Campaigns

5a. CONTRACT NUMBER

5b. GRANT NUMBER

5c. PROGRAM ELEMENT NUMBER
AETC

6. AUTHOR(S)
Harrah, Steven
Hunt, Patricia
Strickland, Justin

5d. PROJECT NUMBER
HIWC

5e. TASK NUMBER

5f. WORK UNIT NUMBER

7. PERFORMING ORGANIZATION NAME(S) AND ADDRESS(ES)
NASA Langley Research Center
Hampton, VA 23681-2199

8. PERFORMING ORGANIZATION REPORT NUMBER

9. SPONSORING/MONITORING AGENCY NAME(S) AND ADDRESS(ES)
National Aeronautics and Space Administration
Washington, DC 20546-0001

10. SPONSOR/MONITOR'S ACRONYM(S)

11. SPONSOR/MONITOR'S REPORT NUMBER(S)
NASA-TM-2020-5007394

12. DISTRIBUTION/AVAILABILITY STATEMENT
Unclassified
Subject Category
Availability: NASA STI Program (757) 864-9658

13. SUPPLEMENTARY NOTES

14. ABSTRACT
This document presents a summary of the airborne weather radar observations made during joint EU/US flight campaigns to study High Altitude Ice Crystal (HAIC) atmospheric conditions. These flight campaigns were conducted near Darwin, Australia and Cayenne, French Guiana in 2014 and 2015, respectively. A variety of analyses were conducted resulting in statistical descriptions of the radar reflectivities of HAIC encountered during storm penetrations. These results are presented along with descriptions of the set of visualization tools that aided flight operations and post-flight assessments. A summary of HAIC radar reflectivities observed during these flight campaigns corroborates reports by commercial pilots during HAIC encounters.

15. SUBJECT TERMS
radar, aviation safety, engine ice, flight test

16. SECURITY CLASSIFICATION OF:			17. LIMITATION OF ABSTRACT	18. NUMBER OF PAGES	19a. NAME OF RESPONSIBLE PERSON
a. REPORT	b. ABSTRACT	c. THIS PAGE			STI Help Desk (email: help@sti.nasa.gov)
U	U	U	UU	79	19b. TELEPHONE NUMBER *(Include area code)* (757) 864-9658